The characterization of Dbf4 interactions and roles in genome replication and stability in *Saccharomyces cerevisiae*

by

Larasati

A thesis

presented to the University of Waterloo

in fulfilment of the thesis requirement for the degree of

Doctor of Philosophy

in

Biology

Waterloo, Ontario, Canada, 2020

Examining Committee Membership

The following served on the Examining Committee for this thesis. The decision of the Examining Committee is by majority vote.

External Examiner	Dr. Caroline Schild-Poulter Associate Professor
Internal-external Member	Dr. Jonathan Blay Professor
Supervisor	Dr. Bernard Duncker Professor
Internal Member	Dr. Bruce Reed Associate Professor
Internal Member	Dr. Andrew Doxey Associate Professor

Author's Declaration

This thesis consists of material all of which I authored or co-authored: see Statement of Contributions included in the thesis. This is a true copy of the thesis, including any required final revisions, as accepted by my examiners.

I understand that my thesis may be made electronically available to the public

Statement of Contributions

Exception to sole authorship of materials are as follows:

Portions of Chapter 2 and research presented in Chapter 3 and Appendix A.

Larasati and P. Myrox (from the laboratory of Dr. Duncker, University of Waterloo) performed the *in vivo* experiments. Dr. R. Ghirlando (National Institutes of Health) conducted, interpreted, and analyzed the ultracentrifugation data. Dr. L. Matthews (from the laboratory of Dr. Guarné, McMaster University) performed the NMR experiments and provided technical and intellectual input to the crystallographic work. S. Boulton (from the laboratory of Dr. Melacini, McMaster University) analyzed the NMR data. C. Lai (from the laboratory of Dr. Moraes, University of Toronto) provided technical and intellectual input to analyze the affinities of the Dbf4-Rad53 and Dbf4-Rad53-Cdc7 complexes. With the guidance of Dr. Alba Guarné, Dr. Ahmad Almawi conducted the experiments, interpreted the data, prepared several figures, and assisted with the writing of the published manuscript.

Abstract

Dbf4-dependent kinase (DDK) is a complex composed of the Cdc7 kinase and its regulatory subunit, Dbf4. Initiation of eukaryotic DNA replication requires phosphorylation of Mcm2-7 helicase by DDK. Due to its essential role in replication, DDK is also an S phase checkpoint response target of Rad53 kinase. Dbf4 is conserved among eukaryotes and interacts with its ligands to regulate DNA replication initiation. In the studies detailed in this thesis, I characterized the molecular details of Dbf4 binding with its targets and their in vivo significance in the budding yeast *Saccharomyces cerevisiae*.

Previous structural studies revealed that Dbf4 HBRCT directly binds to the Rad53 FHA1 domain in a non-canonical way as part of the DNA damage checkpoint response. This interaction is phosphorylation independent, which is novel and distinctive since both BRCT and FHA are known as a phospoepitope recognition module. Work included in this thesis presents the crystal structures of Rad53 FHA1 bound to Dbf4, in the presence of a phosphorylated Cdc7 peptide. FHA1 was shown to interact with both subunits of DDK by using the canonical binding mode to recognize the Cdc7 phosphopeptide and a non-canonical surface to interact with Dbf4. Two interfaces that mediate the Dbf4-Rad53 interaction were also identified and revealed that HBRCT and FHA1 do not contribute equally in this binding.

To prevent precocious DDK activation in G1 phase, Rif1 targets Glc7 phosphatase to origins of DNA replication where it dephosphorylates Mcm2-7. As cells approach S phase, both DDK and cyclin dependent kinase (CDK) phosphorylate the Glc7 binding region of Rif1, inhibiting the Rif1-Glc7 association. A previous study showed that the Dbf4 N-terminus interacts with the Rif1 C-terminus to mediate DDK phosphorylation. This Dbf4 region includes a HBRCT domain that binds to Rad53 during checkpoint conditions. Two-hybrid

analysis revealed the Dbf4 HBRCT domain mediates interaction with Rif1 in a fashion distinct from the way it promotes the Dbf4-Rad53 association. The Rif1 C-terminus is also known to bind the telomere-associated ligand Rap1. A combination of bioinformatics and two-hybrid analysis uncovered a proline-rich (PPDSPP) C-terminal Rif1 motif that is required for Dbf4 binding, but not Rap1. Combining a deletion of this motif (Δ*PPDSPP*) with mutation of RIF1 CDK target sites, (5*A*), resulted in a slow growth phenotype and hypersensitivity to bleocin and phleomycin, suggesting impaired function in DNA double-strand break repair. *rif1 5A*Δ*PPDSPP* was further combined with mutations affecting either non-homologous end-joining (NHEJ) or homologous recombination (HR) and revealed that HR disruption causes increased *rif1 5A*Δ*PPDSPP* sensitivity to a range of genotoxic agents while NHEJ disruption resulted in a striking rescue of this strain. Therefore, Rif1, besides being modulated by DDK and CDK in DNA replication initiation, appears to be regulated by the same kinases during cellular recovery from genotoxic stress.

Recent reports on Mrc1/Claspin suggest a novel checkpoint-independent function in DNA replication initiation in fission yeast and humans. This role involves the Mrc1/Claspin interaction with DDK through its Cdc7 subunit. As part of the investigations conducted for this thesis, two-hybrid assays were carried out and demonstrated that budding yeast Mrc1 associates with DDK via Dbf4, not Cdc7. Moreover, preliminary in vivo data revealed that deletion of budding yeast *MRC1* exacerbated cell growth when DDK activity was compromised, which is different from what was previously seen in fission yeast. Therefore, our initial findings indicate that Mrc1 may function differently in budding and fission yeast DNA replication.

Acknowledgements

Science is not done in isolation. This thesis would not have been finished without many amazing individuals that have contributed along the way. I am greatly indebted to them.

My heartfelt gratitude goes first to my mentor, Dr. Bernard Duncker. Bernie, thank you for everything you have taught me, for the freedom you gave me to explore questions that fascinated me, for your support and guidance, and for pushing me and showing what I can do. You are a wonderful teacher! Thank you to Drs. Bruce Reed and Andrew Doxey for serving as my committee members and the valuable advice throughout the grad school years. I also thank my internal-external examiner Dr. Jonathan Blay and my external examiner Dr. Caroline Schild-Poulter for their time and constructive analysis of this thesis.

Thank you to Dr. Alba Guarné and Dr. Ahmad Almawi for our collaboration and scientific discussion. I learnt a lot about structural biology from you!

Next, I must also thank my lab friends, who made my grad school years much more enjoyable. Mark Hamilton, you were always so kind in answering my endless questions when I started my PhD. You were always helpful. I will never forget all your help, from checking my first PCR primers design until making the 3D sleigh for the Holiday lab door decorating contest. I truly appreciate it! Swathi Jeedigunta, it was a privilege to work with you and I wish we can collaborate again in the future! Thank you for the countless hours you have spent listening to my rambling. You are an amazing friend! To my Rif1 collaborator, Matt Schmitz, it was (still is!) a pleasure working alongside with you and sharing the unexpected twist of Rif1! To the Mrc1 team, Celine Aziz, Zohaib Merali and Karen Chen, I enjoyed working with all of you and will cherish the friendships I have made. To Bradley D'souza, good luck in

continuing the Mrc1 project, and also for your master. To all the undergraduate students who have been a part of our lab (not in a particular order): Polina Myrox, Alana Desouza, Danny Liu, Allison Guitor, Kevin Murray, Denez Bokhari, Kathleen Zhang, Robert Dziamarga, Maryam Najib, Michael Siciak and Vincent Halim, it was great working with you! I wish you all the very best in your future endeavours!

I would like to extend a special thank you to Dr. Hawa Gyamfi, you set a solid example of being a mother and also a PhD student at the same time. Your positive vibe is contagious!

I also want to thank people, from faculty to students, at the University of Waterloo. To Dr. Moira Glerum, Dr. Raffaele Camasta and Alicia Dubinski, thank you for your valuable input and conversation (and sometimes chemicals) during my project. To Dr. Dragana Miskovic, thank you for encouraging me to TA BIOL 331 back in 2015. I truly enjoyed every conversation that I had with you. To April Wettig and Katelyn Fehrenbach, thank you for your help. To Drs. Matt Scott and Brian Ingalls, thank you for letting me use the Amnis FACS machine.

I acknowledge the generous financial support from my sponsor, Lembaga Dana Pengelola Pendidikan, from the Republic of Indonesia.

Finally, I would like to thank my parents, in-laws and family for their unconditional love, prayers, and support. To my husband and best friend, Alfan, I cannot thank you enough for your endless love and incredible support and sacrifices. You always make sure you take care of everything so I can focus on my research. To the best daughter a mother could ever want and my biggest cheerleader, Olivia, I am blessed to have you in my life! I love you!

Dedication

I dedicate this thesis to my late father who passed away from cancer.

He was my biggest source of inspiration.

Table of Contents

List of Figures

List of Tables

List of Abbreviations

ACS:	ARS consensus sequence
APC-C:	Anaphase promoting complex-cyclosome
ARS:	Autonomously replicating sequence
BRCT:	BRCA1 carboxyl terminus
BrdU:	5-bromo-2'-deoxyuridine
CDK:	Cyclin dependent kinase
ChIP:	Chromatin immunoprecipitation
CldU:	5-chloro-2'-deoxyuridine
CMG:	Cdc45, Mcm2-7, GINS
Co-IP:	Co-immunoprecipitation
DDK:	Dbf4 dependent kinase
DNA:	Deoxyribonucleic acid
dNTP:	deoxynucleotide phosphate
DSB:	Double strand break
DTT:	Dithiothreitol
EDTA:	Ethylenediaminetetraacetic acid
FHA:	Forkhead homology associated
FACS:	Fluorescence activated cell sorting
GINS:	Go-Ichi-Ni-San
HA:	Hemagglutinin
HR:	Homologous recombination
HU:	Hydroxyurea
IdU:	5-iodo-2'-deoxyuridine
IPTG:	Isopropyl β-D-1-thiogalactopyranoside
Kb:	Kilobases
kD:	Kilodalton
MCM:	Minichromosome maintenance
MMS:	Methyl methanesulfonate
MRN	Mre11-Rad50-Nbs1 (MRX in yeast)
MRX	Mre11-Rad50-Xrs2 (MRN in higher eukaryotes)
MYC:	Myelocytamatosis
NHEJ:	Non-homologous end-joining
NMR:	Nuclear Magnetic Resonance
ONPG:	2-Nitrophenyl-β-D-galactopyranoside
ORC:	Origin recognition complex
PCR:	Polymerase chain reaction
PMSF:	Phenylmethylsulphonyl fluoride
Pre-IC:	Pre-initiation complex

Pre-LC:	Pre-loading complex
Pre-RC:	Pre-replicative complex
RNR:	Ribonucleotide reductase
RPA:	Replication protein A
SC:	Synthetic complete
SDS:	Sodium dodecyl sulfate
UV:	Ultraviolet
WCE:	Whole cell extract
YPD:	Yeast extract, peptone, dextrose

List of Protein Names

53BP1:	p53-binding protein 1
ATM:	Ataxia telangiectasia mutated
ATR:	ATM and Rad3-related
Bax:	Bcl-2-associated X
BLM:	Bloom syndrome protein
BRCA1/2:	BReast CAncer 1/2
Cdc:	Cell division cycle
Ctf19:	Chromosome transmission fidelity 19
Dbf4:	Dumbbell former 4
Dna2:	DNA synthetic defective 1
Dnl4:	DNA ligase 4
Dpb11:	DNA polymerase B (11)
Exo1:	Exonuclease 1
Fkh1/2:	ForK head Homolog 1/2
Lif1:	Ligase interacting factor 1
Mcm:	Minichromosome maintenance
Mec1:	Mitosis entry checkpoint 1
Mrc1:	Mediator of the replication checkpoint
Mre11:	Meiotic Recombination 11
Nej1:	Nonhomologous end-joining defective 1
PARP-1:	Poly (ADP-ribose) polymerase 1
PCNA:	Proliferating cell nuclear antigen
Rad53:	RADiation sensitive 53
Rap1	Repressor/activator protein 1
Rif1:	Rap1-interacting factor 1
Sae2:	Sporulation in the Absence of Spo11
Sgs1:	Slow growth suppressor 1
Tel1:	TELomere maintenance 1
Yku70/80:	Yeast Ku protein 70/80
WRN:	Werner syndrome protein

Chapter 1

Literature Review and Project Goals

1.1 Budding yeast

1.1.1 Budding yeast as a research model

Cells are marvellous entities. Many fundamental discoveries of cell biology have been made, and translated into medical science applications. However, cells are still a big puzzle; there is so much that we do not know, and the curiosity about them unites scientists to unlock their mysteries.

The cell was first discovered by Robert Hooke in 1665 when he observed a honeycomb structure of the cork cell wall. He then drew and published it in his book *Micrographia.* The honeycomb structure also reminded him of a chamber, which he then called a cell. Almost a decade later, in 1674, Antonie van Leeuwenhoek observed protozoa and bacteria under a microscope for the first time. These findings not only shaped the initial theory of cell biology but gave insights to other scientists for the use of microscopes that led to later discoveries in biology (reviewed in Gest, 2004; Lawson, 2016).

Since their discovery, scientists have been formulating theories and performing research on how cells work, how they communicate with each other to make up an organism, and what happens if they become dysfunctional. Model organisms have been the powerhouse to address these biological questions. The budding yeast, *Saccharomyces cerevisiae*, serves as an excellent research model. This organism is also popular as the baker's yeast and brewer's yeast. It got these names due to its ability to break down sugar and convert it into ethanol, a feature that has been appreciated greatly in human civilization from ancient times.

Yeast research was pioneered by Øjvind Winge, who introduced the concept of yeast mating type in the 1940s (reviewed in Szybalski, 2001), and Carl Lindegreen, who published a book "The Yeast Cell: Its Genetics and Cytology" in 1949 (Pomper, 1950). A couple of decades later, the yeast researchers adopted and domesticated a yeast strain s288c for laboratory use. They selected the cells to be a non-clumpy suspension in liquid culture that can grow in medium with minimum supplements (sugar, biotin, a nitrogen source, and various salts and trace elements) (Mortimer & Johnston, 1986). This strain has been utilized until now, but it has also given rise to several other strains that are widely used in yeast research (reviewed in Louis, 2016). Yeast is a single-celled eukaryote that belongs to the Ascomycete (fungi that can generate spores inside asci) division. These cells can be grown easily in a laboratory setting with relatively inexpensive maintenance. The "*wild type"* laboratory strain has a doubling time of approximately 90 minutes in YPD media (1% yeast extract, 2% peptone, and 2% dextrose/glucose) at a temperature of 30°C. The daughter cell grows by pinching off from its mother cell. Thus it is called budding yeast (Burgess et al., 2017; Duina et al., 2014). Its relative, fission yeast (*Schizosaccharomyces pombe*) has also gained popularity as a eukaryotic research model.

1.1.2 Budding yeast genetics

Besides being the first domesticated yeast lab strain, s288c is also the first eukaryotic organism whose whole genome was sequenced (Goffeau et al., 1996) and this was catalogued comprehensively in the *Saccharomyces* Genome Database (SGD). The budding yeast genome consists of 16 chromosomes that with a total size of 12,068 kilobases (Goffeau et al., 1996) that designate 5885 open reading frames (ORFs). When this sequencing project came to an

end, scientists stepped forward to understand gene function through the *Saccharomyces* Genome Deletion Project (reviewed in Giaever & Nislow, 2014). This loss-of-function based approach was facilitated by PCR-based gene deletion (Baudin et al., 1993). Budding yeast is also the first eukaryote that was transformed by plasmid for research purposes (Hinnen et al., 1978). At the gene level, budding yeast shares a high degree of gene function conservation with humans, with 47% of its 414 essential genes being replaceable with their human orthologs (Kachroo et al., 2015).

Yeasts facilitate not only cell biology research, but also molecular biology and genetics experiments. The ease of its genetic manipulation is most likely the basis of why budding yeast has been a preferred model organism. Thanks to its high rate of homologous recombination (Baudin et al., 1993; Manivasakam et al., 1995), precise modifications can be integrated efficiently into its genome. A promoter modification to modify gene expression, gene deletion and epitope tagging can be done in a one-step gene manipulation method (Longtine et al., 1998). Seamless gene modification that does not leave any scar or foreign DNA sequence in the genome can be done with several techniques, including the classic methods pop-in/pop-out (Guthrie & Fink, 2004) and *delitto perfetto* (Storici et al., 2001). Additionally, the yeast research community has also been enjoying the effectiveness of CRISPR/Cas9 which provides a highly efficient new method to mutate essential genes (Akhmetov et al., 2018). Therefore, this microorganism has earned a good reputation, “the APOYG” (the awesome power of yeast genetics).

Budding yeast can live stably as a haploid or diploid organism. The haploid state is excellent for studying recessive mutations, and their phenotypes are generally easy to observe. Since a loss-of-function mutation of an essential gene is lethal for haploid yeast, this organism

accommodates conditional mutations that disrupt but do not eliminate the gene function completely. For example, this condition can be achieved by changing the temperature for thermo- (ts) and cold-sensitive (cs) mutant strains (Hartwell et al., 1974).

In addition to vegetative reproduction by budding, *S. cerevisiae* also produce offspring by sexual mating. Haploid budding yeast has a mating-type, either "a" or "α". The *MAT* locus on chromosome III determines the mating type by expressing either the *MAT*a or *MAT*α allele. Budding yeasts that are capable of switching their sex type (homothallic) have their MAT locus flanked by both *Hidden MAT Left* (HMLα) and *Hidden MAT Right* (HMRa), the precursors of *MATα* and *MAT*a respectively, and express HO endonuclease that produces a double-stranded DNA break at the *MAT* locus. This leads to recombination and gene conversion to either *MAT*α or *MAT*a. For haploid budding yeast, which requires a partner with the opposite mating type (heterothallic) to mate, the mating between a and α results in diploid yeast. When budding yeast cells sense that cells with a different mating type are around, they initiate mating by producing pheromone (a-factor for a cells and α-factor for α cells) and both change their cell morphology from spherical into a pear-shape cell (This look is called "shmoo" due its resemblance to the fictional Al Capp 1948 Li'l Abner character) to form the mating projection. From the cell cycle perspective, they also arrest themselves in G1 phase to maintain the haploid number of chromosomes before mating. Once formed, diploid cells continue onto vegetative reproduction to generate daughter cells. Budding yeast in its diploid state is utilized to study meiosis and recombination. This requires forcing diploid cells back into a haploid state through sporulation. Under nutrient starvation conditions, diploid cells undergo sporulation to generate four progeny haploid cells (tetrad) in an ascus (a sac-like cell). The tetrad can be separated into four individual spores by ascus digestion and manual

dissection using a micromanipulator. The spores are then grown in the appropriate media for subsequent investigation (Bardwell, 2005; Ni et al., 2011; Steensels et al., 2014).

Based on the characteristics mentioned above, yeast cells have proven themselves to be a fantastic eukaryotic research model. For example, yeast has accelerated the understanding of biology by facilitating gene discovery and the investigation of gene function. Numerous Nobel Prizes have been awarded for fundamental yeast discoveries. Leland Hartwell who worked with *S. cerevisiae,* Paul Nurse with *S. pombe* and Timothy Hunt with sea urchin eggs shared a Nobel Prize in 2001 for their discoveries of the regulators of the cell cycle. This was then followed by several other Nobel Prizes for yeast research, including those for Jack Szostak with *S. cerevisiae,* Elizabeth Blackburn and Carol Greider who worked with *Tetrahymena thermophila* in 2009 for their discovery of telomere function in protecting the chromosome ends and telomerase that extends telomere length, and most recently, Yoshinori Ohsumi for his discoveries of mechanisms for autophagy in *S. cerevisiae* in 2016 (reviewed in Hohmann, 2016). So far, yeast research does not seem to be slowing down, and it will be exciting to see what more it uncovers in the future.

1.2 Overview of the cell cycle

Organisms proliferate and grow by increasing their cell numbers. For budding yeast, cell proliferation accommodates asexual reproduction. To accomplish this, a parental cell divides to make two new daughter cells through the cell cycle. This consists of two main events: interphase, where a cell grows and duplicates its genome, and M phase, where the replicated chromosomes separate, the nucleus splits and a cell divides to give rise to two identical daughter cells. Interphase facilitates cellular growth in G1 (gap 1) and G2 (gap 2) phases and

replicates the cell's DNA content in S (synthesis) phase in between. The duplicated chromosomes are connected as sister chromatids during interphase, which are then separated after the break down of nuclear envelope during mitosis in metazoan. In budding yeast, nuclear envelope remains intact but expands to accommodate the chromosome segregation; hence it is called as closed mitosis (Arnone et al., 2013; De Magistris & Antonin, 2018; Souza & Osmani, 2007). The chromosomes are moved to opposite poles of the cell during mitosis, followed by cell division (cytokinesis) (reviewed in Alberts et al., 2002). Cytokinesis in budding yeast is asymmetrical, where the initial size of the daughter cell (bud) is much smaller than the mother. The process takes place at the narrow neck (bud-neck) between the mother and the bud. The budding emergence leaves a chitin-rich ring that remains on the mother cell wall, termed the bud scar, which determines the reproductive age of budding yeast and can be stained with Calcofluor (Pringle, 1991). After cytokinesis, the duplicated cell organelles are distributed equally between the two cells. An overview of the cell cycle is presented below, with the focus on S phase in budding yeast (Figure 1.1). However, the processes and the factors involved in it are mostly conserved among eukaryotes.

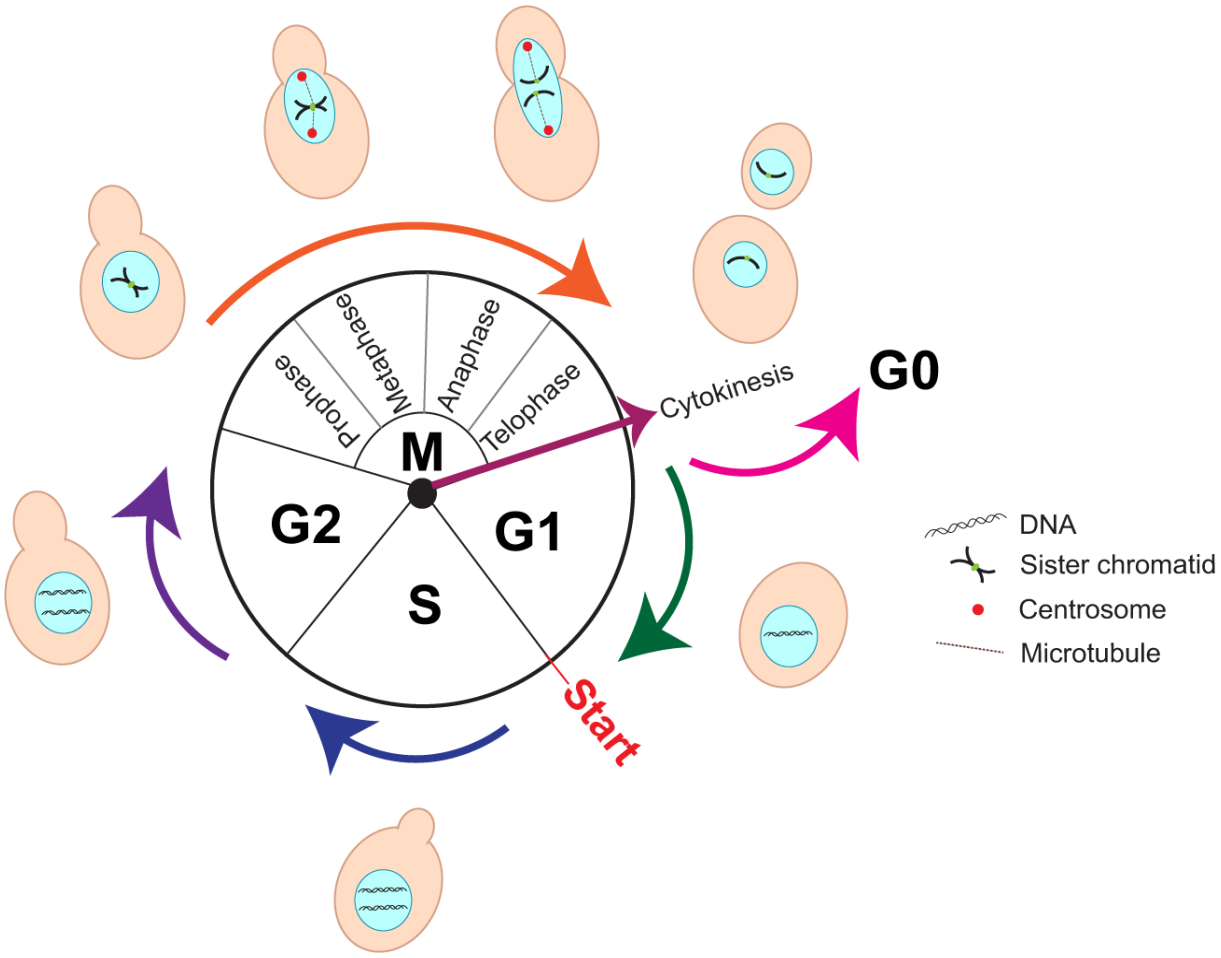

Figure 1.1. The budding yeast cell cycle. The stages of the yeast cell cycle including the formation of the bud/daughter cells: the first growth phase (G1), the DNA synthesis phase (S), the second growth phase (G2), mitosis (M). The cells that are not dividing stay in the quiescent phase (G0). START represents the checkpoint between G1/S phase transition. In budding yeast, the bud emerges at the onset of S phase and eventually pinches off from the mother cell during cell division.

1.3 DNA Replication

During S phase, DNA is duplicated in a semi-conservative way in which each parental strand serves as a template for nascent strand synthesis. Two kinases govern this stage, cyclin-dependent kinase (CDK) and Dbf4-dependent kinase (DDK), with their regulatory subunits, S phase cyclins (Clb5 and-6), and Dbf4, respectively. DNA duplication starts when the replication machinery finds eligible positions on the chromosome and unwinds them. The

machinery then elongates the newly synthesized DNA until every single base of DNA is replicated. Finally, DNA synthesis is terminated by removing the machinery from the chromosomes. The accuracy of DNA replication is robustly maintained to preserve the correct genetic information passed on to the newly formed cells.

1.3.1 DNA replication initiation

DNA replication is facilitated by the assembly of replication factors onto specific locations in the genome of budding yeast, termed origins of DNA replication. The loading of these factors takes place in late M and G1 phases and marks all the eligible origins that may be activated in S phase, this process is therefore called origin licensing. In budding yeast, origins are also called Autonomously Replicating Sequences (ARSs) due to their ability to drive the replication of episomal plasmids (Stinchcomb et al., 1979). The length of an ARS is generally 100-200 bp and contains 11 bp of T-rich ARS consensus sequence (ACS) (domain A) and an adjacent domain B both of which are essential for loading the replication factors (Theis & Newlon, 1997). The ACS element is recognized and bound by the initiator of the loading process, a six subunit origin recognition complex (ORC; Orc1-6), in an ATP-dependent manner (Bell & Stillman, 1992). ORC then recruits another loading factor, Cdc6, which also requires the presence of ATP (Speck et al., 2005). Orc1-5, but not Orc6, and Cdc6 belong to the AAA (ATPases associated with diverse cellular activities) ATPase family, in which the ATPase activity stabilizes the binding of ORC and Cdc6 (Speck & Stillman, 2007). ORC-Cdc6 then recruits the main motor of the replicative helicase, Mcm2-7, in complex with Cdt1. The Mcm3 subunit mediates Mcm-Cdt1 loading via its C-terminus and Cdt1 stabilizes this association (Frigola et al., 2013). Since DNA unwinding requires two helicase hexamers that move

bidirectionally, the first helicase loading is then followed by a second one in the opposite orientation. Single-molecule studies performed by Ticau et al. (2015) proposed that each hexamer is loaded individually by a different mechanism to achieve this particular configuration. The first hexamer is loaded by the ORC-hexamer interaction, whereas the second is facilitated by its interaction with the first hexamer (Ticau et al., 2015). The final result of this loading is double Mcm2-7 hexamers facing each other in an N-terminal head to head configuration to complete the pre-replicative complex (pre-RC) (Figure 1.2). Pre-RCs are then bound by the Sld3-Sld7-Cdc45 complex in a DDK-dependent manner (Kamimura et al., 2001; Tanaka et al., 2011; Yabuuchi et al., 2006). Cdc45 is essential in activating the helicase (Owens et al., 1997; Rios-Morales et al., 2019; Zou et al., 1997) and translocates along the DNA with the helicase. Sld3 loads Cdc45 onto origins, while Sld7 weakens the binding between Sld3 and Cdc45 to help Sld3 dissociate from Cdc45 prior to elongation (Tanaka et al., 2011).

Licensed origins are activated in S phase through a series of phosphorylation events performed by DDK and CDK (Figure 1.2). The resulting event is termed origin firing. At the onset of S phase, there is a spike of expression of the regulatory subunits of the kinases, Dbf4 (Jackson et al., 1993; Nougarède et al., 2000; Oshiro et al., 1999; Pasero et al., 1999) and S-phase cyclins, Clb5 and Clb6 (Schwob & Nasmyth, 1993). DDK phosphorylates Mcm4 (Randell et al., 2010; Sheu & Stillman, 2006) on its N-terminus relieving its inhibitory effect on helicase activity (Sheu & Stillman, 2010). CDK phosphorylates Sld3 and Sld2 thereby promoting their interaction with the scaffold protein Dpb11 (Muramatsu et al., 2010; Tanaka et al., 2007; Zegerman & Diffley, 2007), followed by the formation of a pre-Loading complex (pre-LC) between Sld2, Dpb11, GINS (go-ichi-ni-san), and DNA polymerase ε (Muramatsu et al., 2010).

The result of phosphorylation by DDK and CDK is an active helicase in the form of Cdc45-Mcm2-7-GINS (CMG), that moves along the DNA template bi-directionally, associated with DNA polymerase ε, ensuring that DNA unwinding activity by the helicase is always followed by DNA synthesis.

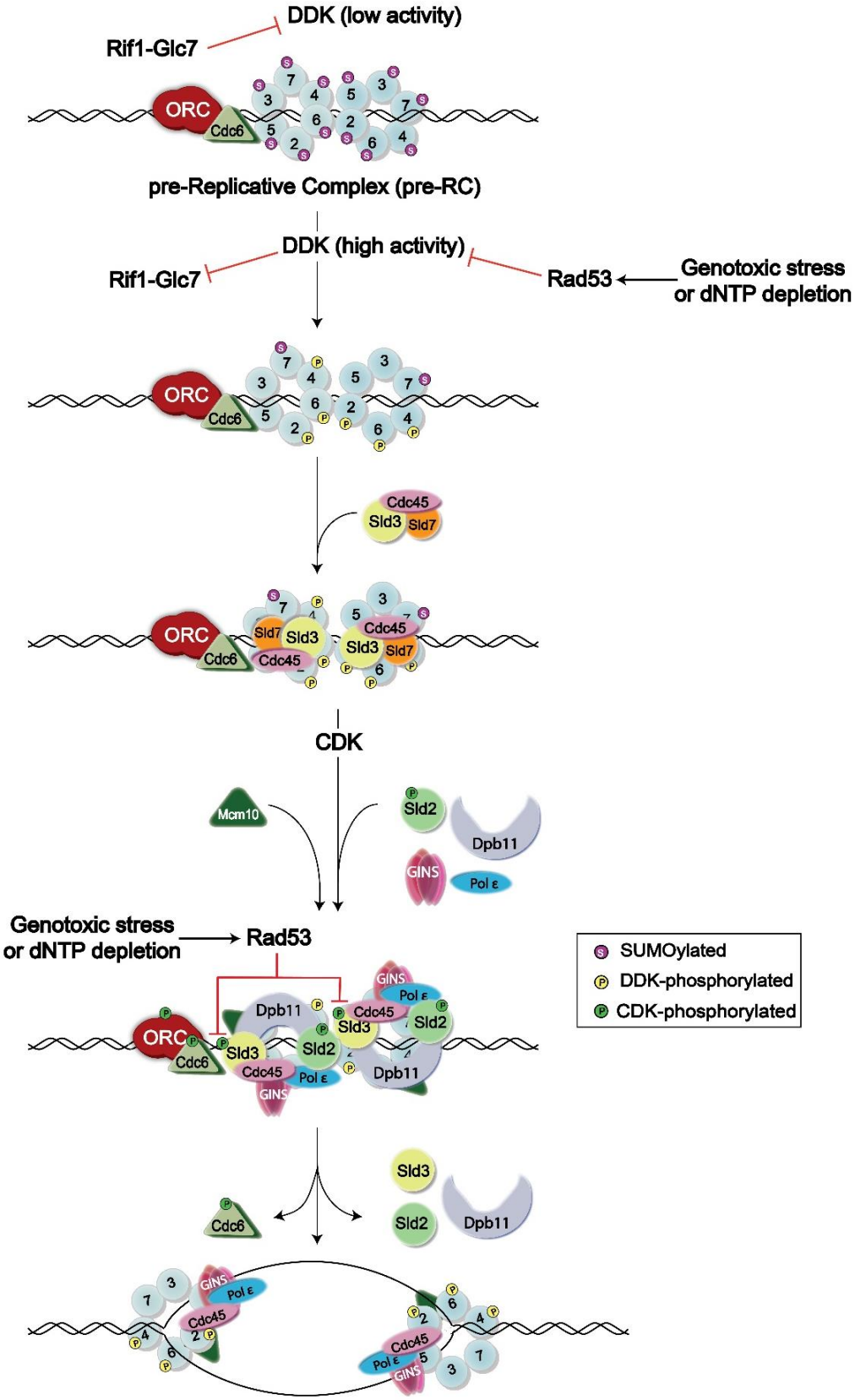
DDK (low activity)
Rif1-Glc7
ORC
Cdc6
pre-Replicative Complex (pre-RC)
DDK (high activity)
Rif1-Glc7
Rad53
Genotoxic stress
or dNTP depletion
Cdc45
Sld3
Sld7
CDK
Mcm10
Sld2
Dpb11
GINS
Pol ε
Genotoxic stress
or dNTP depletion
Rad53
SUMOylated
DDK-phosphorylated
CDK-phosphorylated

Figure 1.2. Model of DNA replication initiation. DNA replication is initiated by the loading of pre-Replicative complex (pre-RC), which also licenses the eligible origin of replication in G1 phase (origin licensing). This loading is then followed by origin activation (origin firing) by a series of phosphorylations events by Dbf4-dependent kinase (DDK) and S-phase Cyclin-dependent Kinase (CDK). DDK precocious phosphorylation to Mcm2-7 subunits is prevented by Rif1-Protein Phosphatase 1 (Glc7 in budding yeast) complex in G1 phase. Under DNA replication stress or depletion of dNTP, Rad53 checkpoint kinase inhibits subsequent origin firing by phosphorylating Dbf4 and Sld3 to target direct DDK and indirect CDK deactivation, respectively (reproduced with permission from Larasati & Duncker, 2016).

Since phosphorylation of CMG helicase components is integral for origin firing, the timing of phosphorylation is robustly regulated. DDK activity coincides with the rise of Dbf4 expression level in late G1/early S phase (Jackson et al., 1993; Nougarède et al., 2000; Oshiro et al., 1999; Pasero et al., 1999). Thus, DDK activity is low through most of G1 phase and peaks during S phase. However, the basal DDK activity in early G1 phase may phosphorylate Mcm2-7 subunits prematurely. Cells counteract this by recruiting Rif1 (Rap1-interacting factor 1) to origins, which in turn targets Protein Phosphatase-1 (PP1; Glc7 in budding yeast) to reverse precocious Mcm2-7 phosphorylation. Indeed, cells with deletion of *RIF1* or expressing a Rif1 mutant that is defective in Glc7 binding exhibit Mcm4 hyperphosphorylation in G1 phase (Davé et al., 2014; Hiraga et al., 2014; Mattarocci et al., 2014). Interestingly, Rif1, which acts in opposition to DDK in G1 phase, is also a DDK phosphorylation substrate in S phase. DDK phosphorylates Rif1 at sites adjacent to its Glc7 binding region, consequently breaking the association between Rif1 and Glc7. Rif1 then no longer promotes Mcm2-7 dephosphorylation. DDK phosphorylation of Rif1 is mediated by an interaction between Dbf4 and Rif1 (Hiraga et al., 2014) (Figure 1.3).

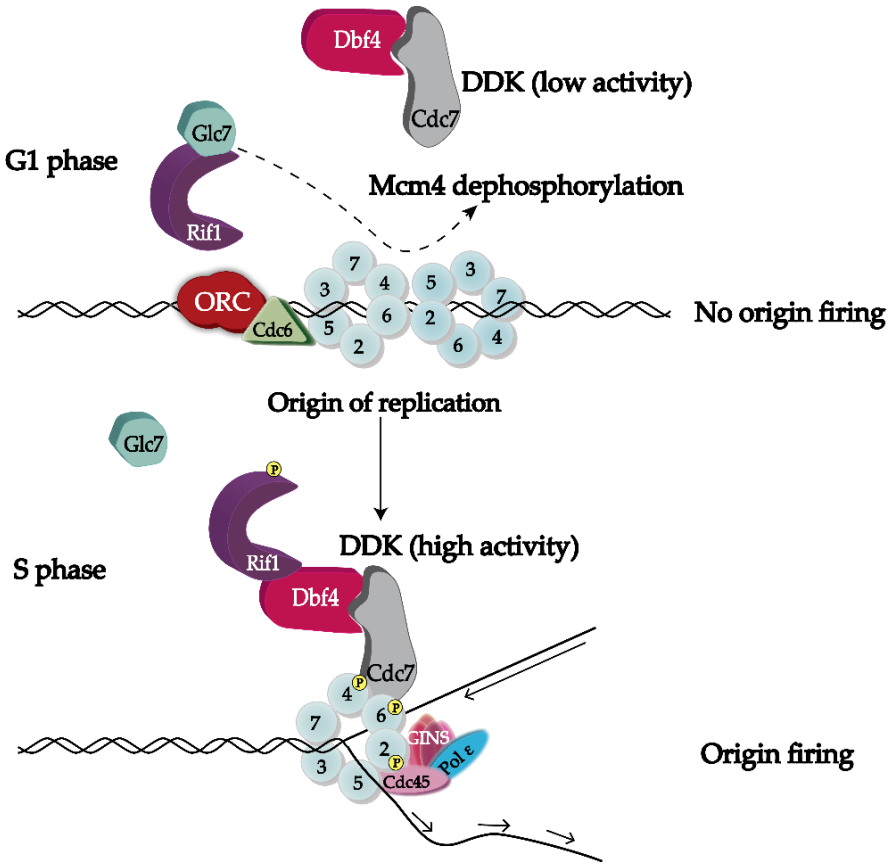

Figure 1.3. The proposed model of Rif1 as a replication timing regulator. In G1 phase when DDK activity is low, Rif1 recruits Glc7 to dephosphorylate Mcm4 and prevent premature helicase activation. In S phase when DDK activity is high, DDK deactivates Rif1-Glc7 activity by binding and phosphorylating Rif1 to disrupt the Rif1-Glc7 association (adapted from Hiraga et al., 2014).

On top of Rif1-Glc7 dephosphorylation activity, cells have another safeguard mechanism to keep Mcm2-7 subunits inactive prior to origin firing. After MCM loading to form the pre-RC, Mcm2-6 subunits undergo SUMOylation, peaking in G1 phase, and diminishing in S phase. This MCM SUMOylation stabilizes the association between MCM subunits and Glc7, and cells expressing a mutant form of Mcm6 that maintain stable SUMOylation throughout the cell cycle are defective in initiating DNA replication. Interestingly, the declining level of MCM SUMOylation coincides with the rise of MCM phosphorylation, consistent with SUMOylation and phosphorylation of MCM proteins being incompatible during S phase (Wei & Zhao, 2016).

1.3.1.1 Origin Firing Timing

Eukaryotes have a larger genome size compared to prokaryotes. To accomplish genome duplication efficiently, eukaryotes have many replication origins distributed throughout the genome. Therefore, the length of S phase is not proportional to genome size. In G1 phase, all the potential origins are licensed by pre-RC formation. However, only a subset of them will be activated each S phase in a given cell. Among those origins that are activated, each must fire no more than once during S phase to avoid overreplication of the genome. Moreover, these origins do not fire simultaneously during S phase, but are rather activated sequentially. This pattern raises the question of whether origin replication timing follows a predetermined or stochastic rule. The favoured notion is that mammalian cells mainly activate origins randomly (Löb et al., 2016; White et al., 2004; Demczuk et al., 2012). However, they set up replication timing immediately after pre-RC formation in G1 phase, termed as timing decision point (TDP) (Dimitrova & Gilbert, 1999; Rhind & Gilbert, 2013). TDP is defined in a spatial and temporal manner which depends on several elements including the access of limiting firing factors (Collart et al., 2013; Mantiero et al., 2011; Tanaka et al., 2011; Wong et al., 2011), histone modifications (Bar-Ziv et al., 2016; Unnikrishnan et al., 2010), local chromatin status (Hoggard et al., 2018; Méchali et al., 2013), and transcription sites (MacAlpine et al., 2004). Furthermore, TDP is not a fixed pattern. In multicellular eukaryotes, TDP can change based on cellular cues during cell development and differentiation (Dixon et al., 2015; Nordman & Orr-Weaver, 2012; Pope et al., 2010).

In contrast to mammals, budding yeast replication initiation sites are well-defined (Newlon & Theis, 1993). Among budding yeast active origins, some of them fire at the beginning of S phase and others fire later (Figure 1.4) (Fangman et al., 1983; Raghuraman et

al., 2001). In general, early-firing origins are the ones that have enriched association with limiting firing factors at the onset of S phase, such as Dbf4, Sld3, Sld2, Dpb11, and Cdc45 (Köhler et al., 2016; Mantiero et al., 2011; Osborn & Elledge, 2003; Tanaka et al., 2011). Several early-firing origin clusters also have enhanced Mrc1 association in fission yeast. In budding yeast, Mrc1 is shown to associate with early origin ARS 305 (discussed further below) (Hayano et al., 2011; Matsumoto et al., 2017; Osborn & Elledge, 2003). In contrast, late origins associate with proteins that prevent firing in early S phase, such as Rif1 (Hafner et al., 2018; Hayano et al., 2012; Peace et al., 2014; Yamazaki et al., 2012) and Rpd3 deacetylase (Aparicio et al., 2004). In mid/late S phase, late-firing origins eventually recruit the limiting factors to initiate DNA replication. Since some limiting firing factors are also part of the replisome, for example Cdc45, they are thought to be recycled from the completed forks that emanated from early origins to new forks from late origins (Aparicio, 2013; Tanaka et al., 2011).

Origins that are licensed in G1 phase but are inactive in S phase serve as 'back-up' dormant origins (Figure 1.4). During elongation, the active forks may encounter DNA damage or replicative stress that stall their progression. In case the forks stall irreversibly or collapse (disassembly of replisome components) and cannot resume DNA replication when the problem is fixed, DNA replication initiation from dormant origins can compensate (Alver et al., 2014; McIntosh & Blow, 2012). Similar to late origins, dormant origins in eukaryotes also have enriched Rif1 association which helps to ensure they are not activated prematurely (Hayano et al., 2012; Moiseeva et al., 2019; Peace et al., 2014).

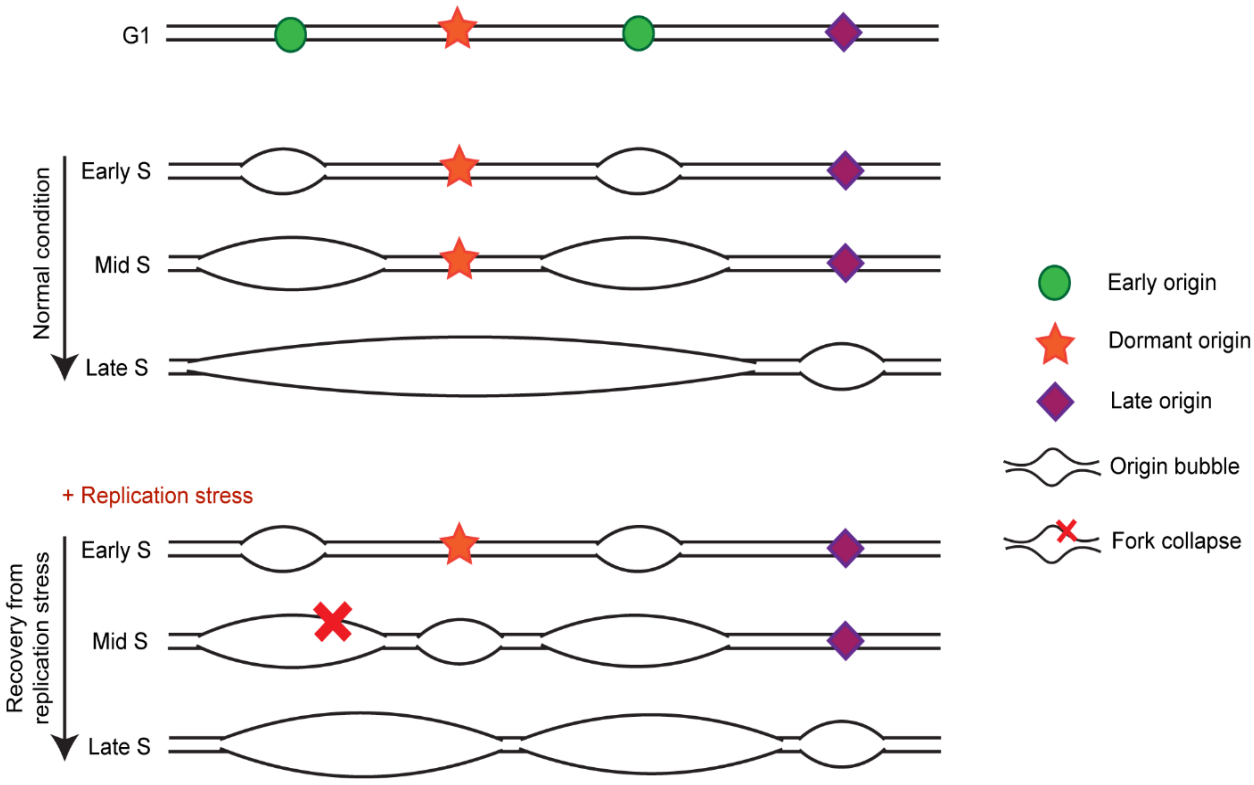

Figure 1.4. Replication firing timing in eukaryotes. In general, the origins of replication can be divided into three groups based on their firing timing during S phase: early, late, and dormant. Origin bubble represents when the origin DNA template is unwound by the helicase. It gets bigger as the helicase progresses during S phase (replication forks). Under normal conditions when dormant origin firing is not needed, they are passively replicated by forks emanating from neighbouring origins. When there is replication stress, forks that stall and then collapse are no longer able to resume DNA replication during recovery. This can be compensated for through DNA synthesis initiating from normally dormant origins.

1.3.2 DNA replication elongation

DNA is synthesized in a 5' to 3' orientation, meaning that the nascent DNA chains generated using Watson (top/left-hand) and Crick (bottom/right-hand) strands grow in opposite directions. More importantly, the elongation of both strands occurs differently, with one strand growing continuously (leading strand) and the other discontinuously (lagging strand). The products of lagging strand synthesis are called Okazaki fragments, named after one of the

Japanese scientists who discovered them in 1968 (Okazaki et al., 1968a, 1968b). Due to the complexity of DNA replication, the CMG helicase and DNA polymerase require accessory factors, which together make a multiproteins complex called the replisome (Figure 1.5).

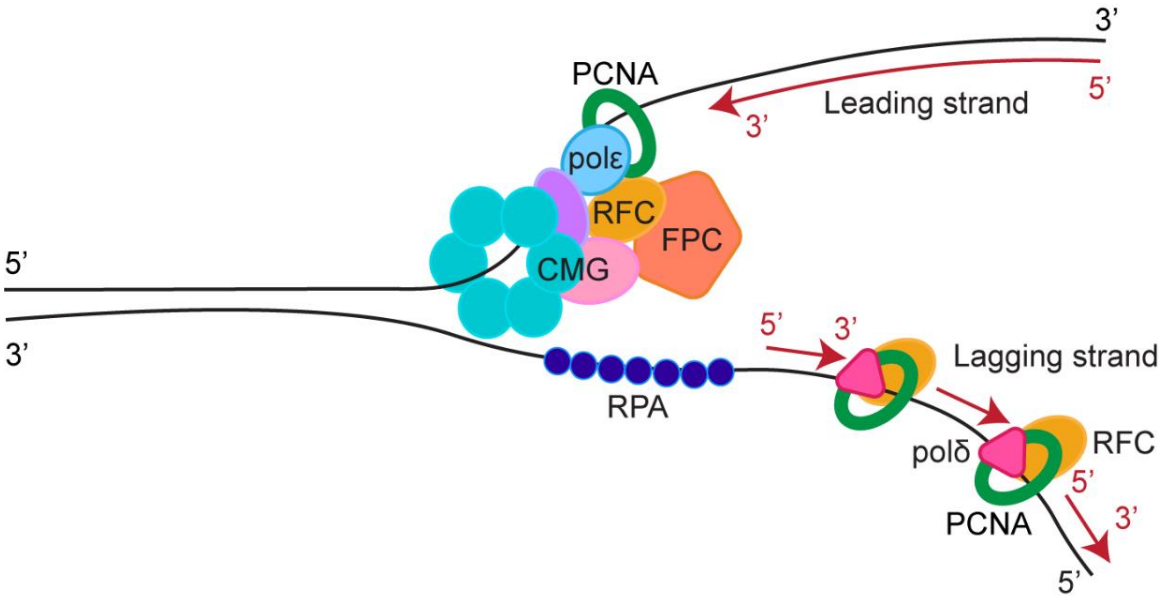

Figure 1.5. Model of the eukaryotic replication fork and the replisome. The CMG helicase unzips the double-stranded duplex into single-stranded DNA (ssDNA) templates. Replication Protein A (RPA) stabilizes and prevents ssDNA from re-annealing. Replication Factor C (RFC) and PCNA tether and promote the polymerase processivity. Nascent DNA is synthesized bi-directionally, with pol ε acting as the leading strand polymerase, and pol δ generating the Okazaki fragments of the lagging strand. Fork protection complex (FPC) maintains the stable association of the helicase and polymerase as a replisome. For simplicity, the RNA primer and the primase-pol α complex are not shown in this diagram.

Budding yeast has 3 DNA polymerases (pol α, pol ε, and pol δ). Their DNA synthesis task follows the unwinding activity of the CMG helicase that converts duplex DNA into single-stranded template. The ssDNA is kept separated by binding of Replication Protein A (RPA) to allow DNA duplication. However, the polymerase does not immediately generate nascent DNA from the template. DNA polymerase works by adding new nucleotides to a preexisting strand (primer). The primer consists of a short RNA fragment with 8-10 nucleotides in length synthesized by primase. Pol α extends the primer length by adding 10-15 nucleotides (reviewed

in Pellegrini, 2012). This polymerase is linked to the helicase by Ctf4 (Zhu et al., 2007). Pol α is then replaced by pol ε and pol δ, for the leading and lagging strands, respectively. The reason why pol α does not function as the main polymerase is that it has a high error rate (Kunkel, 2004) and a lack of proofreading activity (Pavlov et al., 2006). Pol ε is readily available replisome as it is loaded during DNA replication initiation. Its synthesis activity is stimulated by Proliferating Cell Nuclear Antigen (PCNA) sliding clamp, the recruitment of which to DNA requires the clamp loader Replication Factor C (RFC) (Georgescu et al., 2014; Langston et al., 2014). RFC also aids the recruitment of pol δ to the lagging strand and tethers it to PCNA. This sliding clamp also functions as a processivity factor for pol δ (Hedglin et al., 2016; Mondol et al., 2019; Schauer & O'Donnell, 2017).

Pol ε reads the template in a 3' to 5' direction and generates the leading strand in a 5' to 3' direction without any interruption. Pol δ also synthesizes the lagging strand in a 5' to 3' orientation, but it works discontinuously as it generates approximately 100-200 nucleotides per Okazaki fragment. Thus, in contrast with pol ε, pol δ requires multiple RNA primase-pol α-generated primers to replicate the whole template. Moreover, when pol δ elongates an Okazaki fragment, it will finally reach the 5' end of the RNA primer of the neighbouring Okazaki fragment. Pol δ, instead of stopping the DNA extension, continues to elongate the DNA until it displaces the RNA primer of the adjacent fragment, which creates a flap (Garg et al., 2004). This flap is removed during Okazaki fragment maturation by Rad27/Fen1 flap endonuclease (Tishkoff et al., 1997). Next, the short Okazaki fragments are joined into one complete DNA strand by DNA ligase I (Waga & Stillman, 1994).

1.3.2.1 The telomere replication problem

DNA polymerase cannot replicate the template without the presence of primers that provide 3' OH ends. Due to this, the ends of linear DNA chromosomes (telomeres) pose a DNA replication problem. After primer removal, the lagging strand duplicated from the very end of the 3' template will be shorter than its template during every successive round of DNA replication. A reverse transcriptase, telomerase, solves this problem by extending the length of the 3' telomere end so that the precise copy and length of the telomere sequence can be passed on to the newly synthesized DNA (reviewed in Maestroni et al., 2017).

However, the telomere replication problem does not stop just by extending the telomere length. The 3' end of telomeres consists of conserved G-rich repeats (TTAGGG)n in mammals or (TG)n in yeast that have the potential to form a secondary structure G-quadruplex (stacked guanine-tetrad conformation) (reviewed in Víglaský et al., 2010). Moreover, telomeres also recruit a telomere specific protein complex called the telosome (shelterin in mammals). This complex protects the telomere ends from being recognized as DNA double-strand breaks and prevents end-to-end fusion (dicentric chromosome). The G-rich repeats and the telomeric proteins pose a replication barrier during S phase since they may impede the progression of active forks (Makovets et al., 2004; Masuda-Sasa et al., 2008). The Pif1 and Rrm3 helicase family can relieve this threat by disrupting the G-quadruplex motif and clearing out the barriers ahead of the forks (Anand et al., 2012; Geronimo & Zakian, 2016; Maestroni et al., 2017; Paeschke et al., 2011).

The relationship between telomere length and its elongation by telomerase is tightly regulated. If the telomeric single-stranded end is too long, a checkpoint will be activated and halt cell cycle progression. Besides capping the telomere ends, the telosome also prevents

telomerase from accessing them (de Lange, 2018; de Lange, 2005). In budding yeast, the telosome consists of Rap1, Rif1, and Rif2 (Hardy et al., 1992). The loss of telomerase regulation has been associated with cancer as several types of cancer cells upregulate telomerase expression by mutating the human TERT gene that encodes telomerase (Jafri et al., 2016).

1.3.2.2 Natural barriers of DNA replication elongation

During elongation, the replisome faces natural impediments that can stall active forks from replicating the DNA template. When this happens, it is crucial to stabilize the fork components to stay together so that the forks can restart when the problem has been fixed. Failure to do this leads to the decoupling of the helicase and the polymerase that results in excessive unwinding or the disassembly of the fork components (fork collapse). A complex that stabilizes forks is called the fork protection complex (FPC), which is also an integral part of the replisome. FPC consists of four conserved proteins Tof1, Csm3, Mrc1, and Ctf4 (human Timeless, Tipin, Claspin, and And1) (Bando et al., 2009; Uzunova et al., 2014).

The progression of DNA replication poses a hurdle to itself as it creates a DNA topology problem. As the active forks grow, there is more conversion of dsDNA into relaxed ssDNA conformation. This puts torsional stress on the unreplicated region in front of the forks, which, in turn, stimulates the formation of positive supercoiling. The accumulation of this DNA overtwisting impedes fork progression. Topoisomerase II, in an ATP-dependent manner, relieves this formation by generating a transient DNA double-strand break (DSB) at the tangled DNA, allowing strand passing , and re-ligation of the DSB ends (Devbhandari et al., 2017; Mariezcurrena & Uhlmann, 2017; Wang, 1998). Topoisomerase II forms a reversible complex

with DSB ends so that the broken ends are not recognized as DNA damage (Furniss et al., 2013). Alternatively, the positive supercoils ahead of the fork can also be relieved by fork rotation at the replication branching point. This comes with a cost of nascent DNA intertwining behind the forks, which is termed precatenate (precursor of catenates) (Postow et al., 2001). Due to their position relative to the moving forks, precatenates may not interfere with fork progression. However, unresolved catenates during DNA replication termination generate a stable joining of sister chromatids that interrupts their segregation during mitosis. Fortunately, topoisomerase II can also remove precatenates from the replicated DNA (Bermejo et al., 2007; Schalbetter et al., 2015).

Furthermore, replication forks can face a topological conflict when they encounter transcription machinery. Transcription, similar to DNA replication, involves unwinding dsDNA to allow access to the template strand. RNA polymerase II can translocate along the DNA in two different orientations relative to the replication forks: the same orientation (co-directional) or opposite direction (head-on fashion). The head-on conflict is considered more detrimental. Similar to replication, transcription generates positive supercoils in front of RNA polymerase (Liu & Wang, 1987). As the replication and transcription machineries approach each other, the positive supercoil in between becomes more twisted and its removal requires topoisomerase activity. The head-on traffic increases the occurrence of R-loops (the hybrid of DNA template and nascent RNA product) behind RNA polymerase (Hamperl et al., 2017), which can be resolved by RNase-H. More importantly, the collision between replication and transcription can harm both machineries and lead to genome instability (Pomerantz & O'Donnell, 2010). Co-directional translocation can also be dangerous when the replication and transcription machineries do not move at the same speed.

DNA secondary structure itself can pose another topological challenge. With the help of Raymond Gosling and Rosalind Franklin's X-ray photograph "Photo 51" (Franklin & Gosling, 1953), James Watson and Francis Crick elucidated the conformation of DNA. It is a three-dimensional right-handed double helix (Watson & Crick, 1953). Aside from this canonical structure, DNA can adopt several other configurations such as Z-form (left-handed helix) (Wang et al., 1979), triplex (dsDNA hybrid with ssDNA) (Morgan & Wells, 1968), inverted repeat-induced cruciform (Lilley, 1980), and G-quadruplex (Gellert et al., 1962). These various structures can be resolved by a RecQ helicase family that has flexibility in recognizing a broad array of DNA substrates (Manthei et al., 2015). Mutation of the genes encoding these helicases has been associated with Bloom (Ellis et al., 1995) and Werner syndromes (Prince et al., 2001). Yeast has one known homolog of RecQ helicase, Sgs1, that is capable of resolving DNA secondary structures (Cejka & Kowalczykowski, 2010; Gangloff et al., 1994).

Among all these natural impediments, there are cases where the slowing down of the replication machinery is desirable. In eukaryotes, such a slowing zone is called a replication fork barrier (RFB). The highly transcribed ribosomal DNA (rDNA) locus located on chromosome XII of budding yeast is an excellent RFB example. This locus contains approximately 150 tandem repeats each comprised of 35S and 5S transcription units and two non-transcribed spacers. This repeat is followed immediately by an ARS, which creates the possibility of fork collapse if the replication machinery clashes with RNA polymerase. Thus, the replication fork must be temporarily paused to let RNA polymerase pass through the replisome. This pausing event is DNA sequence-independent and relies on a barrier protein called Fob1 that binds to the non-transcribed region. DNA replication at the Fob1-binding site

requires an additional helicase (Rrm3 or Pif1) to displace the barrier from DNA (Ivessa et al., 2000). Cells can also prevent collision of replication and transcription machineries by employing Rif1. This protein has been shown to control the replication of rDNA origins (Shyian et al., 2016). Besides the rDNA locus, Rif1 is also enriched at highly-transcribed loci during S phase (Hiraga et al., 2018).

1.3.3 DNA replication termination

In contrast to both DNA replication initiation and elongation that have been extensively studied, termination is less well understood. In prokaryotes, termination happens at a sequence-specific region called the Ter site (Hidaka et al., 1988; Hill et al., 1988). However, termination in eukaryotes seems to be sequence-independent, occurring when two emanating replisomes from neighbouring origins on the same template meet, which likely takes place in the midpoint between two origins, or at the end of telomeres. Converging replisomes result in their physical displacement from DNA. At the chromosome ends, the replication machinery seems to slide off since the DNA substrate is no longer available. Following this model, termination timing is predicted to agree with origin firing patterns, with replisomes from early origins terminating earlier than those from late origins (Graham et al., 2017; Hawkins et al., 2013; McGuffee et al., 2013).

Identical to DNA replication initiation, termination must not occur prematurely since the helicase loading will not take place again until the next round of G1 phase. However, when DNA replication has terminated, all replisomes must be removed to ensure that they do not unnecessarily unwind already replicated DNA. When two active forks meet, they create a head-to-head collision that leads to replisome disassembly. This dissociation is also aided by F-

box protein Dia2-dependent Mcm7 ubiquitination. Cdc48 segregase/protein remodeler then destabilizes CMG helicase from DNA binding, and consequently, its interaction with nascent DNA is terminated (Maric et al., 2014). Additionally, when two forks converge, they do not reduce the elongation speed (Dewar et al., 2015). This increases the torsional force on DNA in front of them. As the forks get closer to each other, the tension in front of the forks is transmitted to the region behind the forks, which generates catenates. Similar to topoisomerase II activity on precatenates during elongation, it also relieves the catenation when DNA synthesis terminates (Ziraldo et al., 2019).

1.3.4 DNA Damage and Replication Checkpoint

During elongation, the replisomes may encounter exogenous and endogenous obstacles that halt DNA replication. The source of the replication barriers can be external (for example, UV light or hydroxyurea-dependent dNTP pool depletion) or internal factors (for example, DNA topology problems or DNA-binding proteins). However, how cells respond to natural impediments may be different than with those caused by external factors. The natural barriers of replication are discussed above. This chapter focuses on the cell's response to external obstacles.

In the presence of DNA damage or replication stress, cells have a surveillance mechanism (checkpoint) to detect fork stalling and carry out the appropriate response depending on the kind of obstacle. This relies on signalling cascades and the checkpoint protein network. The main function of the checkpoint is to ensure that the cells do not proceed to the next phase of cell cycle before the problem is solved.

The checkpoint factors include the sensors that recognize damaged DNA and activate the regulators of the checkpoint pathway, transducers that mediate the signal cascade from the upstream to the downstream targets, and effectors that target and regulate the response the cells execute, which include cell cycle arrest, DNA repair, transcriptional up- or downregulation of specific genes, and apoptosis. In budding yeast, the set of sensor proteins includes Rad24, Ddc1, Rad17, and Mec3. Rad24 associates with Replication Factor C (RFC) subunits and acts as a chaperone-like clamp loader that binds to ssDNA or ss-dsDNA junctions. Rad17, Ddc1, and Mec3 (analogous to human Rad9/Rad1/Hus1) form a checkpoint clamp and accumulate at the DNA damage site through the Rad-RFC complex. RFC mediates the activation of the upstream regulator of the checkpoint response, Tel1 or Mec1 in budding yeast (Ataxia telangiectasia-mutated (ATM) or Ataxia-telangiectasia and Rad3-related (ATR) proteins in mammals, respectively) (Peng et al., 2019).

ATM/Tel1 responds predominantly to DNA-double strand breaks (DSBs; discussed further in the DNA repair section) while ATR/Mec1 recognizes ssDNA generated by various types of DNA damage and replication blockage. Single-stranded DNA is immediately coated by replication protein A (RPA) upon its formation (Zou & Elledge, 2003). ATR/Mec1 binds to ATR-interacting protein (ATRIP)/Ddc2. This complex then associates with RPA-bound ssDNA and co-localizes with the Rad17/Ddc1/Mec3 clamp, thereby promoting Mec1 phosphorylation of downstream targets (Majka et al., 2006) (Figure 1.6).

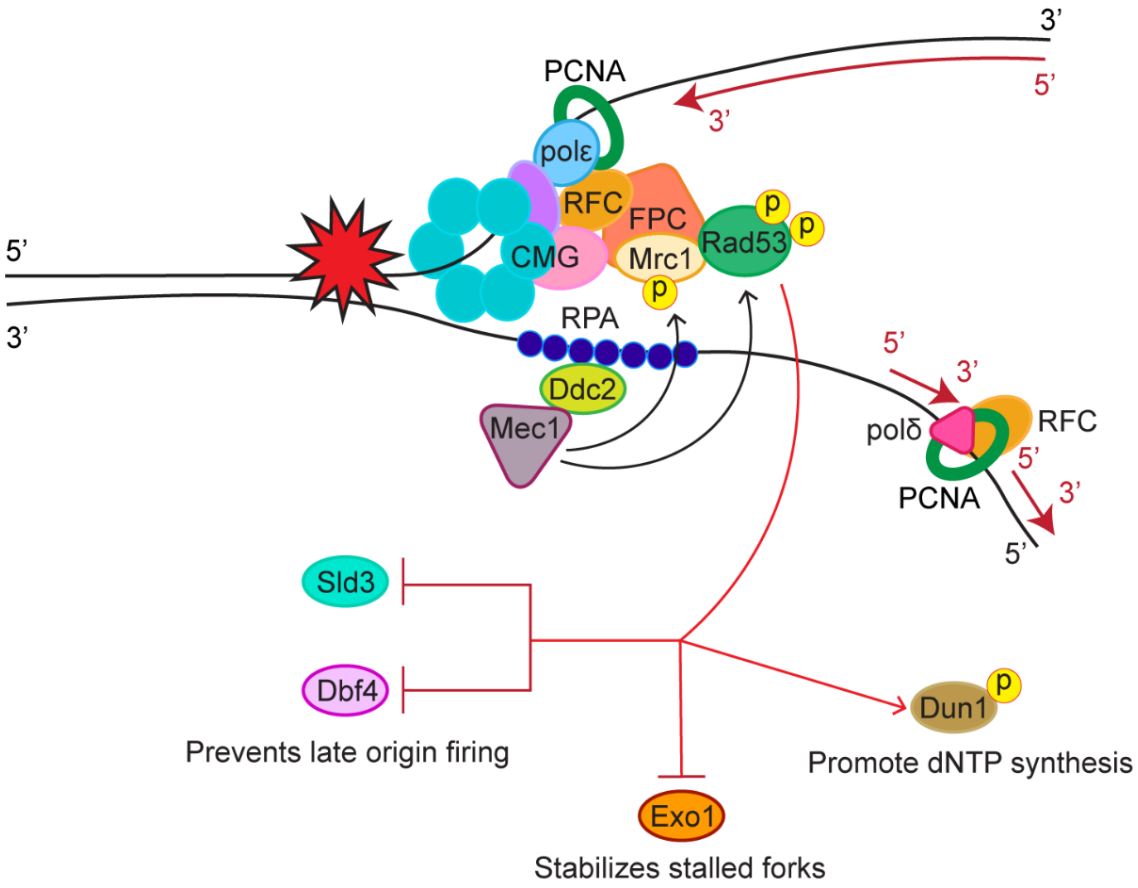

Figure 1.6. A schematic illustration of the Mec1-dependent replication checkpoint. When replication forks stall due to the presence of DNA lesions in front of them (red star), the single-stranded DNA (ssDNA) behind the forks causes the activation of the replication checkpoint. Replication Protein A (RPA) coats ssDNA and facilitates the recruitment of the Ddc2-Mec1 complex. Mec1 phosphorylates Mrc1, which in turn promotes the recruitment and activation of Rad53. Rad53 then executes the checkpoint response by phosphorylating its downstream targets.

A checkpoint mediator group transduces the signal cascade to the effector kinases, Chk1 and Rad53 (Chk2 in mammals). This group includes Mrc1 and Rad9 in budding yeast and Claspin, Mdc1, BRCA1 and 53BP1 in mammals. Mrc1 and Rad9 have a redundant role in transmitting the signal from Mec1, but Mec1 phosphorylates Mrc1 predominantly when the replication fork stalls during S phase (Osborn & Elledge, 2003), and Rad9 when DNA damage is detected throughout cell cycle (Pardo et al., 2017; Vialard et al., 1998). Mrc1/Rad9 then

scaffolds Rad53 and enables Rad53 phosphorylation by Mec1 (Chen & Zhou, 2009; Sweeney et al., 2005). Activated Rad53 executes checkpoint responses by promoting transient cell cycle arrest, preventing the progression of DNA replication, and protecting stalled forks (Figure 1.6).

1.3.4.1 Rad53 as a checkpoint effector in budding yeast

Genomic integrity needs to be maintained at every step of DNA replication. This includes when the forks encounter DNA damage and replication stress. Under these conditions Rad53 blocks the progression of DNA replication by stabilizing stalled forks (Gan et al., 2017), preventing late origin firing (Lopez-Mosqueda et al., 2010; Zegerman & Diffley, 2010), and boosting the production of dNTP (Zhao et al., 1998) (Figure 1.6).

Rad53 targets the kinase activity of both CDK and DDK to prevent late origin firing. To block the CDK pathway, Rad53 phosphorylates Sld3, which then impedes the loading of replication factors, Dpb11 and Cdc45 (Lopez-Mosqueda et al., 2010; Zegerman & Diffley, 2010). Rad53 does not target CDK directly since CDK is required for other functions during DNA replication, such as preventing DNA re-replication and controlling the DNA repair pathway choice (Huertas et al., 2008). In contrast, Rad53 targets DDK directly. Rad53 binds and phosphorylates the regulatory subunit of DDK, Dbf4, thus promoting DDK removal from chromatin (Duch et al., 2011; Duncker et al., 2002; Lopez-Mosqueda et al., 2010; Pasero et al., 1999; Zegerman & Diffley, 2010).

Stalled forks must be stabilized to allow resumption of DNA synthesis later when the checkpoint is no longer active. Rad53 plays a role in stabilizing stalled replisomes and, indeed, cells lacking functional Rad53 cannot restart forks (Tercero et al., 2003). A downstream target of this function seems to be the Exo1, a nuclease that can degrade DNA at the stall sites, which

consequently, destabilizes the forks. Cdc45, an integral replisome component, also mediates Rad53 recruitment to stalled forks (Can et al., 2019).

Rad53 also promotes fork restart by boosting the production of dNTP during stress recovery through phosphorylation of another checkpoint kinase, Dun1 (Chen et al., 2007; Zhou & Elledge, 1993). To produce dNTP, ribonucleotide reductase (RNR) catalyzes the reduction of nucleoside diphosphates (NDP). The active form of RNR requires the assembly of its subunits Rnr1, Rnr2, and Rnr4 in the cytoplasm (Yao et al., 2003). Another RNR subunit, Rnr3, is not required under normal conditions and its expression increases during replication stress conditions (Chabes et al., 2003; Elledge & Davis, 1990). Active Dun1 phosphorylates and promotes degradation of its downstream targets including Sml1, an allosteric inhibitor of Rnr1 (Zhao & Rothstein, 2002); Wtm1, a factor that tethers Rnr2 and Rnr4 to stay inside the nucleus (Lee et al., 2008b); Dif1, a nuclear importer for Rnr2 (Lee et al., 2008b); and Crt1, a transcription repressor for *RNR2, RNR3,* and *RNR4* (Huang et al., 1998).

1.3.5 DNA double strand break repair pathways

Chromosomal DSBs occur when the phosphate backbones of both strands of the DNA duplex break at the same time. DSBs can lead to genome rearrangements, such as deletions, insertions, and translocations. Thus, a DSB is considered the most lethal form of DNA lesion. Two distinct pathways mainly repair DSBs, classical non-homologous end joining (NHEJ) and homologous recombination (HR), the choice of which depends on the activity of CDK and the presence of a homologous template (Figure 1.7).

In mammals, the broken ends are rapidly recognized by Poly (ADP-ribose) polymerase 1 (PARP-1) (Haince et al., 2008). However, this function seems to be absent in yeasts as they

do not have any known PARP-1 homolog. Another factor that recognizes DSBs immediately is the complex of Mre1-Rad50-Xrs2 (yeast)/ Nbs1 (mammals) (MRX/N). At the initial repair stage, MRX plays a structural role by tethering the DNA ends together through a transient dimerization between two Mre11 and two Rad50 proteins in an ATP-dependent manner (de Jager et al., 2001; Deshpande et al., 2014; Lammens et al., 2011). Ku70-Ku80 heterodimers also associate with the broken ends to protect against DNA degradation (Walker et al., 2001). Additionally, Ku70 inhibits DNA translocations (Weinstock et al., 2007), which depend on the Ku70-Ku80 ability to limit DNA end mobility (Soutoglou et al., 2007). The next important step is the cell decision on which pathway to carry out. Since NHEJ and HR are mutually exclusive, the chosen pathway automatically makes the other route ineligible. The choice is settled by keeping the broken dsDNA intact as the substrate for NHEJ, or converting double-stranded into single-stranded DNA for homologous recombination (Figure 1.7).

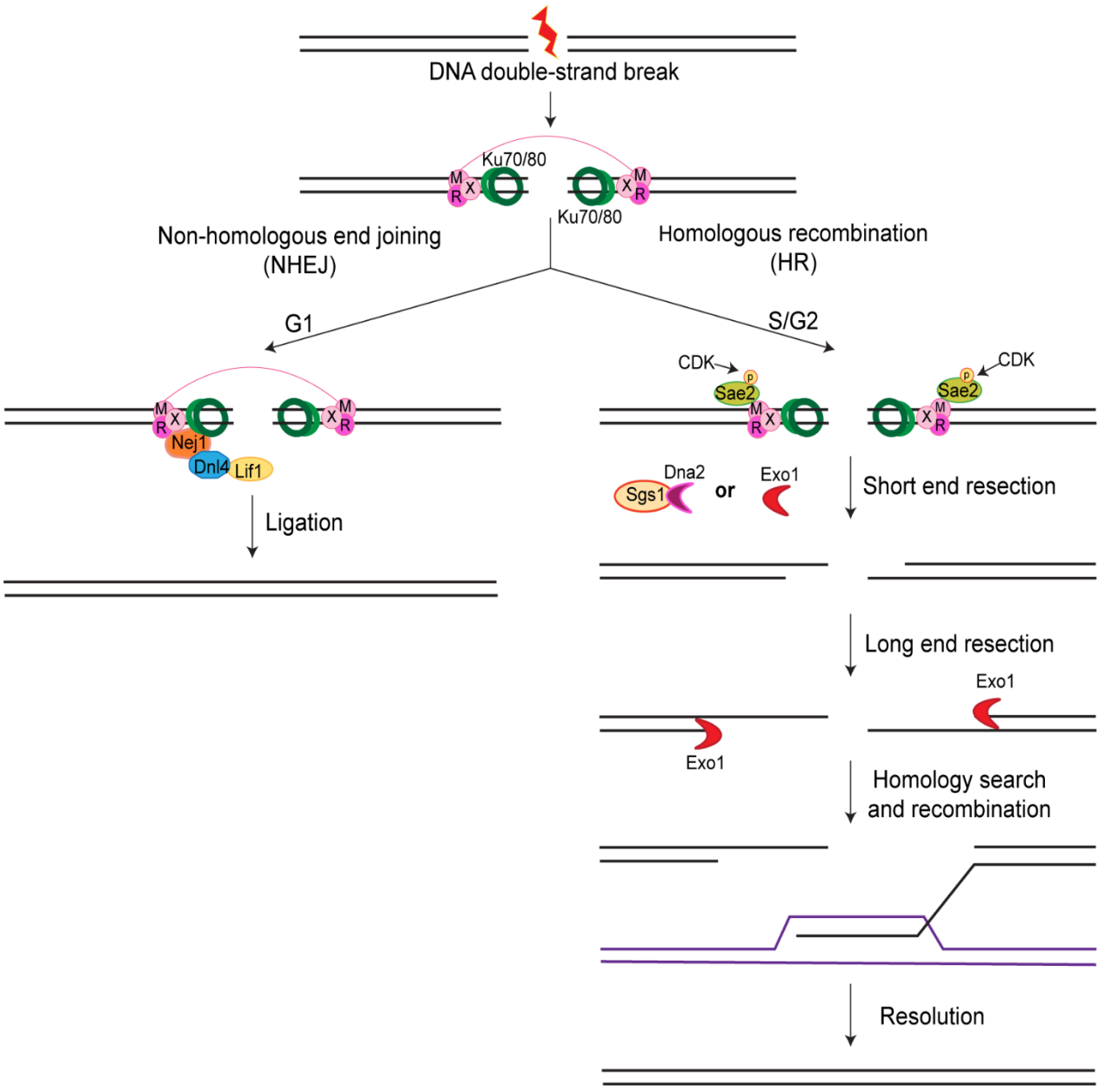

Figure 1.7. Yeast DNA double strand break repair pathways. When cells sense that DNA double-strand breaks are present, the broken ends are immediately recognized and protected by the Mre11-Rad50-Xrs2 complex (MRX) and yeast Ku70/80 ring heterodimers. If the cells decide to do NHEJ, Nej1 is recruited to the broken sites, which in turn, loads the Dnl4-Lif1 ligase complex to perform end-joining. If HR is the repair choice, MRX recruits CDK-phosphorylated Sae2 to start the short endonucleolytic activity, which is then continued by Exo1 or Sgs1-Dna2 to generate the single-stranded DNA (ssDNA) overhangs. The ssDNA stretches find the homologous region on the sister chromatid and use it as the repair template.

NHEJ can take place at any stage of the cell cycle, but it predominantly occurs in G1 phase (Mao et al., 2008). In this pathway, Ku-protected DNA ends recruit Nej1 (XLF in mammals), which functions by stabilizing the accumulation of Ku proteins at the DSB sites and promoting end-joining by the Dnl4-Lif1 ligase complex (mammalian DNA ligase IV-XRCC) (Chen & Tomkinson, 2011). Nej1 also inhibits long nuclease activity by HR factors, Sgs1 and Dna2 (Sorenson et al., 2017). Ku80 loads Dnl4 and concomitantly, Xrs2 recruits Lif1 (Palmbos et al., 2008). The Dnl4-Lif1 complex then joins the broken ends through direct ligation (Zhang et al., 2007)

Cells commit to HR if they detect DSBs in S or G2 phase. This pathway requires a nucleolytic resection on both 5' DNA ends to create 3' ssDNA overhangs to initiate pairing between homologous strands. Thus, the presence of the homologous template, either sister chromatid or homologous chromosome, is a prerequisite for the recombination. However, even in diploid organisms, sister chromatid is the favoured template (Kadyk & Hartwell, 1992) since crossing over between homologous chromosomes may lead to loss of heterozygosity. HR starts when the MRX complex recruits Sae2 (CtIP in mammals). CDK phosphorylates Sae2/CtIP to promote the 3' to 5' endonucleolytic activity of MRX (Huertas et al., 2008; Huertas & Jackson, 2009). Additionally, Tel1/ATM, which is recruited to DSB sites through direct binding to Xrs2/Nbs1 (Nakada et al., 2003), also phosphorylates Sae2/CtIP to support resection (Baroni et al., 2004; Wang et al., 2013). The range of resection at this stage is relatively short (around 300 base pairs) (Garcia et al., 2011) but sufficient to remove the Ku barrier from DNA ends (Chanut et al., 2016). This initial DNA degradation is then followed by long resection (up to thousands of base pairs) by the 5' end exonuclease Exo1 or helicase/nuclease Sgs1/Dna2. Exo1 and Sgs1/Dna2 serve a redundant role in providing long stretches of 3' end ssDNA overhangs.

However, their substrate preference is different. Exo1 targets dsDNA, whereas Dna2 chooses ssDNA. Hence, Dna2 nucleolytic activity couples with Sgs1 helicase. The ssDNA tail is then stabilized by RPA coating. When this tail is ready to invade the homologous template, the recombinase factor Rad51 subsequently replaces RPA for DNA binding. Following the invasion, a Holliday Junction is formed and cleaved by resolvase. Subsequently, DSBs are repaired (Figure 1.7).

Over the last couple of years, mammalian Rif1 has emerged as a repair factor that promotes NHEJ. In contrast with yeast, mammalian DNA repair choice is initiated by the competition between 53BP1 and BRCA1. ATM phosphorylated-53BP1 forms a complex with Rif1 at DSB sites to repair them in G1 phase and limit resection (Feng et al., 2013, 2015). Recently, the detailed mechanism of 53BP1-Rif1 has come to light. Rif1 recruits a protein complex called shieldin, which in turn promotes the recruitment of the primase-pol α complex to fill the gap at the DSB site (Ghezraoui et al., 2018; Mirman et al., 2018; Noordermeer et al., 2018), Rif1 also controls the CDK phosphorylation level of WRN helicase (mammalian Sgs1) (Garzón et al., 2019) and Dna2 nuclease (Mukherjee et al., 2019) which has direct implications for the nuclease's resection rate. In S phase where HR is more dominant, BRCA1 negates these functions by promoting 53BP1 dephosphorylation, and thereby Rif1 decumulation from DSB sites (Chapman et al., 2013; Escribano-Díaz et al., 2013). Even though the 53BP1-BRCA1 antagonistic relationship is not observed in yeasts due to lack of protein conservation, Rif1 function to support NHEJ is retained (Fontana et al., 2019; Mattarocci et al., 2017). Thus, the precise mechanism of how yeast Rif1 leads the repair choice to NHEJ requires further investigation.

1.3.6 DNA damage tolerance mechanisms

If DNA damage is irreparable, cells may escape from persistent cell cycle arrest through DNA damage tolerance mechanisms. In some cases, bypassing the DNA lesion is still better for cell survival than accumulating ssDNA, which can generate more stalled forks. The tolerance mechanism can be divided into two main mechanisms: polymerase-switching (translesion synthesis) and template-switching.

Error-prone translesion DNA synthesis (TLS) switches DNA polymerase from high-fidelity (pol ε or pol δ) to low-fidelity ones (Rev3, Rev1, pol η). These polymerases can traverse the damaged template and bypass the lesion (Shcherbakova & Fijalkowska, 2006). Due to the lack of proofreading activity, these polymerases may incorporate some wrong dNTPs that do not complement the template (Tissier et al., 2000). The second possibility is the error-free template switching pathway (Nikolaishvili-Feinberg & Cordeiro-Stone, 2000), which is similar to DNA repair via homologous recombination. In this pathway, the stalled nascent strand temporarily invades undamaged sister chromatid DNA and uses this strand as the template for DNA replication at the lesion area (Branzei & Szakal, 2016). Cells decide the suitable pathway for damage adaptation through Rad18-Rad6-dependent PCNA ubiquitination (Hoege et al., 2002; Kannouche et al., 2004; Stelter & Ulrich, 2003). PCNA promotes TLS when it is monoubiquitinated, and leads to the template-switching route when it is polyubiquitinated. Modified PCNA then recruits the downstream adaptation factors to execute the appropriate pathway (Gallo et al., 2019).

1.4 DDK interaction in cell cycle signalling

1.4.1 Dbf4

Dbf4 (ASK in mammals, Dfp1/Him1 in fission yeast) is the regulatory subunit of DDK. This protein has three conserved motifs: N, M and C, which denote their relative positions (Masai & Arai, 2000) (Figure 1.8). Each of these motifs mediates Dbf4 interaction with specific ligands, and their biological implications have been extensively studied (Matthews & Guarne, 2013).

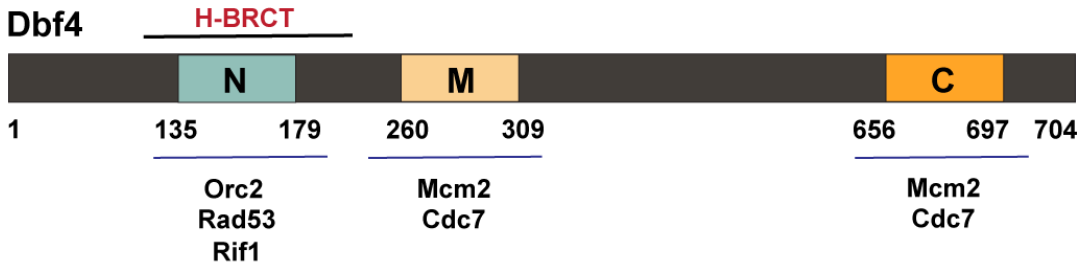

Figure 1.8. A schematic map of Dbf4. Three Dbf4 conserved motifs (Masai & Arai, 2000) along with their corresponding amino acid positions and known binding ligands.

Dbf4 motif N (residues 135-179 (Masai & Arai, 2000)), is necessary for association with Orc2, Rad53 (Duncker et al., 2002) and Rif1 (Hiraga et al., 2014). Cells expressing a Dbf4 mutant lacking motif N (*dbf4*Δ*N*) are viable, but they grow slowly under normal conditions (Varrin et al., 2005). Motif N itself does not form a specific configuration, but is part of larger BRCT fold (Gabrielse et al., 2006; Matthews et al., 2009). with an additional N-terminal alpha-helix. This whole unit is therefore termed HBRCT (Helix α0-BRCT), which is both required and sufficient to bind Rad53 (Matthews et al., 2012).

Dbf4 motif M is essential for cell viability and is necessary for Mcm2 binding (Varrin et al., 2005). In fission yeast and humans, both motif M and C mediate binding to Cdc7 (Ogino et al., 2001; Sato et al., 2003).

Dbf4 motif C contains a CCHH zinc finger that is essential for Cdc7 activation in fission yeast (Ogino et al., 2001), budding yeast (Jones et al., 2010) and humans (Hughes et al.,

2012). Histidine mutation to alanine (CCAA) in this motif impairs Dbf4 binding to Mcm2 and origin of replication ARS1. The *dbf4 CCAA* mutant strain also shows a reduction of Mcm2 phosphorylation and a slow-growth phenotype (Jones et al., 2010). This phenotype indicates that similar to motif M, motif C is also required for viability.

1.4.2 Rad53

As a checkpoint effector protein, Rad53 phosphorylates and interacts with several targets to arrest the cell cycle, and it also helps with cell recovery after the checkpoint is lifted. Rad53 contains two FHA (forkhead-associated) domains and a kinase module in between. The Rad53 FHA1 domain binds to Dbf4 (Duncker et al., 2002; Matthews et al., 2012) as well as variety of other targets, including the checkpoint adaptors Rad9 and Mrc1 (Sun et al., 1998), Protein Phosphatase 2C Ptc2 and Ptc3 (Leroy et al., 2003), and a cytosolic protein Cdc11 (Smolka et al., 2006). Rad53 association with Rad9 is also facilitated by the second FHA domain, FHA2 (Sun et al., 1998). FHA domains are made of an 11 β-sheet sandwich. Their canonical binding mode relies on recognizing phosphothreonine/serine (pT/S) containing motifs on the targets (Durocher et al., 1999). When a pT/S motif is present, Arg70 of the Rad53 FHA1 domain engages with the oxygen group of the pT/S to create a hydrogen bond. This binding is stabilized by the presence of aspartic acid in the three residues position immediately after the phosphorylated residue (Durocher & Jackson, 2002; Durocher et al., 2000). A further Rad53 FHA1 characterization study has revealed a novel binding mode of this domain to Dbf4. Instead of using its phosphopeptide recognition motif, FHA1 engages Dbf4 via its lateral β-sandwich surface (Matthews et al., 2014). Multiple mutations on this surface disrupt binding to Dbf4 and make the cells hypersensitive to genotoxic stress. Furthermore, the FHA1 R70A

mutant is capable of maintaining intact binding to Dbf4, indicating the existence of a non-canonical Rad53-Dbf4 association (Matthews et al., 2014).

1.4.3 Rif1

Rif1 is a conserved protein that was originally identified as part of the telosome in budding yeast. It is recruited to telomeres by binding to the Rap1 C-terminus (Hardy et al., 1992). Budding yeast Rif1 consists of 1916 amino acids and has distinct features at its N and C-termini. The N-terminus has been crystallized and contains two Protein Phosphatase-1 (PP1; Glc7 in budding yeast) binding motifs, RVxF (residues 115-118) and SILK (residues 146-149), both of which are required for Rif1 function in preventing precocious origin firing by promoting Mcm4 dephosphorylation in G1 phase (Davé et al., 2014; Hiraga et al., 2014; Mattarocci et al., 2017, 2014; Sreesankar et al., 2012). This is different from mammalian Rif1 which harbors both PP1 interaction motifs on its C-terminus (Sukackaite et al., 2017). The N-terminal part of Rif1 also includes an NTD (N-terminal domain, residues 177-1283), that binds to DNA in a direct and sequence-independent manner, which is associated with Rif1 function in promoting DNA repair through NHEJ (Mattarocci et al., 2017). Additionally, the Rif1 NTD region undergoes acylation (cysteine 466 and 473) that increases Rif1 hydrophobicity and, in turn, aids in anchoring Rif1 to the inner nuclear membrane. This posttranslational modification also facilitates Rif1 repair of chromosomal DSBs at the nuclear periphery (Fontana et al., 2019). The C-terminal region of Rif1 can be subdivided into three parts: the linear Rap1-binding module (residues 1752-1772) (Shi et al., 2013), Dbf4-binding region (residues 1790-1916) (Hiraga et al., 2014); and tetramerization module (residues 1857-1916) (Shi et al., 2013). Interaction between the Rif1 C-terminus and Dbf4 brings DDK and

the Rif1 N-terminus into close proximity. DDK phosphorylates an area near the Glc7-binding motifs on the Rif1 N-terminus to abolish Glc7 binding to Rif1. Certain DDK phosphorylation sites on Rif1 are CDK-primed while others are CDK-independent. Rif1 without binding Glc7 can no longer promote Mcm4 dephosphorylation, and subsequently, permits S-phase progression (Hiraga et al., 2014).

1.4.4 Mrc1

Budding yeast Mrc1 is conserved among eukaryotes and is comprised of 1096 amino acids. It has multiple roles during the cell cycle. During normal conditions, Mrc1 maintains the replisome progression rate during elongation, shown by the slow S-phase progression in cells with a deletion of *MRC1* (Szyjka et al., 2005). In agreement with this, an in vitro DNA replication assay using purified proteins demonstrated that Mrc1 is required for the maximum DNA synthesis rate on the leading strand (Yeeles et al., 2017), which likely relies on its function to stimulate the enzymatic activity of the leading strand polymerase, pol ε (Zhang et al., 2018). Mrc1, through its residues 312-655, is tethered to the replisome by direct binding to Mcm6 (Komata et al., 2009). Furthermore, it forms the fork protection complex (FPC) with other proteins, Ctf4, Tof1 and Csm1. FPC travels along with the replisome during elongation and stabilizes the replisome by keeping the helicase and polymerase together during DNA synthesis (Katou et al., 2003; Noguchi et al., 2003) FPC co-precipitates with both normal and stalled replisomes (Nedelcheva et al., 2005), indicating that it associates with the forks stably under various conditions. When replisomes stall, Mrc1 has an additional role in bridging Mec1 phosphorylation to Rad53 (Alcasabas et al., 2001; Chen & Zhou, 2009; Tanaka & Russell,

2001). Beyond DNA replication, FPC aids sister chromatid cohesion during mitosis, and the deletion of *MRC1*, in particular, increases the loss of sister cohesion events (Xu et al., 2004).

Mrc1 has been shown to associate with early origins in S phase and regulate their firing in fission yeast (Hayano et al., 2011). In budding yeast, Mrc1 interacts with early and late origins in a timely manner (Osborn & Elledge, 2003). The association of Mrc1 with ARS305, a representative early origin, is DDK-dependent, as Mrc1 binding to the origin diminishes when DDK activity is compromised (Osborn & Elledge, 2003).

In fission yeast, knockout of *MRC1* rescues the growth of the temperature-sensitive strain *hsk1-89* at the semi-restrictive temperature of 30°C, indicating that Δ*mrc1* cells allows origin firing when there is less Hsk1-Dfp1(budding yeast ortholog of Cdc7-Dbf4) activity (Matsumoto et al., 2011). Some details of how Mrc1 regulates origin firing in fission yeast have come to the light. Mrc1 acts as a 'built-in' brake for DNA replication. It exhibits intramolecular binding when it binds to DNA origins and this conformation prevents origins from firing. In early S phase, Hsk1-Dfp1 binds to and phosphorylates Mrc1 to disrupt the intramolecular binding. Next, Mrc1 in open conformation allows Hsk1-Dfp1 to activate the origins. The possible explanation for why Δ*mrc1/hsk1-89* cells are viable at 30°C is that there is no Mrc1 'brake' so even the low activity of *hsk1-89* suffices to maintain cell growth (Matsumoto et al., 2017).

1.5 Project goals

Dbf4 is required to activate DDK and initiate DNA replication. During S phase, it interacts with several other replication factors. The dynamics of its interactions change with different stages and circumstances in the cell cycle. Despite the importance of its binding with its

ligands, many of the details are still unclear. In this thesis, I aimed to pursue the following objectives.

1. To characterize how Dbf4 binds to Rif1 to inactivate the dephosphorylation activity of the Rif1-Glc7 complex.
2. To further investigate the association between Rad53 and Dbf4.
3. To characterize DDK binding to and regulation of Mrc1 in budding yeast.

1.6 Research significance

Various cancer types have been shown to overexpress DDK to support cell proliferation. This phenomenon has been studied in both cancer cell lines and primary tissue samples (Bonte et al., 2008; Cheng et al., 2013; Zhuang et al., 2018). DDK overexpression is associated with p53 inactivation (Bonte et al., 2008) and resistance to radio- and chemotherapy (Gad et al., 2019; Li et al., 2018). Furthermore, the depletion of Cdc7 in HeLa cells can inhibit DNA replication (Jiang et al., 1999) and lead to apoptotic death (Montagnoli et al., 2004). The knockdown of DDK also helps to limit metastasis by preventing esophageal squamous cell carcinoma (ESCC) cell invasion and sensitize them to the chemotherapy agents, Cisplatin and 5-Fluorourea (Cao & Lu, 2019). As a result of these findings, targeting DDK seems promising as one of the strategies for cancer therapy. At the moment this thesis is being written, the ATP-competitive DDK inhibitor, TAK-931, is undergoing two clinical trials (Iwai et al., 2019). Their trial identifiers are NCT02699749 (phase 1 in participants with advanced nonhematologic tumor) and NCT03261947 (phase 2 in participants with metastatic pancreatic cancer, metastatic colorectal cancer, and other advanced solid tumors). Both trials are expected to be completed in 2020. Moreover, protein-protein interaction-based therapy has been getting attention as a

novel approach for chemotherapy drugs (Gupta et al., 2019). Therefore, understanding the mechanistic details of DDK roles and interactions during the cell cycle can contribute to setting the future direction of DDK-targeted cancer therapy.

Chapter 2

Material and Methods

Portions of this chapter appear in the following article and are reproduced with permission. Almawi AW, Matthews LA, Larasati, Myrox P, Boulton S, Lai C, Moraes T, Melacini G, Ghirlando R, Duncker BP, and Guarné A. (2016). 'AND'logic gates at work: Crystal structure of Rad53 bound to Dbf4 and Cdc7. Sci Rep 6:34327. 10.1038/srep34237.

2.1 Construction of yeast strains and plasmids

Yeast strains and plasmids used in this study are listed in Tables 1 and 2, respectively. DY-1 was used for all yeast two-hybrid experiments. DY-30 was used to generate *RIF1 MYC* (DY-361), Δ*rif1* (DY-362), *rif1* Δ*PPDSPP MYC* (DY-363), and Δ*mre11* (DY-364) strains using a one-step genome modification method (Longtine et al., 1998). To create DY-363, the last 534 bp of *RIF1* (encoding amino acids 1739-1916 without stop codon) was amplified from pJG4-6 Rif11739-1916 ΔPPDSPP (see below) and cloned into pFA6A-13Myc-HIS3MX6 (Longtine et al., 1998) using HindIII and PacI sites incorporated into the forward and reverse primers, respectively. From this construct, the Rif1 1739-1916 ΔPPDSPP-13Myc-HIS3MX6 cassette was amplified, transformed into yeast cells using standard procedures (Gietz et al., 1992) and then plated onto synthetic complete medium lacking histidine (SC-His). To identify correct integration, genomic DNA was extracted from single colonies and used as template for PCR using primers with DNA sequences reflecting the genomic sequence flanking the desired site of integration of the replacement cassette. The identity of DY-363 was further confirmed via DNA sequencing of the PCR product obtained (SickKids, Toronto, Ontario, Canada).

To generate *rif1 5A MYC* (DY-379) and *rif1 5A*Δ*PPDSPP MYC* (DY-380) strains, from DY-361 and DY-363, respectively, we employed a seamless gene modification method inspired by the *delitto perfetto* approach (Storici et al., 2001) with modification. A *URA3* cassette was amplified from pRS406 (Sikorski & Hieter, 1989) and integrated at the *RIF1* locus to replace 216 bp of RIF1 containing CDK target sites (nucleotides 328-543) (Hiraga et al., 2014). The modified strain was then grown on synthetic complete medium lacking uracil. The replacement cassette bearing the 5A point mutations (S110A, S125A, S134A, S138A, and S181A) and having end homology to *RIF1* regions up- and downstream of the integrated *URA3* cassette was

generated through site-directed mutagenesis (Agilent). Cells were transformed with this second cassette and plated onto YPD. Integrants were selected through replica plating on synthetic complete medium supplemented with 5-Fluoroorotic acid (BioShop #FOA555). Strain modifications were confirmed through PCR and DNA sequencing (SickKids, Toronto, Ontario, Canada), and Western blotting (described below).

We used DY-361 and DY-380 to generate Δ*nej1* (DY-381), Δ*nej1/rif1 5A*Δ*PPDSPP MYC* (DY-382), Δ*sae2* (DY-383), Δ*sae2/rif1 5A*Δ*PPDSPP MYC* (DY-384), Δ*exo1* (DY-385), Δ*exo1/rif1 5A*Δ*PPDSPP MYC* (DY-386), Δ*yku70* (DY-387) and Δ*yku70/rif1 5A*Δ*PPDSPP MYC* (DY-388) using a one-step genome modification method (Longtine et al., 1998). A *URA3* cassette was amplified from pRS406 (Sikorski & Hieter, 1989) and integrated at the gene of interest locus. The modified strain was then grown on synthetic complete medium lacking uracil. Strain modifications were confirmed through PCR analysis as described above.

To generate Δ*mrc1 dna52-1*, a *URA3* cassette was amplified from pRS406 (Sikorski & Hieter, 1989) and integrated at the *MRC1* locus to replace the whole coding sequence in a *dna52-1* strain (DY-2). The modified strain was then grown on synthetic complete medium lacking uracil. Strain modification was confirmed through PCR analysis.

Table 2.1 Yeast strains used in this study.

Strain	Genotype	Source
DY-1	*MATa, ade2-1, can1-100, trp1-1, his3-11, his3-15, ura3-1, leu2-3, leu2-112, pep4::LEU2*	R. Rothstein (W303-1a)
DY-2	*MATa, can1-11, ura3-52, dna52-1*	(Solomon et al., 1992)
DY-30	*MATa, hisΔ1, leu2Δ0, met15Δ0, ura3Δ0*	(Brachmann et al., 1998)
DY-26	*MATa, his3Δ200, leu2Δ0, met15Δ0, trp1Δ63, ura3Δ0*	(Brachmann et al., 1998)
DY-361	*MATa, hisΔ1, leu2Δ0, met15Δ0, ura3Δ0, RIF1 MYC::HIS3MX6*	This study
DY-362	*MATa, hisΔ1, leu2Δ0, met15Δ0, ura3Δ0, Δrif1::HIS3MX6*	This study
DY-363	*MATa, hisΔ1, leu2Δ0, met15Δ0, ura3Δ0, rif1 ΔPPDSPP MYC::HIS3MX6*	This study
DY-364	*MATa, hisΔ1, leu2Δ0, met15Δ0, ura3Δ0, Δmre11::URA3*	This study
DY-374	*MATa, can1-11, ura3-52, dna52-1 Δmrc1::URA3*	This study
DY-379	*MATa, hisΔ1, leu2Δ0, met15Δ0, ura3Δ0, rif1 5A MYC::HIS3MX6*	This study
DY-380	*MATa, hisΔ1, leu2Δ0, met15Δ0, ura3Δ0, rif1 5AΔPPDSPP MYC::HIS3MX6*	This study
DY-381	*MATa, hisΔ1, leu2Δ0, met15Δ0, ura3Δ0, RIF1 MYC::HIS3MX6 Δnej1::URA3*	This study
DY-382	*MATa, hisΔ1, leu2Δ0, met15Δ0, ura3Δ0, rif1 5AΔPPDSPP MYC::HIS3MX6 Δnej1::URA3*	This study
DY-383	*MATa, hisΔ1, leu2Δ0, met15Δ0, ura3Δ0, RIF1 MYC::HIS3MX6 Δsae2::URA3*	This study
DY-384	*MATa, hisΔ1, leu2Δ0, met15Δ0, ura3Δ0, rif1 5AΔPPDSPP MYC::HIS3MX6 Δsae2::URA3*	This study
DY-385	*MATa, hisΔ1, leu2Δ0, met15Δ0, ura3Δ0, RIF1 MYC::HIS3MX6 Δexo1::URA3*	This study
DY-386	*MATa, hisΔ1, leu2Δ0, met15Δ0, ura3Δ0, rif1 5AΔPPDSPP MYC::HIS3MX6 Δexo1::URA3*	This study
DY-387	*MATa, hisΔ1, leu2Δ0, met15Δ0, ura3Δ0, RIF1 MYC::HIS3MX6 Δyku70::URA3*	This study
DY-388	*MATa, hisΔ1, leu2Δ0, met15Δ0, ura3Δ0, rif1 5AΔPPDSPP MYC::HIS3MX6 Δyku70::URA3*	This study

Plasmid construction was carried out using standard cloning techniques. For yeast two-hybrid constructs, *DBF4* (full-length without start codon or nucleotides 313-663 encoding amino acids 105-221) was amplified from DY-1 genomic DNA, digested with EcoRI and NcoI, and cloned into EcoRI-NcoI linearized pEG202 as an in frame fusion with sequence encoding the N-terminal epitope tag (LexA for pEG202 and HA for pJG4-6). Using the same technique, ApaI-XhoI digested *RIF1* fragments (nucleotides 5368-5751 encoding amino acids 1790-1916 or nucleotides 5215-5751 encoding amino acid 1739-1916) were cloned into ApaI-XhoI linearized pJG4-6. EcoRI-XhoI digested *RAP1* fragment (nucleotides 1957-2484 encoding amino acids 653-827) was cloned into EcoRI-XhoI linearized pEG202. Plasmids bearing point mutant alleles were created by site-directed mutagenesis (Agilent). pCM190 Rif1-Myc *ura3::LEU2* was constructed step-wise. *LEU2* was amplified from pRS405, digested with SmaI and cloned into EcoRV linearized pCM190 Myc to disrupt *URA3* locus. EcoRV was chosen as it cuts pCM190 Myc backbone once in the middle of *URA3* locus. The construct was confirmed by transforming it into DY-26 and growing the transformant on synthetic complete medium lacking uracil (SC-ura) and synthetic complete medium lacking leucine (SC-leu). The transformant grew on SC-leu, but not on SC-ura. *RIF1* (full-length without stop codon) was amplified from DY-1 genomic DNA, digested with BamHI and NotI, and cloned into BamHI-NotI linearized pCM190 Myc *ura3::LEU2*. pEG202 Mrc1 was created by amplifying *MRC1* (full-length) from DY-1 genomic DNA, digested with Nco1I and XhoI, and cloned into NcoI-XhoI linearized pEG202. pEG Mrc1 1-684 was created by amplifying *MRC1* nucleotides 4-2052, digested with BamHI and EcoRI, and cloned into BamHI-EcoRI linearized pEG202. pEG Mrc1 679-1096 was created by amplifying *MRC1* nucleotides 2035-3291, digested with BamHI and XhoI, and cloned into

BamHI-XhoI linearized pEG202. pJG4-6 Dbf4 variants were created by amplifying *DBF4* from either pEG202 Dbf4 L109A/W112S, pEG202 Dbf4 ΔM (Varrin et al., 2005) or pEG202 Dbf4 CCAA (Jones et al., 2010), digested with NcoI and EcoRI, and cloned into NcoI-EcoRI linearized pJG4-6. Clones were confirmed through DNA sequencing (SickKids, Toronto, Ontario, Canada).

Point mutations within Rad53 FHA1 (F146A and N112A/F146A) were generated by site-directed mutagenesis using pJG4-6 FHA1 (including residues 1–165 of Rad53) as the template. Single point mutations on Dbf4 (Y198A and K200A) were generated from the pEG202-Dbf4 full-length template. These constructs were verified by DNA sequencing (MOBIX, McMaster University).

Table 2.2 Plasmids used in this study.

Plasmid	Reference
pEG202	(Ausubel et al., 1994)
pEG202 Dbf4 FL WT	(Duncker et al., 2002)
pEG202 Dbf4 105-221 (Dbf4 HBRCT)	(Matthews et al., 2012)
pEG202 Dbf4 FL L109A/W112S	This study
pEG202 Dbf4 FL K121D/R122E	(Matthews et al., 2012)
pEG202 Dbf4 FL E111R/K118D	(Matthews et al., 2012)
pEG202 Dbf4 FL W116D/M120A	(Matthews et al., 2012)
pEG202 Dbf4 FL K200A	This study
pEG202 Dbf4 FL Y198A	This study
pEG202 Rap1 653-827	This study
pJG4-6	(Gyuris et al., 1993; Varrin et al., 2005)
pJG4-6 Rif1 1790-1916	This study
pJG4-6 Rif1 1790-1916 R1895A	This study
pJG4-6 Rif1 1790-1916 L1905R	This study
pJG4-6 Rif1 1739-1916	This study
pJG4-6 Rif1 1739-1916 E1839K	This study
pJG4-6 Rif1 1739-1916 N1847A	This study
pJG4-6 Rif1 1739-1916 ΔPPDSPP	This study
pJG4-6 Rad53 1-165 (Rad53 FHA1)	This study
pJG4-6 Rad53 FHA1 F146A	This study
pJG4-6 Rad53 FHA1 N112A/F146A	This study
pSH18-34	(Ausubel et al., 1994)
YCplac111	(Gietz & Sugino, 1988)
pRS406	(Sikorski & Hieter, 1989)
pRS405	(Sikorski & Hieter, 1989)
pCM190 Myc *ura3::LEU2*	This study
pCM190 Rif1-Myc *ura3::LEU2*	This study
pEG202 Mrc1 FL WT	This study
pEG202 Mrc1 1-684	This study
pEG202 Mrc1 679-1096	This study
pJG4-6 Dbf4 FL L109A/W112S	This study
pJG4-6 Dbf4 ΔM	This study, (Varrin et al., 2005)
pJG4-6 Dbf4 CCAA	This study, (Jones et al., 2010)

2.2 Yeast two-hybrid analysis

Yeast two-hybrid analysis was performed as described previously (Varrin et al., 2005). pEG202-derived bait, pJG4-6-derived prey and pSH18-34 reporter plasmids (Ausubel et al., 1994; Gyuris

et al., 1993; Varrin et al., 2005) were transformed into 100 µl of DY-1 culture with a density of $1x10^7$ cells/ml. Triple transformants were selected on solid medium lacking histidine, tryptophan and uracil (SC-His/Trp/Ura) then individual colonies were used to inoculate 10 mL of SC-His/Trp/Ura and grown to a concentration of $1x10^7$ cells/ml. $1x10^8$ cells were then washed and induced in 20 ml 2% Galactose-1% Raffinose lacking uracil, histidine, and tryptophan for 6 hours to promote the expression of the prey protein. The cell density was measured at 600 nm (A_{600}) and cell number was counted using a hemocytometer. $5x10^6$ cells were harvested and subjected to a quantitative β-galactosidase assay. The cells were resuspended in 500 µl Z buffer pH 7 (60 mM Na_2HPO_4, 40 mM NaH_2PO_4, 10 mM KCl, and 1 mM MgSO4) and permeabilized with one drop of 0.1% SDS and two drops of chloroform. The reaction was immediately started upon addition of 100 µl 4 mg/ml *o*-nitrophenyl-β-galactoside (ONPG) at 28ºC and stopped with 250 µl 1M Na_2CO_3 when a faint yellow color was apparent. The supernatant was separated from the pellet via centrifugation at 16,000 g for 10 minutes and the intensity of yellow color was measured at 420 nm (A_{420}). The quantification of β-Galactosidase activity was determined as β-Galactosidase unit $= 1{,}000 \times A_{420}/(t \times V \times A_{600})$, where t = time of reaction (in minute) and V = volume (in ml).

2.3 Western blotting

20 ml yeast cultures ($1x10^7$ cells/ml) were centrifuged at 4,000 rpm for 5 minutes and the pellets were resuspended in 300 µl ice-cold lysis buffer (50 mM HEPES-KOH pH 7.5, 140 mM NaCl, 1 mM EDTA, 1% Triton X-100, 0.1% (w/v) Na-deoxycholate, 1% (v/v) protease inhibitor cocktail (Fisher), and 1mM PMSF (BioShop)). Following addition of 0.5 g glass beads, the

cells were lysed at 4°C with a bead beater (BioSpec Products, Inc.) for 30 seconds, eight times, with rests in ice for 30 seconds in between pulses. Cell lysates were centrifuged at 16,000g for 1 minute to obtain the supernatant. Protein concentration was measured using the Bradford assay (Bio-Rad) and 100 µl of the supernatant was mixed with 50 µl sample buffer (41.5 mM Tris pH 6.8, 10% glycerol, 3.75% SDS, 0.01% bromophenol blue, 100 mM DTT). The protein samples were denatured at 95ºC for 10 minutes and 80 µg of each sample was used for Western blots. SDS-PAGE was performed using a 10% acrylamide separating gel and the proteins were transferred onto a BioTrace nitrocellulose membrane (Pall #66485) overnight. Proteins tagged with LexA, HA and Myc were detected with rabbit polyclonal anti-LexA (Pierce #PA1-4966), mouse monoclonal anti-HA (Sigma #H9658) and mouse monoclonal anti-Myc (Sigma #M5546) primary antibodies, respectively. Alexa Fluor 647 goat-anti rabbit IgG (Invitrogen #A-21244) and Alexa Fluor 488 goat anti-mouse IgG (Invitrogen #A-11001) were used as the secondary antibodies. All detections were performed using a PharosFX Imager (Bio-Rad).

2.4 Bioinformatics analysis

A multiple sequence alignment of *RIF1* homologs was generated using MUSCLE (Edgar, 2004) and visualized within Jalview (Waterhouse et al., 2009). Structure-prediction was performed using Phyre2 (Kelley et al., 2015) and I-TASSER (Zhang, 2008). Secondary structure prediction was performed using Jpred3 (Cole et al., 2008a). Phosphorylation sites were identified based on information retrieved from the UniProt database record (accession # P29539). Protein binding sites were predicted using the BSPred algorithm (Mukherjee & Zhang, 2011).

2.5 Plasmid stability assay

Plasmid stability assays (Kapoor et al., 2001) were carried out with modification. DY-361, DY-362, and DY-363 were transformed with low copy number plasmid YCplac111 (Gietz & Sugino, 1988) and grown on synthetic complete plates lacking leucine (SC-Leu). A single colony from each strain was picked and grown in 10 ml SC-Leu liquid medium until the cells reached stationary phase. $2x10^3$ cells from this initial culture were then used to inoculate 10 ml synthetic complete (including leucine) liquid medium and grown until they reached stationary phase. The cells were diluted, concentration determined using a hemocytometer, and a total number of 400 were plated onto each SC-Leu (selective) and YPD (non-selective) plate. The rate of plasmid loss per generation was calculated as the percentage of plasmid loss = (1-(colony number on SC-Leu/colony number on YPD))/number of cell divisions. The total number of replicates was ten sets for each strain.

2.6 Yeast spot plate assay

Yeast strains were grown in liquid media overnight, serially diluted ten-fold each time, and spotted onto YPD plates with or without added compounds. Plates were incubated for 2 days at 30°C. The compounds added were hydroxyurea (BioShop #HYD023), methyl methanesulfonate (Millipore Sigma #129925); bleocin (Millipore Sigma #203408-M); phleomycin (Millipore Sigma #P9654); camptothecin (Millipore Sigma #C9911); and caffeine (BioShop #CAF114).

2.7 β-galactosidase-based competition assay

pEG202-derived bait, pJG4-6-derived prey, pSH18-34 reporter plasmids (Ausubel et al., 1994; Gyuris et al., 1993; Varrin et al., 2005) and pCM190 Myc *ura3::LEU2*-derived competitor were transformed into 100 µl of DY-26 culture with a density of $1x10^7$ cells/ml. Quadruple transformants were selected on solid medium lacking histidine, tryptophan, uracil and leucine (SC-His/Trp/Ura/Leu) then individual colonies were used to inoculate 10 mL of SC-His/Trp/Ura/Leu and grown to a concentration of $1x10^7$ cells/ml. $1x10^8$ cells were then washed and induced in 20 ml 2% Galactose-1% Raffinose lacking uracil, histidine, leucine and tryptophan for 6 hours to promote the expression of the prey protein. The cell density was measured at 600 nm (A_{600}) and cell number was counted using a hemocytometer. $5x10^6$ cells were harvested and subjected to a quantitative β-galactosidase assay, as previously mentioned in yeast two-hybrid experiment.

2.8 Mcm4 phosphorylation detection

10 ml yeast cultures ($1x10^7$ cells/ml) were centrifuged at 4,000 rpm for 5 minutes. The supernatant was discarded and the pellet was washed with 20 ml sterile water. The suspension was spun down again, and the pellet was resuspended in fresh YPD supplemented with 50 µg/ml α-factor. The cell culture was shaken at 200 rpm and incubated at 30°C for 3 hours. After incubation, approximately 2.5×10^7 cells were harvested at 1000 *g* and spheroplasted as performed previously (Semple et al., 2006) with modifications. Cells were washed with sterile water and incubated at 30°C for 10 minutes with gentle mixing in 10 ml/g pre-spheroplasting buffer (100 mM EDTA-KOH (pH 8), 10 mM DTT), followed by incubation in 10 mL/g

spheroplasting buffer (0.5X YPD, 1.1 M sorbitol) containing 0.5 mg/mL Zymolyase 20T (Seikagaku Corp., Japan) at 30°C for 10–15 minutes with gentle mixing. Cells were washed once with 20 ml spheroplasting buffer containing 0.5 mM PMSF (BioShop), 2 mM NaF (Sigma #201154) and 1mM Na_3VO_4 (Sigma #450243), followed by resuspension in 1 ml ice-cold wash buffer (5 mM Tris–HCl (pH 7.4), 20 mM KCl, 2 mM EDTA-KOH (pH 7.4), 1 M sorbitol, 1% thiodiglycol, 125 μM spermidine, 50 μM spermine) and protease and phosphatase inhibitors (1% (v/v) protease inhibitor cocktail (Fisher), 0.5 mM PMSF, 2 mM NaF and 1mM Na_3VO_4). Cells were pelleted at 400 *g* for 2 minutes in a microcentrifuge at 4°C, washed twice with 1 mL ice-cold wash buffer, and resuspended in 0.4 mL ice-cold breakage buffer (5 mM Tris–HCl (pH 7.4), 20 mM KCl, 2 mM EDTA-KOH (pH 7.4), 0.4 M sorbitol, 1% thiodiglycol, 125 μM spermidine, 50 μM spermine) and protease and phosphatase inhibitors as above. Cells were lysed with 0.5 ml ice-cold breakage buffer containing 2% Triton X-100 and incubated on ice for 5 minutes with occasional mixing. The lysed cells were spun at 16,000 *g* for 5 minutes in a microcentrifuge at 4°C. The supernatant (SUP) was separated from the pellet (PEL), and the protein concentration was measured using the Bradford assay (Bio-Rad). The pellet and 100 μL of the supernatant were prepared as the protein sample, as previously described in Section 2.3. SDS-PAGE was performed using 6% acrylamide separating gels and the proteins were transferred to a PVDF membrane (Millipore # IPVH00010) overnight at 30V. Mcm4 was detected with goat polyclonal Mcm4 primary antibody (Santa Cruz #sc-6685) and donkey anti-goat IgG HRP-conjugated secondary antibody (Promega #V8051). The detections were performed using the Bio-Rad Clarity ECL substrate (Bio-Rad #1705060) and a Bio-Rad ChemiDoc.

2.9 Flow cytometry/fluorescence-activated cell sorting (FACS) analysis

10 ml yeast cultures ($1x10^7$ cells/ml) were centrifuged at 4,000 rpm for 5 minutes. The supernatant was discarded and the pellet was washed with 20 ml sterile water. The suspension was spun down again, and the pellet was resuspended in fresh YPD supplemented with 30-50 µg/ml α-factor. The cell culture was shaken at 200 rpm and incubated at 30°C for 2.5 hours. After α-factor arrest, the shmoo (the pear-shape morphology that orients the mating position) appearance was checked under microscope. The cells were washed with sterile water and spun down 4,000 rpm for 5 minutes for four times. The cell pellet was resuspended in fresh YPD supplemented with 50 µg/mL Pronase E to degrade any residual α-factor (Sigma #P6911) and incubated at 30°C. The samples for FACS were taken at several time points during incubation. Approximately 1×10^7 cells were harvested at 16,000 *g* for 1 minute. The pellet was resuspended in 1 mL 70% EtOH. Next, 500 µl of this suspension was transferred to a new tube, spun down at 16,000 *g* for 1 minute, and the pellet was washed using 500 µL sterile water. The suspension was spun down again and the pellet was resuspended in 500 µL of 50 mM Tris-HCl pH 8. RNaseA (BioShop #RNA675.250) was added to a concentration of 0.2 mg/ml, and the suspension was incubated at 37°C for 3 hours. The suspension was spun down, and the pellet was resuspended in 500 µL of 50 mM Tris-HCl pH 7.5 containing 2 mg/ml Proteinase K (Sigma #P2308) and incubated at 50°C for 1 hour. The suspension was again spun down, and the pellet was resuspended in 100 µL of FACS buffer (200 mM Tris-HCl pH 7.5, 200 mM NaCl, 78 mM $MgCl_2$) and transferred to a new tube containing 750 µL Sytox solution (50 mM Tris-HCl pH7.5 and 1:5000 diluted 5 mM Sytox in DMSO (Molecular Probes #S7020). Prior to FACS reading,

the suspension was sonicated at low-intensity for 5 seconds. FACS was performed using Amnis ImageStream Flow Cytometry.

2.10 Cloning and expression of Dbf4-Rad53 chimeras

Dbf4-Rad53 chimeras were created by subcloning a codon-optimized fragment of Dbf4 encompassing amino acids 105–220 (Matthews et al., 2014) followed by the FHA1 domain of Rad53 (amino acids 22–162) into a modified pET15b vector including His6-SUMO tag with a TEV protease cleavage site (pAG8586). The two protein fragments were connected directly (Dbf4(0)Rad53) or separated by a five-residue linker (Dbf4-SGASG-Rad53, herein referred to as Dbf4(5)Rad53). Clones were confirmed by DNA sequencing (MOBIX, McMaster University). Plasmids encoding the Dbf4(0)Rad53 (pAG8801) and Dbf4(5)Rad53 (pAG8805) chimeras were transformed in BL21(DE3) cells containing a plasmid encoding rare tRNAs. Cultures were grown to A600 = 0.7, induced by addition of 1 mM isopropyl β-D-1-thiogalactopyranoside, and incubated overnight at 16 °C with orbital agitation.

2.11 Protein purification

Cell pellets were resuspended in buffer A (20 mM TRIS-HCl pH 8.0, 500 mM NaCl, 1.4 mM 2-mercaptoethanol, 5% glycerol) and lysed by sonication. Lysates were cleared by centrifugation at 39,000 *g*, and the supernatants were loaded onto a HiTrap nickel-chelating HP column (GE Healthcare) equilibrated with buffer A. The His6-SUMO-tagged chimeras were eluted with a linear gradient to 300 mM imidazole. The fractions containing the chimera were pooled and injected onto a HiPrep 26/10 desalting column (GE Healthcare) equilibrated with

buffer B (20 mM TRIS-HCl pH 8.0, 150 mM NaCl, 1.4 2-mercaptoethanol, 5% glycerol). The His6-SUMO tag was removed with tobacco etch virus (TEV) protease, and the tagless chimeras further purified by affinity (HiTrap nickel-chelating HP column, GE Healthcare) and size-exclusion chromatography (Superdex 75 (10/300) GL column, GE Healthcare). The purified proteins were concentrated to 9–12 mg/mL and stored in buffer B. Protein concentrations were determined using the Beer-Lambert equation with an extinction coefficient of 36,440 M−1 cm−1.

2.12 Analytical ultracentrifugation

Sedimentation velocity experiments were conducted at 50,000 rpm and 20°C on a Beckman Coulter ProteomeLab XLI analytical ultracentrifuge following standard protocols (Zhao et al., 2013). Samples of the Dbf4(5)Rad53 chimera were studied at various loading concentrations ranging from 2 to 310 μM in 0.2 M NaCl, 0.02 M TRIS-HCl pH 8.0, 1.4 mM 2-mercaptoethanol and 5% v/v glycerol. Samples were loaded in 2-channel centerpiece cells and data were collected using both the absorbance (280 nm) and Rayleigh interference (655 nm) optical detection systems when possible. Standard 12 mm centerpieces were used, whereas shorter 3 mm centerpieces were used for the higher concentration protein samples (>70 μM). Sedimentation data were time-corrected (Ghirlando et al., 2013) and analyzed in SEDFIT 15.01b (Schuck, 2000) in terms of a continuous c(s) distribution of sedimenting species with a resolution of 0.05 S and a maximum entropy regularization confidence level of 0.68. The solution density, solution viscosity and protein partial specific volume were calculated in SEDNTERP (Cole et al., 2008b) (http://sednterp.unh.edu/), and sedimentation

coefficients s were corrected to standard conditions s20,w. Weighted-average sedimentation coefficients obtained by integration of the c(s) distributions were used to create an isotherm that was analyzed in SEDPHAT 13.0a in terms of a reversible monomer-dimer equilibrium. The protein extinction coefficient at 280 nm and the interference signal increment were calculated based on the amino acid composition in SEDFIT 15.01b (Zhao et al., 2011).

2.13 Crystallization, structure determination and refinement

Crystals of the Dbf4(5)Rad53 grew in 50 mM sodium cacodylate pH 6.5, 12% PEG 4000 (v/v), and 250 mM MgCl2 and cryo-protected by addition of 10% ethylene glycol. A complete data set was collected at the X29 beamline of NSLS-I (Brookhaven National Laboratory). Data was processed and scaled in HKL2000 (see Table 2.3) (Otwinowski & Minor, 1997). A phosphorylated peptide (pPEP) derived from Cdc7 (480DGESpTDEDDVVS491) was purchased from GenScript and resuspended in buffer B. The Dbf4(0)Rad53 chimera was mixed with the phosphorylated peptide at a 10-fold molar excess and incubated at 4°C for one hour prior to crystallization trials. Crystals of the Dbf4(0)Rad53-pPEP complex were grown in 100 mM TRIS pH 8.5, and 12.5% PEG 3350 (v/v) and cryo-protected by addition of 15% glycerol. A complete data set was collected at the O8B1-1 beamline of the Canadian Light Source and processed using XDS (see Table 2.3) (Kabsch, 2010).

Table 2.3 Data collection and refinement statistics.

	Dbf4(5)Rad53	Dbf4(0) Rad53 + pPEP
Data Collection		
Beamline	X29 (NSLS)	08B1-1 (CLS)
Wavelength (Å)	1.1	0.979
Space group	P 1	$P\ 2_1$
Cell dimensions		
a, b, c	57.7, 66.6, 86.6	64.5, 87.3, 66.1
α, β, γ	109.5, 90.1, 90.1	90, 94, 90
Resolution	35–2.3 (2.34–2.3)	44.6–2.25 (2.31–2.25)
Reflections (total/unique)	887,843/55,038	101,589/36,580
Completeness (%)	87.2 (57.3)	98.3 (97.4)
CC1/2 (%)	97.1 (92.5)	99.3 (31.8)
I/σ (I)	13.6 (1.4)	8.15 (1)
Redundancy	1.6 (1.4)	2.8 (2.8)
Refinement		
Resolution (Å)	35–2.66	44.6–2.4
Completeness (%)	91.1	98.3
R_{work}/R_{free} (%)	20.6/23.7	20.7/22.9
Atoms refined	15,338	8,312
Solvent Atoms	175	192
rmsd in bonds (Å)	0.004	0.003
rmsd in angles (°)	0.834	0.733
Mean B values ($Å^2$)	45.6	51.5

Both structures were determined by molecular replacement using the FHA1 domain of Rad53 (PDB 1G6G) and the HBRCT domain of Dbf4 (PDB 3QBZ) as search models. The initial models were refined by iterative cycles of manual model building in Coot and refinement in

PHENIX (Adams et al., 2010). The refined models have 98% (Dbf4(5)Rad53) and 98.4% (Dbf4(0)Rad53-pPEP) of the residues in the most favored regions of the Ramachandran plot and none in the disallowed regions. Quantitative analysis of the Dbf4(L)Rad53 (±pPEP) interfaces was done using the online Protein Interfaces Structures and Assemblies (PISA) server (Krissinel & Henrick, 2007). Figures showing molecular structures were generated using PyMOL(Matthews et al., 2014) (DeLano, 2002).

2.14 Analysis of the NMR data

Gradient and sensitivity enhanced [1H-15N] heteronuclear single quantum coherence (HSQC) spectra were acquired at 306 K using a Bruker AV-700 MHz spectrometer equipped with a 5 mm TCI cryoprobe. Samples were prepared as described by (Matthews et al., 2014) with an equimolar concentration of FHA1 and HBRCT in either the absence or presence of 200 μM phosphorylated Cdc7 peptide (pPEP, 480DGESpTDEDDVVS491). Spectra were processed using NMRPipe (Delaglio et al., 1995) and analyzed in Sparky.

Chapter 3

'AND' logic gates at work: Crystal structure of Rad53 bound to Dbf4 and Cdc7

This research was originally published in Scientific Reports and is reproduced with permission. Almawi AW, Matthews LA, Larasati, Myrox P, Boulton S, Lai C, Moraes T, Melacini G, Ghirlando R, Duncker BP, and Guarné A. (2016). 'AND'logic gates at work: Crystal structure of Rad53 bound to Dbf4 and Cdc7. Sci Rep 6:34327. 10.1038/srep34237.

A.W.A. and L.A.M. conducted, analyzed and interpreted the structural characterization of the complexes.
A.W.A., L., P.M. and B.P.D. Y2H conducted, analyzed and interpreted the Y2H experiments (Figure 3.3 and 3.4 and Appendix A Figure 3 and 4).
L.A.M., S.B. and G.M. designed, conducted, analyzed and interpreted the NMR experiments.
R.G. collected and analyzed analytical ultracentrifugation data.
C.L. and T.M. provided technical and intellectual input to analyze the affinity of the binary and ternary complexes.
A.W.A. and A.G. wrote the manuscript with contributions from all authors.
A.G. designed the research, interpreted data and secured funding.

3.1 Introduction

Stress generated during DNA replication is one of the biggest hurdles proliferating cells face to preserve genome integrity. Therefore, eukaryotic cells have conserved surveillance mechanisms, known as cell cycle checkpoints, to detect and repair damage generated during DNA replication (Branzei & Foiani, 2005; Putnam et al., 2009; Segurado & Tercero, 2009; Zegerman & Diffley, 2009). Rad53, and its mammalian ortholog the checkpoint kinase 2 (Chk2), are key effector kinases of the DNA replication checkpoint (Bartek & Lukas, 2003; Rouse & Jackson, 2002). Loss-of-function mutations in *RAD53* cause loss of viability due to an essential function in maintaining dNTP levels during DNA replication, while hypomorphic *RAD53* mutations result in DNA damage sensitivity and deficits in checkpoint responses (Allen et al., 1994; Fay et al., 1997; Moore, 1978; Paulovich & Hartwell, 1995). Similarly, loss-of-function mutations in Chk2 lead to a defective checkpoint response (Hirao et al., 2000; Matsuoka et al., 1998).

Rad53 contains two forkhead-associated (FHA) domains, as well as two SQ/TQ cluster domains (SCD), flanking its kinase domain. FHA domains are commonly found in DNA damage response proteins and mediate protein-protein interactions by recognizing phosphorylated epitopes on their binding partners (Durocher et al., 2000). During the replication checkpoint, phosphorylation-dependent interactions mediated by the FHA domains of Rad53 trigger hyperphosphorylation of the N-terminal SCD domain and lead to the full activation of Rad53 (Pellicioli & Foiani, 2005). It was generally believed that FHA domains recognize unstructured sequences containing a phosphorylated amino acid –often a threonine. Recent studies, however, have shown that FHA domains can also use alternate surfaces for

protein oligomerization and to mediate protein-protein interactions (Luo et al., 2015; Matthews et al., 2014; Nott et al., 2009; Raasch et al., 2014; Weng et al., 2015). The Dbf4-dependent kinase (DDK) and Rad9 are two binding partners of Rad53 during the replication checkpoint response. Dbf4 preferentially interacts with the N-terminal FHA domain (FHA1) of Rad53 (Duncker et al., 2002), whereas Rad9 binds the C-terminal FHA domain (FHA2) (Sun et al., 1998), reinforcing the idea that the two FHA domains recognize distinct features on their binding partners. DDK, a heterodimer the Ser/Thr kinase Cdc7 and its regulatory subunit Dbf4, is one of the kinases known to hyperphosphorylate Rad53 (Ogi et al., 2008). Reciprocally, Rad53 phosphorylates DDK to inhibit its activity, thereby preventing the firing of late replication origins (Zegerman & Diffley, 2010). This is crucial as it inhibits S-phase progression and allows cells to recover from replication stress.

The interaction between Rad53 and DDK is of special interest because it involves multiple interfaces of the FHA1 domain. The phosphoepitope-binding site recognizes an epitope present in DDK (Aucher et al., 2010), whereas one of the lateral surfaces of FHA1 interacts with the modified BRCT domain of Dbf4 (Matthews et al., 2014), herein referred to as HBRCT domain due to the presence of an additional a-helix at the N-terminus of the domain. However, like many other relevant signaling interactions, the Rad53 and Dbf4 association is weak and presumably transient. The latter are especially difficult to study for effector proteins like Rad53, because they often interact with multiple partners using a common interface. To understand how Rad53 manages its multiple interactions during the steps leading to Cdc7 inhibition, we stabilized the Rad53:Dbf4 complex using glycine-rich linkers. We generated chimeras expressing the BRCT (Dbf4) and FHA1 (Rad53) domains in

tandem and solved the crystal structures of these chimeras in the absence and presence of a phosphorylated epitope derived from Cdc7. These are the first structures of an FHA domain bound to a binding partner through a non-canonical interface and they reveal a unique bipartite interface between Rad53 and Dbf4 that provides exquisite specificity despite the minimal interaction surface.

3.2 Results

3.2.1 The Dbf4(L)Rad53 chimeras have a weak self-association

We have previously shown that the HBRCT domain of Dbf4, consisting of a BRCT fold immediately preceded by a helix, is necessary and sufficient for the interaction with the FHA1 domain of Rad53 (Matthews et al., 2012). The interaction with this domain of Dbf4 is mediated by one of the lateral surfaces of the FHA1 domain rather than its phosphopeptide-binding pocket (Matthews et al., 2012). However, the instability of the HBRCT domain at high concentrations prevented the characterization of the reciprocal surface in Dbf4. Based on our biochemical, genetic and structural data, we generated a preliminary model of the Dbf4-Rad53 complex using the Rosetta software. In this model, the lateral surface of the FHA1 domain interacted with the concave surface of the HBRCT domain of Dbf4 leaving the termini of both domains in close proximity. Therefore, we anticipated that we could stabilize the interaction by producing the two domains as a single polypeptide chain. We fused the FHA1 domain of Rad53 at the C-terminus of the HBRCT domain of Dbf4 directly, or using a five-residue glycine/serine-rich linkers (Dbf4(0)Rad53 and Dbf4(5)Rad53; Figure 3.1A). The resulting chimeras were monodisperse and behaved as monomers in solution as judged by dynamic light

scattering and size exclusion chromatography. Despite being predominantly monomeric, the elution times from an analytical size exclusion chromatography varied in a concentration-dependent manner suggesting a weak intermolecular association (Figure 3.1B and Appendix A Figure 1).

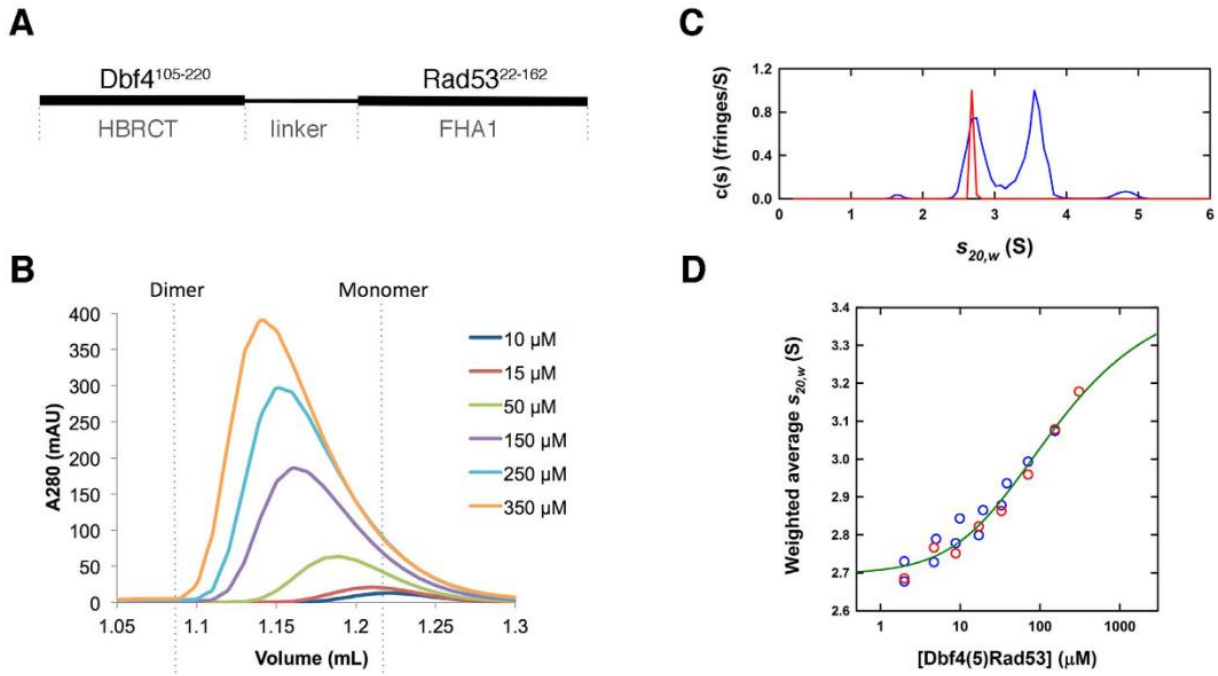

Figure 3.1. The Rad53(5)Dbf4 chimera exists in a monomer-dimer equilibrium. (A) Cartoon depicting how the Rad53(L)Dbf4 chimeras were generated. (B) Size exclusion chromatography profiles of Dbf4(5)Rad53 at increasing protein concentrations. Elution volumes for a ideal Dbf4(5)Rad53 monomer and dimer are indicated as dashed lines. (C) Normalized interference c(*s*) profiles for Dbf4(5)Rad53 at 2 µM (red) and 310 µM (blue) supporting a reversible monomer-dimer equilibrium. (D) Dependence of the weighted-average $s_{20,w}$ on the loading concentration for absorbance (blue) and interference (red) sedimentation velocity data, along with the global best-fit monomer-dimer isotherm (green).

We carried out a series of sedimentation velocity experiments on the Dbf4(5)Rad53 chimera at increasing loading concentrations. The sedimentation experiments demonstrated the absence of very large species and yielded c(*s*) profiles that supported a reversible monomer-

dimer equilibrium (Figure 3.1C). Dimerization of chimeric proteins is not uncommon and it indicates that the two components of the chimera associate intermolecularly (Foss et al., 2005; Wang et al., 2008; Williams et al., 2014). A weighted-average sedimentation coefficient isotherm was constructed and analyzed in terms of reversible monomer-dimer equilibrium (Figure 3.1D), to obtain a dissociation constant K_d of 130 μM. As the isotherm does not adequately cover the high concentration region there may be significant errors in this value. Based on the reduced chi-squared, using the method of F-statistics (Johnson, 1992), we estimate 68% and 95% confidence limits of the K_d to be 70–260 μM and 50–400 μM. These values indicate the order of magnitude of the interaction and confirm that the HBRCT domain of Dbf4 and the FHA1 domain of Rad53 associate weakly.

3.2.2 The Dbf4(L)Rad53 chimeras recreate the Dbf4:Rad53 interaction

To avoid constraints imposed by the presence of the linker joining the two proteins, we set crystallization trials of two chimeras: Dbf4(0)Rad53 and Dbf4(5)Rad53. The chimera containing a five-residue linker readily yielded diffraction-quality crystals (See Table 2.3). The asymmetric unit contained four copies of the Dbf4(5)Rad53 chimera arranged to form four Dbf4:Rad53 complexes. The C-terminal end of Dbf4 (residues 216-220) and the N-terminal end of Rad53 (residues 22-29), as well as the five amino acid linker, were disordered in the structure (Appendix A Figure 2). This results in almost twenty amino acids missing in each polypeptide chain. The distance between the last ordered residue of the HBRCT domain of Dbf4 and the first ordered residue in the closest FHA1 neighbors, the crystal packing contacts and the behavior in solution of the chimeras, confirms that the Dbf4:Rad53 complex forms

inter-molecularly. Importantly, the four complexes in the asymmetric unit had identical interfaces, indicating that the linkers did not constrain complex formation.

The FHA1 and HBRCT domains have identical architectures in the complex as in their unbound structures (Figure 3.2A). However, the helix α0 of the HBRCT domain swivels about twenty degrees upon complex formation (Figure 3.2A). In good agreement with our previous results showing that the pThr-binding pocket of the FHA1 domain does not mediate the interaction with Dbf4 (Matthews et al., 2014), the complex forms through the lateral surface of the FHA1 domain defined by the β2-β1-β11-β10-β7-β8 strands and the concave surface of the HBRCT domain (Figure 3.2B). This interface, however, is quite limited because Dbf4 only contacts two small regions on each side of the lateral surface of Rad53. On one side of the interface, the side chains of residues Arg35 (β1), Ile37 (β1), Val144 (β11) and Phe146 (β11) of Rad53 are cradled by the α0 helix of the HBRCT domain, specifically by residues Glu111, Trp112, Asn115 and Trp116, defining interface I (Figure 3.2C). On the other side, the loop containing residues Tyr198 and Lys200 of Dbf4 wraps around the β7/β8 loop of the FHA1 domain enabling the interaction between the amine group of Lys200 and Asn112 (β7) in Rad53 defining interface II (Figure 3.2D). Globally the two interfaces bury a mere 10% of the total accessible surface area of the FHA1 (755 out of 6,664 $Å^2$) and the HBRCT (801 out of 7,799 $Å^2$) domains, a value that is below the cutoff for specific interactions as judged using the PISA server (Krissinel & Henrick, 2007). This is not surprising in light of the dissociation constant estimated from the sedimentation velocity and NMR analysis (Figure 3.1 and (Matthews et al., 2014)).

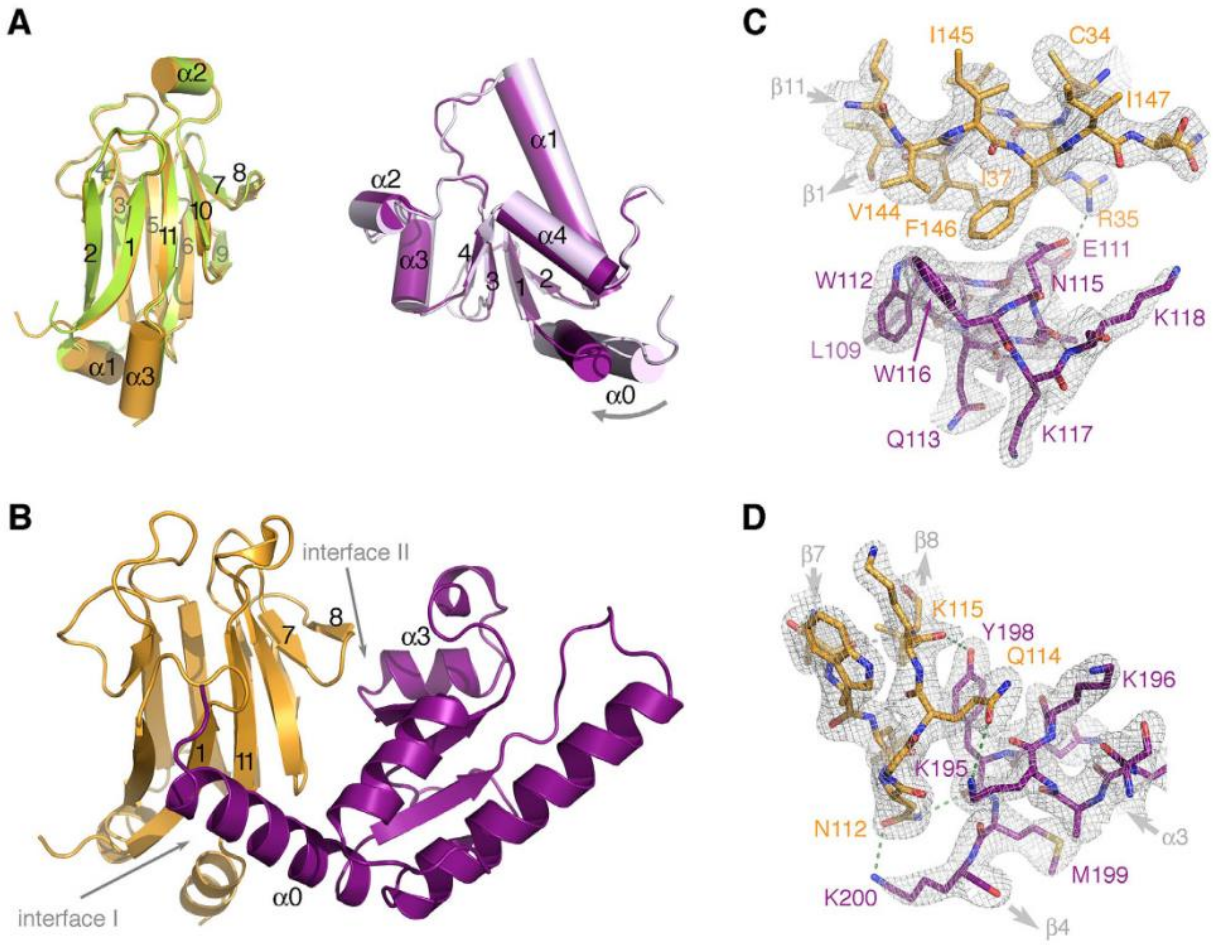

Figure 3.2. Structure of the Rad53(5)Dbf4 chimera. (A) Comparison of the structures of the FHA1 domain of Rad53 and the HBRCT domain of Dbf4 when crystallized on their own (PDB ID: 1G6G and 3QBZ) or forming a complex. The FHA1 domain is shown in green (1G6G) or gold (complex) and the HBRCT domain is shown in lilac (3QBZ) or purple (complex) with secondary structure elements labeled for clarity. (B) Ribbon diagram of the crystal structure of the Rad53:Dbf4 complex with Rad53 colored gold and Dbf4 colored purple. The interfaces mediating the complex, as well as the pThr-binding groove, are labeled. Detailed views of the interactions defining interface I (C) and interface II (D). Rad53 and Dbf4 residues are shown as sticks colored as in (B) and labeled. Refined 2Fo-Fc electron density maps are shown as a grey mesh contoured at σ = 1.2. Hydrogen bonds are shown as dashed lines.

3.2.3 Rad53 and Dbf4 contribute asymmetrically to the interface of the complex

The residues of the FHA1 domain mediating the interaction with Dbf4 in the crystal structure of the Dbf4(5)Rad53 chimera are the same as those previously identified using NMR

(Matthews et al., 2014). Our previous work, however, could not explain why multiple point mutations on the FHA1 surface were required to abrogate complex formation (Matthews et al., 2014). These results were intriguing because Rad53 and Dbf4 interact with low affinity and, hence, we had not anticipated the need of multiple mutations to abrogate the interaction. Since the point mutations in Rad53 were designed based on sequence conservation, we had a better sampling of interface I than interface II (Figure 3.2). Therefore, we decided to dissect the contributions of both interfaces to the complex formation.

We generated single point mutations in the FHA1 domain affecting either interface I (Phe146Ala) or interface II (Asn112Ala), as well as a double point mutation affecting both interfaces (Asn112Ala/Phe146Ala). We then measured the ability of these variants to interact with full-length Dbf4 using a yeast two-hybrid assay. As we expected from our previous work, the FHA1-Asn112Ala had a mild, yet significant, binding defect (Figure 3.3A and Appendix A Figure 3A). Conversely, the FHA1-Phe146Ala variant interacted with Dbf4 better than wild type FHA1 suggesting that a smaller side chain at this position may help accommodate helix α0 of the HBRCT. The combination of both changes had a stronger defect than the FHA1-Asn112Ala variant, but retained about half of the residual binding to Dbf4 (Figure 3.3A). When we conducted the reciprocal experiment, the results were more drastic. The Dbf4-Leu109Ala/Trp112Asp variant (affecting interface I) completely abrogated the interaction with the FHA1 domain, whereas variants affecting interface II had wide-ranging effects (Figure 3.3B). On our structure, the loop containing residues Tyr198 and Lys200 of Dbf4 wraps around the β7/β8 loop of the FHA1 domain enabling the interaction with Asn112 (β7) in Rad53 (Figure 3.2D). Mutation of Tyr198Ala did not affect the interaction with the FHA1

domain, whereas mutation of Lys200Ala disrupted binding to the FHA1 domain (Figure 3.3B). Collectively these data suggest that hydrophobic contacts and the relative rigid body movement of helix α0 drive the interaction at interface I, whereas polar interactions determine interface II. Furthermore, they confirm that Dbf4 and Rad53 do not contribute equally to each interface, but both contact points are important for complex formation.

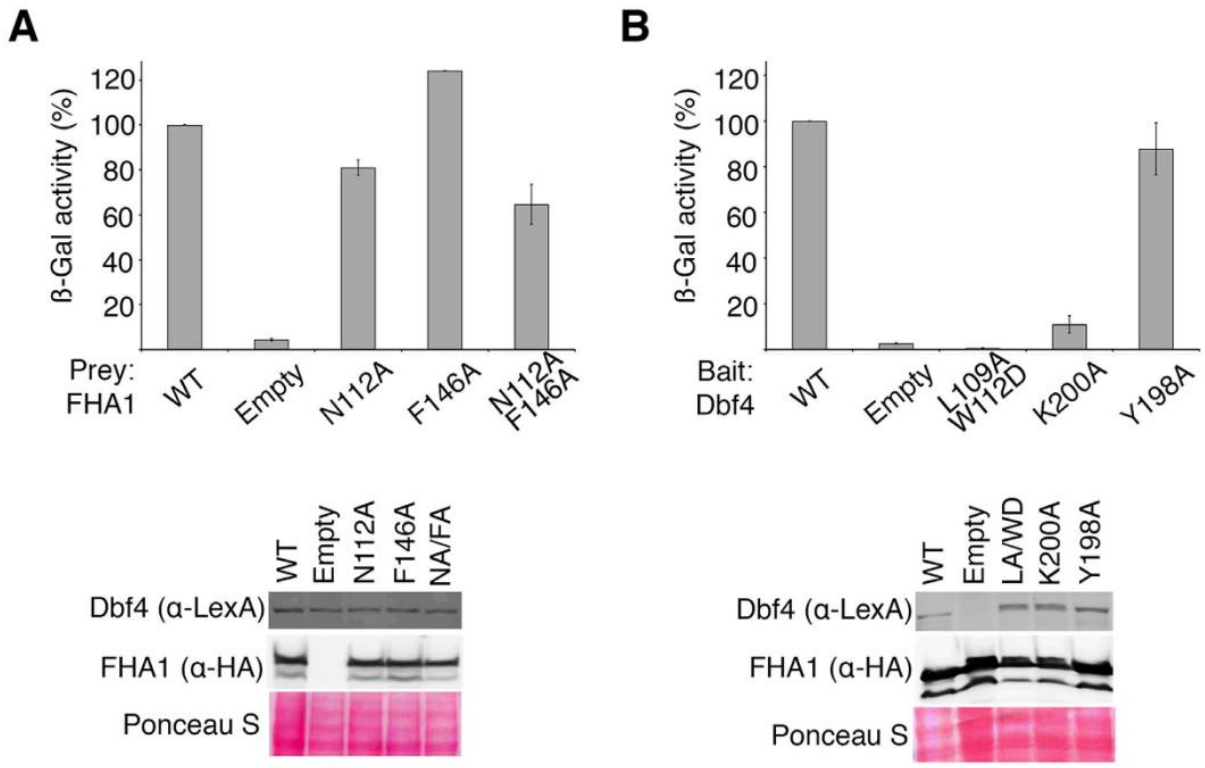

Figure 3.3. Two discrete interfaces contribute to the Rad53:Dbf4 interaction. (**A**) Yeast two-hybrid analysis using wild type Dbf4 as the bait and variants of the FHA1 domain of Rad53 as the preys. (**B**) Yeast two-hybrid analysis using variants of Dbf4 as the baits and the wild type FHA1 domain of Rad53 as the prey. In each case, the interaction is shown as a percentage of β-galactosidase activity for the interaction between wild-type proteins and represents the mean of three independent measurements (error bars represent S.D). Bait and prey expression levels were analyzed by the representative Western blotting (of three independent experiments performed) and relative protein loading assessed by Ponceau S staining. See Appendix A Figure 3 for original gels/blots.

3.2.4 Rad53 interacts simultaneously with Dbf4 and a phosphorylated peptide

The combination of hydrophobic and polar interactions segregated in two different contact areas could provide the means to regulate complex formation upon binding of additional partners. Since a phosphorylated binding epitope is necessary for the interaction of Rad53 with DDK, we sought to determine the structure of the Dbf4(L)Rad53 chimera bound to a phosphorylated peptide (Table 2.3).

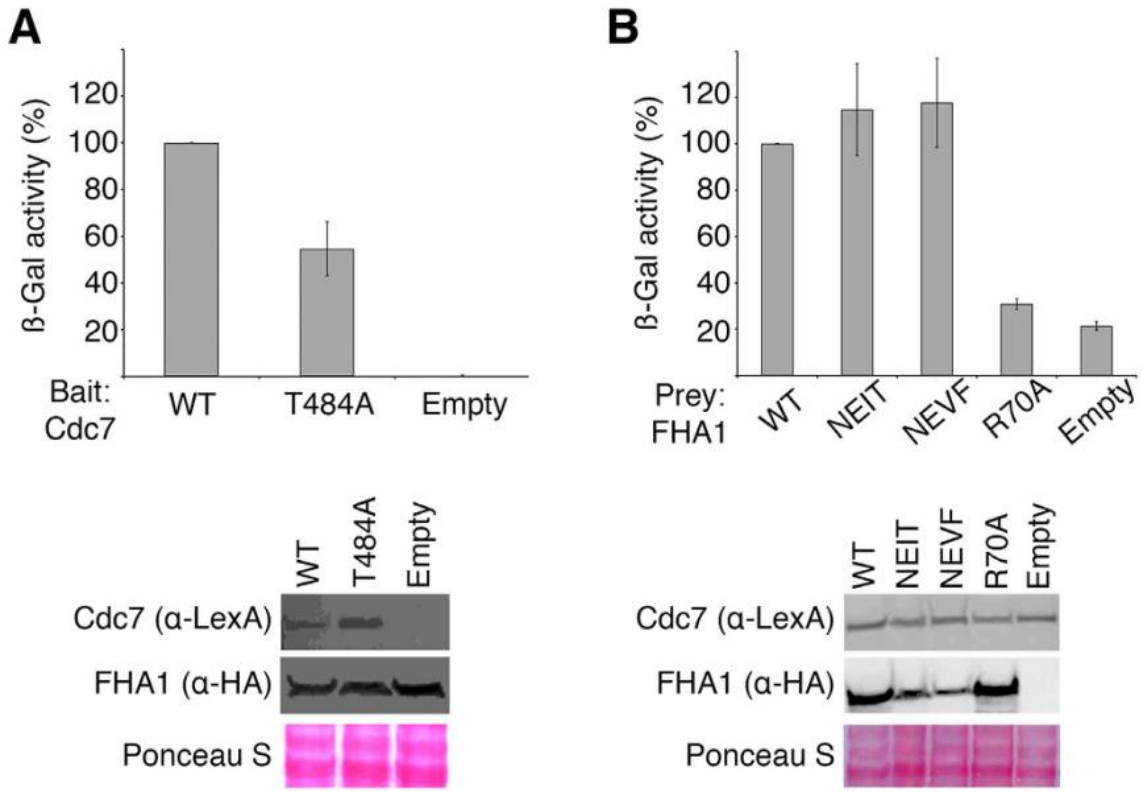

Figure 3.4. Rad53 recognizes a phosphorylated epitope in the Cdc7 subunit of the DDK complex. (**A**) Yeast two-hybrid analysis using either wild type or a T484A variant of Cdc7 as the baits and wild type FHA1 domain of Rad53 as the prey. (**B**) Yeast two-hybrid analysis using wild type Cdc7 as the bait and variants of the FHA1 domain of Rad53 as the prey. Bait and prey expression levels were analyzed by the representative Western blotting (of three independent experiments performed) and relative protein loading assessed by Ponceau S staining. See Appendix A Figure 4 for original gels/blots.

The fragment of Cdc7 encompassing residues 294-493 interacts reproducibly with the FHA1 domain of Rad53 (Aucher et al., 2010). This region only contains one TXXD motif (^{484}TDED^{487}) that is conserved and has high phosphorylation probability (Aucher et al., 2010). In good agreement, a Cdc7 variant encompassing a Thr484Ala point mutation reduces the interaction of Cdc7 with the FHA1 domain of Rad53 to 50% of wild type (Figure 3.4A and Appendix A Figure 4). Reciprocally, a variant of Rad53-FHA1 unable to bind phosphorylated targets (FHA1-Arg70Ala) abrogates the interaction with Cdc7 (Figure 3.4B). The differences between the Cdc7-Thr484Ala and Rad53-Arg70Ala variants suggest that Rad53 may be able to bind other epitopes in Cdc7 in the absence of Thr484.

Conversely, variants disrupting the Rad53:Dbf4 interface do not affect binding to Cdc7 (Figure 3.4B and (Matthews et al., 2014)). Since we have previously shown that a peptide derived from this motif of Cdc7 (pPEP, ^{480}DGES**pT**DEDDVVS^{491}) binds to the FHA1 domain of Rad53 in a phosphorylation-dependent manner in vitro, we used this peptide for subsequent crystallographic studies. Crystals of the ternary Rad53-Dbf4-Cdc7 complex grew in the $P2_1$ space group and diffracted X-rays beyond 2.3 Å resolution. We determined the structure by molecular replacement using the structures of the individual FHA1 and HBRCT domains as search models. The molecular replacement solution showed well-defined electron density for the two domains, as well as the main chain and most side chains of the phosphorylated peptide (Figure 3.5A-B). Similar to other structures of FHA1 domains bound to phosphorylated peptides, pPEP is bound at one end of the FHA1 domain and interacts with residues in the β3/β4, β4/β5 and β6/β7 loops (Durocher et al., 2000). The phosphate moiety of pThr484 is held in place through hydrogen bonds with Arg70, Ser85, Asn86 and Thr106 (Figure 3.5C); the

pT+3 aspartate residue (Asp487) is anchored through a salt bridge with Arg83; and the main chain of the intervening residues is further stabilized through hydrogen-bonds with the main chain carbonyl of Ser82 and the side chain of Asn107 (Figure 3.5D).

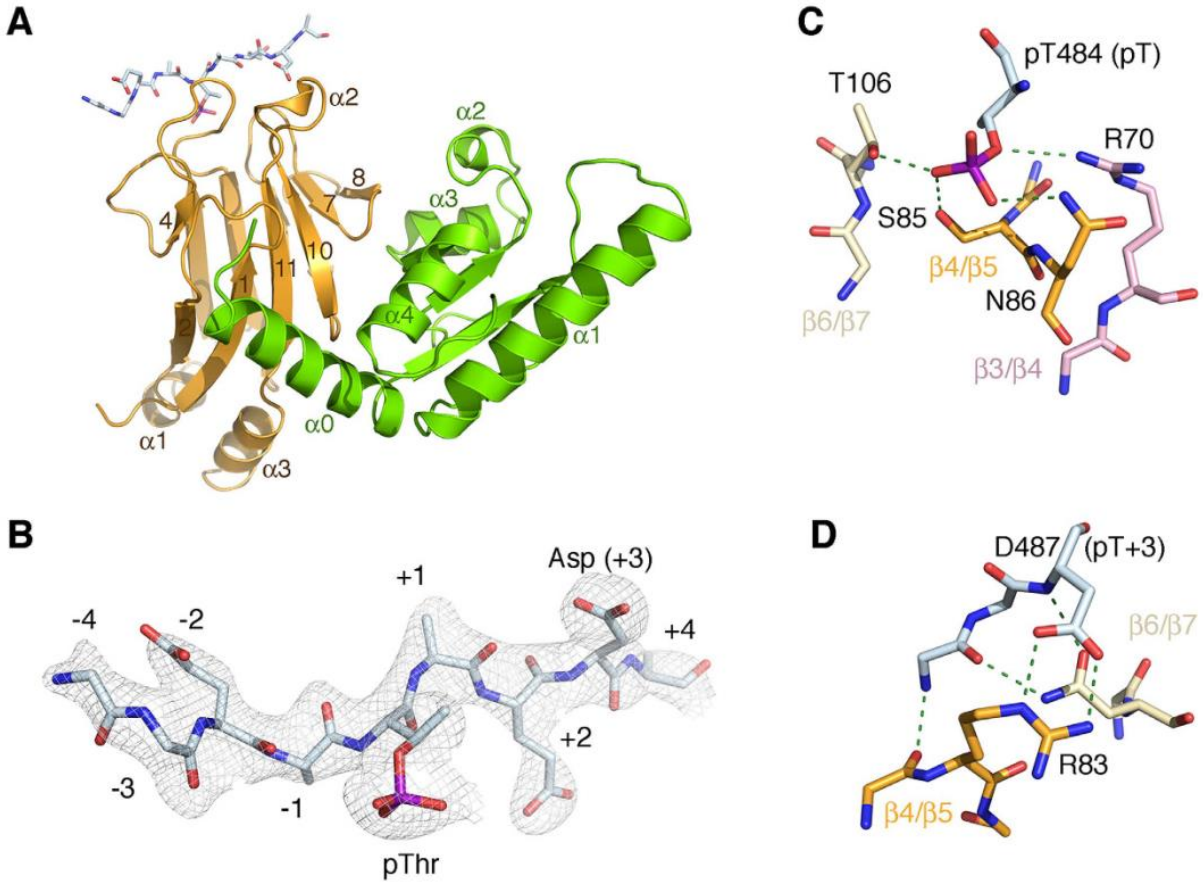

Figure 3.5. Structure of Rad53:Dbf4:Cdc7 ternary complex. (A) Ribbon representation of the ternary complex on a similar view as in Figure 3.2. Rad53 (orange) and Dbf4 (green) are shown as ribbons. The Cdc7-derived peptide (pPEP) is shown as colored coded sticks. (B) Detail of the electron density map around the phosphorylated peptide shown as a grey mesh contoured at σ = 1.0. (C) Detail of the hydrogen-bond network stabilizing pThr484. (D) Detail of the hydrogen bond interactions defining the specificity at the pT + 3 position of the peptide, as well as additional hydrogen bonds stabilizing the main chain of the peptide. Hydrogen bonds are shown as green dashed lines.

The Dbf4:Rad53 interface is similar, but not identical, to the binary complex. Superimposition of the FHA1 domains in the binary and ternary complexes revealed that the β1 strand and the β1/β2 loop were virtually invariant (r.m.s.d. < 0.1 $Å^2$). Therefore, we used this region of the FHA1 to superimpose and compare the two complexes. As expected, the loops defining the pThr-binding groove of the FHA1 domain had larger deviations (0.34 < r.m.s.d. < 0.63), caused by the binding of the phosphopeptide. Conversely, the residues in FHA1 mediating the interaction with Dbf4 were barely affected by phosphopeptide binding (0.15 < r.m.s.d. < 0.35).

Binding of the phosphopeptide, however, induces a small rigid body movement of Dbf4 around the two interfaces holding the complex (Figure 3.6A). The HBRCT domain seesaws pushing helix α1 away from the FHA1 domain while pulling the α0/β1 loop towards the FHA1 domain. This rotation is identical for both complexes in the asymmetric unit and, though subtle, the movement is enough to reorganize some of the residues at both interfaces. Upon binding to pPEP, the side-chain of Lys118 (interface I in Dbf4) comes close to the side-chains of Asp123 (Dbf4) and Asp149 (Rad53) stabilizing the interaction of the C-terminus of helix α0 in Dbf4 with Rad53 (Figure 3.6B). On the ternary complex, Lys200 (interface II in Dbf4) is not hydrogen-bonded to Asn112. Binding to pPEP pushes the α3/β4 loop of Dbf4 closer to the β10 strand where the new conformation of Lys200 is stabilized through hydrogen bonds with Gln126 and Asp128 (Figure 3.6C).

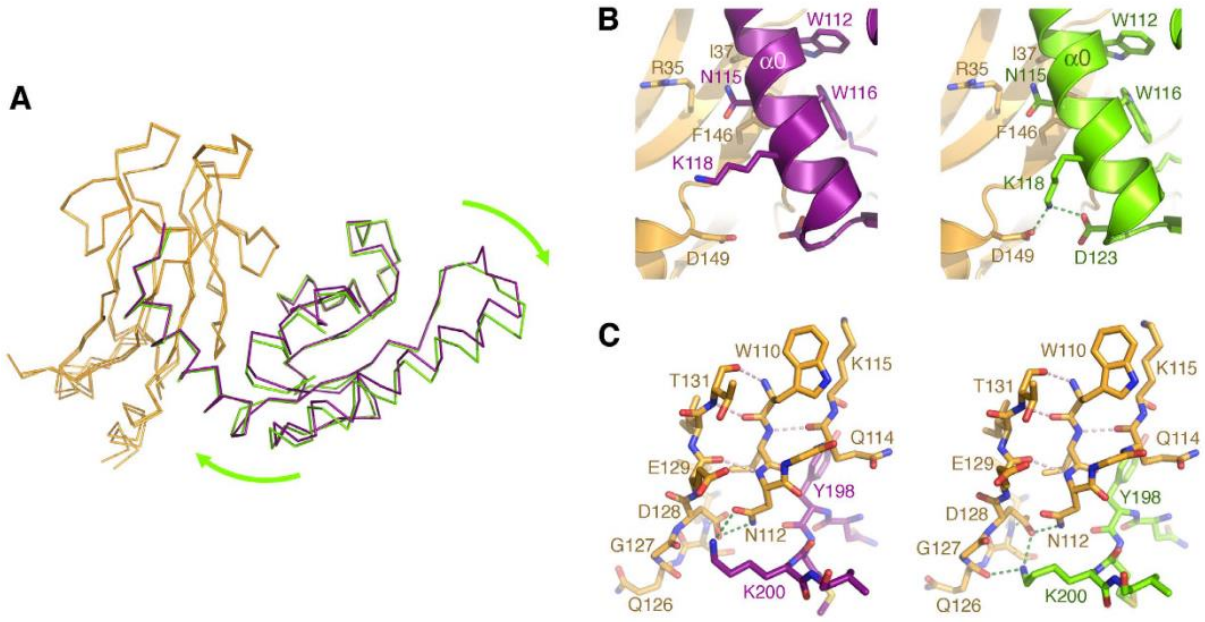

Figure 3.6. Peptide-binding induces a rigid body movement of Dbf4. (A) Opposite views of the Rad53:Dbf4:Cdc7 complex (gold-green) superimposed onto the Rad53:Dbf4 complex (gold-purple). (B) Detail of the different interactions of Lys118 (Dbf4) in in the binary (left) and ternary (right) complexes. (C) Detail of the conformational change imposed onto the side chain of Lys200 (Dbf4) upon binding of the phosphorylated peptide. In the binary complex (left-side panel) Lys200 interacts with Asn112 (Rad53), whereas in the ternary complex (right-side panel) interacts with Gly127 and Asp128 (Rad53).

3.2.5 Phosphopeptide binding modulates the Rad53:Dbf4 interaction

Given the subtle movement of the HBRCT domain, the analysis of the two interfaces did not show significant differences in the extension of the interface or solvation energy (Table 3.1). Dbf4 had a minimal gain in solvation energy suggesting the HBRCT domain has more surface exposed residues in the ternary than the binary complexes (Table 3.1). The differences between the Dbf4:Rad53 interface in the binary and ternary complexes could indicate that binding of the phosphopeptide allosterically regulates the interaction. However, these differences could also be due to crystal packing environment or the different linker length of the fusions.

Table 3.1. PISA analysis of the Dbf4:Rad53 and Dbf4:Rad53:Cdc7 complexes

Complex	Interface (Å²)	ΔG solvation (kcal/mol)	Solvation Energy contribution			
			Dbf4		Rad53	
			Structure	Average gain	Structure	Average gain
Rad53:Dbf4	684–707	−3.5 – −5.0	−96.3	−3.75	−115	−1.5
Rad53:Dbf4:Cdc7	684	−3.8	−96.7	−2.2	−115.1	−1.3

The asymmetric unit of the binary complex included four Dbf4(5)Rad53 molecules defining four Dbf4:Rad53 interfaces, whereas that of the ternary complex included two Dbf4(0)Rad53 molecules defining two Dbf4:Rad53 interfaces. Superimposition of each ternary complex onto any of the binary complexes revealed that the peptide moiety could only be accommodated in half of the complexes, explaining why crystals of the ternary complex grew in different conditions. However, no other crystal contacts mediated by the FHA1 or HBRCT domains enhanced or prevented the movement in Dbf4. Therefore, phosphopeptide binding rather than crystal packing is the likely driving force of the movement.

We have previously shown that losses of cross-peak intensity in the HSQC spectrum of ^{15}N-labeled Rad53 upon binding Dbf4 serve as sensitive reporters to map the interface of the complex (Matthews et al., 2014). If phosphopeptide binding to the FHA1 domain weakened the interaction, we would expect an enhancement of cross-peak intensities for the Rad53 residues at the interface with Dbf4. Despite maintaining similar conformations in the binary and ternary crystal structures, two residues on interface I (Ile37 and Phe146) showed increased cross-peak intensities in the ternary complex (Appendix A Figure 5). These observations are

consistent with the idea that phosphopeptide binding to the FHA1 domain weakens the Rad53:Dbf4 interaction. However, some surface residues beyond the complex interface also show variations of cross-peak intensities between the two complexes (Appendix A Figure 5). Interestingly, a number of residues within the hydrophobic core of Rad53 display decreased cross-peak intensities upon phosphopeptide binding (Appendix A Figure 5). These residues form a continuous network from the β3/β4 loop (Phe68-Gly69) to the β9/β10 loop (Leu124-Ser125) that propagates across the β-sheet defined by strands β4-β3-β5-β6-β9. Such intensity losses typically reflect changes in internal dynamics and could possibly reveal an allosteric network to report the presence of the phosphorylated peptide to the Rad53:Dbf4 interface. While these changes could explain how the two inputs of the logic gate sense each other to elicit a single output, the idea awaits further validation.

3.3 Discussion

Yeast genetics has delineated the factors and hierarchy of interactions involved in the DNA damage response, but the molecular detail has remained elusive because most of the interactions driving the checkpoint response are transient. This problem is aggravated for 'AND' logic gates because they recognize two or more inputs to produce a single signal (Hasty et al., 2002; Lee et al., 2008a; Zhang & Durocher, 2008), but disruption of any of the inputs disrupts the output leading to technically biased interpretations. We have found that the FHA1 domain of Rad53 functions as a 'AND' logic gate for its interaction with DDK, thereby explaining more than a decade of partly conflicting results (Chen et al., 2013; Duncker et al., 2002; Matthews et al., 2012, 2014; Matthews & Guarne, 2013). The crystal structures of the

FHA1 domain of Rad53 bound to one (HBRCT) or both (HBRCT and phosphoepitope) partners in the DDK complex presented here unveil how this logic gate simultaneously recognizes two inputs and provide the first image of an FHA domain recognizing a binding partner through a non-canonical interface.

The interaction of Rad53 with the DDK complex is reminiscent of the interaction between Chk2 (the human ortholog of Rad53) and BRCA1, where the tandem BRCT repeat of BRCA1 simultaneously recognizes two distal surfaces in the FHA domain of Chk2 (Li et al., 2002). In the BRCA1:Chk2 complex, the interaction involves the pThr-binding site and a conserved hydrophobic patch on one of the lateral surfaces of the FHA domain. Disruption of either contact point prevents the interaction, and mutation of the hydrophobic patch has been linked to Li-Fraumeni syndrome (Li et al., 2002). However, Dbf4 and BRCA1 do not interact with the same lateral surface of the FHA domains of Rad53 and Chk2, exposing the extreme plasticity of FHA domains to enhance binding specificity.

Both Rad53 and Chk2 dimerize in solution and this is important to promote kinase activation by trans-autophosphorylation (Cai et al., 2009; Wybenga-Groot et al., 2014). Dimerization is triggered by damage-induced phosphorylation of a threonine within the SCD of the kinase. The dimers associate in a face-to-face configuration that promotes the swap of the activation loops for phosphorylation in trans (Cai et al., 2009; Schwarz et al., 2003). In the crystal structure of Chk2, one of the lateral surfaces of the FHA domain also contributes to the dimerization interface and, in fact, the requirement of a phosphorylated threonine residue is bypassed by protein overexpression indicating that the kinase and FHA mediated interactions suffice to stabilize the dimer (Cai et al., 2009). The surface of the FHA domain involved in the

dimerization interface is the same as that of Rad53 mediating the interaction with Dbf4 (Appendix A Figure 6). However, the two kinases transition to monomers to phosphorylate downstream targets (Ahn & Prives, 2002; Ahn et al., 2002; Cai et al., 2009), implying that dimer formation and subsequent dissociation may determine the hierarchy of checkpoint events.

In contrast to the Chk2 dimer, where the entire lateral face of the FHA domain contributes to dimer formation, Dbf4 only contacts two points on the lateral face of the FHA1 domain. Interestingly, mutations on the two surfaces are not reciprocal indicating that each partner contributes asymmetrically to the two small interfaces mediating the interaction with Dbf4, thereby suggesting a sophisticated way to gain binding-specificity without strengthening the interaction. To our knowledge, this is the first crystal structure of an FHA domain bound to a binding partner through a non-canonical interface and lays the foundation to study how FHA domains can exploit canonical and non-canonical interactions to increase binding specificity of low-affinity interactions and, in turn, extend the functional repertoire of this phosphoepitope binding module.

Chapter 4

A proline-rich Rif1 motif mediates interaction with Dbf4, promoting DNA replication and resistance to genotoxic stress

Figure 4.4A. Analysis was conducted by Dr. Andrew Doxey.

Figure 4.6B. Experiments were performed by Matthew J. Schmitz.

Figure 4.7. Larasati performed experimental design, yeast strain construction, data interpretation and analysis. Matthew J. Schmitz assisted in yeast strain construction and optimizing the spotting conditions. Larasati and Matthew J. Schmitz performed independent replicates for Figure 4.7A. Matthew J. Schmitz performed independent replicates for Figure 4.7B.

Appendix 4 Figure 1. Larasati performed experimental design, yeast transformation, data interpretation and analysis. Larasati and Matthew J. Schmitz performed independent replicates of the competitive yeast two-hybrid assays.

4.1 Introduction

Faithful DNA replication is fundamental to the proliferation of every living organism. Its mechanisms and levels of regulation have been studied extensively to understand the processes that drive the cell cycle, maintain genomic integrity and, eventually, translate these findings into clinical applications. Eukaryotes normally duplicate their entire genomes once per cell cycle. To maintain the correct ploidy, re-activation of origins of DNA replication during the same cell cycle is strictly inhibited. This is achieved, in part, by temporally separating the assembly of the replicative helicase at origins (origin licensing) and its activation (origin firing) into different stages of the cell cycle (Bell & Labib, 2016).

Origin firing in S phase is triggered by a series of phosphorylation events, involving Dbf4-dependent kinase (DDK) and cyclin-dependent kinase (CDK). As cells progress from G1 to S phase, there are spikes in the expression levels of Dbf4, the regulatory subunit of DDK (Nougarède et al., 2000; Oshiro et al., 1999; Pasero et al., 1999) and the budding yeast S-phase cyclins Clb5 and Clb6 (Schwob & Nasmyth, 1993). DDK phosphorylates the helicase core Mcm2-7, targeting Mcm4 and relieving its inhibitory effect on helicase activity (Sheu & Stillman, 2010). CDK phosphorylates Sld3 and Sld2 and drives their interaction with Dpb11, which promotes the recruitment of the accessory factors of the helicase, Cdc45 and GINS, respectively (Tanaka et al., 2007; Zegerman & Diffley, 2007). CDK phosphorylation also allows the formation of a complex between Sld2, Dpb11, GINS, and DNA polymerase ε (Muramatsu et al., 2010). This ensures that DNA unwinding activity by the helicase is always followed by DNA synthesis. The result of DDK and CDK phosphorylation is the active helicase in the form of Cdc45-Mcm2-7-GINS (CMG).

To avoid any origin firing outside of S phase, the cells restrict DDK and S-phase CDK activities temporally. Dbf4 is degraded by the anaphase-promoting complex/cyclosome (APC/C) during mitosis and its expression level only increases again in late G1/early S phase (Cheng et al., 1999; Ferreira et al., 2000). However, basal levels of Dbf4 escape this process, potentially resulting in residual DDK activity and, consequently, premature phosphorylation of Mcm4 in G1 phase. Indeed, Mcm4 is phosphorylated in a DDK-dependent manner in G1 phase when one of the DNA replication timing regulators, Rap1-interacting factor 1 (Rif1), is removed (discussed further below) (Davé et al., 2014; Hiraga et al., 2014; Mattarocci et al., 2014). Cells are equipped with a safeguard mechanism to counteract this that employs Protein Phosphatase-1 (PP1). This enzyme has been shown to have a broad range of substrates, thus its specificity is determined by the ligand that targets it to the substrates (Virshup & Shenolikar, 2009). Rif1 is an evolutionarily conserved protein that has been characterized as the PP1 regulatory factor that performs this task of preventing precocious DNA replication (Davé et al., 2014; Hiraga et al., 2014; Mattarocci et al., 2014).

Rif1 was originally identified as a telomeric protein in budding yeast (Hardy et al., 1992) and has more recently been implicated as a regulator of DNA replication timing in fission yeast (Hayano et al., 2012), mouse cells (Cornacchia et al., 2012), human cells (Yamazaki et al., 2012), and budding yeast (Davé et al., 2014; Hiraga et al., 2014; Mattarocci et al., 2014). Rif1 recruits PP1 (Glc7 in budding yeast) to dephosphorylate Mcm4 in G1 phase, and deletion of Rif1 allows stable phosphorylation of this helicase subunit (Davé et al., 2014; Hiraga et al., 2014; Mattarocci et al., 2014). As the cells enter S phase, the phosphorylation of the helicase must be maintained and this is achieved, in part, by blocking Rif1-Glc7

dephosphorylation activity. Rif1 has two PP1 binding motifs (Sreesankar et al., 2012) that mediate its association with Glc7, and phosphorylation near these motifs abolishes this interaction (Davé et al., 2014; Hiraga et al., 2014; Mattarocci et al., 2014). These phosphorylations are carried out by both DDK and CDK, and corresponding phosphomimetic mutants have been shown to suppress the sensitivity of a *cdc7-1* strain at semi-permissive temperature (Davé et al., 2014; Hiraga et al., 2014). In addition, the Rif1-Glc7 interaction contributes to telomere length maintenance. Interestingly, the extension of telomeres in Δ*rif1* cells is not due to any effect on origin regulation as this still occurs in this strain background when the telomere proximal origins are deleted (Kedziora et al., 2018).

Since Rif1 is found at telomeres, an intriguing question is whether it affects replication timing locally or globally. Deletion of *RIF1* rescues the lethality of *Δhsk1* in fission yeast (Hayano et al., 2012) and suppresses the growth defect of budding yeast strains *cdc7-1* and *cdc7-4* at semi-permissive temperature (Davé et al., 2014; Hiraga et al., 2014; Mattarocci et al., 2014). Δ*rif1* exhibits late origin firing in the presence of hydroxyurea (Peace et al., 2014), earlier activation of the origins adjacent to telomeres (Davé et al., 2014; Hiraga et al., 2014; Lian et al., 2011; Mattarocci et al., 2014), and early firing of a cluster of origins at the rDNA locus (Shyian et al., 2016) that are normally silenced by Sir2 histone deacetylase (Pasero et al., 2002). Deregulation of origin firing timing through deletion of *RIF1* can result in a more pronounced checkpoint response when the cells are challenged by genotoxic stress (Shyian et al., 2016). Moreover, recent findings revealed that Rif1 binds to the origins it regulates, and a strong preference for telomere-proximal regions is mediated by Rap1 (Hafner et al., 2018).

Rif1 also associates with both early and late non-telomeric origins (Hiraga et al., 2018). These findings support the idea that Rif1 regulates replication timing genome-wide.

Other Rif1 activities besides controlling origin firing timing have also been investigated. Human Rif1 (hRif1) is not recruited to normal telomeres (Silverman et al., 2004; Xu & Blackburn, 2004), which leads to the notion that the telomere length regulation of Rif1 is specific to yeasts (Hardy et al., 1992; Kanoh & Ishikawa, 2001; Sreesankar et al., 2012). hRif1 associates with unprotected telomeres, which resemble double strand DNA breaks (DSBs), and colocalizes with stress-induced DSB foci in an ATM (ataxia telangiectasia mutated) kinase-dependent manner (Silverman et al., 2004; Xu & Blackburn, 2004). Several groups have also shown that mammalian Rif1 belongs to a protein network that promotes non-homologous end joining (NHEJ) (Chapman et al., 2013; Escribano-Díaz et al., 2013; Feng et al., 2013; Virgilio et al., 2013; Zimmermann et al., 2013), while budding yeast studies have indicated that Rif1 is similarly involved in the response to DSBs (Martina et al., 2014; Mattarocci et al., 2017).

Despite the importance of DDK phosphorylating Rif1 for cell cycle progression, the precise way the proteins associate has not been investigated. In the present study, the key determinants of the Dbf4-Rif1 interaction were identified. Furthermore, the abrogation of the Dbf4-Rif1 interaction inhibits DNA replication and, when combined with impairment in CDK phosphorylation of Rif1, results in hypersensitivity to genotoxic stress. This hypersensitivity is further exacerbated or rescued by disrupting the homologous recombination (HR) or NHEJ pathway, respectively, indicating that Rif1 functionality in both DNA replication and DNA damage responses is regulated by DDK and CDK.

4.2 Results

4.2.1 The HBRCT domain of Dbf4 is sufficient for interaction with the Rif1 C-terminus

It was previously reported that Dbf4 interacts with a minimal Rif1 C-terminal region consisting of amino acid residues 1790-1916. A truncated version of Dbf4, lacking its first 221 amino acids, failed to bind Rif1, indicating that this region is necessary to mediate the Rif1-Dbf4 association (Hiraga et al., 2014). Dbf4 residues 105-221 was previously shown to fold as a BRCT domain with an additional N-terminal helix (α0), hence it is termed the HBRCT domain. The HBRCT was further demonstrated to be both required and sufficient to mediate Dbf4 binding to the FHA1 domain of the checkpoint kinase Rad53 (Matthews et al., 2012). Under conditions of DNA damage or replicative stress, Rad53 phosphorylates Dbf4, and displaces DDK from chromatin, thus preventing subsequent origin firing (Pasero et al., 1999). It was interesting to know whether the HBRCT domain also mediates Dbf4 binding to the Rif1 C-terminus. Using yeast two-hybrid analysis, the HBRCT showed a more robust interaction with Rif1 C-terminus relative to that observed for untruncated Dbf4 (Figure 4.1). This may be due, in part, to the higher expression level of the HBRCT domain, relative to full-length Dbf4, in combination with the Rif1 C-terminus, which was consistently observed for different transformants in independent trials. Alternatively, expressing Dbf4 HBRCT on its own may better expose Rif1-binding residues than in the context of full-length Dbf4. In any case, it is concluded that the Dbf4 HBRCT domain is sufficient to interact with Rif1.

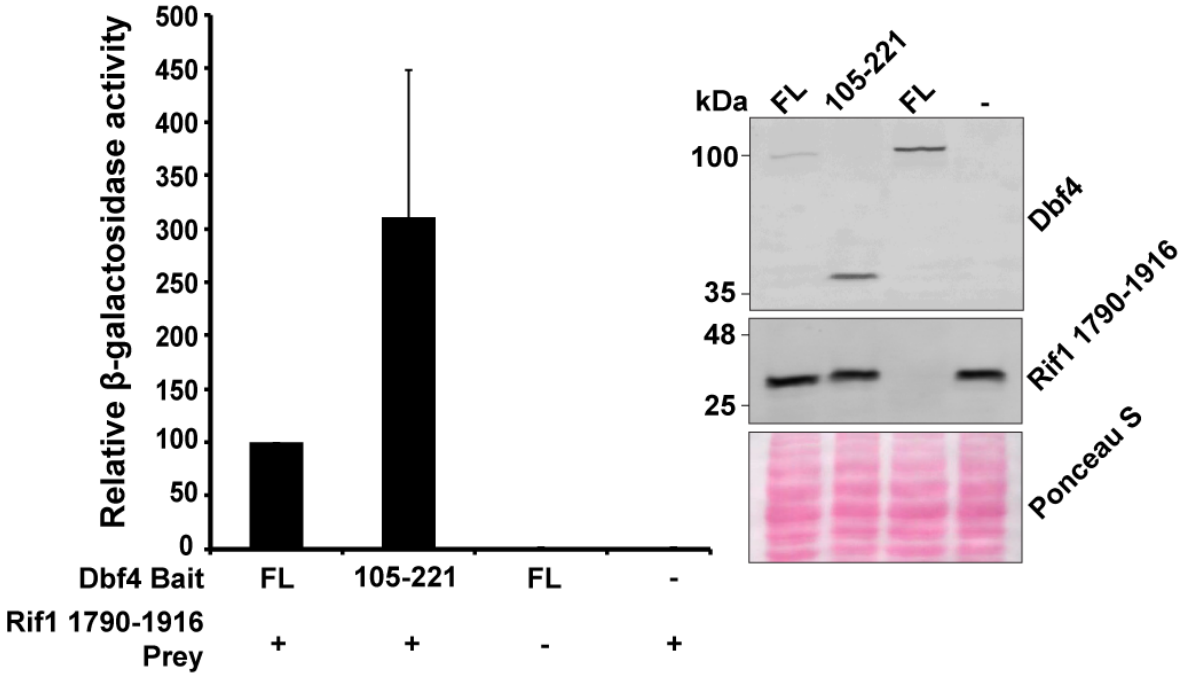

Figure 4.1. Dbf4 HBRCT is sufficient for Rif1 binding. The interaction of the Dbf4 HBRCT domain (amino acids 105-221) and Rif1 amino acids 1790-1916 was assessed through yeast two-hybrid assays. The two-hybrid interaction values are presented as a percentage of the interaction of Dbf4 FL (full-length) and Rif1 1790-1916. Three independent replicates were performed, and error bars represent standard deviation. Representative Western blots (of three independent experiments performed) indicate protein expression levels and Ponceau S staining shows equal protein loading. Bait and prey proteins were detected with anti-LexA (Dbf4) and anti-HA (Rif1) antibodies, respectively.

4.2.2 Dbf4 HBRCT mutations disrupting the helix α0 hydrophobic interaction with the BRCT core abrogate Rif1 C-terminus binding

The observation that HBRCT mediates the interaction of Dbf4 with two key ligands, Rad53 and Rif1, raised the question of whether this domain binds to them in a similar fashion. This is particularly intriguing given these associations promote opposing outcomes, with Rif1-Dbf4 favouring DNA replication and Rad53-Dbf4 opposing it. The Dbf4 HBRCT helix α0 has two

faces, a hydrophobic one that interacts with the hydrophobic core of the BRCT domain, as well as a polar one (Figure 4.2A). Mutations of the non-polar residues on the hydrophobic face disrupt the interaction with the Rad53 FHA1 domain, whereas mutations on the polar face do not (Matthews et al., 2012). Thus, I asked if maintaining the hydrophobic environment of helix α0 and the BRCT core is required for Rif1 interaction. Two-hybrid results demonstrated that double mutations L109A/W112S and W116D/M120A on the hydrophobic face resulted in a dramatic reduction of Dbf4 binding to Rif1 (Figure 4.2B), as previously observed with Rad53 (Matthews et al., 2012). In contrast, double mutations on the polar face, K121D/R122E and E111R/K118D, did not weaken the interaction, suggesting that the maintenance of Rif1 binding is specific to the hydrophobic face of helix α0. These results indicate that the hydrophobic interaction between helix α0 and the BRCT core must be intact for Rif1 binding.

To further investigate whether Dbf4 binds to Rif1 in a similar fashion to Rad53, two-hybrid analysis was performed using an additional Dbf4 mutant. Dbf4 has two contact points with Rad53 (Chapter 3 Figure 3.2 and (Almawi et al., 2016)). The hydrophobic region of Dbf4 HBRCT is pivotal for contact with β-sheets 1 and 11 of Rad53 FHA1 domain. As described above, simultaneous mutation of Leu109 and Trp112 from this HBRCT region severely impaired binding to Rif1, as was the case for Rad53. The polar association of Dbf4 Lys200 and Rad53 FHA1 Asn112 determines the second contact point (Chapter 3 Figure 3.2 and (Almawi et al., 2016)). In contrast to what was seen with Rad53, Dbf4 K200A mutant maintained its interaction with Rif1 (Figure 4.2C). Thus, it is concluded that Dbf4 interacts with both Rad53 and Rif1 via its HBRCT domain, but through a different mechanism.

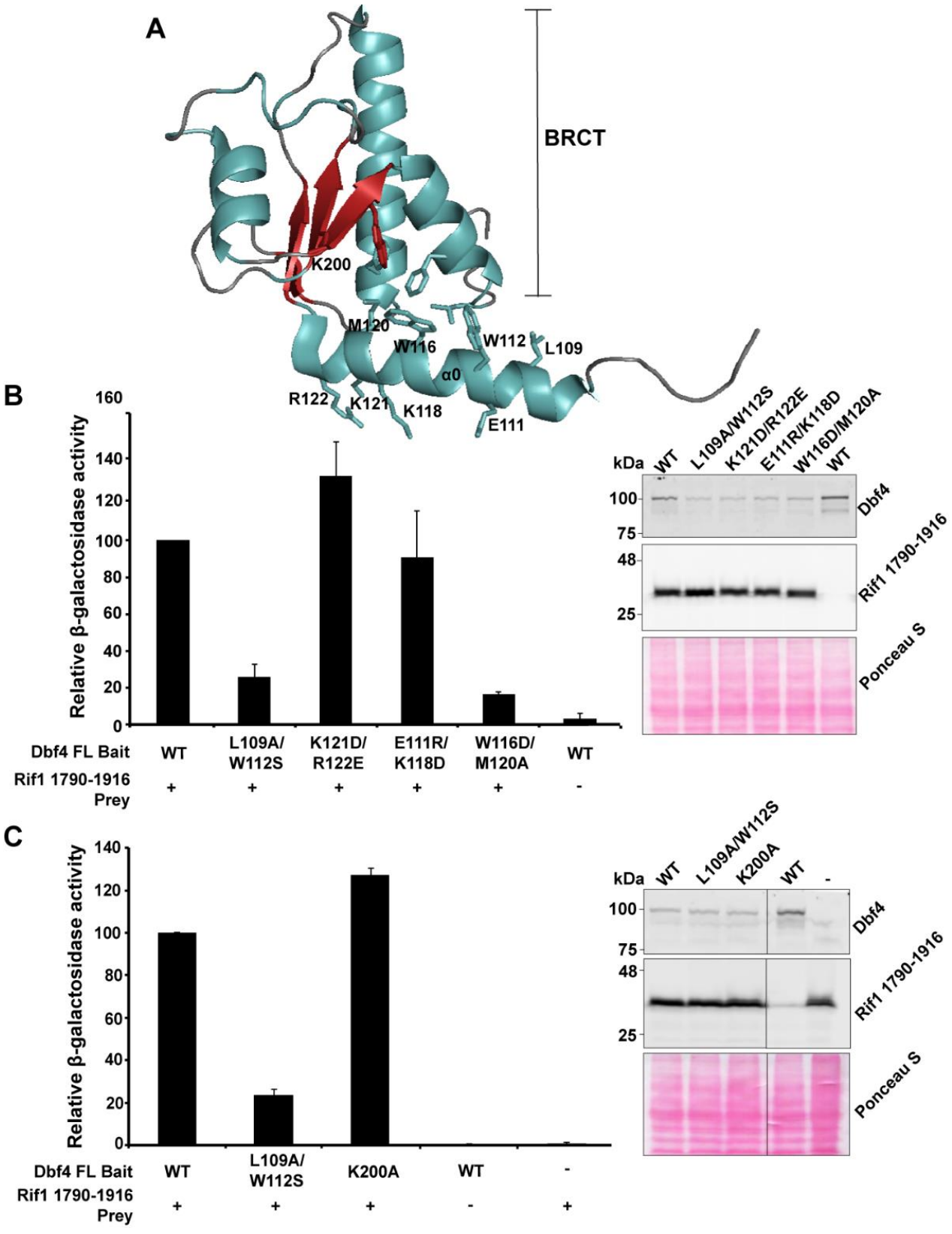
A
BRCT
K200
M120
W116
W112
L109
α0
R122
K121
K118
E111
B
Relative β-galactosidase activity
160
140
120
100
80
60
40
20
0
Dbf4 FL Bait
WT
L109A/ W112S
K121D/ R122E
E111R/ K118D
W116D/ M120A
WT
Rif1 1790-1916 Prey
+
+
+
+
+
-
kDa
WT
L109A/W112S
K121D/R122E
E111R/K118D
W116D/M120A
WT
100
75
48
25
Dbf4
Rif1 1790-1916
Ponceau S
C
Relative β-galactosidase activity
140
120
100
80
60
40
20
0
Dbf4 FL Bait
WT
L109A/ W112S
K200A
WT
-
Rif1 1790-1916 Prey
+
+
+
-
+
kDa
WT
L109A/W112S
K200A
WT
-
100
75
48
25
Dbf4
Rif1 1790-1916
Ponceau S

Figure 4.2. Mutations of hydrophobic residues on HBRCT helix α0 disrupt Dbf4 interaction with Rif1. (A) Illustration of the Dbf4 HBRCT domain (PDB 3QBZ; adapted from (Matthews et al., 2012)). (B, C) Yeast two-hybrid analysis of Dbf4 mutant interaction with Rif11790-1916. The values are presented as a percentage of the Dbf4 WT (wild type) and Rif1 1790-1916 interaction and the experiments were performed as in Figure 4.1. Four (B) and three (C) independent replicates were performed, and error bars represent standard deviation. Representative Western blots (of four (B) or three (C) independent experiments performed) indicate protein expression levels and Ponceau S staining shows equal protein loading. Bait and prey proteins were detected with anti-LexA (Dbf4) and anti-HA (Rif1) antibodies, respectively.

Since the HBRCT domain also mediates Dbf4 interaction with the checkpoint protein Rad53 (Matthews et al., 2012), an intriguing possibility is that Rif1 and Rad53 can displace each other in terms of Dbf4 binding during specific cell cycle stages and growth conditions, with one interaction promoting the initiation of DNA replication and the other one blocking it. Thus, Rad53 may physically displace Rif1 from binding Dbf4 as one of the ways it downregulates DDK activity under checkpoint conditions. If Dbf4 is inhibited from binding Rif1, DDK will no longer phosphorylate the Rif1 PP1-association motifs, thereby promoting Rif1 and Glc7 association, leading to dephosphorylation of Mcm2-7. To investigate the differential affinity between Rad53 and Rif1 in Dbf4 binding, we performed a competitive yeast-two hybrid assay where Rif1 was co-expressed with Dbf4 and Rad53 simultaneously. Rif1's ability to titrate Dbf4 from Rad53 binding was judged by comparing the Dbf4-Rad53 binding intensity to that when Rif1 was absent (Appendix B Figure 1). Rif1 did not disrupt the binding, which supports the idea that Rif1 and Rad53 engage with Dbf4 in a differential mechanism.

4.2.3 Mutation of the Rif1 tetramerization module impairs binding to Dbf4.

Next, I aimed to determine which Rif1 residues are responsible for the Dbf4-Rif1 interaction. The *S. cerevisiae* Rif1 C-terminus interacts with both Rap1 (Hardy et al., 1992) and Dbf4 (Hiraga et al., 2014; Mattarocci et al., 2014). A previous crystallographic study showed that Rif1 residues 1857-1916 form a tetramer, disruption of which abolishes interaction with Rap1 (Shi et al., 2013). I therefore investigated whether Rif1 tetramer formation is also required for association with Dbf4. The dimeric interaction is facilitated by salt bridges and a hydrophobic interaction of the non-polar residues. Mutation of one of the hydrophobic residues, Leu1905 to Arg, severely impaired the interaction with Dbf4 (Figure 4.3), as was the case for Rap1. The two dimers form a tetramer through the aid of salt bridges between Arg1895 and Glu1906, and mutation of Arg1895 into Glu similarly disrupts the interaction of Rap1 and Rif1 (Shi et al., 2013). The result showed that the Rif1 R1895E mutation also had a negative effect on interaction with Dbf4, reducing its strength by more than half (Figure 4.3). The tetramerization domain does not likely directly mediate any interactions with other ligands, but is required to support the structural stability of this region (Shi et al., 2013). These findings demonstrate that the tetramerization of the Rif1 C-terminus is required for robust Dbf4 binding, with disruption of either intra- or interdimer contacts having detrimental effects.

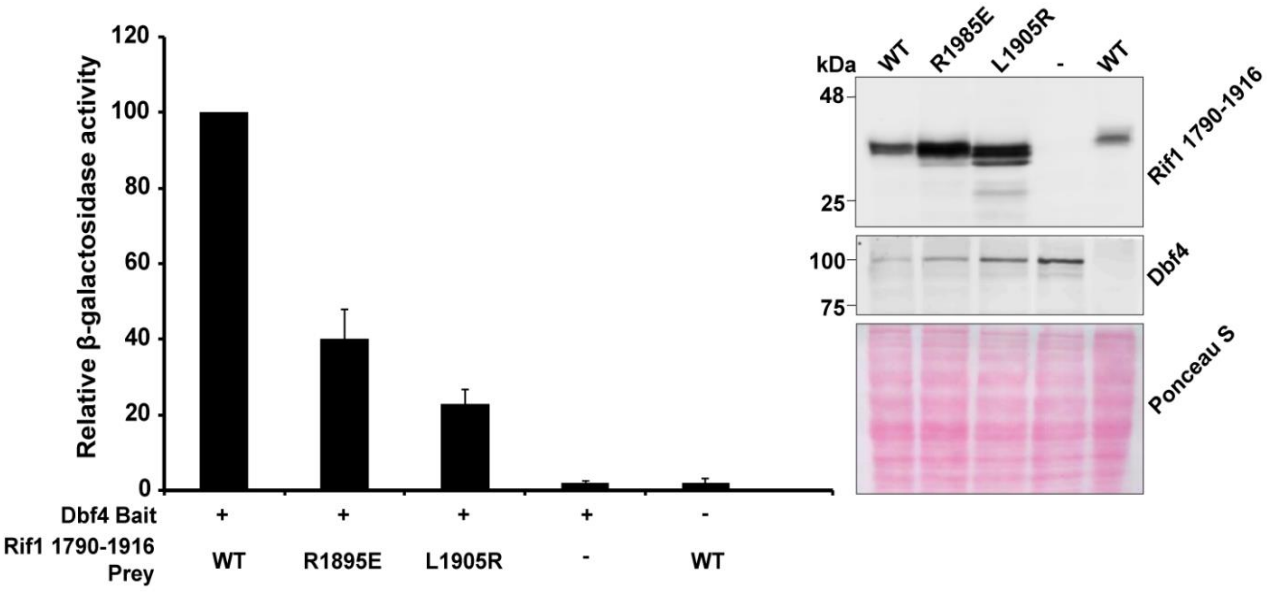

Figure 4.3. The tetramerization module of Rif1 is required for Dbf4 binding. The two-hybrid interaction values of Dbf4 and Rif1 1790-1916 mutants are presented as a percentage of the Dbf4 and Rif1 1790-1916 (WT) interaction. Three independent replicates were performed, and error bars represent standard deviation. Representative Western blots (of three independent experiments performed) indicate protein expression levels and Ponceau S staining shows equal protein loading. Bait and prey proteins were detected with anti-LexA (Dbf4) and anti-HA (Rif1) antibodies, respectively.

4.2.4 The Rif1 C-terminus binds to Rap1 and Dbf4 in a differential manner

The Rif1 fragment (residues 1790-1916) that interacts with Dbf4 is encompassed by the region (residues 1739-1916) that suffices to bind Rap1 (Hiraga et al., 2014). To dissect the in vivo significance of the Dbf4-Rif1 interaction, I asked if a separation-of-function mutation that maintains Rif1 binding to Rap1, but not to Dbf4, could be found. To identify potential motifs responsible for the Rif1-Dbf4 interaction, the region 1790 to 1857 in budding yeast Rif1, which lies outside of the tetramerization module described above, was analyzed. Analysis based on multiple sequence alignment indicated poor conservation within this region. However, across orthologous Rif1 regions from diverse species, an abundance of proline-rich

segments (data not shown) was observed, indicating possible conservation of short linear interaction motifs (SLIMs) within an unstructured linker (Kay et al., 2000; Neduva & Russell, 2005). Therefore, the region 1790 to 1857 was further assessed based on four criteria: 1) predicted secondary structure (Cole et al., 2008a), since interaction motifs often occur in disordered/unstructured regions (Mészáros et al., 2009; Neduva & Russell, 2005); 2) proline composition, because proline residues are overrepresented in interaction motifs (Kay et al., 2000); 3) phosphorylated serine or threonine residues (as determined from the UniProt database), since cell cycle protein-protein interactions are often mediated by phosphopeptides; and 4) predicted protein binding sites using a sequence-based machine-learning algorithm (Mukherjee & Zhang, 2011) (Figure 4.4A).

This analysis identified one amino acid segment in particular (1792-PPDSPP-1797) as matching all four criteria, whereas the next highest candidate region (1812-DTVPK-1816) matched only one criterion. The PPDSPP motif is proline-rich, occurs in an unstructured loop segment as judged by Jpred3/JNETJURY analysis (Cole et al., 2008a) and confirmed through both I-TASSER (Zhang, 2008) (Appendix B Figure 2) and Phyre2 (Kelley et al., 2015) (data not shown) structure predictions, contains a phosphoserine residue previously identified based on a proteomic screen (Holt et al., 2009), and includes three putative interface residues predicted by the BSPred algorithm (Mukherjee & Zhang, 2011).

Two-hybrid analysis was performed and Rif1 1739-1916 lacking the PPDSPP stretch maintained the interaction with Rap1 653-827, the binding domain for Rif1 (Hardy et al., 1992) (Figure 4.4B). This is consistent with previous work indicating that Rif1 requires residues 1752-1772 to interact with Rap1 (Shi et al., 2013). In contrast, Rif1 1739-1916 ΔPPDSPP had

severely impaired Dbf4 binding (Figure 4.4C). When two conserved sites distal to the PPDSPP motif were mutated (E1839K and N1847A), neither had a significant effect on either Rap1 or Dbf4 binding. Therefore, these data demonstrate that Rif1 binding to Dbf4 and Rap1 is mediated by distinct regions within the Rif1 C-terminus.

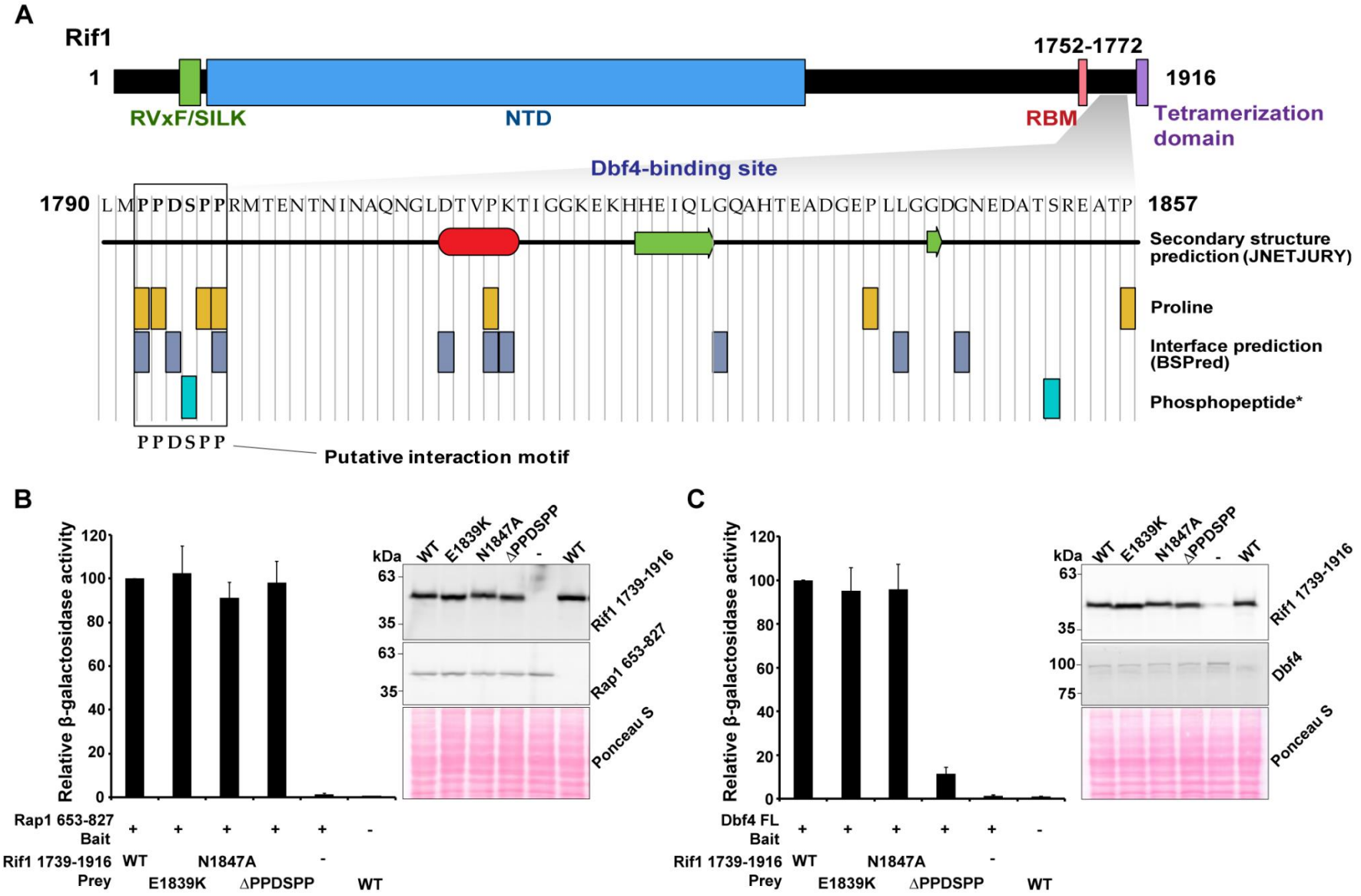
A
Rif1
1
1752-1772
1916
RVxF/SILK
NTD
RBM
Tetramerization domain
Dbf4-binding site
1790
L M P P D S P P R M T E N T N I N A Q N G L D T V P K T I G G K E K H H E I Q L G Q A H T E A D G E P L L G G D G N E D A T S R E A T P
1857
Secondary structure prediction (JNETJURY)
Proline
Interface prediction (BSPred)
Phosphopeptide*
P P D S P P
Putative interaction motif
B
Relative β-galactosidase activity
120
100
80
60
40
20
0
Rap1 653-827 Bait
Rif1 1739-1916 Prey
+ + + + + -
WT E1839K N1847A ΔPPDSPP - WT
kDa
WT E1839K N1847A ΔPPDSPP - WT
63
35
Rif1 1739-1916
63
35
Rap1 653-827
Ponceau S
C
Relative β-galactosidase activity
120
100
80
60
40
20
0
Dbf4 FL Bait
Rif1 1739-1916 Prey
+ + + + + -
WT E1839K N1847A ΔPPDSPP - WT
kDa
WT E1839K N1847A ΔPPDSPP - WT
63
35
Rif1 1739-1916
100
75
Dbf4
Ponceau S

Figure 4.4. The Rif1 PPDSPP motif mediates interaction with Dbf4, but not with Rap1. (A) Assessment of Rif1 1790-1857 characteristics to identify potential binding motifs for Rif1 and Dbf4 interaction. RVxF and SILK are Glc7-binding motifs (Hiraga et al., 2014; Mattarocci et al., 2014; Sreesankar et al., 2012), NTD is N-terminal domain and RBM is Rap1-binding module (Shi et al., 2013). We evaluated the Dbf4-binding region based on these criteria: Jpred3/JNETJURY secondary structure prediction which indicates helices as red ovals and sheets as green arrows (Cole et al., 2008a), proline content, BSPred protein binding site prediction (Mukherjee & Zhang, 2011) and phosphorylated serine or threonine residues (UniProt database). (B and C) Yeast two-hybrid analysis of Rif1 1739-1916 (WT and mutants, as indicated) binding to Rap1 653-827 (B) and Dbf4 (C). Three independent replicates were performed, and error bars represent standard deviation. Representative Western blots (of three independent experiments performed) indicate protein expression levels and Ponceau S staining shows equal protein loading. Bait and prey proteins were detected with anti-LexA (Dbf4 and Rap1) and anti-HA (Rif1) antibodies, respectively.

4.2.5 Disruption of the Rif1-Dbf4 association does not have a major effect on cell growth and DNA replication

I next made a genomic *rif1 ΔPPDSPP* mutant strain and predicted that it would display a defect in cell cycle progression, since the failure of Rif1 to be bound by Dbf4 would impede its phosphorylation by DDK, perpetuating the Rif1-Glc7 complex and consequentially Mcm4 dephosphorylation, delaying DNA replication. Yeast growth in liquid cultures was measured (Figure 4.5A). In contrast with my prediction, *rif1 ΔPPDSPP* did not have a strikingly reduced growth rate compared to isogenic *wild type* cells, and neither did the *Δrif1* cells.

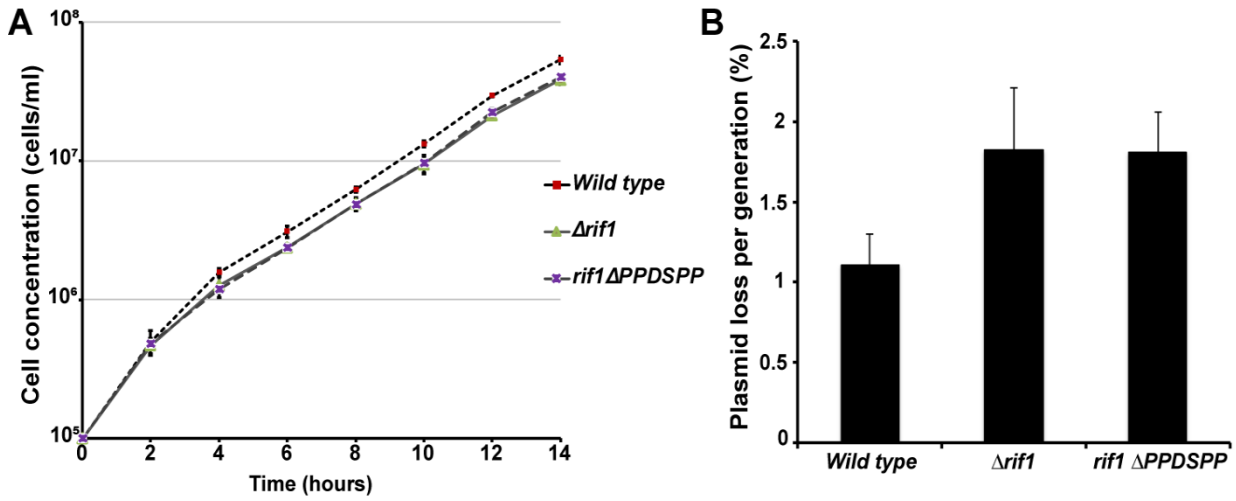

Figure 4.5. Removal of the Rif1 PPDSPP motif does not dramatically disrupt cell proliferation and DNA replication. (A) Yeast cultures at exponential phase were diluted to $1x10^5$ cells per milliliter and grown in YPD at 30°C. The cell concentrations were counted at the indicated time points. Three independent growth measurements were performed, and error bars represent standard deviation. (B) Plasmid stability assay (Kapoor et al., 2001) with modification was performed by transforming the cells with YCplac111 (Gietz & Sugino, 1988). The transformants were grown in non-selective liquid medium to allow plasmid loss prior to plating on both selective and non-selective medium to assess plasmid stability. Four hundred cells were plated on synthetic complete medium lacking leucine and YPD medium for two days at 30°C. The plasmid loss per generation rate was determined as the percentage of plasmid loss = (1-(colony number on SC-Leu/colony number on YPD))/number of cell divisions. The total number of replicates was ten sets for each strain.

Since Mcm4 phosphorylation is associated with origin activation, its phosphorylation level in the *Δrif1* cells in G1 phase was checked. Indeed, deletion of *RIF1* resulted in the increased phosphorylation level of chromatin-bound Mcm4 in G1 phase (Appendix B Figure 3). However, since *Δrif1* cells did not show a notable growth defect, there are probably other cell cycle regulations that can restrict origin firing events in G1 phase.

To investigate whether a defect in DNA replication was contributing to the minor reduced growth rate observed for *Δrif1* and *rif1 ΔPPDSPP* strains, a plasmid stability assay was performed (Kapoor et al., 2001) (Figure 4.5B). Each yeast strain was transformed with

YCpLac111, a CEN vector that contains an ARS1 origin (Gietz & Sugino, 1988). The transformants were grown in non-selective liquid medium to allow plasmid loss prior to plating on both selective and non-selective medium to assess the plasmid stability. Both the *Δrif1* (mean 1.82%) and *rif1 ΔPPDSPP* (mean 1.81%) strains resulted in a higher rate of plasmid loss per generation than observed for isogenic wild-type cells (mean 1.10%). However, these plasmid loss values are not remarkable since the loss rate of CEN/ARS plasmid is generally 1-3% per generation (Fitzgerald-Hayes et al., 1982; Hieter et al., 1985).

To further confirm the growth phenotype of *rif1 ΔPPDSPP* cells, FACS analysis was performed and the growth defect of *rif1 ΔPPDSPP* strain was minor compared to the *wild type* in a single cell cycle (Appendix B Figure 4). Both *wild type* and *rif1 ΔPPDSPP* cells were efficiently arrested in G1 phase. However, in contrast to *wild type*, *rif1 ΔPPDSPP* experienced delayed S phase entry, indicated by a more prominent G1 peak at the 15 minutes time point after release, which explains the minimal growth rate reduction of *rif1 ΔPPDSPP*.

4.2.6 Combining *rif1 ΔPPDSPP* and CDK phosphorylation site mutations results in hypersensitivity to genotoxic stress

The disruption of Dbf4 and Rif1 association likely results in less efficient origin firing due to greater MCM dephosphorylation activity of a stabilized Rif1-Glc7 complex. During recovery from genotoxic stress, this effect could have both beneficial and detrimental consequences. On the one hand, a greater number of origins not firing before checkpoint arrest could increase opportunities for new initiation events, which are of particular importance in the case of collapsed or compromised replication forks. On the other hand, initiation from these same

unfired origins during recovery could be compromised by enhanced Rif1-Glc7 dephosphorylation activity. To examine whether removal of the Rif1 PPDSPP motif has a net positive or negative effect on resistance to genotoxic stress, the cell spotting assays were performed on solid growth media supplemented with hydroxyurea (HU), methyl methanesulfonate (MMS), phleomycin (Phleo), bleocin (Bleo), camptothecin (CPT) or caffeine (Figure 4.6A).

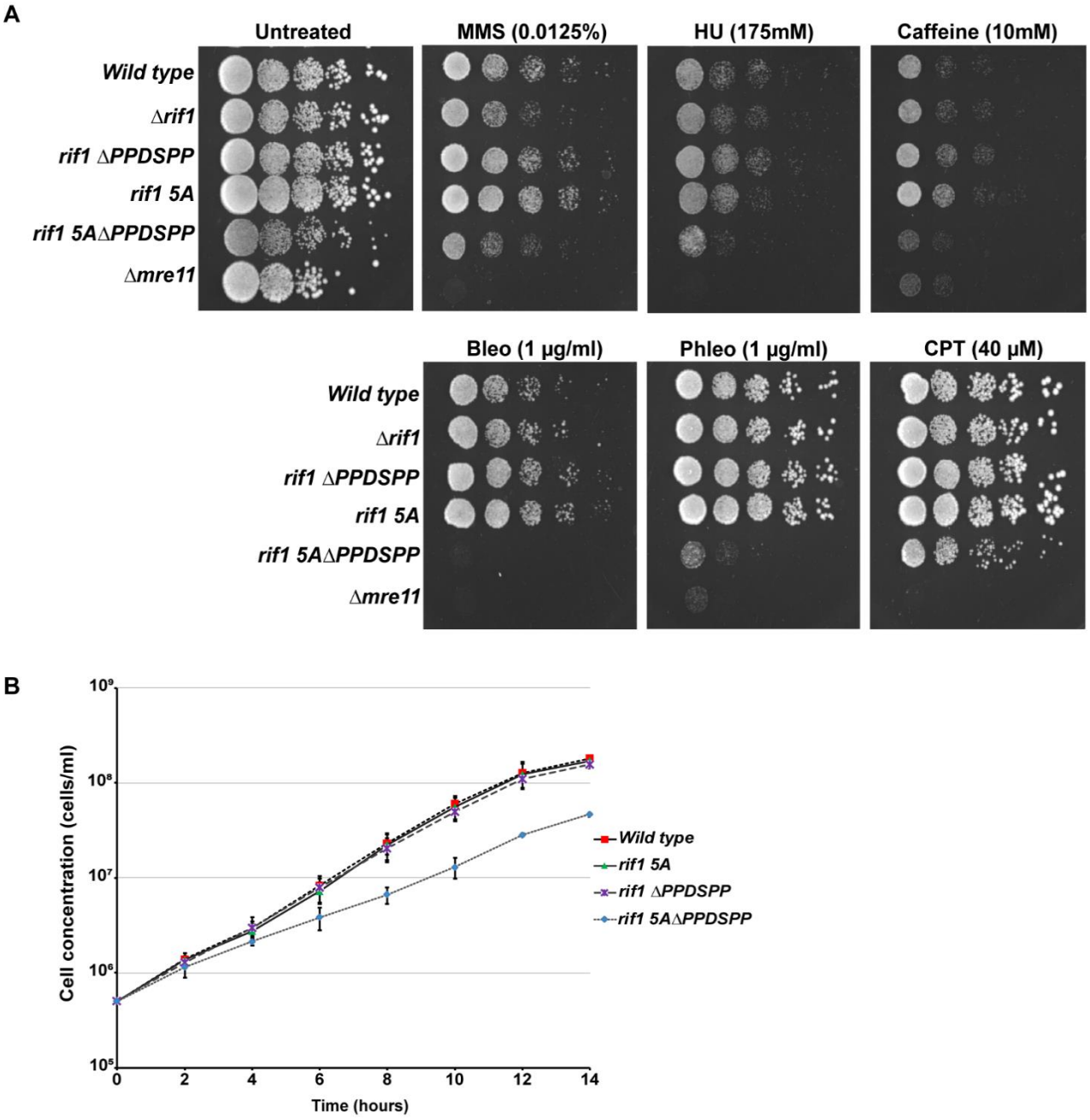
A
Untreated
MMS (0.0125%)
HU (175mM)
Caffeine (10mM)
Wild type
Δrif1
rif1 ΔPPDSPP
rif1 5A
rif1 5AΔPPDSPP
Δmre11
Bleo (1 μg/ml)
Phleo (1 μg/ml)
CPT (40 μM)
Wild type
Δrif1
rif1 ΔPPDSPP
rif1 5A
rif1 5AΔPPDSPP
Δmre11
B
Cell concentration (cells/ml)
10⁹
10⁸
10⁷
10⁶
10⁵
0
2
4
6
8
10
12
14
Time (hours)
Wild type
rif1 5A
rif1 ΔPPDSPP
rif1 5AΔPPDSPP

Figure 4.6. *rif1 5AΔPPDSPP* cells demonstrate impaired growth in normal conditions and hypersensitivity to genotoxic stress. (A) Cells from liquid cultures of the indicated yeast strains were serially diluted ten-fold and spotted onto YPD plates with or without genotoxic compounds hydroxyurea (HU), methyl methanesulfonate (MMS), phleomycin (Phleo), bleocin (Bleo), camptothecin (CPT) or caffeine. Pictures were taken after incubation for two days at 30°C. Three independent spotting experiments were performed. The *Δmre11* strain was used as a control that has been shown to be sensitive to genotoxic stress (Ajimura et al., 1993). (B) Yeast cultures at exponential phase were diluted to $5x10^5$ cells per milliliter and grown in YPD at 30°C. Cell concentrations were counted at the indicated time points. Three independent growth measurements were performed, and error bars represent standard deviation.

The *rif1 ΔPPDSPP* strain did not show a change in sensitivity towards any of the genotoxic agents used, indicating that disrupting DDK interaction with Rif1 by itself is not sufficient to alter resistance to these compounds. Rif1 has 9 and 5 potential phosphorylation sites for DDK and CDK, respectively, which are located near the PP1-binding motifs (Davé et al., 2014; Hiraga et al., 2014). Three of these CDK sites prime DDK phosphorylation (Hiraga et al., 2014). Thus, it was interesting to see whether CDK phosphorylation of Rif1 also plays a role during stress recovery. All the CDK phosphorylation sites on Rif1 were mutated into alanine (*rif1 5A*) and combined with the PPDSPP deletion. Under normal conditions, the *rif1 5A* cells grew as well as wild type and *rif1 ΔPPDSPP* cells on solid media (Figure 4.6A). When subjected to a wide range of genotoxic stress, *rif1 5A* did not show any change in sensitivity relative to wildtype. However, the combination of the *5A* and *ΔPPDSPP* mutations had a dramatically different effect (Figure 4.6A). Even under normal conditions, fewer colonies of the *rif1 5AΔPPDSPP* strain were observed, reflecting slower growth and consistent with continuous MCM helicase dephosphorylation facilitated by Rif1. Through cell counts at numerous time intervals in liquid medium, it was confirmed that *rif1 5AΔPPDSPP* indeed grows poorly relative

to the *5A* and *ΔPPDSPP* strains (Figure 4.6B). Under genotoxic stress conditions, *rif1 5AΔPPDSPP* cells demonstrated hypersensitivity, the most pronounced effects coming from exposure to bleocin and phleomycin (Figure 4.6A). This finding suggests that DDK and CDK phosphorylation of Rif1 are largely redundant with respect to imparting resistance to genotoxic stress.

4.2.7 *rif1 5A*Δ*PPDSPP* hypersensitivity to double-strand breaks is enhanced or rescued by compromising HR or NHEJ, respectively

The hypersensitivity of *rif1 5A*Δ*PPDSPP* cells to DSB-inducing agents, bleocin and phleomycin, prompted us to speculate that robust dephosphorylation activity of the Rif1-Glc7 complex may impede the DNA repair process. There are two main pathways that deal with correcting DSBs, HR and NHEJ. In yeasts, HR repairs DSBs more efficiently than NHEJ (Chen & Tomkinson, 2011; Clikeman et al., 2001; Zhang et al., 2007). Thus, to examine which pathway is affected by the dephosphorylation activity of Rif1-Glc7, the *rif1 5A*Δ*PPDSPP* mutation was combined with gene deletions impairing HR *(*Δ*sae2*, Δ*exo1*) or NHEJ *(*Δ*nej1*). A spotting assay was then performed and the Δ*sae2/rif1 5A*Δ*PPDSPP* strain was more sensitive compared to Δ*sae2* or *rif1 5A*Δ*PPDSPP* strains to an array of genotoxic stressors, with the exception of caffeine (Figure 4.7A). Δ*exo1/rif1 5A*Δ*PPDSPP* cells did not phenocopy Δ*sae2/rif1 5A*Δ*PPDSPP,* showing no enhancement of sensitivity when compared to *rif1 5A*Δ*PPDSPP*, except upon exposure to MMS. To confirm that the disruption of NHEJ suppresses the genotoxic hypersensitivity of the *rif1 5A*Δ*PPDSPP* strain, this mutant was combined with deletion of *YKU70,* a component of the yKu70/80 ring heterodimer that protects broken DNA ends from HR initiation (Bonetti et al.,

2010; Mimitou & Symington, 2010; Shim et al., 2010). As anticipated, Δ*yku70* rescued the hypersensitivity of *rif1 5A*Δ*PPDSPP* cells to a degree that was similar to Δ*nej1* (Figure 4.7B). For the spotting experiments in Figure 4.7, the genotoxic compound concentrations, except for camptothecin, were lower than that used in Figure 4.6 to accommodate the growth of the most sensitive strain Δ*sae2/rif1 5A*Δ*PPDSPP*.

Sae2 lies upstream of Exo1 in the HR response and, when phosphorylated by CDK, is responsible for stimulating the initial endonuclease activity of MRX (Mre11-Rad50-Xrs1) complex (Cannavo & Cejka, 2014; Huertas et al., 2008). This short nucleolytic resection is then followed by long-range resection by Exo1 or Dna2 in complex with Sgs1 helicase (Gnügge & Symington, 2017; Huertas, 2010; Longhese et al., 2010; Symington, 2016). The redundancy between Exo1 and Dna2 is likely the reason for the mild Δ*exo1/rif1 5A*Δ*PPDSPP* phenotype. Moreover, the contrast in sensitivity between Δ*sae2/rif1 5A*Δ*PPDSPP* and Δ*exo1/rif1 5A*Δ*PPDSPP* suggests that the detrimental effect of *rif1 5A*Δ*PPDSPP* is more harmful toward the initial step of resection. Strikingly, the deletion of *NEJ1* or *YKU70* rescued the sensitivity of *rif1 5A*Δ*PPDSPP* cells for all compounds tested with the most dramatic results observed for exposure to bleocin or phleomycin, indicating that the hypersensitivity of *rif1 5A*Δ*PPDSPP* cells might stem from lack of DNA end resection. yKu70 prevents the resection initiation by inhibiting DSB access to nucleases (Mimitou & Symington, 2010; Shim et al., 2010) and recruits the loading of others NHEJ factors to DNA ends, including Nej1 (Chen & Tomkinson, 2011; Zhang et al., 2007). Nej1 also blocks resection by stabilizing the recruitment of yKu to DSB sites (Chen & Tomkinson, 2011), inhibiting Dna2-Sgs1 activity (Mojumdar et al., 2019; Sorenson et al., 2017), and stimulating ligation by Dnl4/Lif1 (Chen & Tomkinson, 2011). Thus, the rescue

observed through yKu70 or Nej1 deletion is consistent with relief of a resection defect. Taken together, these results suggest a deleterious effect of constitutive Rif1-Glc7 activity in the context of HR is alleviated when the NHEJ pathway is compromised and cells are shifted towards HR.

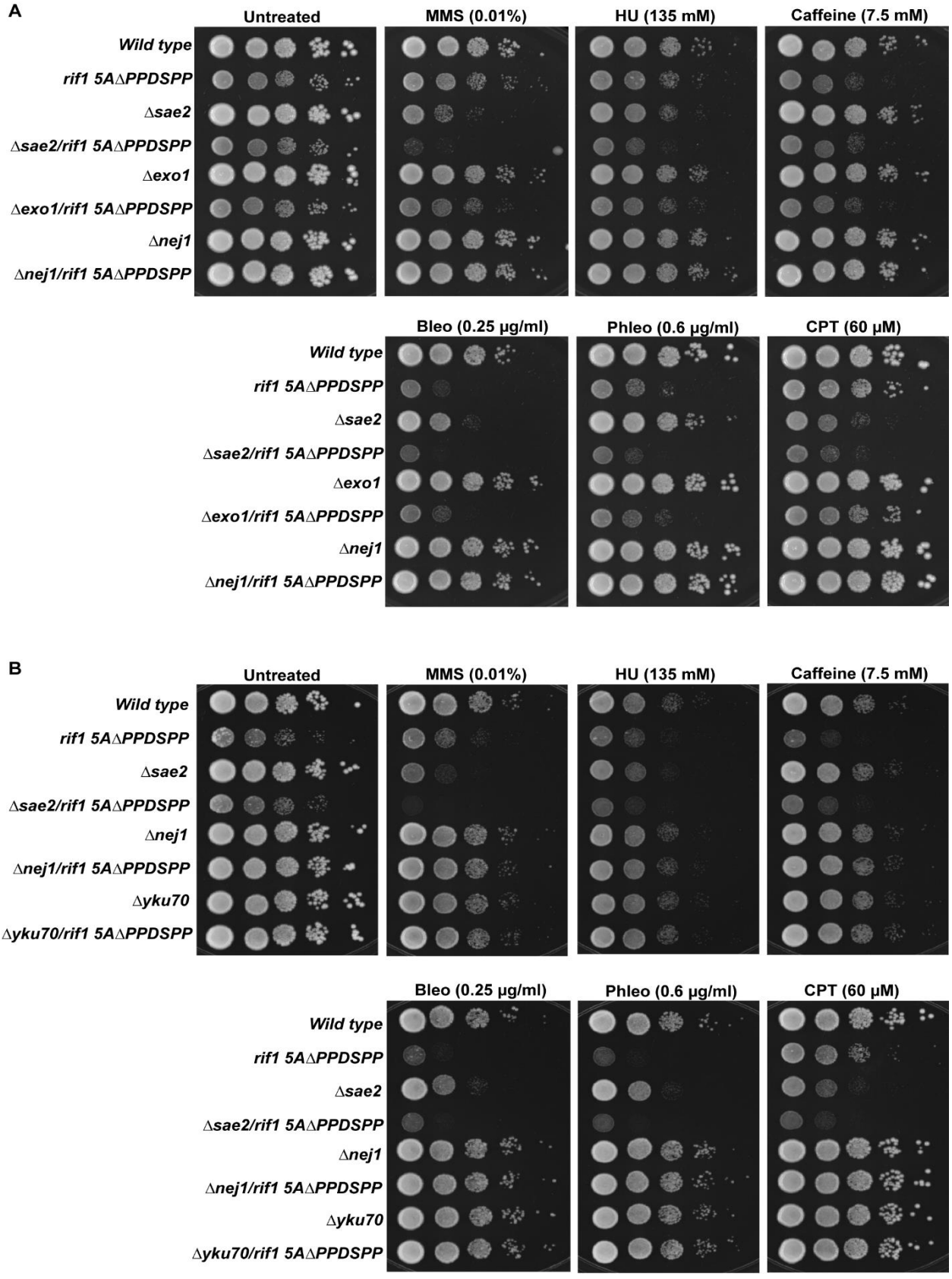
A
Untreated
MMS (0.01%)
HU (135 mM)
Caffeine (7.5 mM)
Wild type
rif1 5AΔPPDSPP
Δsae2
Δsae2/rif1 5AΔPPDSPP
Δexo1
Δexo1/rif1 5AΔPPDSPP
Δnej1
Δnej1/rif1 5AΔPPDSPP
Bleo (0.25 μg/ml)
Phleo (0.6 μg/ml)
CPT (60 μM)
Wild type
rif1 5AΔPPDSPP
Δsae2
Δsae2/rif1 5AΔPPDSPP
Δexo1
Δexo1/rif1 5AΔPPDSPP
Δnej1
Δnej1/rif1 5AΔPPDSPP
B
Untreated
MMS (0.01%)
HU (135 mM)
Caffeine (7.5 mM)
Wild type
rif1 5AΔPPDSPP
Δsae2
Δsae2/rif1 5AΔPPDSPP
Δnej1
Δnej1/rif1 5AΔPPDSPP
Δyku70
Δyku70/rif1 5AΔPPDSPP
Bleo (0.25 μg/ml)
Phleo (0.6 μg/ml)
CPT (60 μM)
Wild type
rif1 5AΔPPDSPP
Δsae2
Δsae2/rif1 5AΔPPDSPP
Δnej1
Δnej1/rif1 5AΔPPDSPP
Δyku70
Δyku70/rif1 5AΔPPDSPP

Figure 4.7. Deletion of *SAE2* exacerbates the genotoxic sensitivity of *rif1 5AΔPPDSPP* cells, while deletion of *NEJ1* or *YKU70* rescues it. Cells from liquid cultures of the indicated yeast strains were serially diluted ten-fold and spotted onto YPD plates with or without genotoxic compounds, as indicated previously in Figure 4.6. Two different sets of spotting results that include Δ*exo1* or Δ*yku70* variants are shown on panel (A) and (B), respectively. Pictures were taken after incubation for two days at 30°C. Three independent spotting experiments for each of the strain combinations shown in panels A and B were performed.

4.3 Discussion

In the present study, I characterize the way in which Rif1 and Dbf4 interact and demonstrate that this association is important for cell cycle progression under both unperturbed conditions and following exposure to genotoxic stress. I found that DDK association with Rif1 is mediated by the Dbf4 HBRCT domain, which is sufficient for Rif1 binding on its own. This binding mode differs from that of the HBRCT-Rad53 interaction. Additionally, a proline-rich PPDSPP fragment was also found on the Rif1 C-terminus that distinguishes its binding to Rap1 and Dbf4.

The *rif1 ΔPPDSPP* mutation by itself did not result in a remarkable growth defect or any sensitivity to genotoxic stress (Figure 4.6A). In order to further examine the in vivo effect of Rif1 ΔPPDSPP, this mutant was combined with mutation of its five CDK target sites, thus disrupting phosphorylation by both DDK and CDK. *rif1 5AΔPPDSPP* cells show slower growth under unperturbed and increased sensitivity under perturbed conditions, with the most apparent effect was observed during DSBs condition (Figure 4.6A). This implies that Rif1 is not only a DDK/CDK phosphorylation target during DNA replication initiation, but also a target during cell recovery from genotoxic stress exposure. It has been reported that Rif1 is recruited to stalled forks under HU treatment and protects nascent DNA from degradation, but removal of 594 amino acids at its C terminus (which includes the PPDSPP stretch) weakens this protection (Hiraga et al., 2018). This indicates that the C-terminal region of Rif1 is

required for a robust response to DNA replication stress, even though the precise mechanism remains unclear. HU sensitivity was not observed with the *rif1* Δ*PPDSPP* mutant, arguing that interaction with Dbf4 is not required for RIF1's role in nascent DNA protection.

Yeast Rif1, like its mammalian counterpart, has been implicated in promoting NHEJ to repair DSBs (Fontana et al., 2019; Mattarocci et al., 2017). In the present report, it is shown that attenuation of the NHEJ pathway rescues the genotoxic sensitivity of *rif1 5AΔPPDSPP* cells, suggesting that constitutively active Rif1-Glc7 has a detrimental effect by shifting cells too much towards reliance on NHEJ as a response to DNA damage while HR is the preferred means to deal with genotoxic stress in budding yeast (Chen & Tomkinson, 2011; Clikeman et al., 2001; Zhang et al., 2007). Consistent with this model, combination of *rif1 5A*Δ*PPDSPP* with Δ*sae2* results in greater sensitivity than for either mutant alone, suggesting severe impairment of DNA resection (Figure 4.7). Interestingly, *RIF1* deletion also exacerbates the effects of Δ*sae2* in both unperturbed and perturbed conditions (Martina et al., 2014). Taken together, these findings suggest that productive Rif1 involvement in DNA repair requires its wild type activity level.

Since Rif1 roles in DNA replication and telomere maintenance require its binding to Glc7, it is tempting to postulate that its DNA repair function also involves its ability to target Glc7 dephosphorylation activity. CDK phosphorylation controls DNA repair pathway choice by directing HR to take place in S and G2 phases (Ferretti et al., 2013; Longhese et al., 2010). CDK phosphorylation of CtIP, the human homolog of Sae2, stimulates resection and also prevents hRif1 accumulation at DSBs (Escribano-Díaz et al., 2013; Huertas & Jackson, 2009). Thus, an appealing notion is that the complete absence of Sae2 in the Δ*sae2/rif1 5A*Δ*PPDSPP*

strain allows high levels of Rif1 to associate with DSBs and promote NHEJ over the more favourable HR pathway (Chen & Tomkinson, 2011; Clikeman et al., 2001; Zhang et al., 2007). Interestingly, CDK also phosphorylates Exo1 in human cells thereby promoting HR (Tomimatsu et al., 2014). Thus, Exo1 is another potential candidate for Rif1-mediated dephosphorylation by Glc7 at DSBs in budding yeast. Moreover, DDK has been reported to phosphorylate human Exo1 in vitro (Sasi et al., 2018), thus Exo1 may be analagous to Mcm4 as a factor that DDK both phosphorylates directly and whose dephosphorylation is prevented through DDK inhibition of Rif1-Glc7 activity. Along similar lines, recent reports show that hRif1, through PP1 binding, prevents nascent DNA degradation by over-resection during HU exposure and controls the phosphorylation level of Dna2 (Mukherjee et al., 2019) and WRN helicase, one of the human homologs of Sgs1 (Garzón et al., 2019). Future investigation, combining the Rif1 RVxF/SILK mutations, which abrogate its association with Glc7 (Hiraga et al., 2014; Mattarocci et al., 2014; Sreesankar et al., 2012) and *5AΔPPDSPP* will confirm whether the repair defect in *rif1 5AΔPPDSPP* is due to Rif1 gain-of function in stably tethering Glc7 or not. Another mechanism whereby mammalian Rif1 inhibits resection is via its interaction with 53BP1 and the shieldin complex, limiting access to resection nucleases at DSBs, as well as mediating the co-localization of the CST (CTC1-STN1-TEN1) complex and DNA polymerase-α to DSBs resulting in CST-polα dependent fill-in activity (Ghezraoui et al., 2018; Mirman et al., 2018; Noordermeer et al., 2018). It will be interesting to determine if similar mechanisms exist in other eukaryotes, and, if so, whether the Rif1-Dbf4 interaction plays a role.

With the present report, I demonstrate that the Dbf4-Rif1 interaction is important for cell cycle progression under both unperturbed and perturbed conditions. Impairment of this association through deletion of the Rif1 C-terminal PPDSPP motif and mutation of Rif1 CDK phosphorylation sites renders cells acutely sensitive to DSBs. The identification of key Glc7 targets that are hypophosphorylated as a consequence of the disrupted Rif1-Dbf4 interaction will be an important step in better understanding of cellular responses to genotoxic stress.

Chapter 5

Characterization of a novel mode of DDK-Mrc1 association in *Saccharomyces cerevisiae*

Figure 5.1. Larasati performed experimental design, data interpretation and analysis. Celine Aziz carried out plasmid construction and performed yeast-two hybrid experiments and analysis.

Figure 5.2 and 5.3. Larasati carried out experimental design, data interpretation and analysis. Zohaib Merali carried out plasmid construction and performed yeast-two hybrid analysis.

Figure 5.4. Larasati generated the yeast strain and carried out experimental design, data interpretation and analysis. Zohaib Merali carried out yeast strain confirmation and performed the spotting assay.

Appendix C Figure 1. Larasati and Zohaib Merali carried out Mrc1 multiple sequence alignment.

5.1 Introduction

Eukaryotes initiate DNA replication from multiple loci, ranging from around 400 origins in budding yeast to 50,000 in humans (Cvetic & Walter, 2005; Diffley, 2011; Méchali, 2010). Each origin must fire no more than once per cell cycle. Any origin that does not follow this rule is a threat to genomic integrity, since over-replication can result in a change of ploidy level and DNA damage (Muñoz et al., 2017; Neelsen et al., 2013). Budding yeast origins follow a temporal order of activation during S-phase. Similarly, fission yeast origins have been shown to fire sequentially, where origins near to centromeres fire early and origins adjacent to telomeres fire later in S phase (Hayano et al., 2012; Kim & Huberman, 2001; Tazumi et al., 2012). This has raised long-standing questions: why are there early and late origins and what differentiates them?

All origins do not fire simultaneously due to the limited abundance of certain firing (Mantiero et al., 2011; Tanaka et al., 2011) and elongation factors (Poli et al., 2012), local transcription activity (Fraser, 2013), and chromatin status (Bellush & Whitehouse, 2017). The loading of the pre-Replicative complex (pre-RC) at origins in budding yeast marks them as eligible candidates of DNA replication start sites in G1 phase. Therefore, the sequential timing pattern of origin firing is established after pre-RC formation. It has been shown that limiting firing factors, such as Dbf4, are enriched at early origins at the beginning of S phase, whereas inhibitory factors that delay origin firing, such as Rif1, accumulate at the late origins (reviewed in Boos & Ferreira, 2019; Yamazaki et al., 2013).

A checkpoint protein, Mrc1, has been shown to associate with a subset of early origins during early S phase in fission yeast (Hayano et al., 2011). Budding yeast Mrc1 has also been

reported to accumulate at early (ARS 305) and late (ARS 603) origins in a sequential fashion (Osborn & Elledge, 2003). These findings indicate that Mrc1 recruitment to origins may coincide with or precede their activations. Consistently, its human ortholog Claspin is loaded onto origins in a Cdc45-dependent but RPA-independent manner, demonstrating that its loading occurs before origin unwinding (Lee et al., 2005, 2003). In budding yeast, Mrc1 engages with the pre-RC components, Cdc45 (Gambus et al., 2006), Mcm6 (Komata et al., 2009) and pol2 (a subunit of pol ε) (Lou et al., 2008). While this binding is considered as one of the Mrc1 mechanisms in guarding replisome stability (Bando et al., 2009; Nedelcheva et al., 2005), this also indicates that Mrc1 may be involved in origin firing regulation.

Evidence of a Claspin/Mrc1 role in replication timing regulation has come from experiments in higher eukaryotes and fission yeast. The depletion of Claspin reduces the rate of fork progression in *Xenopus* oocyte extracts (Lee et al., 2003), HeLa cells (Scorah & McGowan, 2009), and murine cells (Yang et al., 2016). However, the slower DNA synthesis rate in HeLa cells treated with Claspin siRNA is accompanied by a higher level of origin firing (Scorah & McGowan, 2009). The deletion of *MRC1* in fission yeast advances early origin firing, which results in a slightly accelerated speed of S-phase progression (Hayano et al., 2011). In contrast with the observation in HeLa cells (Scorah & McGowan, 2009), Δ*mrc1* fission yeast cells do not have significantly altered fork rates in, suggesting the modestly escalated speed of S-phase is due to more efficient origin firing. Indeed, Δ*mrc1* cells exhibit earlier loading of Cdc45 onto a subset of early origins (Hayano et al., 2011). Additionally, Δ*mrc1* rescues the temperature-sensitive mutation *hsk1-89* (fission yeast ortholog of Cdc7) at a semi-restrictive temperature of 30°C (Matsumoto et al., 2011).

It has been proposed that Claspin/Mrc1 directs origin firing through its recruitment of DDK (Hsk1-Dfp1 in fission yeast or Cdc7-ASK in mammals) (reviewed in Masai et al., 2017). Both Claspin and fission yeast Mrc1 have been reported to interact with Cdc7/Hsk1 (Shimmoto et al., 2009; Yang et al., 2016). Moreover, Mrc1 forms an intramolecular interaction, where its C-terminal interacts with a region in the middle of the protein. The C-terminal portion is called the Hsk1-bypass segment (HBS) due to corresponding mutant fission yeast cells' ability to bypass the need for Hsk1 in supporting growth. The middle region is termed the N-terminal target of HBS (NTHBS). Both NTHBS and HBS are required for Hsk1 binding, whereas neither of them efficiently mediates the Hsk1 interaction on its own. This indicates that this Mrc1 intramolecular interaction facilitates Hsk1 recruitment (Matsumoto et al., 2017). Additionally, the NTHBS-HBS interaction has been postulated to control the functionality of fission yeast Mrc1. As previously mentioned, deletion of the HBS portion on Mrc1 can rescue the temperature sensitivity of *hsk1-89* (*hsk1-89 mrc1*Δ*HBS* strain) at 30°C. An increased level of early origin firing in this mutant strain and the loss of NTHBS-HBS binding are considered as the basis of the rescue phenotype. When the HBS polypeptide is expressed ectopically to restore this binding in the *hsk1-89 mrc1*Δ*HBS* strain, the rescue phenotype at 30°C is suppressed. Therefore, this intramolecular NTHBS-HBS interaction is proposed to act as a 'built-in' brake for DNA replication as it possesses an inhibitory property for origin firing (Matsumoto et al., 2017). Consistently, the N-terminal segment of Claspin also interacts with an acidic patch located on its C-terminus in human 293T cells. This binding is reported to reduce Claspin association with DNA and PCNA (Yang et al., 2016). These findings demonstrate that Mrc1 loading at a subset of early origins in fission yeast not only

differentiates these origins from others in early S phase, but also acts as a replication constraint to prevent their precocious firing. Thus, Mrc1 loading at origins adds another layer of control for replication timing in fission yeast and possibly in humans too.

Claspin/Mrc1 is phosphorylated by DDK (Kim et al., 2008; Matsumoto et al., 2010). The association between Claspin/Mrc1 and Cdc7/Hsk1 is postulated to enable DDK phosphorylation of this protein (reviewed in Masai et al., 2017). Furthermore, DDK phosphorylation of Mrc1/Claspin disrupts its intramolecular binding, and in turn, promotes DNA replication in fission yeast (Matsumoto et al., 2017) and its DNA and PCNA binding in human cells (Yang et al., 2016). Given that Mrc1 and Claspin associate with DDK through Hsk1 and Cdc7 in fission yeast and human cells, respectively, we aimed to assess whether this binding is conserved in budding yeast. Such confirmation would then lead to further characterization of how these factors interact and the significance for dictating DNA replication timing.

5.2 Results

5.2.1 Budding yeast Mrc1 engages with DDK by binding Dbf4, not Cdc7

To examine the association between Mrc1 and budding yeast DDK, yeast-two hybrid analysis of Mrc1 binding to each subunit of DDK, Dbf4 and Cdc7 was performed. In contrast to what had previously been seen in fission yeast and human cells, Mrc1 was found to interact with Dbf4 and not Cdc7. The intensity of Mrc1-Cdc7 binding was insignificant, as it was similar to the negative controls (Figure 5.1). The Western-blot result confirmed that the absence of interaction between Cdc7 and Mrc1 is not due to a lack of protein expression. Furthermore, the

protein expression level of the Dbf4 bait seemed to be weaker than was the case for the Cdc7 bait, yet it still demonstrated stronger binding to Mrc1 (Figure 5.1).

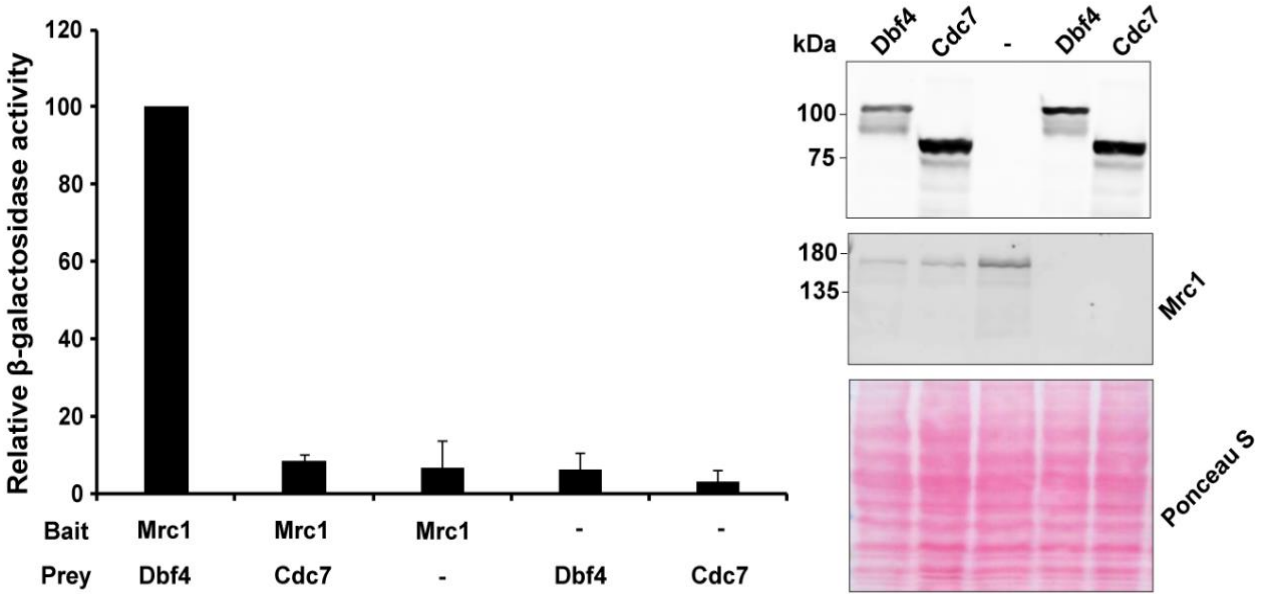

Figure 5.1. Budding yeast Mrc1 interacts with Dbf4, not Cdc7. The interaction of the DDK subunits and Mrc1 was assessed through yeast two-hybrid assays. The two-hybrid interaction values are presented as a percentage of the interaction of Dbf4 and Mrc1. Three independent replicates were performed, and error bars represent standard deviation. Representative Western blots (of three independent experiments performed) indicate protein expression levels and Ponceau S staining shows equal protein loading. Bait and prey proteins were detected with anti-LexA (Mrc1) and anti-HA (Dbf4 or Cdc7) antibodies, respectively.

5.2.2 Dbf4 HBRCT domain and motif C are required for Mrc1 binding

Dbf4 has three conserved motifs, N, M and C, that all mediate protein-protein interactions. They are named based on their relative amino acid positions (Chapter 1 Figure 1.8) (Masai & Arai, 2000). To determine which of the motifs may facilitate Mrc1 binding, yeast-two hybrid experiments of Mrc1 and Dbf4 variants, either with point mutations or full deletions of the aforementioned motifs were conducted. Dbf4 motif N is part of the HBRCT domain (residues 105-221); thus, the Dbf4 mutant L109A/W112S that disrupts the structural stability of this

domain (Matthews et al., 2012) was used. Dbf4 ΔM has its motif M removed (Varrin et al., 2005). To examine Dbf4 motif C investigation, the Dbf4 CCAA mutant that disrupts this zinc finger motif by altering two conserved histidines 674 and 680 into alanines (Jones et al., 2010) was used. The result shows that the Dbf4 L109A/W112S and Dbf4 CCAA mutations abrogated Mrc1 binding by more than 60% and 40%, respectively (Figure 5.2), indicating that both HBRCT domain and motif C contribute to the interaction. In contrast to the two other conserved Dbf4 regions, motif M is not required to mediate Mrc1 binding.

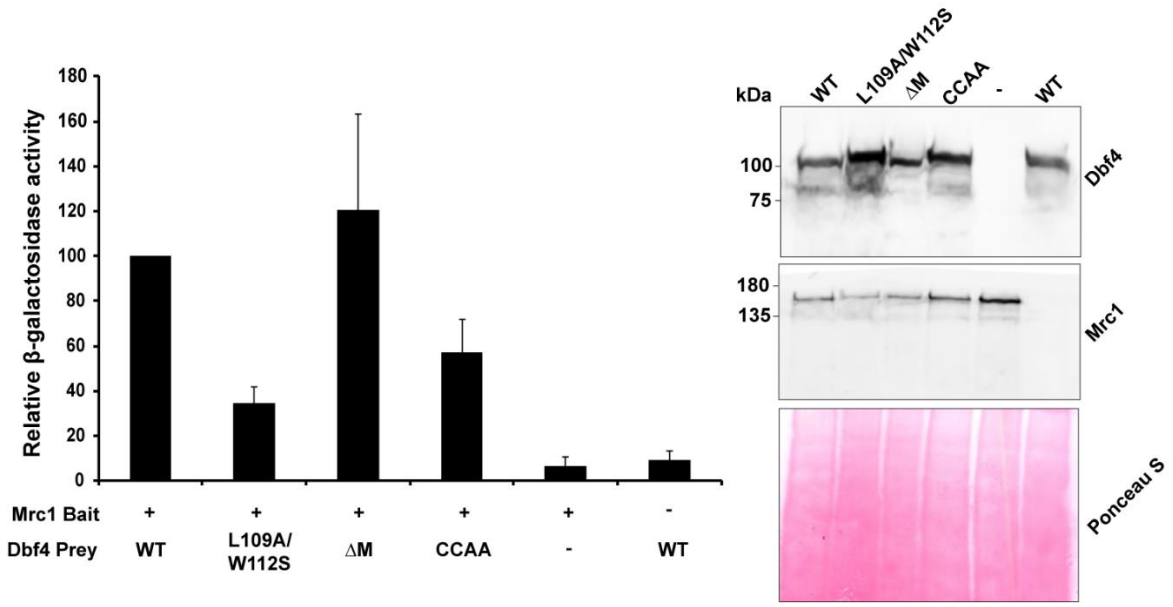

Figure 5.2. Dbf4 binds to Mrc1 through its HBRCT domain and motif C. Yeast two-hybrid assay of Mrc1 with Dbf4 L109A/W112S that represents motif N/HBRCT domain disruption (Matthews et al., 2012), Dbf4 with full deletion of motif M (ΔM) (Varrin et al., 2005), and Dbf4 CCAA that disrupts the zinc finger of motif C (Jones et al., 2010). The two-hybrid interaction values are presented as a percentage of the interaction of wild-type Dbf4 and Mrc1. Three independent replicates were performed, and error bars represent standard deviation. Representative Western blots (of three independent experiments performed) indicate protein expression levels and Ponceau S staining shows equal protein loading. Bait and prey proteins were detected with anti-LexA (Mrc1) and anti-HA (Dbf4) antibodies, respectively.

5.2.3 The Mrc1 N-terminal region, not its C-terminus, mediates binding to Dbf4

Next, attention was turned to Mrc1. To examine the conservation of this protein, multiple sequence alignment of Mrc1 orthologs from yeast species was performed (Appendix C Figure 1). Fission yeast central NTHBS and C-terminal HBS motifs do not seem to be highly conserved among fungi. However, it was noticed that the budding yeast Mrc1 C-terminus has three acidic patches: 720 EMEAEESEDE 729, 808 DDDEDD 813 and 986 EDEDEVE 992. One is located in the HBS equivalent region of budding yeast Mrc1. Acidic patches are known to mediate charge-based protein-protein interactions (Mersman et al., 2012). Therefore, budding yeast Mrc1was truncated to produce two regions with a small overlap: N (residues 1-684) and C (residues 679-1096), and these variants were used for yeast two-hybrid experiments with Dbf4 (Figure 5.3).

The results demonstrated that the Mrc1 N-region, not its C-region, interacts with Dbf4. Interestingly, the Mrc1 N-region consistently showed a stronger binding intensity for Dbf4 than the full-length version. The higher expression level of the Mrc1 N-region compared to other versions may have contributed to this stronger signal. However, since the Mrc1 C-region fails to interact with Dbf4 on its own while its expression level looked similar to Mrc1 full-length, it was concluded that Mrc1 binding to Dbf4 requires its N-terminal region.

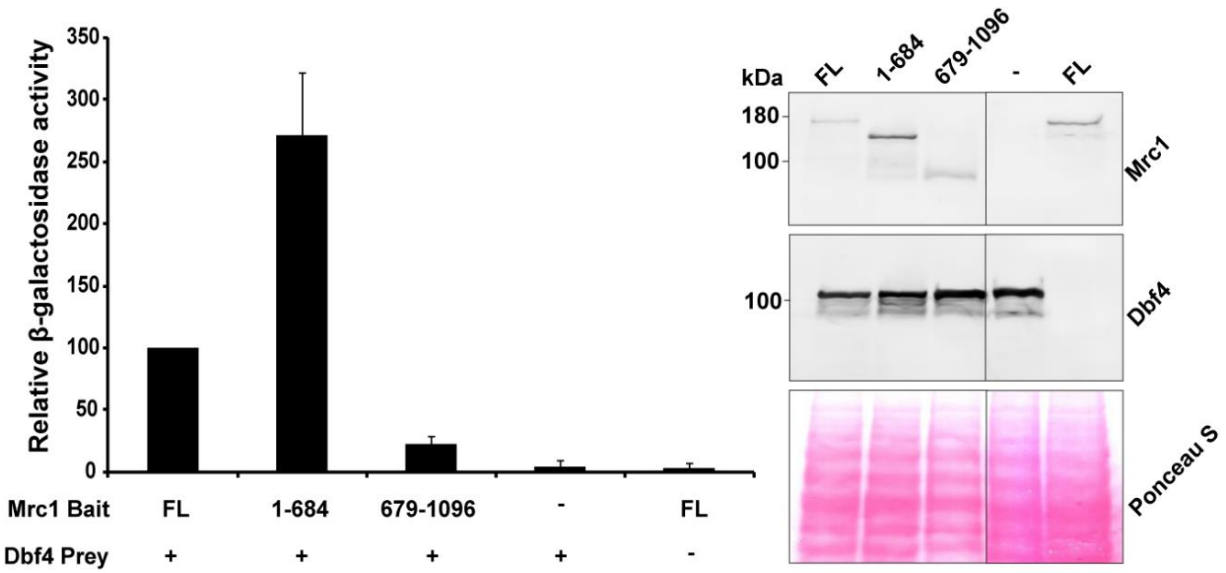

Figure 5.3. Mrc1 engages with Dbf4 via its N-terminal region. Yeast two-hybrid assays with truncated versions of Mrc1 and full-length Dbf4 were performed. Mrc1 is divided into two parts: N-region (residues 1-684) and C-region (residues 679-1096). The two-hybrid interaction values are presented as a percentage of the interaction of Dbf4 and full-length Mrc1. Three independent replicates were performed, and error bars represent standard deviation. Representative Western blots indicate (of three independent experiments performed) protein expression levels and Ponceau S staining shows equal protein loading. Bait and prey proteins were detected with anti-LexA (Mrc1) and anti-HA (Dbf4) antibodies, respectively.

5.2.4 Deletion of *MRC1* exacerbates the *dna52-1* growth defect at 30°C

Knockout of fission yeast *MRC1* rescues the temperature sensitivity of a DDK mutant strain, *hsk1-89,* at non-permissive temperature 30°C. (Matsumoto et al., 2011). To evaluate whether budding yeast Mrc1 behaves the same way as its fission yeast ortholog with respect to its interaction with DDK, *MRC1* was deleted in a budding yeast DDK temperature sensitive strain, *dna52-1*. The *dna52-1* strain expresses a Dbf4 P227L mutant with impaired binding to Mcm2 and Cdc7 at the semi-restrictive temperature of 30°C (Varrin et al., 2005). The P227L mutation is located within motif M. Since this motif is not required for Mrc1 binding (Figure 5.2), it can

be assumed that the temperature sensitivity of *dna52-1* is not due to any defect in Mrc1 association with Dbf4.

dna52-1 and Δ*mrc1 dna52-1* cells were spotted on solid media and incubated in parallel at permissive (22°C), semi-restrictive (30°C) and restrictive (37°C) temperatures (Figure 5.4). To our surprise, Δ*mrc1* worsened the growth of *dna52-1* at 30°C. While our data is still preliminary and requires more validation in different strain backgrounds, this spotting result indicates that Δ*mrc1* behaves in a different manner in supporting growth of fission and budding yeast DDK temperature-sensitive strains.

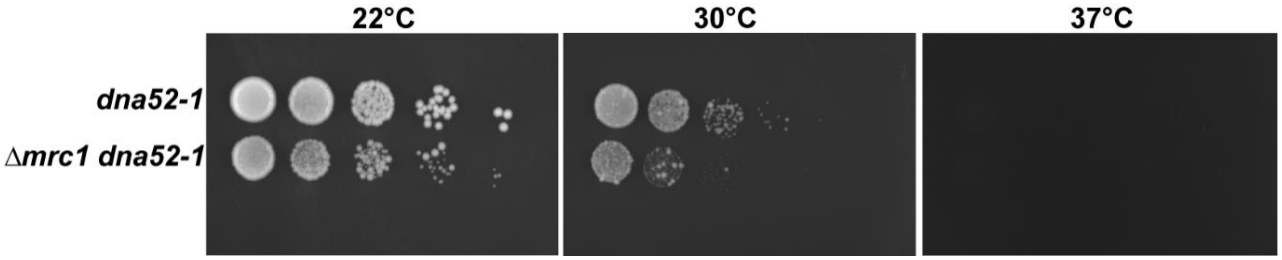

Figure 5.4. Deletion of *MRC1* exacerbates the temperature sensitivity of a *dna52-1* strain. Cells from liquid cultures of the indicated yeast strains were serially diluted ten-fold and spotted onto YPD plates. Pictures were taken after incubation for two days at 22°C, 30°C or 37°C. Three independent replicates were performed, with high reproducibility. A representative image of one trial is shown.

5.3 Discussion

Eukaryotes not only maintain the accuracy of DNA replication to preserve genomic integrity, but they also robustly control when DNA replication can take place. The limiting abundance of certain firing factors greatly contributes to replication timing regulation. Despite the vast progression in the study of eukaryotic DNA replication timing since the findings of its sequential pattern a couple of decades ago (Fangman et al., 1983; McCarroll & Fangman, 1988; Raghuraman et al., 2001; Reynolds et al., 1989), the precise mechanisms whereby the

limiting factors distinguish which the origins to associate with remain to be characterized. Here, we began to investigate whether budding yeast Mrc1 has a checkpoint-independent role in origin firing, as previously demonstrated in fission yeast (Hayano et al., 2011; Matsumoto et al., 2011, 2017) and human cells (Yang et al., 2016).

In fission yeast, Mrc1 is known to be enriched at a cluster of early origins and prevents their premature firing by adopting the 'brake-on' intramolecular binding. DDK then carries out a dual role in initiating DNA replication: phosphorylating Mrc1 to break its intramolecular binding and activating the MCM helicase (Hayano et al., 2011; Matsumoto et al., 2011, 2017). Similarly, human DDK targets Claspin to prevent its self-interaction and, additionally, stimulates Claspin binding to DNA and PCNA (Yang et al., 2016). Inspired by the binding of Mrc1-Hsk1 and Claspin-Cdc7 in mediating DDK phosphorylation, it was decided to investigate whether this is also true in budding yeast. However, it was found that the DDK-interacting subunit for Mrc1 is Dbf4, not Cdc7 (Figure 5.1). Living yeast cells were used in our two-hybrid experiments. Thus, the possibility that another protein may bridge the Dbf4-Mrc1 association cannot be eliminated. An in vitro pull-down assay using purified recombinant proteins can validate whether Dbf4 interaction with Mrc1 is mediated by their direct binding or not. This Dbf4-Mrc1 association is also unique since it depends on the Dbf4 HBRCT domain and motif C (Figure 5.2). To the best of my knowledge, this is the first binding mode of Dbf4 that requires both regions. The data in this chapter also provides another example of HBRCT and motif C versatility in mediating protein-protein interactions. Since Dbf4 HBRCT is known to bind Rad53 during checkpoint conditions (Matthews et al., 2012), it will be interesting to see

if Mrc1 binding to Dbf4 is maintained during replication stress and whether Rad53 displaces it or not.

It was further shown that Mrc1 does not need its C-region to engage with Dbf4 (Figure 5.3). This result argues against the idea that budding yeast Mrc1 must carry out intramolecular binding to recruit DDK, as shown in fission yeast. To evaluate the importance of the Mrc1 N-region, further truncation can be done to find the minimum sufficient binding area, through yeast two-hybrid and/or co-immunoprecipitation experiments. For example, since Mrc1 contains 17 Mec1-dependent checkpoint phosphorylation sites (S/T-Q) (Osborn & Elledge, 2003) and 12 of them reside in the N-terminal region (residues 89-273), the Mrc1 truncation that separates the checkpoint target sites may help to distinguish whether Mrc1-Dbf4 binding is checkpoint-dependent or independent. After the minimum sufficient Dbf4-binding area is obtained, bioinformatic analysis can be conducted on this truncated Mrc1 to find a domain or motif candidate that mediates protein-protein interaction. Mrc1 point mutations of the putative key residues on the domain/motif candidate can be generated through site-directed mutagenesis and its interaction strength can be evaluated as described above. The significance of the Mrc1-Dbf4 interaction can be tested by introducing into the genome a mutant version of *MRC1,* whose product specifically does not bind to Dbf4, as the sole copy of the gene, and the growth phenotype of cells expressing this mutant can be judged by culture cell counts at regular time intervals and FACS analysis.

The Mrc1 N-region, besides being the portion that interacts with Dbf4, is also enriched for serines followed by negatively charged residues (S-E/D), which are the consensus phosphorylation sites of DDK (Randell et al., 2010). Similarly, in fission yeast DDK

phosphorylates an S/T-E rich region that is located immediately N-terminal to the NTHBS region of Mrc1 (Matsumoto et al., 2017). Since the association between a kinase and its substrate generally facilitates phosphorylation, a study to test whether budding yeast Mrc1 is phosphorylated by DDK can be conducted by performing an in vitro kinase assay using purified Mrc1, Dbf4, Cdc7 and [γ^{32}P] ATP. As a negative control, the kinase-deficient Cdc7 that bears mutation on ATP-binding site can be used (Ohtoshi et al., 1997).

In fission yeast, DDK interaction with and phosphorylation of Mrc1 has implications for DNA replication timing. Mrc1 adopts the "brake-on" intramolecular binding and marks a subset of early origins in the beginning of S phase. This Mrc1 "brake-on" is converted to "brake-off" conformation by DDK phosphorylation (Matsumoto et al., 2017). Fission yeast Mrc1 loading at early origins is DDK-independent, indicating that Mrc1 association with the origins may precede DDK recruitment at these sites (Hayano et al., 2011). In budding yeast, Mrc1 loading at the early origin ARS305 is dependent on DDK function where Mrc1 is recruited less efficiently when DDK activity is compromised (Osborn & Elledge, 2003). To obtain more precise data on how DDK regulates Mrc1 loading at origins, further Mrc1 chromatin immunoprecipitation can be carried out with more examples of early origins in budding yeast. Further investigation of Mrc1 as an early origin determinant can be accomplished by observing the genome-wide origin firing pattern in budding yeast *wild type* and Δ*mrc1* strains, as judged by BrdU (5-bromo-2'-deoxyuridine) incorporation as previously described in (Viggiani et al., 2010). Cells are arrested in G1 phase and released into S phase in the presence of BrdU. After this thymidine analog incorporation in the synchronous cell culture, the genomic DNA is extracted at specific time points (early and late S phases),

sonicated, denatured, and the BrdU-labeled DNA is immunoprecipitated using anti-BrdU antibody. The immunoprecipitated DNA is then purified, amplified using PCR, labelled with fluorophore and subjected onto DNA microarrays (BrdU-IP-chip). Unbound genomic DNA fraction is used as a control and labelled with a different fluorophore. BrdU peak heights of known origins are quantified and compared with the peak heights at different genomic locations. Early origins incorporate a higher level of BrdU than late origins in early S phase. If Mrc1 contributes in controlling the replication timing, then the deletion of *MRC1* would result in the failure to differentiate between early and late origins. Consequently, Δ*mrc1* cells may allow normally late origins to access the limiting firing factor(s), such as Dbf4, and their BrdU peaks could appear at the beginning of S phase. Dbf4, as an essential limiting firing factor and activator of DDK, seems to be enriched at different groups of early origins in different ways. A kinetochore protein, Ctf19, recruits Dbf4 to centromeric origins in G1 phase to facilitate their early DNA replication (Natsume et al., 2013). Additionally, Dbf4 localization to the non-centromeric early origins is facilitated by its interaction with the transcription factor Fkh1/2 (Fang et al., 2017; Knott et al., 2012; Lõoke et al., 2013; Ostrow et al., 2014). Recruitment of Dbf4 is then followed by the loading of another limiting factor, Sld3 (Deegan et al., 2016). If Mrc1 is indeed a determinant of origin activation in budding yeast, then it is analogous to Ctf19 or Fkh1/2 in marking early origins and promoting DDK loading onto these sites.

Our preliminary in vivo analysis showed that budding yeast Mrc1 does not act the same way as its fission yeast ortholog (Figure 5.4). Knockout of *MRC1* supports the cell growth of fission yeast when DDK activity is compromised. In contrast in budding yeast, Δ*mrc1* suppresses it. To follow-up on this initial result, Δ*mrc1* can be combined with other non-DDK

temperature sensitive mutants that reduce origin firing efficiency under restrictive temperature, such as *orc2-1* (Fox et al., 1995). Moreover, our preliminary spotting assay requires additional controls, *wild type* and Δ*mrc1*, which can indicate whether the deletion of *MRC1* is also detrimental or not in a non-temperature sensitive strain background.

At this point, we have observed two novel results that may differentiate Mrc1 in budding and fission yeasts: Mrc1 binding to Dbf4 and the slow growth phenotype of Δ*mrc1 dna52-1* at the semi-permissive temperature of 30°C. While it is still interesting to investigate whether budding yeast Mrc1 contributes in origin firing timing by marking early origins, these results also lead us to new questions in investigating the non-checkpoint role of Mrc1 in DNA replication of budding yeast. What is the in vivo significance of Dbf4-Mrc1 binding? What is the basis of the growth defect in Δ*mrc1 dna52-1* cells? Are our new findings related to other known Mrc1 functions in budding yeast, such as maintaining the stability of pol ε binding (Lou et al., 2008) or sustaining the DNA replication speed (Szyjka et al., 2005)? Further studies will be required to elucidate precisely the function of Mrc1 in DNA replication.

Chapter 6

General Discussion and Further Directions

Proteins can dictate the phenotypic traits of an organism. However, they never act alone. Instead, they belong to networks where they can interact with other proteins, DNA and RNA. Thus, characterizing protein interactions provides mechanistic details on how proteins determine the biological processes in cells. Here I summarize the key findings of Dbf4 interactions with its ligands in this thesis and discuss possible future directions in the field.

6.1 The dissection of the novel binding mode between Dbf4 and Rad53

Dbf4 interacts with Rad53 through the phospho-independent binding of HBRCT and FHA1 domains (Matthews et al., 2012, 2014). This interaction is extraordinary since both BRCT and FHA normally function as a phospho-recognition module (Durocher et al., 1999; Manke et al., 2003; Rodriguez et al., 2003; Yu et al., 2003). This non-canonical binding is essential for Rad53 in targeting Dbf4 during checkpoint conditions, and disruption of it results in genotoxic hypersensitivity (Matthews et al., 2014). We further characterized the binding interface and found that HBRCT binds to FHA1 through two contact points. Both domains do not contribute equally to the association with HBRCT is being the dominant partner. Single or dual point mutations on the HBRCT interface result in a more severe binding defect than that on the FHA1 domain (Chapter 3 Figure 3.3). Additionally, quadruple mutations on FHA1 are required to show the same effect (Matthews et al., 2014).

Asymmetrical dimerization, where one subunit acts as a donor and the other as an acceptor, has also been shown in cyclin A-CDK2 interaction. Binding of CDK2 to cyclin A induces a conformational change in this kinase, repositions its ATP-binding site, and exposes its Thr160 for subsequent phosphorylation (Jeffrey et al., 1995) by CDK-activating kinase (CAK) (Gu et al., 1992). Interestingly, cyclin A does not show any structural change upon binding to CDK2 (Brown et al., 1995). Another asymmetrical dimer is represented by the HER2-HER3 pair where their dimer acts as a potent oncoprotein (Amin et al., 2010). In this case, HER2 behaves as the acceptor and HER3 as the donor (Collier et al., 2013). Thus, HER2 dimerization has been a chemotherapy target (Capelan et al., 2013; Wehrman et al., 2006). Unexpectedly, a HER2 inhibitor lapatinib can promote this dimerization in a non-canonical way that is distinct from the native HER2-HER3 dimer (Claus et al., 2018). This may explain a possible resistance mechanism of HER2+ patients to lapatinib, and as Claus et al. (2018) speculated, the failure of lapatinib in increasing the efficacy of trastuzumab in HER2+ breast cancer clinical trials (Piccart-Gebhart et al., 2015).

A second example of a protein with a HBRCT domain has been recently found in yeast, Sir4 (Deshpande et al., 2019). When the HBRCT domains from Sir4 and Dbf4 are superimposed, the structures are similar except for the conformation of the connecting loops between β-strands or β-strand and α-helix. Interestingly, Sir4 HBRCT does not bind to Rad53 (Deshpande et al., 2019). Dbf4 HBRCT interacts with Rad53 FHA1 through two interfaces (Chapter 3 Figure 3.2). The Dbf4 interface I in engaging with Rad53 FHA1 is partially conserved in Sir4 HBRCT, however, the interface II (Dbf4 Lys200) is not. The structural equivalent of this Lys200 residue is Sir4 Arg1066, showing that the positive charge is retained

at that position. However, this site on Sir4 is preceded by a seven residue insert that make it a longer loop than that of Dbf4 (Deshpande et al., 2019). Thus, this research and the Rif1 data (Chapter 4 Figure 4.2C) strongly suggest that Dbf4 Lys200 is specific for Rad53 binding.

Even though Rad53 FHA1 appears to engage with Dbf4 HBRCT in a phospho-independent fashion, it is still competent to act as phospho-recognition module to bind other ligands. We showed that Rad53 FHA1 also interacts with a Cdc7 phospho-peptide (Chapter 3 Figure 3.4) which demonstrates that Rad53 can associate with both DDK subunits simultaneously (Chapter 3 Figure 3.5). Dbf4 HBRCT can also recognize proline-rich phosphopeptide ligands (Esc1 and Ubp10) that are shown to interact with Sir4 HBRCT. These peptide bindings to Dbf4 are phosphorylation specific since the unphosphorylated counterparts do not engage with Dbf4 (Deshpande et al., 2019).

Taken together, additional details of the novel non-canonical Dbf4-Rad53 interaction are presented in this thesis. It will be interesting to explore whether this mode of binding is found in other proteins containing FHA or BRCT domains.

6.2 The characterization of Dbf4 and Rif1 interaction

The Dbf4 HBRCT domain and Rif1 short linear PPDSPP fragment facilitate Dbf4-Rif1 binding. In general, protein-protein associations are mediated by domain-domain interactions (DDIs) or domain-motif interactions (DMIs). DDIs exist as the interface between globular domains, and DMIs occur between globular domains and 3-10 residue Short Linear Motifs (SLIMs). DMIs are thought to require a smaller interface and lower affinity than DDIs do. Thus, they are less stable and linked to transient signalling pathways (Davey et al., 2011;

Mosca et al., 2014; Scott & Pawson, 2009; Stein & Aloy, 2010). Consistent with this, Dbf4-Rif1 binding may reflect a temporary protein-protein interaction that acts as a molecular switch for DNA replication.

A proline-rich fragment, PPDSPP, on the Rif1 C-terminus seems to fit as a SLIM. Proline by itself is already unique because the side chain forms a pyrrolidine ring. Therefore, the occurrence of repetitive prolines in a motif makes it an exceptionally distinct protein recognition face. Proline's side chain possesses a rotational constraint; thus this amino acid is normally located at disordered regions (Imai & Mitaku, 2005). Proline-rich segments tend to occupy the protein's surface instead of being buried in the interior (Holt & Koffer, 2001). Due to these properties, the proline residues on the PPDSPP motif may also help to expose the residues between them to the surface, which can facilitate a unique interface recognition. These characteristics seem to support the Rif1 C-terminus I-TASSER structural prediction (Appendix B Figure 1). Moreover, proline-rich regions are highly represented among eukaryotes proteomes (Rubin et al., 2000) and known to interact with proline-recognition domains (PRDs) such as Src homology-3 (SH3), WW (named after a conserved Trp-Trp motif) and Enabled/VASP homology (EVH1) domains (Li, 2005; Zarrinpar et al., 2003).

While the exploration of Dbf4 HBRCT recognizing a Rif1 proline-rich motif was being conducted, another study was published revealing that, similar to Dbf4, a budding yeast silencing protein Sir4 HBRCT domain interacts with proline-rich phosphopeptides in a nuclear periphery protein Esc1 and a ubiquitin-specific protease Ubp10 in a nanomolar, and a Ty5 retrotransposon integrase in a micromolar range (Deshpande et al., 2019). Therefore, it would be interesting to co-crystalize the PPDSPP-containing Rif1 C-terminal peptide and HBRCT

domain. However, since Dbf4-Rif1 binding is postulated to be cell-cycle dependent, I expect that this interaction is weak and transient. Thus, the detailed interface of this binding can be mapped using Nuclear Magnetic Resonance (NMR) spectroscopy which can capture weak protein-protein interactions that are difficult to crystallize (Qin & Gronenborn, 2014; Vinogradova & Qin, 2012). Moreover, a study to investigate whether a post-translational modification, such as phosphorylation, is required or not for Dbf4-Rif1 binding can be conducted, as in the case of Sir4 HBRCT with its aforementioned targets (Deshpande et al., 2019). The serine residue on the PPDSPP motif follows the CDK consensus phosphorylation target rule (Ser/Thr-Pro). Therefore, mutation of the serine or the following proline to alanine may abolish the Dbf4-Rif1 interaction. In contrast, phosphomimetic mutations changing the targeted serine into glutamic or aspartic acid may stabilize this binding. These results will provide a better insight into how the HBRCT domain engages with its targets in a phospho-dependent or -independent manner.

Protein-protein interactions have gained attention as drug discovery targets with the development of small molecules that act as binding inhibitors. These molecules are said to be peptidomimetics and can occupy the binding site of a protein so that its natural ligand cannot bind to it. However, any comprehensive characterization of the binding interface does not guarantee successful drug development. The proteins that are considered to be undruggable (or not yet druggable) usually have flat and large binding interfaces on both sides (about 1,000-2,000 $Å^2$) (Hwang et al., 2010). In contrast, the druggable targets must have an obvious catalytic site (Sperandio et al., 2008) and a binding cleft/pocket, with the size around 300-500 $Å^2$ (Fuller et al., 2009) where the small molecule can attack. Many examples of the druggable

proteins have been collected in a public repository "Druggable Cavity Directory" (DCD) (http://fpocket.sourceforge.net/dcd/) (Schmidtke & Barril, 2010). A good example of a druggable DMI-based protein-protein interaction is the binding of tumor suppressor p53 and E3-ubiquitin ligase Mdm2. p53 interacts with Mdm2 via a hydrophobic motif on its C-terminus that fits in a small pocket of Mdm2 (Blommers et al., 1997; Kussie et al., 1996). This binding results in the loss of p53 transcriptional activity in promoting the expression of anti-oncogenic proteins, such as p21 and Bax (Clegg et al., 2012; Momand et al., 1992; Oliner et al., 1993). Therefore, inhibiting Mdm2-p53 interaction is promising for cancer therapy, and indeed, several corresponding small molecule inhibitors have been tested in clinical trials (Kocik et al., 2019; Tisato et al., 2017). DDK itself has been proposed as a promising target candidate for cancer chemotherapy. Its selective inhibitor, TAK-931, is undergoing two clinical trials at this moment (Iwai et al., 2019). Additionally, since Dbf4-Rif1 acts as a molecular switch for DNA replication, further structural investigation of the Dbf4-Rif1 interaction will shed light on whether this binding has potential as a target in DDK-based cancer drug development.

Proline-rich motifs have been shown to be useful in the development of proline-rich antimicrobial peptides (Graf et al., 2017). Additionally, proline-rich polypeptides possess a positive immunomodulatory property in human studies of patients with Alzheimer's disease (Janusz & Zabłocka, 2010; Sochocka et al., 2019). These suggest that proline-rich motifs can be used as a platform for polyproline peptidomimetic drug discovery, where the peptides can block proline-specific protein-protein interactions.

In the context of this thesis and its connection to cancer-related research, inhibition of Rif1 and Dbf4 interaction via disruption of the Rif1 proline-rich segment may help to

deactivate the helicase which, in turn, could reduce DNA replication initiation and cell proliferation levels. The combination of Rif1 CDK and DDK phosphorylation defects on *rif1 5A*Δ*PPDSPP* results in dramatic growth inhibition (Chapter 4 Figure 4.6). In human cells, CDK phosphorylation of Rif1 disrupts Rif1-PP1's ability to repress dormant origin firing (Moiseeva et al., 2019). Thus, it is interesting to study how human DDK regulates Rif1 in normal conditions and whether there is an overlap between the two kinases.

The parallel inhibitions of CDK and DDK targeting Rif1 also impair cell resistance to genotoxic stress, with the most notable lethality shown under DNA double-strand break conditions (bleocin and phleomycin). Since these kinases' phosphorylation of Rif1 breaks its binding to Glc7 (Davé et al., 2014; Hiraga et al., 2014), the in vivo results indicate that Rif1 gain-of-function in maintaining a stable Glc7 interaction is detrimental for the cells when dealing with genotoxic insults. In contrast, the *rif1* mutant strain that is defective in Glc7 binding (*rif1 RVxF/SILK*) does not show a sickness under phleomycin treatment when compared to *wild type* (Shyian et al., 2016). The genotoxic hypersensitivity of *rif1 5A*Δ*PPDSPP* may stem from the failure to activate dormant origins, incompetency in DNA damage repair, or both. The fact that *rif1 5A*Δ*PPDSPP* genotoxic sensitivity is worsened when homologous recombination (HR) is compromised (Δ*sae2/rif1 5A*Δ*PPDSPP*), but not in NHEJ disruption (Δ*nej1/rif1 5A*Δ*PPDSPP* and Δ*yku70/ rif1 5A*Δ*PPDSPP*) (Chapter 4 Figure 4.7), is consistent with the continuous Rif1-Glc7 dephosphorylation activity being detrimental to the HR pathway. Further investigations combining *rif1 RVxF/SILK* with Δ*sae2* and Δ*sae2/rif1 5A*Δ*PPDSPP* can be conducted to pinpoint whether Glc7 is indeed the Rif1 downstream target in threatening homologous recombination.

The increased sensitivity of Δ*sae2/rif1 5A*Δ*PPDSPP* to genotoxic stress, when compared to the individual mutant strains, aligns well with the concept of synthetic toxicity (conditional synthetic lethality) (O'Neil et al., 2017). The term synthetic lethality in cancer studies conveys the idea of killing cancer cells by inhibiting a DNA repair pathway while another pathway is already blocked by mutations accumulated in the cells (reviewed in Lord et al., 2015; O'Neil et al., 2017). Since the basis of this strategy is using the deficiency that the cancer cells already bear, synthetic lethality can increase the selectivity of cancer therapy. Conventional chemotherapy drugs, such as doxorubicin and cisplatin, are cytotoxic to not only cancer but to healthy cells as well (Buzdar et al., 1985; Safirstein et al., 1986). A major leap of synthetic lethality-based therapy was the discovery and usage of olaparib, a PARP-1 inhibitor, in treating cancer with *BRCA1/2* mutations (Farmer et al., 2005; Helleday et al., 2005). Conditional synthetic lethality adds another twist by sensitizing the mutant cells to specific circumstances. An example of this strategy is combining a PARP inhibitor with lapatinib (epidermal growth factor receptor/EGFR and HER2 inhibitor) in treating triple negative breast cancer (negative to estrogen receptor, progesterone receptor, and excess of HER2) (Nowsheen et al., 2012). An example in budding yeast research is the combination of a checkpoint mutant strain Δ*tel1* and flap endonuclease mutant Δ*rad27* that is lethal under camptothecin treatment (Li et al., 2014). In the research reported in my thesis, another example of synthetic cytotoxicity was identified. The Δ*sae2/rif1 5A*Δ*PPDSPP* strain is sick/lethal when being challenged by genotoxic stress, with the most noteworthy result obtained from treatment of the alkylating agent MMS, while the single mutants showed reduced viability. More importantly, we were able to lower the concentrations of the genotoxic compounds in our experiments,

except for camptothecin, to see the cytotoxic effect in Δ*sae2/rif1 5A*Δ*PPDSPP* (Chapter 4 Figure 4.7) compared to that for *rif1 5A*Δ*PPDSPP* (Chapter 4 Figure 4.6). In cancer therapy, lower doses of anticancer drugs are linked to less severe side effects. Thus, the concept of synthetic toxicity can broaden the scope of the therapeutic targets which, optimistically, may attack the cancerous cells more effectively than standard chemotherapy without increasing the risks of their side effects.

In contrast to the results discussed above, a rescue from genotoxic stress was observed when the NHEJ pathway was disrupted (Δ*nej1* or Δ*yku70*) in the *rif1 5A*Δ*PPDSPP* strain. Since NHEJ and HR are incompatible, the possible explanation for this phenotype is Δ*nej1* or Δ*yku70* can reverse the resection defect in *rif1 5A*Δ*PPDSPP.* This hypothesis could be confirmed through a sequential dual pulse-labelling DNA fibre assay (IdU-CldU) followed by genotoxic stress exposure. In this experiment, cells (Δ*sae2/rif1 5A*Δ*PPDSPP,* Δ*nej1/rif1 5A*Δ*PPDSPP* and Δ*yku70/rif1 5A*Δ*PPDSPP*) are arrested in G1 phase and released into S phase. The nascent DNA from the synchronized cell culture before genotoxic stress can be sequentially labelled by incorporation of the thymidine analogs, IdU (5-iodo-2'-deoxyuridine) and CldU (5-chloro-2'-deoxyuridine) for 20 minutes each followed by genotoxic compound treatment for 3-4 hours. Cells are harvested and individual DNA fibres are spread on a slide and incubated with fluorophore-tagged antibodies directed against IdU and CldU, each with specific fluorophore. The signals are visualized by fluorescence microscopy. The first (IdU) and second (CldU) labelled tracks indicate the initial position and polarity of replication, respectively. The shortening of the second labelled-track represents the rate of DNA resection (Higgs et al., 2015). Moreover, the synthetic rescue that was obtained in this research

emphasizes the importance of genetic background when revealing a new phenotype. This is true especially in cancer where each type has specific gene mutations, meaning that a "one size fits all" chemotherapy approach is not always the best strategy. Additionally, synthetic rescue can arise when cancer cells develop mutation-based drug resistance. For instance, loss of 53BP1 results in resistance to PARP inhibitor in *BRCA1*-deficient mammary tumors, which is aided by the re-establishment of homologous recombination (Jaspers et al., 2013).

Collectively, the results presented in Chapter 4 further the understanding of protein-protein binding based on domain-motif interaction, and the employment of in vivo synthetic cytotoxicity/rescue approaches.

6.3 Initial investigation of Dbf4 and Mrc1 association in budding yeast

In this study, we explored the possibility that Mrc1 associates with DDK in budding yeast, as previously reported in fission yeast and humans (Hayano et al., 2011; Kim et al., 2008; Matsumoto et al., 2011; Yang et al., 2016). To facilitate DDK phosphorylation, fission yeast Mrc1 and its human orthologs Claspin interact with DDK subunit, Cdc7 (Kim et al., 2008; Matsumoto et al., 2017; Shimmoto et al., 2009; Yang et al., 2016). However, our work showed that Dbf4, not Cdc7, is the subunit that engages with Mrc1 in budding yeast (Chapter 5 Figure 5.1). More importantly, deletion of *MRC1* exacerbated the growth defect of a temperature-sensitive DDK strain at a semi-permissive temperature (Chapter 5 Figure 5.4), instead of rescuing it as in fission yeast (Matsumoto et al., 2011, 2017). Even though our preliminary data still requires more validation of how DDK regulates Mrc1, as I proposed in Chapter 5, they indicate that budding and fission yeast Mrc1 may act differently in DNA replication initiation.

Additionally, the efficient loading of budding yeast Mrc1 onto the early origin ARS305 requires DDK activity (Osborn & Elledge, 2003). In contrast, fission yeast Mrc1 enrichment at early origins is not affected by DDK (Hayano et al., 2011). This discrepancy suggests that DDK may modulate a different role of budding yeast Mrc1.

In budding yeast, Mrc1 is not included in the minimum set of the initiation factors to reconstitute DNA replication in vitro (Yeeles et al., 2015). However, Mrc1 increases the DNA replication speed, and combining it with Csm3/Tof1 promotes the maximum replication rate (Yeeles et al., 2017). Fission yeast Mrc1 exhibits another difference by not significantly controlling the replication rate (Hayano et al., 2011). Thus, if future investigations do not support Mrc1 as a marker of early origins in budding yeast, it is interesting to see whether DDK-Mrc1 binding can control other known Mrc1 functions, such as the maintenance of DNA replication speed.

In summary, we show here that Mrc1 interacts with the Dbf4 subunit of DDK and is required to support cell growth when DDK activity is compromised. The in vivo significance of the DDK-Mrc1 association awaits furthers exploration.

6.4 Final thoughts

Over many years, yeast-based assays have been developed to study fundamental questions in cell cycle and cancer biology-related research. The major contribution of this thesis is to advance our understanding of how Dbf4 interactions with various ligands regulate DNA replication and safeguard its integrity in budding yeast. While the escalation of our findings to cancer research will require rigorous exploration and validation, they provide an insight on

how Dbf4 association with other proteins can have critical consequences in the cell cycle. More importantly, understanding basic science is undoubtedly essential in the development of better and more effective cancer treatments. We cannot offer solutions to problems that we do not fully understand.

Bibliography

Adams, P. D., Afonine, P. V., Bunkóczi, G., Chen, V. B., Davis, I. W., Echols, N., … Zwart, P. H. (2010). PHENIX: A comprehensive Python-based system for macromolecular structure solution. *Acta Crystallographica. Section D, Biological Crystallography*, *66*(Pt 2), 213–221.

Ahn, J., & Prives, C. (2002). Checkpoint Kinase 2 (Chk2) Monomers or Dimers Phosphorylate Cdc25C after DNA Damage Regardless of Threonine 68 Phosphorylation. *Journal of Biological Chemistry*, *277*(50), 48418–48426.

Ahn, J.-Y., Li, X., Davis, H. L., & Canman, C. E. (2002). Phosphorylation of Threonine 68 Promotes Oligomerization and Autophosphorylation of the Chk2 Protein Kinase via the Forkhead-associated Domain. *Journal of Biological Chemistry*, *277*(22), 19389–19395.

Ajimura, M., Leem, S. H., & Ogawa, H. (1993). Identification of new genes required for meiotic recombination in Saccharomyces cerevisiae. *Genetics*, *133*(1), 51–66.

Akhmetov, A., Laurent, J. M., Gollihar, J., Gardner, E. C., Garge, R. K., Ellington, A. D., … Marcotte, E. M. (2018). Single-step Precision Genome Editing in Yeast Using CRISPR-Cas9. *Bio-Protocol*, *8*(6).

Alberts, B., Johnson, A., Lewis, J., Raff, M., Roberts, K., & Walter, P. (2002). An Overview of the Cell Cycle. *Molecular Biology of the Cell. 4th Edition*.

Alcasabas, A. A., Osborn, A. J., Bachant, J., Hu, F., Werler, P. J. H., Bousset, K., … Elledge, S. J. (2001). Mrc1 transduces signals of DNA replication stress to activate Rad53. *Nature Cell Biology*, *3*(11), 958–965.

Allen, J. B., Zhou, Z., Siede, W., Friedberg, E. C., & Elledge, S. J. (1994). The SAD1/RAD53 protein kinase controls multiple checkpoints and DNA damage-induced transcription in yeast. *Genes & Development*, *8*(20), 2401–2415.

Almawi, A. W., Matthews, L. A., Larasati, Myrox, P., Boulton, S., Lai, C., … Guarné, A. (2016). 'AND' logic gates at work: Crystal structure of Rad53 bound to Dbf4 and Cdc7. *Scientific Reports*, *6*, 34237.

Alver, R. C., Chadha, G. S., & Blow, J. J. (2014). The contribution of dormant origins to genome stability: From cell biology to human genetics. *DNA Repair*, *19*(100), 182–189.

Amin, D. N., Sergina, N., Ahuja, D., McMahon, M., Blair, J. A., Wang, D., … Moasser, M. M. (2010). Resiliency and Vulnerability in the HER2-HER3 Tumorigenic Driver. *Science Translational Medicine*, *2*(16), 16ra7-16ra7.

Anand, R. P., Shah, K. A., Niu, H., Sung, P., Mirkin, S. M., & Freudenreich, C. H. (2012). Overcoming natural replication barriers: Differential helicase requirements. *Nucleic Acids Research*, *40*(3), 1091–1105.

Aparicio, J. G., Viggiani, C. J., Gibson, D. G., & Aparicio, O. M. (2004). The Rpd3-Sin3 histone deacetylase regulates replication timing and enables intra-S origin control in Saccharomyces cerevisiae. *Molecular and Cellular Biology*, *24*(11), 4769–4780.

Aparicio, O. M. (2013). Location, location, location: It's all in the timing for replication origins. *Genes & Development*, *27*(2), 117–128.

Arnone, J. T., Walters, A. D., & Cohen-Fix, O. (2013). The dynamic nature of the nuclear envelope. *Nucleus*, *4*(4), 261–266.

Aucher, W., Becker, E., Ma, E., Miron, S., Martel, A., Ochsenbein, F., … Guerois, R. (2010). A strategy for interaction site prediction between phospho-binding modules and their partners identified from proteomic data. *Molecular & Cellular Proteomics: MCP*, *9*(12), 2745–2759.

Ausubel, F. M., Brent, R., Kingston, R. E., Moore, D. D., Seidman, J. G., Smith, J. A., & Struhl, K. (1994). *Current Protocols in Molecular Biology*. New York: Wiley.

Bando, M., Katou, Y., Komata, M., Tanaka, H., Itoh, T., Sutani, T., & Shirahige, K. (2009). Csm3, Tof1, and Mrc1 Form a Heterotrimeric Mediator Complex That Associates with DNA Replication Forks. *Journal of Biological Chemistry*, *284*(49), 34355–34365.

Barberis, M., Spiesser, T. W., & Klipp, E. (2010). Replication Origins and Timing of Temporal Replication in Budding Yeast: How to Solve the Conundrum? *Current Genomics*, *11*(3), 199–211.

Bardwell, L. (2005). A walk-through of the yeast mating pheromone response pathway. *Peptides*, *26*(2), 339–350.

Baroni, E., Viscardi, V., Cartagena-Lirola, H., Lucchini, G., & Longhese, M. P. (2004). The Functions of Budding Yeast Sae2 in the DNA Damage Response Require Mec1- and Tel1-Dependent Phosphorylation. *Molecular and Cellular Biology*, *24*(10), 4151–4165.

Bartek, J., & Lukas, J. (2003). Chk1 and Chk2 kinases in checkpoint control and cancer. *Cancer Cell*, *3*(5), 421–429.

Bar-Ziv, R., Voichek, Y., & Barkai, N. (2016). Chromatin dynamics during DNA replication. *Genome Research*, *26*(9), 1245–1256.

Baudin, A., Ozier-Kalogeropoulos, O., Denouel, A., Lacroute, F., & Cullin, C. (1993). A simple and efficient method for direct gene deletion in Saccharomyces cerevisiae. *Nucleic Acids Research*, *21*(14), 3329–3330.

Bell, S. P., & Labib, K. (2016). Chromosome Duplication in Saccharomyces cerevisiae. *Genetics*, *203*(3), 1027–1067.

Bell, S. P., & Stillman, B. (1992). ATP-dependent recognition of eukaryotic origins of DNA replication by a multiprotein complex. *Nature*, *357*(6374), 128.

Bellush, J. M., & Whitehouse, I. (2017). DNA replication through a chromatin environment. *Philosophical Transactions of the Royal Society B: Biological Sciences*, *372*(1731), 20160287.

Bermejo, R., Doksani, Y., Capra, T., Katou, Y.-M., Tanaka, H., Shirahige, K., & Foiani, M. (2007). Top1- and Top2-mediated topological transitions at replication forks ensure fork progression and stability and prevent DNA damage checkpoint activation. *Genes & Development*, *21*(15), 1921–1936.

Blommers, M. J. J., Fendrich, G., García-Echeverría, C., & Chêne, P. (1997). On the Interaction Between p53 and MDM2: Transfer NOE Study of a p53-Derived Peptide Ligated to MDM2. *Journal of the American Chemical Society*, *119*(14), 3425–3426.

Bonetti, D., Clerici, M., Anbalagan, S., Martina, M., Lucchini, G., & Longhese, M. P. (2010). Shelterin-Like Proteins and Yku Inhibit Nucleolytic Processing of Saccharomyces cerevisiae Telomeres. *PLoS Genetics*, *6*(5).

Bonte, D., Lindvall, C., Liu, H., Dykema, K., Furge, K., & Weinreich, M. (2008). Cdc7-Dbf4 Kinase Overexpression in Multiple Cancers and Tumor Cell Lines Is Correlated with p53 Inactivation. *Neoplasia*, *10*(9), 920-IN4.

Boos, D., & Ferreira, P. (2019). Origin Firing Regulations to Control Genome Replication Timing. *Genes*, *10*(3).

Brachmann, C. B., Davies, A., Cost, G. J., Caputo, E., Li, J., Hieter, P., & Boeke, J. D. (1998). Designer deletion strains derived from Saccharomyces cerevisiae S288C: A useful set of strains and plasmids for PCR-mediated gene disruption and other applications. *Yeast*, *14*(2), 115–132.

Branzei, D., & Foiani, M. (2005). The DNA damage response during DNA replication. *Current Opinion in Cell Biology*, *17*(6), 568–575.

Branzei, D., & Szakal, B. (2016). DNA damage tolerance by recombination: Molecular pathways and DNA structures. *DNA Repair*, *44*, 68–75.

Brown, N. R., Noble, M. E. M., Endicott, J. A., Garman, E. F., Wakatsuki, S., Mitchell, E., … Johnson, L. N. (1995). The crystal structure of cyclin A. *Structure*, *3*(11), 1235–1247.

Buonomo, S. B. C., Wu, Y., Ferguson, D., & Lange, T. de. (2009). Mammalian Rif1 contributes to replication stress survival and homology-directed repair. *The Journal of Cell Biology*, *187*(3), 385–398.

Burgess, S. M., Powers, T., & Mell, J. C. (2017). Budding Yeast Saccharomyces Cerevisiae as a Model Genetic Organism. In *ELS* (pp. 1–12).

Buzdar, A. U., Marcus, C., Smith, T. L., & Blumenschein, G. R. (1985). Early and delayed clinical cardiotoxicity of doxorubicin. *Cancer*, *55*(12), 2761–2765.

Cai, Z., Chehab, N. H., & Pavletich, N. P. (2009). Structure and Activation Mechanism of the CHK2 DNA Damage Checkpoint Kinase. *Molecular Cell*, *35*(6), 818–829.

Can, G., Kauerhof, A. C., Macak, D., & Zegerman, P. (2019). Helicase Subunit Cdc45 Targets the Checkpoint Kinase Rad53 to Both Replication Initiation and Elongation Complexes after Fork Stalling. *Molecular Cell*, *73*(3), 562-573.e3.

Cannavo, E., & Cejka, P. (2014). Sae2 promotes dsDNA endonuclease activity within Mre11–Rad50–Xrs2 to resect DNA breaks. *Nature*, *514*(7520), 122–125.

Cao, J.-X., & Lu, Y. (2019). Targeting CDC7 improves sensitivity to chemotherapy of esophageal squamous cell carcinoma. *OncoTargets and Therapy*, *12*, 63–74.

Capelan, M., Pugliano, L., De Azambuja, E., Bozovic, I., Saini, K. S., Sotiriou, C., … Piccart-Gebhart, M. J. (2013). Pertuzumab: New hope for patients with HER2-positive breast cancer. *Annals of Oncology*, *24*(2), 273–282.

Cejka, P., & Kowalczykowski, S. C. (2010). The Full-length Saccharomyces cerevisiae Sgs1 Protein Is a Vigorous DNA Helicase That Preferentially Unwinds Holliday Junctions. *Journal of Biological Chemistry*, *285*(11), 8290–8301.

Chabes, A., Georgieva, B., Domkin, V., Zhao, X., Rothstein, R., & Thelander, L. (2003). Survival of DNA Damage in Yeast Directly Depends on Increased dNTP Levels Allowed by Relaxed Feedback Inhibition of Ribonucleotide Reductase. *Cell*, *112*(3), 391–401.

Chanut, P., Britton, S., Coates, J., Jackson, S. P., & Calsou, P. (2016). Coordinated nuclease activities counteract Ku at single-ended DNA double-strand breaks. *Nature Communications*, *7*, 12889.

Chapman, J. R., Barral, P., Vannier, J.-B., Borel, V., Steger, M., Tomas-Loba, A., … Boulton, S. J. (2013). RIF1 Is Essential for 53BP1-Dependent Nonhomologous End Joining and Suppression of DNA Double-Strand Break Resection. *Molecular Cell*, *49*(5), 858–871.

Chen, S., Smolka, M. B., & Zhou, H. (2007). Mechanism of Dun1 activation by Rad53 phosphorylation in Saccharomyces cerevisiae. *The Journal of Biological Chemistry*, *282*(2), 986–995.

Chen, S.-H., & Zhou, H. (2009). Reconstitution of Rad53 activation by Mec1 through adaptor protein Mrc1. *The Journal of Biological Chemistry*, *284*(28), 18593–18604.

Chen, X., & Tomkinson, A. E. (2011). Yeast Nej1 Is a Key Participant in the Initial End Binding and Final Ligation Steps of Nonhomologous End Joining. *Journal of Biological Chemistry*, *286*(6), 4931–4940.

Chen, Y.-C., Kenworthy, J., Gabrielse, C., Hänni, C., Zegerman, P., & Weinreich, M. (2013). DNA Replication Checkpoint Signaling Depends on a Rad53–Dbf4 N-Terminal Interaction in Saccharomyces cerevisiae. *Genetics*, *194*(2), 389–401.

Cheng, A. N., Jiang, S. S., Fan, C.-C., Lo, Y.-K., Kuo, C.-Y., Chen, C.-H., … Lee, A. Y.-L. (2013). Increased Cdc7 expression is a marker of oral squamous cell carcinoma and overexpression of Cdc7 contributes to the resistance to DNA-damaging agents. *Cancer Letters*, *337*(2), 218–225.

Cheng, L., Collyer, T., & Hardy, C. F. J. (1999). Cell Cycle Regulation of DNA Replication Initiator Factor Dbf4p. *Molecular and Cellular Biology*, *19*(6), 4270–4278.

Claus, J., Patel, G., Autore, F., Colomba, A., Weitsman, G., Soliman, T. N., … Parker, P. J. (2018). Inhibitor-induced HER2-HER3 heterodimerisation promotes proliferation through a novel dimer interface. *ELife*, *7*.

Clegg, H. V., Itahana, Y., Itahana, K., Ramalingam, S., & Zhang, Y. (2012). Mdm2 RING Mutation Enhances p53 Transcriptional Activity and p53-p300 Interaction. *PLOS ONE*, *7*(5), e38212.

Clikeman, J. A., Khalsa, G. J., Barton, S. L., & Nickoloff, J. A. (2001). Homologous Recombinational Repair of Double-Strand Breaks in Yeast Is Enhanced by MAT Heterozygosity Through yKU-Dependent and -Independent Mechanisms. *Genetics*, *157*(2), 579–589.

Cole, C., Barber, J. D., & Barton, G. J. (2008a). The Jpred 3 secondary structure prediction server. *Nucleic Acids Research*, *36*(suppl_2), W197–W201.

Cole, J. L., Lary, J. W., P Moody, T., & Laue, T. M. (2008b). Analytical ultracentrifugation: Sedimentation velocity and sedimentation equilibrium. *Methods in Cell Biology*, *84*, 143–179.

Collart, C., Allen, G. E., Bradshaw, C. R., Smith, J. C., & Zegerman, P. (2013). Titration of Four Replication Factors is essential for the Xenopus laevis Mid-Blastula Transition. *Science (New York, N.Y.)*, *341*(6148), 893–896.

Collier, T. S., Diraviyam, K., Monsey, J., Shen, W., Sept, D., & Bose, R. (2013). Carboxyl Group Footprinting Mass Spectrometry and Molecular Dynamics Identify Key Interactions in the HER2-HER3 Receptor Tyrosine Kinase Interface. *Journal of Biological Chemistry*, *288*(35), 25254–25264.

Cornacchia, D., Dileep, V., Quivy, J.-P., Foti, R., Tili, F., Santarella-Mellwig, R., … Buonomo, S. B. C. (2012). Mouse Rif1 is a key regulator of the replication-timing programme in mammalian cells. *The EMBO Journal*, *31*(18), 3678–3690.

Cvetic, C., & Walter, J. C. (2005). Eukaryotic origins of DNA replication: Could you please be more specific? *Seminars in Cell & Developmental Biology*, *16*(3), 343–353.

Davé, A., Cooley, C., Garg, M., & Bianchi, A. (2014). Protein Phosphatase 1 Recruitment by Rif1 Regulates DNA Replication Origin Firing by Counteracting DDK Activity. *Cell Reports*, *7*(1), 53–61.

Davey, N. E., Roey, K. V., Weatheritt, R. J., Toedt, G., Uyar, B., Altenberg, B., … Gibson, T. J. (2011). Attributes of short linear motifs. *Molecular BioSystems*, *8*(1), 268–281.

de Jager, M., van Noort, J., van Gent, D. C., Dekker, C., Kanaar, R., & Wyman, C. (2001). Human Rad50/Mre11 Is a Flexible Complex that Can Tether DNA Ends. *Molecular Cell*, *8*(5), 1129–1135.

de Lange, T. (2005). Shelterin: The protein complex that shapes and safeguards human telomeres. *Genes & Development*, *19*(18), 2100–2110.

de Lange, T. (2018). Shelterin-Mediated Telomere Protection. *Annual Review of Genetics*, *52*, 223–247.

DeLano, W. L. (2002). *The PyMOL Molecular Graphic Systems*, (DeLano Scientific, Palo Alto, CA, USA.

De Magistris, P., & Antonin, W. (2018). The Dynamic Nature of the Nuclear Envelope. *Current Biology*, *28*(8), R487–R497.

Deegan, T. D., Yeeles, J. T., & Diffley, J. F. (2016). Phosphopeptide binding by Sld3 links Dbf4-dependent kinase to MCM replicative helicase activation. *The EMBO Journal*, *35*(9), 961–973.

Delaglio, F., Grzesiek, S., Vuister, G. W., Zhu, G., Pfeifer, J., & Bax, A. (1995). NMRPipe: A multidimensional spectral processing system based on UNIX pipes. *Journal of Biomolecular NMR*, *6*(3), 277–293.

Demczuk, A., Gauthier, M. G., Veras, I., Kosiyatrakul, S., Schildkraut, C. L., Busslinger, M., … Norio, P. (2012). Regulation of DNA Replication within the Immunoglobulin Heavy-Chain Locus During B Cell Commitment. *PLOS Biology*, *10*(7), e1001360.

Deshpande, I., Keusch, J. J., Challa, K., Iesmantavicius, V., Gasser, S. M., & Gut, H. (2019). The Sir4 H-BRCT domain interacts with phospho-proteins to sequester and repress yeast heterochromatin. *The EMBO Journal*, *38*(20), e101744.

Deshpande, R. A., Williams, G. J., Limbo, O., Williams, R. S., Kuhnlein, J., Lee, J.-H., … Paull, T. T. (2014). ATP-driven Rad50 conformations regulate DNA tethering, end resection, and ATM checkpoint signaling. *The EMBO Journal*, *33*(5), 482–500.

Devbhandari, S., Jiang, J., Kumar, C., Whitehouse, I., & Remus, D. (2017). Chromatin Constrains the Initiation and Elongation of DNA Replication. *Molecular Cell*, *65*(1), 131–141.

Dewar, J. M., Budzowska, M., & Walter, J. C. (2015). The mechanism of DNA replication termination in vertebrates. *Nature*, *525*(7569), 345–350.

Diffley, J. F. X. (2011). Quality control in the initiation of eukaryotic DNA replication. *Philosophical Transactions of the Royal Society B: Biological Sciences*, *366*(1584), 3545–3553.

Dimitrova, D. S., & Gilbert, D. M. (1999). The Spatial Position and Replication Timing of Chromosomal Domains Are Both Established in Early G1 Phase. *Molecular Cell*, *4*(6), 983–993.

Dixon, J. R., Jung, I., Selvaraj, S., Shen, Y., Antosiewicz-Bourget, J. E., Lee, A. Y., … Ren, B. (2015). Chromatin architecture reorganization during stem cell differentiation. *Nature*, *518*(7539), 331–336.

Duch, A., Palou, G., Jonsson, Z. O., Palou, R., Calvo, E., Wohlschlegel, J., & Quintana, D. G. (2011). A Dbf4 mutant contributes to bypassing the Rad53-mediated block of origins of replication in response to genotoxic stress. *The Journal of Biological Chemistry*, *286*(4), 2486–2491.

Duina, A. A., Miller, M. E., & Keeney, J. B. (2014). Budding Yeast for Budding Geneticists: A Primer on the Saccharomyces cerevisiae Model System. *Genetics*, *197*(1), 33–48.

Duncker, B. P., Shimada, K., Tsai-Pflugfelder, M., Pasero, P., & Gasser, S. M. (2002). An N-terminal domain of Dbf4p mediates interaction with both origin recognition complex (ORC) and Rad53p and can deregulate late origin firing. *Proceedings of the National Academy of Sciences*, *99*(25), 16087–16092.

Durocher, D., Henckel, J., Fersht, A. R., & Jackson, S. P. (1999). The FHA domain is a modular phosphopeptide recognition motif. *Molecular Cell*, *4*(3), 387–394.

Durocher, D., & Jackson, S. P. (2002). The FHA domain. *FEBS Letters*, *513*(1), 58–66.

Durocher, D., Taylor, I. A., Sarbassova, D., Haire, L. F., Westcott, S. L., Jackson, S. P., … Yaffe, M. B. (2000). The molecular basis of FHA domain:phosphopeptide binding specificity and implications for phospho-dependent signaling mechanisms. *Molecular Cell*, *6*(5), 1169–1182.

Edgar, R. C. (2004). MUSCLE: Multiple sequence alignment with high accuracy and high throughput. *Nucleic Acids Research*, *32*(5), 1792–1797.

Elledge, S. J., & Davis, R. W. (1990). Two genes differentially regulated in the cell cycle and by DNA-damaging agents encode alternative regulatory subunits of ribonucleotide reductase. *Genes & Development*, *4*(5), 740–751.

Ellis, N. A., Groden, J., Ye, T. Z., Straughen, J., Lennon, D. J., Ciocci, S., … German, J. (1995). The Bloom's syndrome gene product is homologous to RecQ helicases. *Cell*,

Escribano-Díaz, C., Orthwein, A., Fradet-Turcotte, A., Xing, M., Young, J. T. F., Tkáč, J., … Durocher, D. (2013). A Cell Cycle-Dependent Regulatory Circuit Composed of 53BP1-RIF1 and BRCA1-CtIP Controls DNA Repair Pathway Choice. *Molecular Cell*, *49*(5), 872–883.

Fang, D., Lengronne, A., Shi, D., Forey, R., Skrzypczak, M., Ginalski, K., … Lou, H. (2017). Dbf4 recruitment by forkhead transcription factors defines an upstream rate-limiting step in determining origin firing timing. *Genes & Development*, *31*(23–24), 2405–2415.

Fangman, W. L., Hice, R. H., & Chlebowicz-Sledziewska, E. (1983). ARS replication during the yeast S phase. *Cell*, *32*(3), 831–838.

Farmer, H., McCabe, N., Lord, C. J., Tutt, A. N. J., Johnson, D. A., Richardson, T. B., … Ashworth, A. (2005). Targeting the DNA repair defect in BRCA mutant cells as a therapeutic strategy. *Nature*, *434*(7035), 917–921.

Fay, D. S., Sun, Z., & Stern, D. F. (1997). Mutations in SPK1/RAD53 that specifically abolish checkpoint but not growth-related functions. *Current Genetics*, *31*(2), 97–105.

Feng, L., Fong, K.-W., Wang, J., Wang, W., & Chen, J. (2013). RIF1 Counteracts BRCA1-mediated End Resection during DNA Repair. *Journal of Biological Chemistry*, *288*(16), 11135–11143.

Feng, L., Li, N., Li, Y., Wang, J., Gao, M., Wang, W., & Chen, J. (2015). Cell cycle-dependent inhibition of 53BP1 signaling by BRCA1. *Cell Discovery*, *1*(1), 1–11.

Ferreira, M. G., Santocanale, C., Drury, L. S., & Diffley, J. F. X. (2000). Dbf4p, an Essential S Phase-Promoting Factor, Is Targeted for Degradation by the Anaphase-Promoting Complex. *Molecular and Cellular Biology*, *20*(1), 242–248.

Ferretti, L. P., Lafranchi, L., & Sartori, A. A. (2013). Controlling DNA-end resection: A new task for CDKs. *Frontiers in Genetics*, *4*.

Fitzgerald-Hayes, M., Clarke, L., & Carbon, J. (1982). Nucleotide sequence comparisons and functional analysis of yeast centromere DNAs. *Cell*, *29*, 235-244.

Fontana, G. A., Hess, D., Reinert, J. K., Mattarocci, S., Falquet, B., Klein, D., … Rass, U. (2019). Rif1 S- acylation mediates DNA double-strand break repair at the inner nuclear membrane. *Nature Communications*, *10*(1), 2535.

Foss, T. R., Kelker, M. S., Wiseman, R. L., Wilson, I. A., & Kelly, J. W. (2005). Kinetic Stabilization of the Native State by Protein Engineering: Implications for Inhibition of Transthyretin Amyloidogenesis. *Journal of Molecular Biology*, *347*(4), 841–854.

Fox, C. A., Loo, S., Dillin, A., & Rine, J. (1995). The origin recognition complex has essential functions in transcriptional silencing and chromosomal replication. *Genes & Development*, *9*(8), 911–924.

Franklin, R. E. & Gosling, R. G. (1953). Molecular Configuration in Sodium Thymonucleate. *Nature*, *171*, 740-741.

Fraser, H. B. (2013). Cell-cycle regulated transcription associates with DNA replication timing in yeast and human. *Genome Biology*, *14*(10), R111.

Frigola, J., Remus, D., Mehanna, A., & Diffley, J. F. X. (2013). ATPase-dependent quality control of DNA replication origin licensing. *Nature*, *495*(7441), 339–343.

Fuller, J. C., Burgoyne, N. J., & Jackson, R. M. (2009). Predicting druggable binding sites at the protein–protein interface. *Drug Discovery Today*, *14*(3), 155–161.

Furniss, K. L., Tsai, H.-J., Byl, J. A. W., Lane, A. B., Vas, A. C., Hsu, W.-S., … Clarke, D. J. (2013). Direct Monitoring of the Strand Passage Reaction of DNA Topoisomerase II Triggers Checkpoint Activation. *PLoS Genetics*, *9*(10).

Gabrielse, C., Miller, C. T., McConnell, K. H., DeWard, A., Fox, C. A., & Weinreich, M. (2006). A Dbf4p BRCA1 C-terminal-like domain required for the response to replication fork arrest in budding yeast. *Genetics*, *173*(2), 541–555.

Gad, S. A., Ali, H. E. A., Gaballa, R., Abdelsalam, R. M., Zerfaoui, M., Ali, H. I., … Abd Elmageed, Z. Y. (2019). Targeting CDC7 sensitizes resistance melanoma cells to BRAFV600E-specific inhibitor by blocking the CDC7/MCM2-7 pathway. *Scientific Reports*, *9*(1), 14197.

Gallo, D., Kim, T., Szakal, B., Saayman, X., Narula, A., Park, Y., … Brown, G. W. (2019). Rad5 Recruits Error-Prone DNA Polymerases for Mutagenic Repair of ssDNA Gaps on Undamaged Templates. *Molecular Cell*, *73*(5), 900-914.e9.

Gambus, A., Jones, R. C., Sanchez-Diaz, A., Kanemaki, M., Deursen, F. van, Edmondson, R. D., & Labib, K. (2006). GINS maintains association of Cdc45 with MCM in replisome progression complexes at eukaryotic DNA replication forks. *Nature Cell Biology*, *8*(4), 358–366.

Gan, H., Yu, C., Devbhandari, S., Sharma, S., Han, J., Chabes, A., … Zhang, Z. (2017). Checkpoint kinase Rad53 couples leading and lagging strand DNA synthesis under replication stress. *Molecular Cell*, *68*(2), 446-455.e3.

Gangloff, S., McDonald, J. P., Bendixen, C., Arthur, L., & Rothstein, R. (1994). The yeast type I topoisomerase Top3 interacts with Sgs1, a DNA helicase homolog: A potential eukaryotic reverse gyrase. *Molecular and Cellular Biology*, *14*(12), 8391–8398.

Garcia, V., Phelps, S. E. L., Gray, S., & Neale, M. J. (2011). Bidirectional resection of DNA double-strand breaks by Mre11 and Exo1. *Nature*, *479*(7372), 241–244.

Garg, P., Stith, C. M., Sabouri, N., Johansson, E., & Burgers, P. M. (2004). Idling by DNA polymerase δ maintains a ligatable nick during lagging-strand DNA replication. *Genes & Development*, *18*(22), 2764–2773.

Garzón, J., Ursich, S., Lopes, M., Hiraga, S., & Donaldson, A. D. (2019). Human RIF1-Protein Phosphatase 1 Prevents Degradation and Breakage of Nascent DNA on Replication Stalling. *Cell Reports*, *27*(9), 2558-2566.e4.

Gellert, M., Lipsett, M. N., & Davies, D. R. (1962). Helix formation by guanylic acid. *Proceedings of the National Academy of Sciences of the United States of America*, *48*,

Georgescu, R. E., Langston, L., Yao, N. Y., Yurieva, O., Zhang, D., Finkelstein, J., … O'Donnell, M. E. (2014). Mechanism of asymmetric polymerase assembly at the eukaryotic replication fork. *Nature Structural & Molecular Biology*, *21*(8), 664–670.

Geronimo, C. L., & Zakian, V. A. (2016). Getting it done at the ends: Pif1 family DNA helicases and telomeres. *DNA Repair*, *44*, 151–158.

Gest, H. (2004). The discovery of microorganisms by Robert Hooke and Antoni Van Leeuwenhoek, fellows of the Royal Society. *Notes and Records of the Royal Society of London*, *58*(2), 187–201.

Ghezraoui, H., Oliveira, C., Becker, J. R., Bilham, K., Moralli, D., Anzilotti, C., … Chapman, J. R. (2018). 53BP1 cooperation with the REV7–shieldin complex underpins DNA structure-specific NHEJ. *Nature*, *560*(7716), 122–127.

Ghirlando, R., Balbo, A., Piszczek, G., Brown, P. H., Lewis, M. S., Brautigam, C. A., … Zhao, H. (2013). Improving the thermal, radial, and temporal accuracy of the analytical ultracentrifuge through external references. *Analytical Biochemistry*, *440*(1), 81–95.

Giaever, G., & Nislow, C. (2014). The Yeast Deletion Collection: A Decade of Functional Genomics. *Genetics*, *197*(2), 451–465.

Gietz, D., St Jean, A., Woods, R. A., & Schiestl, R. H. (1992). Improved method for high efficiency transformation of intact yeast cells. *Nucleic Acids Research*, *20*(6), 1425.

Gietz, R. D., & Sugino, A. (1988). New yeast-Escherichia coli shuttle vectors constructed with in vitro mutagenized yeast genes lacking six-base pair restriction sites. *Gene*, *74*(2), 527–534.

Gnügge, R., & Symington, L. S. (2017). Keeping it real: MRX–Sae2 clipping of natural substrates. *Genes & Development*, *31*(23–24), 2311–2312.

Goffeau, A., Barrell, B. G., Bussey, H., Davis, R. W., Dujon, B., Feldmann, H., … Oliver, S. G. (1996). Life with 6000 Genes. *Science*, *274*(5287), 546–567.

Graf, M., Mardirossian, M., Nguyen, F., Seefeldt, A. C., Guichard, G., Scocchi, M., … Wilson, D. N. (2017). Proline-rich antimicrobial peptides targeting protein synthesis. *Natural Product Reports*, *34*(7), 702–711.

Graham, J. E., Marians, K. J., & Kowalczykowski, S. C. (2017). Independent and Stochastic Action of DNA Polymerases in the Replisome. *Cell*, *169*(7), 1201-1213.e17.

Gu, Y., Rosenblatt, J., & Morgan, D. o. (1992). Cell cycle regulation of CDK2 activity by phosphorylation of Thr160 and Tyr15. *The EMBO Journal*, *11*(11), 3995–4005.

Gupta, A., Shah, K., Oza, M. J., & Behl, T. (2019). Reactivation of p53 gene by MDM2 inhibitors: A novel therapy for cancer treatment. *Biomedicine & Pharmacotherapy*, *109*, 484–492.

Guthrie, C., & Fink, G. R. (2004). *Guide to Yeast Genetics and Molecular Biology*. Gulf Professional Publishing.

Gyuris, J., Golemis, E., Chertkov, H., & Brent, R. (1993). Cdi1, a human G1 and S phase protein phosphatase that associates with Cdk2. *Cell*, *75*(4), 791–803.

Hafner, L., Lezaja, A., Zhang, X., Lemmens, L., Shyian, M., Albert, B., … Mattarocci, S. (2018). Rif1 Binding and Control of Chromosome-Internal DNA Replication Origins Is Limited by Telomere Sequestration. *Cell Reports*, *23*(4), 983–992.

Haince, J.-F., McDonald, D., Rodrigue, A., Déry, U., Masson, J.-Y., Hendzel, M. J., & Poirier, G. G. (2008). PARP1-dependent Kinetics of Recruitment of MRE11 and NBS1 Proteins to Multiple DNA Damage Sites. *Journal of Biological Chemistry*, *283*(2), 1197–1208.

Hamperl, S., Bocek, M. J., Saldivar, J. C., Swigut, T., & Cimprich, K. A. (2017). Transcription-Replication Conflict Orientation Modulates R-Loop Levels and Activates Distinct DNA Damage Responses. *Cell*, *170*(4), 774-786.e19.

Hardy, C. F., Sussel, L., & Shore, D. (1992). A RAP1-interacting protein involved in transcriptional silencing and telomere length regulation. *Genes & Development*, *6*(5), 801–814.

Hartwell, L. H., Culotti, J., Pringle, J. R., & Reid, B. J. (1974). Genetic Control of the Cell Division Cycle in Yeast: A model to account for the order of cell cycle events is deduced from the phenotypes of yeast mutants. *Science*, *183*(4120), 46–51.

Hasty, J., McMillen, D., & Collins, J. J. (2002). Engineered gene circuits. *Nature*, *420*(6912), 224–230.

Hawkins, M., Retkute, R., Müller, C. A., Saner, N., Tanaka, T. U., de Moura, A. P. S., & Nieduszynski, C. A. (2013). High-Resolution Replication Profiles Define the Stochastic Nature of Genome Replication Initiation and Termination. *Cell Reports*, *5*(4), 1132–1141.

Hayano, M., Kanoh, Y., Matsumoto, S., & Masai, H. (2011). Mrc1 Marks Early-Firing Origins and Coordinates Timing and Efficiency of Initiation in Fission Yeast. *Molecular and Cellular Biology*, *31*(12), 2380–2391.

Hayano, M., Kanoh, Y., Matsumoto, S., Renard-Guillet, C., Shirahige, K., & Masai, H. (2012). Rif1 is a global regulator of timing of replication origin firing in fission yeast. *Genes & Development*, *26*(2), 137–150.

Hedglin, M., Pandey, B., & Benkovic, S. J. (2016). Stability of the human polymerase δ holoenzyme and its implications in lagging strand DNA synthesis. *Proceedings of the National Academy of Sciences*, *113*(13), E1777–E1786.

Helleday, T., Bryant, H. E., & Schultz, N. (2005). Poly(ADP-ribose) polymerase (PARP-1) in homologous recombination and as a target for cancer therapy. *Cell Cycle (Georgetown, Tex.)*, *4*(9), 1176–1178.

Hidaka, M., Akiyama, M., & Horiuchi, T. (1988). A consensus sequence of three DNA replication terminus sites on the E. coli chromosome is highly homologous to the terR sites of the R6K plasmid. *Cell*, *55*(3), 467–475.

Hieter, P., Mann, C., Snyder, M., & Davis, R. W. (1985) Mitotic stability of yeast chromosomes: a colony color assay that measures nondisjunction and chromosome loss. *Cell*, *40*, 381-392.

Higgs, M. R., Reynolds, J. J., Winczura, A., Blackford, A. N., Borel, V., Miller, E. S., … Stewart, G. S. (2015). BOD1L Is Required to Suppress Deleterious Resection of Stressed Replication Forks. *Molecular Cell*, *59*(3), 462–477.

Hill, T. M., Pelletier, A. J., Tecklenburg, M. L., & Kuempel, P. L. (1988). Identification of the DNA sequence from the E. coli terminus region that halts replication forks. *Cell*, *55*(3), 459–466.

Hinnen, A., Hicks, J. B., & Fink, G. R. (1978). Transformation of yeast. *Proceedings of the National Academy of Sciences of the United States of America*, *75*(4), 1929–1933.

Hiraga, S., Alvino, G. M., Chang, F., Lian, H., Sridhar, A., Kubota, T., … Donaldson, A. D. (2014). Rif1 controls DNA replication by directing Protein Phosphatase 1 to reverse Cdc7-mediated phosphorylation of the MCM complex. *Genes & Development*, *28*(4), 372–383.

Hiraga, S., Monerawela, C., Katou, Y., Shaw, S., Clark, K. R., Shirahige, K., & Donaldson, A. D. (2018). Budding yeast Rif1 binds to replication origins and protects DNA at blocked replication forks. *EMBO Reports*, e46222.

Hirao, A., Kong, Y. Y., Matsuoka, S., Wakeham, A., Ruland, J., Yoshida, H., … Mak, T. W. (2000). DNA damage-induced activation of p53 by the checkpoint kinase Chk2. *Science (New York, N.Y.)*, *287*(5459), 1824–1827.

Hoege, C., Pfander, B., Moldovan, G.-L., Pyrowolakis, G., & Jentsch, S. (2002). RAD6 - dependent DNA repair is linked to modification of PCNA by ubiquitin and SUMO. *Nature*, *419*(6903), 135–141.

Hoggard, T. A., Chang, F., Perry, K. R., Subramanian, S., Kenworthy, J., Chueng, J., … Fox, C. A. (2018). Yeast heterochromatin regulators Sir2 and Sir3 act directly at euchromatic DNA replication origins. *PLOS Genetics*, *14*(5), e1007418.

Hohmann, S. (2016). Nobel Yeast Research. *FEMS Yeast Research*, *16*(8).

Holt, L. J., Tuch, B. B., Villén, J., Johnson, A. D., Gygi, S. P., & Morgan, D. O. (2009). Global Analysis of Cdk1 Substrate Phosphorylation Sites Provides Insights into Evolution. *Science*, *325*(5948), 1682–1686.

Holt, M. R., & Koffer, A. (2001). Cell motility: Proline-rich proteins promote protrusions. *Trends in Cell Biology*, *11*(1), 38–46.

Huang, M., Zhou, Z., & Elledge, S. J. (1998). The DNA Replication and Damage Checkpoint Pathways Induce Transcription by Inhibition of the Crt1 Repressor. *Cell*, *94*(5), 595–605.

Huertas, P. (2010). DNA resection in eukaryotes: Deciding how to fix the break. *Nature Structural & Molecular Biology*, *17*(1), 11–16.

Huertas, P., Cortés-Ledesma, F., Sartori, A. A., Aguilera, A., & Jackson, S. P. (2008). CDK targets Sae2 to control DNA-end resection and homologous recombination. *Nature*, *455*(7213), 689–692.

Huertas, P., & Jackson, S. P. (2009). Human CtIP Mediates Cell Cycle Control of DNA End Resection and Double Strand Break Repair. *Journal of Biological Chemistry*, *284*(14), 9558–9565.

Hughes, S., Elustondo, F., Di Fonzo, A., Leroux, F. G., Wong, A. C., Snijders, A. P., … Cherepanov, P. (2012). Crystal structure of human CDC7 kinase in complex with its activator DBF4. *Nature Structural & Molecular Biology*, *19*(11), 1101–1107.

Hwang, H., Vreven, T., Janin, J., & Weng, Z. (2010). Protein–protein docking benchmark version 4.0. *Proteins: Structure, Function, and Bioinformatics*, *78*(15), 3111–3114.

Imai, K., & Mitaku, S. (2005). Mechanisms of secondary structure breakers in soluble proteins. *Biophysics, 1*, 55–65.

Ivessa, A. S., Zhou, J. Q., & Zakian, V. A. (2000). The Saccharomyces Pif1p DNA helicase and the highly related Rrm3p have opposite effects on replication fork progression in ribosomal DNA. *Cell*, *100*(4), 479–489.

Iwai, K., Nambu, T., Dairiki, R., Ohori, M., Yu, J., Burke, K., … Ohashi, A. (2019). Molecular mechanism and potential target indication of TAK-931, a novel CDC7-selective inhibitor. *Science Advances*, *5*(5).

Jackson, A. L., Pahl, P. M., Harrison, K., Rosamond, J., & Sclafani, R. A. (1993). Cell cycle regulation of the yeast Cdc7 protein kinase by association with the Dbf4 protein. *Molecular and Cellular Biology*, *13*(5), 2899–2908.

Jafri, M. A., Ansari, S. A., Alqahtani, M. H., & Shay, J. W. (2016). Roles of telomeres and telomerase in cancer, and advances in telomerase-targeted therapies. *Genome Medicine*, *8*.

Janusz, M., & Zabłocka, A. (2010). Colostral proline-rich polypeptides—Immunoregulatory properties and prospects of therapeutic use in Alzheimer's disease. *Current Alzheimer Research*, *7*(4), 323–333.

Jaspers, J. E., Kersbergen, A., Boon, U., Sol, W., van Deemter, L., Zander, S. A., … Rottenberg, S. (2013). Loss of 53BP1 causes PARP inhibitor resistance in Brca1-mutated mouse mammary tumors. *Cancer Discovery*, *3*(1), 68–81.

Jeffrey, P. D., Russo, A. A., Polyak, K., Gibbs, E., Hurwitz, J., Massagué, J., & Pavletich, N. P. (1995). Mechanism of CDK activation revealed by the structure of a cyclinA-CDK2 complex. *Nature*, *376*(6538), 313–320.

Jiang, W., McDonald, D., Hope, T. J., & Hunter, T. (1999). Mammalian Cdc7–Dbf4 protein kinase complex is essential for initiation of DNA replication. *The EMBO Journal*, *18*(20), 5703–5713.

Johnson, M. L. (1992). Why, when, and how biochemists should use least squares. *Analytical Biochemistry*, *206*(2), 215–225.

Jones, D. R., Prasad, A. A., Chan, P. K., & Duncker, B. P. (2010). The Dbf4 motif C zinc finger promotes DNA replication and mediates resistance to genotoxic stress. *Cell Cycle (Georgetown, Tex.)*, *9*(10), 2018–2026.

Kabsch, W. (2010). XDS. *Acta Crystallographica Section D: Biological Crystallography*, *66*(Pt 2), 125–132.

Kachroo, A. H., Laurent, J. M., Yellman, C. M., Meyer, A. G., Wilke, C. O., & Marcotte, E. M. (2015). Evolution. Systematic humanization of yeast genes reveals conserved functions and genetic modularity. *Science (New York, N.Y.)*, *348*(6237), 921–925.

Kadyk, L. C., & Hartwell, L. H. (1992). Sister chromatids are preferred over homologs as substrates for recombinational repair in Saccharomyces cerevisiae. *Genetics*, *132*(2), 387–402.

Kamimura, Y., Tak, Y.-S., Sugino, A., & Araki, H. (2001). Sld3, which interacts with Cdc45 (Sld4), functions for chromosomal DNA replication in Saccharomyces cerevisiae. *The EMBO Journal*, *20*(8), 2097–2107.

Kannouche, P. L., Wing, J., & Lehmann, A. R. (2004). Interaction of Human DNA Polymerase η with Monoubiquitinated PCNA: A Possible Mechanism for the Polymerase Switch in Response to DNA Damage. *Molecular Cell*, *14*(4), 491–500.

Kanoh, J., & Ishikawa, F. (2001). SpRap1 and spRif1, recruited to telomeres by Taz1, are essential for telomere function in fission yeast. *Current Biology*, *11*(20), 1624–1630.

Kapoor, P., Shire, K., & Frappier, L. (2001). Reconstitution of Epstein–Barr virus-based plasmid partitioning in budding yeast. *The EMBO Journal*, *20*(1–2), 222–230.

Katou, Y., Kanoh, Y., Bando, M., Noguchi, H., Tanaka, H., Ashikari, T., … Shirahige, K. (2003). S-phase checkpoint proteins Tof1 and Mrc1 form a stable replication-pausing complex. *Nature*, *424*(6952), 1078–1083.

Kay, B. K., Williamson, M. P., & Sudol, M. (2000). The importance of being proline: The interaction of proline-rich motifs in signaling proteins with their cognate domains. *The FASEB Journal*, *14*(2), 231–241.

Kedziora, S., Gali, V. K., Wilson, R. H., Clark, K. R., Nieduszynski, C. A., Hiraga, S., & Donaldson, A. D. (2018). Rif1 acts through Protein Phosphatase 1 but independent of replication timing to suppress telomere extension in budding yeast. *Nucleic Acids Research*, *46*(8), 3993–4003.

Kelley, L. A., Mezulis, S., Yates, C. M., Wass, M. N., & Sternberg, M. J. (2015). The Phyre2 web portal for protein modelling, prediction and analysis. *Nature Protocols*, *10*(6), 845–858.

Kim, J. M., Kakusho, N., Yamada, M., Kanoh, Y., Takemoto, N., & Masai, H. (2008). Cdc7 kinase mediates Claspin phosphorylation in DNA replication checkpoint. *Oncogene*, *27*(24), 3475–3482.

Kim, S. M., & Huberman, J. A. (2001). Regulation of replication timing in fission yeast. *The EMBO Journal*, *20*(21), 6115–6126.

Knott, S. R. V., Peace, J. M., Ostrow, A. Z., Gan, Y., Rex, A. E., Viggiani, C. J., … Aparicio, O. M. (2012). Forkhead transcription factors establish origin timing and long-range clustering in S. cerevisiae. *Cell*, *148*(1–2), 99–111.

Kocik, J., Machula, M., Wisniewska, A., Surmiak, E., Holak, T. A., & Skalniak, L. (2019). Helping the Released Guardian: Drug Combinations for Supporting the Anticancer Activity of HDM2 (MDM2) Antagonists. *Cancers*, *11*(7), 1014.

Köhler, C., Koalick, D., Fabricius, A., Parplys, A. C., Borgmann, K., Pospiech, H., & Grosse, F. (2016). Cdc45 is limiting for replication initiation in humans. *Cell Cycle*, *15*(7), 974–985.

Komata, M., Bando, M., Araki, H., & Shirahige, K. (2009). The Direct Binding of Mrc1, a Checkpoint Mediator, to Mcm6, a Replication Helicase, Is Essential for the Replication Checkpoint against Methyl Methanesulfonate-Induced Stress. *Molecular and Cellular Biology*, *29*(18), 5008–5019.

Krissinel, E., & Henrick, K. (2007). Inference of Macromolecular Assemblies from Crystalline State. *Journal of Molecular Biology*, *372*(3), 774–797.

Kunkel, T. A. (2004). DNA Replication Fidelity. *Journal of Biological Chemistry*, *279*(17), 16895–16898.

Kussie, P. H., Gorina, S., Marechal, V., Elenbaas, B., Moreau, J., Levine, A. J., & Pavletich, N. P. (1996). Structure of the MDM2 Oncoprotein Bound to the p53 Tumor Suppressor Transactivation Domain. *Science*, *274*(5289), 948–953.

Lammens, K., Bemeleit, D. J., Möckel, C., Clausing, E., Schele, A., Hartung, S., … Hopfner, K.-P. (2011). The Mre11:Rad50 structure shows an ATP dependent molecular clamp in DNA double-strand break repair. *Cell*, *145*(1), 54–66.

Langston, L. D., Zhang, D., Yurieva, O., Georgescu, R. E., Finkelstein, J., Yao, N. Y., … O'Donnell, M. E. (2014). CMG helicase and DNA polymerase ε form a functional 15-subunit holoenzyme for eukaryotic leading-strand DNA replication. *Proceedings of the National Academy of Sciences*, *111*(43), 15390–15395.

Larasati, & Duncker, B. P. (2016). Mechanisms Governing DDK Regulation of the Initiation of DNA Replication. *Genes*, *8*(1).

Lawson, I. (2016). CRAFTING THE MICROWORLD: HOW ROBERT HOOKE CONSTRUCTED KNOWLEDGE ABOUT SMALL THINGS. *Notes and Records of the Royal Society of London*, *70*(1), 23–44.

Lee, H., Yuan, C., Hammet, A., Mahajan, A., Chen, E. S.-W., Wu, M.-R., … Tsai, M.-D. (2008a). Diphosphothreonine-Specific Interaction between an SQ/TQ Cluster and an FHA Domain in the Rad53-Dun1 Kinase Cascade. *Molecular Cell*, *30*(6), 767–778.

Lee, J., Gold, D. A., Shevchenko, A., Shevchenko, A., & Dunphy, W. G. (2005). Roles of Replication Fork-interacting and Chk1-activating Domains from Claspin in a DNA Replication Checkpoint Response. *Molecular Biology of the Cell*, *16*(11), 5269–5282.

Lee, J., Kumagai, A., & Dunphy, W. G. (2003). Claspin, a Chk1-Regulatory Protein, Monitors DNA Replication on Chromatin Independently of RPA, ATR, and Rad17. *Molecular Cell*, *11*(2), 329–340.

Lee, Y. D., Wang, J., Stubbe, J., & Elledge, S. J. (2008b). Dif1 is a DNA Damage Regulated Facilitator of Nuclear Import for Ribonucleotide Reductase. *Molecular Cell*, *32*(1), 70–80.

Leroy, C., Lee, S. E., Vaze, M. B., Ochsenbein, F., Ochsenbien, F., Guerois, R., … Marsolier-Kergoat, M.-C. (2003). PP2C phosphatases Ptc2 and Ptc3 are required for DNA checkpoint inactivation after a double-strand break. *Molecular Cell*, *11*(3), 827–835.

Li, J., Williams, B. L., Haire, L. F., Goldberg, M., Wilker, E., Durocher, D., … Smerdon, S. J. (2002). Structural and Functional Versatility of the FHA Domain in DNA-Damage Signaling by the Tumor Suppressor Kinase Chk2. *Molecular Cell*, *9*(5), 1045–1054.

Li, Q., Xie, W., Wang, N., Li, C., & Wang, M. (2018). CDC7-dependent transcriptional regulation of RAD54L is essential for tumorigenicity and radio-resistance of glioblastoma. *Translational Oncology*, *11*(2), 300–306.

Li, S. S.-C. (2005). Specificity and versatility of SH3 and other proline-recognition domains: Structural basis and implications for cellular signal transduction. *Biochemical Journal*, *390*(Pt 3), 641–653.

Li, X., O'Neil, N. J., Moshgabadi, N., & Hieter, P. (2014). Synthetic cytotoxicity: Digenic interactions with TEL1/ATM mutations reveal sensitivity to low doses of camptothecin. *Genetics*, *197*(2), 611–623.

Lian, H.-Y., Robertson, E. D., Hiraga, S., Alvino, G. M., Collingwood, D., McCune, H. J., … Donaldson, A. D. (2011). The effect of Ku on telomere replication time is mediated by telomere length but is independent of histone tail acetylation. *Molecular Biology of the Cell*, *22*(10), 1753–1765.

Lilley, D. M. (1980). The inverted repeat as a recognizable structural feature in supercoiled DNA molecules. *Proceedings of the National Academy of Sciences*, *77*(11), 6468–6472.

Liu, L. F., & Wang, J. C. (1987). Supercoiling of the DNA template during transcription. *Proceedings of the National Academy of Sciences*, *84*(20), 7024–7027.

Löb, D., Lengert, N., Chagin, V. O., Reinhart, M., Casas-Delucchi, C. S., Cardoso, M. C., & Drossel, B. (2016). 3D replicon distributions arise from stochastic initiation and domino-like DNA replication progression. *Nature Communications*, *7*(1), 1–11.

Longhese, M. P., Bonetti, D., Manfrini, N., & Clerici, M. (2010). Mechanisms and regulation of DNA end resection. *The EMBO Journal*, *29*(17), 2864–2874.

Longtine, M. S., Iii, A. M., Demarini, D. J., Shah, N. G., Wach, A., Brachat, A., … Pringle, J. R. (1998). Additional modules for versatile and economical PCR-based gene deletion and modification in Saccharomyces cerevisiae. *Yeast*, *14*(10), 953–961.

Lõoke, M., Kristjuhan, K., Värv, S., & Kristjuhan, A. (2013). Chromatin-dependent and -independent regulation of DNA replication origin activation in budding yeast. *EMBO Reports*, *14*(2), 191–198.

Lopez-Mosqueda, J., Maas, N. L., Jonsson, Z. O., DeFazio-Eli, L. G., Wohlschlegel, J., & Toczyski, D. P. (2010). Damage-induced phosphorylation of Sld3 is important to block late origin firing. *Nature*, *467*(7314), 479–483.

Lord, C. J., Tutt, A. N. J., & Ashworth, A. (2015). Synthetic lethality and cancer therapy: Lessons learned from the development of PARP inhibitors. *Annual Review of Medicine*, *66*, 455–470.

Lou, H., Komata, M., Katou, Y., Guan, Z., Reis, C. C., Budd, M., … Campbell, J. L. (2008). Mrc1 and DNA Polymerase ε Function Together in Linking DNA Replication and the S Phase Checkpoint. *Molecular Cell*, *32*(1), 106–117.

Louis, E. J. (2016). Historical Evolution of Laboratory Strains of *Saccharomyces cerevisiae*. *Cold Spring Harbor Protocols*, *2016*(7), pdb.top077750.

Luo, S., Xin, X., Du, L.-L., Ye, K., & Wei, Y. (2015). Dimerization Mediated by a Divergent Forkhead-associated Domain Is Essential for the DNA Damage and Spindle Functions of Fission Yeast Mdb1. *Journal of Biological Chemistry*, *290*(34), 21054–21066.

MacAlpine, D. M., Rodríguez, H. K., & Bell, S. P. (2004). Coordination of replication and transcription along a Drosophila chromosome. *Genes & Development*, *18*(24), 3094–3105.

Maestroni, L., Matmati, S., & Coulon, S. (2017). Solving the Telomere Replication Problem. *Genes*, *8*(2).

Majka, J., Niedziela-Majka, A., & Burgers, P. M. J. (2006). The Checkpoint Clamp Activates Mec1 Kinase during Initiation of the DNA Damage Checkpoint. *Molecular Cell*, *24*(6), 891–901.

Makovets, S., Herskowitz, I., & Blackburn, E. H. (2004). Anatomy and Dynamics of DNA Replication Fork Movement in Yeast Telomeric Regions. *Molecular and Cellular Biology*, *24*(9), 4019–4031.

Manivasakam, P., Weber, S. C., McElver, J., & Schiestl, R. H. (1995). Micro-homology mediated PCR targeting in Saccharomyces cerevisiae. *Nucleic Acids Research*, *23*(14), 2799–2800.

Manke, I. A., Lowery, D. M., Nguyen, A., & Yaffe, M. B. (2003). BRCT repeats as phosphopeptide-binding modules involved in protein targeting. *Science (New York, N.Y.)*, *302*(5645), 636–639.

Manthei, K. A., Hill, M. C., Burke, J. E., Butcher, S. E., & Keck, J. L. (2015). Structural mechanisms of DNA binding and unwinding in bacterial RecQ helicases. *Proceedings of the National Academy of Sciences of the United States of America*, *112*(14), 4292–4297.

Mantiero, D., Mackenzie, A., Donaldson, A., & Zegerman, P. (2011). Limiting replication initiation factors execute the temporal programme of origin firing in budding yeast. *The EMBO Journal*, *30*(23), 4805–4814.

Mao, Z., Bozzella, M., Seluanov, A., & Gorbunova, V. (2008). DNA repair by nonhomologous end joining and homologous recombination during cell cycle in human cells. *Cell Cycle (Georgetown, Tex.)*, *7*(18), 2902–2906.

Maric, M., Maculins, T., De Piccoli, G., & Labib, K. (2014). Cdc48 and a ubiquitin ligase drive disassembly of the CMG helicase at the end of DNA replication. *Science (New York, N.Y.)*, *346*(6208), 1253596.

Mariezcurrena, A., & Uhlmann, F. (2017). Observation of DNA intertwining along authentic budding yeast chromosomes. *Genes & Development*, *31*(21), 2151–2161.

Martina, M., Bonetti, D., Villa, M., Lucchini, G., & Longhese, M. P. (2014). Saccharomyces cerevisiae Rif1 cooperates with MRX-Sae2 in promoting DNA-end resection. *EMBO Reports*, *15*(6), 695–704.

Masai, H., & Arai, K. (2000). Dbf4 motifs: Conserved motifs in activation subunits for Cdc7 kinases essential for S-phase. *Biochemical and Biophysical Research Communications*, *275*(1), 228–232.

Masai, H., Yang, C.-C., & Matsumoto, S. (2017). Mrc1/Claspin: A new role for regulation of origin firing. *Current Genetics*, *63*(5), 813–818.

Masuda-Sasa, T., Polaczek, P., Peng, X. P., Chen, L., & Campbell, J. L. (2008). Processing of G4 DNA by Dna2 helicase/nuclease and replication protein A (RPA) provides insights into the mechanism of Dna2/RPA substrate recognition. *The Journal of Biological Chemistry*, *283*(36), 24359–24373.

Matsumoto, S., Hayano, M., Kanoh, Y., & Masai, H. (2011). Multiple pathways can bypass the essential role of fission yeast Hsk1 kinase in DNA replication initiation. *The Journal of Cell Biology*, *195*(3), 387–401.

Matsumoto, S., Kanoh, Y., Shimmoto, M., Hayano, M., Ueda, K., Fukatsu, R., … Masai, H. (2017). Checkpoint-Independent Regulation of Origin Firing by Mrc1 through Interaction with Hsk1 Kinase. *Molecular and Cellular Biology*, *37*(7), e00355-16.

Matsumoto, S., Shimmoto, M., Kakusho, N., Yokoyama, M., Kanoh, Y., Hayano, M., … Masai, H. (2010). Hsk1 kinase and Cdc45 regulate replication stress-induced checkpoint responses in fission yeast. *Cell Cycle*, *9*(23), 4627–4637.

Matsuoka, S., Huang, M., & Elledge, S. J. (1998). Linkage of ATM to cell cycle regulation by the Chk2 protein kinase. *Science (New York, N.Y.)*, *282*(5395), 1893–1897.

Mattarocci, S., Reinert, J. K., Bunker, R. D., Fontana, G. A., Shi, T., Klein, D., … Rass, U. (2017). Rif1 maintains telomeres and mediates DNA repair by encasing DNA ends. *Nature Structural & Molecular Biology*, *24*(7), 588–595.

Mattarocci, S., Shyian, M., Lemmens, L., Damay, P., Altintas, D. M., Shi, T., … Shore, D. (2014). Rif1 Controls DNA Replication Timing in Yeast through the PP1 Phosphatase Glc7. *Cell Reports*, *7*(1), 62–69.

Matthews, L. A., Duong, A., Prasad, A. A., Duncker, B. P., & Guarné, A. (2009). Crystallization and preliminary X-ray diffraction analysis of motif N from Saccharomyces cerevisiae Dbf4. *Acta Crystallographica. Section F, Structural Biology and Crystallization Communications*, *65*(Pt 9), 890–894.

Matthews, L. A., Jones, D. R., Prasad, A. A., Duncker, B. P., & Guarné, A. (2012). Saccharomyces cerevisiae Dbf4 Has Unique Fold Necessary for Interaction with Rad53 Kinase. *The Journal of Biological Chemistry*, *287*(4), 2378–2387.

Matthews, L. A., Selvaratnam, R., Jones, D. R., Akimoto, M., McConkey, B. J., Melacini, G., … Guarné, A. (2014). A novel non-canonical forkhead-associated (FHA) domain-binding interface mediates the interaction between Rad53 and Dbf4 proteins. *The Journal of Biological Chemistry*, *289*(5), 2589–2599.

Matthews, L., & Guarne, A. (2013). Dbf4: The whole is greater than the sum of its parts. *Cell Cycle*, *12*(8), 1180–1188.

McCarroll, R. M., & Fangman, W. L. (1988). Time of replication of yeast centromeres and telomeres. *Cell*, *54*(4), 505–513.

McGuffee, S. R., Smith, D. J., & Whitehouse, I. (2013). Quantitative, genome-wide analysis of eukaryotic replication initiation and termination. *Molecular Cell*, *50*(1), 123–135.

McIntosh, D., & Blow, J. J. (2012). Dormant Origins, the Licensing Checkpoint, and the Response to Replicative Stresses. *Cold Spring Harbor Perspectives in Biology*, *4*(10).

Méchali, M. (2010). Eukaryotic DNA replication origins: Many choices for appropriate answers. *Nature Reviews Molecular Cell Biology*, *11*(10), 728–738.

Méchali, M., Yoshida, K., Coulombe, P., & Pasero, P. (2013). Genetic and epigenetic determinants of DNA replication origins, position and activation. *Current Opinion in Genetics & Development*, *23*(2), 124–131.

Mersman, D. P., Du, H.-N., Fingerman, I. M., South, P. F., & Briggs, S. D. (2012). Charge-based Interaction Conserved within Histone H3 Lysine 4 (H3K4) Methyltransferase Complexes Is Needed for Protein Stability, Histone Methylation, and Gene Expression. *Journal of Biological Chemistry*, *287*(4), 2652–2665.

Mészáros, B., Simon, I., & Dosztányi, Z. (2009). Prediction of Protein Binding Regions in Disordered Proteins. *PLoS Computational Biology*, *5*(5).

Mimitou, E. P., & Symington, L. S. (2010). Ku prevents Exo1 and Sgs1-dependent resection of DNA ends in the absence of a functional MRX complex or Sae2. *The EMBO Journal*, *29*(19), 3358–3369.

Mirman, Z., Lottersberger, F., Takai, H., Kibe, T., Gong, Y., Takai, K., … Lange, T. de. (2018). 53BP1–RIF1–shieldin counteracts DSB resection through CST- and Polα-dependent fill-in. *Nature*, *560*(7716), 112–116.

Moiseeva, T. N., Yin, Y., Calderon, M. J., Qian, C., Schamus-Haynes, S., Sugitani, N., … Bakkenist, C. J. (2019). An ATR and CHK1 kinase signaling mechanism that limits origin firing during unperturbed DNA replication. *Proceedings of the National Academy of Sciences of the United States of America*, *116*(27), 13374–13383.

Mojumdar, A., Sorenson, K., Hohl, M., Toulouze, M., Lees-Miller, S. P., Dubrana, K., … Cobb, J. A. (2019). Nej1 Interacts with Mre11 to Regulate Tethering and Dna2 Binding at DNA Double-Strand Breaks. *Cell Reports*, *28*(6), 1564-1573.e3.

Momand, J., Zambetti, G. P., Olson, D. C., George, D., & Levine, A. J. (1992). The mdm-2 oncogene product forms a complex with the p53 protein and inhibits p53-mediated transactivation. *Cell*, *69*(7), 1237–1245.

Mondol, T., Stodola, J. L., Galletto, R., & Burgers, P. M. (2019). PCNA accelerates the nucleotide incorporation rate by DNA polymerase δ. *Nucleic Acids Research*, *47*(4), 1977–1986.

Montagnoli, A., Tenca, P., Sola, F., Carpani, D., Brotherton, D., Albanese, C., & Santocanale, C. (2004). Cdc7 Inhibition Reveals a p53-Dependent Replication Checkpoint That Is Defective in Cancer Cells. *Cancer Research*, *64*(19), 7110–7116.

Moore, C. W. (1978). Responses of radiation-sensitive mutants of Saccharomyces cerevisiae to lethal effects of bleomycin. *Mutation Research*, *51*(2), 165–180.

Morgan, A. R., & Wells, R. D. (1968). Specificity of the three-stranded complex formation between double-stranded DNA and single-stranded RNA containing repeating nucleotide sequences. *Journal of Molecular Biology*, *37*(1), 63–80.

Mortimer, R. K., & Johnston, J. R. (1986). Genealogy of Principal Strains of the Yeast Genetic Stock Center. *Genetics*, *113*(1), 35–43.

Mosca, R., Céol, A., Stein, A., Olivella, R., & Aloy, P. (2014). 3did: A catalog of domain-based interactions of known three-dimensional structure. *Nucleic Acids Research*, *42*(Database issue), D374–D379.

Mukherjee, C., Tripathi, V., Manolika, E. M., Heijink, A. M., Ricci, G., Merzouk, S., … Chaudhuri, A. R. (2019). RIF1 promotes replication fork protection and efficient restart to maintain genome stability. *Nature Communications*, *10*(1), 3287.

Mukherjee, S., & Zhang, Y. (2011). Protein-Protein Complex Structure Predictions by Multimeric Threading and Template Recombination. *Structure*, *19*(7), 955–966.

Muñoz, S., Búa, S., Rodríguez-Acebes, S., Megías, D., Ortega, S., de Martino, A., & Méndez, J. (2017). In Vivo DNA Re-replication Elicits Lethal Tissue Dysplasias. *Cell Reports*, *19*(5), 928–938.

Muramatsu, S., Hirai, K., Tak, Y.-S., Kamimura, Y., & Araki, H. (2010). CDK-dependent complex formation between replication proteins Dpb11, Sld2, Pol ε, and GINS in budding yeast. *Genes & Development*, *24*(6), 602–612.

Nakada, D., Matsumoto, K., & Sugimoto, K. (2003). ATM-related Tel1 associates with double-strand breaks through an Xrs2-dependent mechanism. *Genes & Development*, *17*(16), 1957–1962.

Natsume, T., Müller, C. A., Katou, Y., Retkute, R., Gierliński, M., Araki, H., … Tanaka, T. U. (2013). Kinetochores Coordinate Pericentromeric Cohesion and Early DNA Replication by Cdc7-Dbf4 Kinase Recruitment. *Molecular Cell*, *50*(5), 661–674.

Nedelcheva, M. N., Roguev, A., Dolapchiev, L. B., Shevchenko, A., Taskov, H. B., Shevchenko, A., … Stoynov, S. S. (2005). Uncoupling of Unwinding from DNA Synthesis Implies Regulation of MCM Helicase by Tof1/Mrc1/Csm3 Checkpoint Complex. *Journal of Molecular Biology*, *347*(3), 509–521.

Neduva, V., & Russell, R. B. (2005). Linear motifs: Evolutionary interaction switches. *FEBS Letters*, *579*(15), 3342–3345.

Neelsen, K. J., Zanini, I. M. Y., Mijic, S., Herrador, R., Zellweger, R., Chaudhuri, A. R., … Lopes, M. (2013). Deregulated origin licensing leads to chromosomal breaks by rereplication of a gapped DNA template. *Genes & Development*, *27*(23), 2537–2542.

Newlon, C. S., & Theis, J. F. (1993). The structure and function of yeast ARS elements. *Current Opinion in Genetics & Development*, *3*(5), 752–758.

Ni, M., Feretzaki, M., Sun, S., Wang, X., & Heitman, J. (2011). Sex in Fungi. *Annual Review of Genetics*, *45*, 405–430.

Nikolaishvili-Feinberg, N., & Cordeiro-Stone, M. (2000). Discrimination between Translesion Synthesis and Template Switching during Bypass Replication of Thymine Dimers in Duplex DNA. *Journal of Biological Chemistry*, *275*(40), 30943–30950.

Noguchi, E., Noguchi, C., Du, L.-L., & Russell, P. (2003). Swi1 prevents replication fork collapse and controls checkpoint kinase Cds1. *Molecular and Cellular Biology*, *23*(21), 7861–7874.

Noordermeer, S. M., Adam, S., Setiaputra, D., Barazas, M., Pettitt, S. J., Ling, A. K., … Durocher, D. (2018). The shieldin complex mediates 53BP1-dependent DNA repair. *Nature*, *560*(7716), 117–121.

Nordman, J., & Orr-Weaver, T. L. (2012). Regulation of DNA replication during development. *Development*, *139*(3), 455–464.

Nott, T. J., Kelly, G., Stach, L., Li, J., Westcott, S., Patel, D., … Smerdon, S. J. (2009). An intramolecular switch regulates phosphoindependent FHA domain interactions in Mycobacterium tuberculosis. *Science Signaling*, *2*(63), ra12.

Nougarède, R., Seta, F. D., Zarzov, P., & Schwob, E. (2000). Hierarchy of S-Phase-Promoting Factors: Yeast Dbf4-Cdc7 Kinase Requires Prior S-Phase Cyclin-Dependent Kinase Activation. *Molecular and Cellular Biology*, *20*(11), 3795–3806.

Nowsheen, S., Cooper, T., Stanley, J. A., & Yang, E. S. (2012). Synthetic Lethal Interactions between EGFR and PARP Inhibition in Human Triple Negative Breast Cancer Cells. *PLOS ONE*, *7*(10), e46614.

Ogi, H., Wang, C.-Z., Nakai, W., Kawasaki, Y., & Masumoto, H. (2008). The role of the Saccharomyces cerevisiae Cdc7-Dbf4 complex in the replication checkpoint. *Gene*, *414*(1–2), 32–40.

Ogino, K., Takeda, T., Matsui, E., Iiyama, H., Taniyama, C., Arai, K., & Masai, H. (2001). Bipartite Binding of a Kinase Activator Activates Cdc7-related Kinase Essential for S Phase. *Journal of Biological Chemistry*, *276*(33), 31376–31387.

Ohtoshi, A., Miyake, T., Arai, K., & Masai, H. (1997). Analyses of Saccharomyces cerevisiae Cdc7 kinase point mutants: Dominant-negative inhibition of DNA replication on overexpression of kinase-negative Cdc7 proteins. *Molecular and General Genetics MGG*, *254*(5), 562–570.

Okazaki, R., Okazaki, T., Sakabe, K., Sugimoto, K., Kainuma, R., Sugino, A., & Iwatsuki, N. (1968a). In Vivo Mechanism of DNA Chain Growth. *Cold Spring Harbor Symposia on Quantitative Biology*, *33*, 129–143.

Okazaki, R., Okazaki, T., Sakabe, K., Sugimoto, K., & Sugino, A. (1968b). Mechanism of DNA chain growth. I. Possible discontinuity and unusual secondary structure of newly synthesized chains. *Proceedings of the National Academy of Sciences of the United States of America*, *59*(2), 598–605.

Oliner, J. D., Pietenpol, J. A., Thiagalingam, S., Gyuris, J., Kinzler, K. W., & Vogelstein, B. (1993). Oncoprotein MDM2 conceals the activation domain of tumour suppressor p53. *Nature*, *362*(6423), 857–860.

O'Neil, N. J., Bailey, M. L., & Hieter, P. (2017). Synthetic lethality and cancer. *Nature Reviews Genetics*, *18*(10), 613–623.

Osborn, A. J., & Elledge, S. J. (2003). Mrc1 is a replication fork component whose phosphorylation in response to DNA replication stress activates Rad53. *Genes & Development*, *17*(14), 1755–1767.

Oshiro, G., Owens, J. C., Shellman, Y., Sclafani, R. A., & Li, J. J. (1999). Cell Cycle Control of Cdc7p Kinase Activity through Regulation of Dbf4p Stability. *Molecular and Cellular Biology*, *19*(7), 4888–4896.

Ostrow, A. Z., Nellimoottil, T., Knott, S. R. V., Fox, C. A., Tavaré, S., & Aparicio, O. M. (2014). Fkh1 and Fkh2 Bind Multiple Chromosomal Elements in the S. cerevisiae Genome with Distinct Specificities and Cell Cycle Dynamics. *PLOS ONE*, *9*(2), e87647.

Otwinowski, Z., & Minor, W. (1997). Processing of X-ray diffraction data collected in oscillation mode. *Methods in Enzymology*, *276*, 307–326.

Owens, J. C., Detweiler, C. S., & Li, J. J. (1997). CDC45 is required in conjunction with CDC7/DBF4 to trigger the initiation of DNA replication. *Proceedings of the National Academy of Sciences*, *94*(23), 12521–12526.

Paeschke, K., Capra, J. A., & Zakian, V. A. (2011). DNA replication through G-quadruplex motifs is promoted by the Saccharomyces cerevisiae Pif1 DNA helicase. *Cell*, *145*(5), 678–691.

Palmbos, P. L., Wu, D., Daley, J. M., & Wilson, T. E. (2008). Recruitment of Saccharomyces cerevisiae Dnl4-Lif1 complex to a double-strand break requires interactions with Yku80 and the Xrs2 FHA domain. *Genetics*, *180*(4), 1809–1819.

Pardo, B., Crabbé, L., & Pasero, P. (2017). Signaling pathways of replication stress in yeast. *FEMS Yeast Research*, *17*(2).

Pasero, P., Bensimon, A., & Schwob, E. (2002). Single-molecule analysis reveals clustering and epigenetic regulation of replication origins at the yeast rDNA locus. *Genes & Development*, *16*(19), 2479–2484.

Pasero, P., Duncker, B. P., Schwob, E., & Gasser, S. M. (1999). A role for the Cdc7 kinase regulatory subunit Dbf4p in the formation of initiation-competent origins of replication. *Genes & Development*, *13*(16), 2159–2176.

Patel, P. K., Kommajosyula, N., Rosebrock, A., Bensimon, A., Leatherwood, J., Bechhoefer, J., & Rhind, N. (2008). The Hsk1(Cdc7) Replication Kinase Regulates Origin Efficiency. *Molecular Biology of the Cell*, *19*(12), 5550–5558.

Paulovich, A. G., & Hartwell, L. H. (1995). A checkpoint regulates the rate of progression through S phase in S. cerevisiae in response to DNA damage. *Cell*, *82*(5), 841–847.

Pavlov, Y. I., Frahm, C., McElhinny, S. A. N., Niimi, A., Suzuki, M., & Kunkel, T. A. (2006). Evidence that Errors Made by DNA Polymerase α are Corrected by DNA Polymerase δ. *Current Biology*, *16*(2), 202–207.

Peace, J. M., Ter-Zakarian, A., & Aparicio, O. M. (2014). Rif1 Regulates Initiation Timing of Late Replication Origins throughout the S. cerevisiae Genome. *PLOS ONE*, *9*(5), e98501.

Pellegrini, L. (2012). The Pol α-primase complex. *Sub-Cellular Biochemistry*, *62*, 157–169.

Pellicioli, A., & Foiani, M. (2005). Signal transduction: How rad53 kinase is activated. *Current Biology: CB*, *15*(18), R769-771.

Peng, B., Ortega, J., Gu, L., Chang, Z., & Li, G.-M. (2019). Phosphorylation of proliferating cell nuclear antigen promotes cancer progression by activating the ATM/Akt/GSK3β/Snail signaling pathway. *Journal of Biological Chemistry*, *294*(17), 7037–7045.

Piccart-Gebhart, M., Holmes, E., Baselga, J., de Azambuja, E., Dueck, A. C., Viale, G., … Perez, E. A. (2015). Adjuvant Lapatinib and Trastuzumab for Early Human Epidermal Growth Factor Receptor 2–Positive Breast Cancer: Results From the Randomized Phase III Adjuvant Lapatinib and/or Trastuzumab Treatment Optimization Trial. *Journal of Clinical Oncology*, *34*(10), 1034–1042.

Poli, J., Tsaponina, O., Crabbé, L., Keszthelyi, A., Pantesco, V., Chabes, A., … Pasero, P. (2012). DNTP pools determine fork progression and origin usage under replication stress. *The EMBO Journal*, *31*(4), 883–894.

Pomerantz, R. T., & O'Donnell, M. (2010). Direct restart of a replication fork stalled by a head-on RNA polymerase. *Science (New York, N.Y.)*, *327*(5965), 590–592.

Pomper, S. (1950). The Yeast Cell. Its Genetics and Cytology. Carl C. Lindegren. *The Quarterly Review of Biology*, *25*(2), 215–216.

Pope, B. D., Hiratani, I., & Gilbert, D. M. (2010). Domain-wide regulation of DNA replication timing during mammalian development. *Chromosome Research*, *18*(1), 127–136.

Postow, L., Crisona, N. J., Peter, B. J., Hardy, C. D., & Cozzarelli, N. R. (2001). Topological challenges to DNA replication: Conformations at the fork. *Proceedings of the National Academy of Sciences*, *98*(15), 8219–8226.

Prince, P. R., Emond, M. J., & Monnat, R. J. (2001). Loss of Werner syndrome protein function promotes aberrant mitotic recombination. *Genes & Development*, *15*(8), 933–938.

Pringle, J. R. (1991). [52] Staining of bud scars and other cell wall chitin with Calcofluor. In *Guide to Yeast Genetics and Molecular Biology*: *Vol. 194*. *Methods in Enzymology* (pp. 732–735).

Putnam, C. D., Hayes, T. K., & Kolodner, R. D. (2009). Specific pathways prevent duplication-mediated genome rearrangements. *Nature*, *460*(7258), 984–989.

Qin, J., & Gronenborn, A. M. (2014). Weak protein complexes: Challenging to study but essential for life. *The FEBS Journal*, *281*(8), 1948–1949.

Raasch, K., Bocola, M., Labahn, J., Leitner, A., Eggeling, L., & Bott, M. (2014). Interaction of 2-oxoglutarate dehydrogenase OdhA with its inhibitor OdhI in Corynebacterium glutamicum: Mutants and a model. *Journal of Biotechnology*, *191*, 99–105.

Raghuraman, M. K., Winzeler, E. A., Collingwood, D., Hunt, S., Wodicka, L., Conway, A., … Fangman, W. L. (2001). Replication Dynamics of the Yeast Genome. *Science*, *294*(5540), 115–121.

Randell, J. C. W., Fan, A., Chan, C., Francis, L. I., Heller, R. C., Galani, K., & Bell, S. P. (2010). Mec1 is one of multiple kinases that prime the Mcm2-7 helicase for phosphorylation by Cdc7. *Molecular Cell*, *40*(3), 353–363.

Reynolds, A. E., McCarroll, R. M., Newlon, C. S., & Fangman, W. L. (1989). Time of replication of ARS elements along yeast chromosome III. *Molecular and Cellular Biology*, *9*(10), 4488–4494.

Rhind, N., & Gilbert, D. M. (2013). DNA Replication Timing. *Cold Spring Harbor Perspectives in Biology*, *5*(8).

Rios-Morales, R. Y., Chan, S. H., & Bell, S. P. (2019). Initiation-specific alleles of the Cdc45 helicase-activating protein. *PLOS ONE*, *14*(3), e0214426.

Rodriguez, M., Yu, X., Chen, J., & Songyang, Z. (2003). Phosphopeptide binding specificities of BRCA1 COOH-terminal (BRCT) domains. *The Journal of Biological Chemistry*, *278*(52), 52914–52918.

Rouse, J., & Jackson, S. P. (2002). Interfaces between the detection, signaling, and repair of DNA damage. *Science (New York, N.Y.)*, *297*(5581), 547–551.

Rubin, G. M., Yandell, M. D., Wortman, J. R., Gabor, G. L., Miklos, Nelson, C. R., … Lewis, S. (2000). Comparative Genomics of the Eukaryotes. *Science*, *287*(5461), 2204–2215.

Safirstein, R., Winston, J., Goldstein, M., Moel, D., Dikman, S., & Guttenplan, J. (1986). Cisplatin nephrotoxicity. *American Journal of Kidney Diseases: The Official Journal of the National Kidney Foundation*, *8*(5), 356–367.

Sasi, N. K., Coquel, F., Lin, Y.-L., MacKeigan, J. P., Pasero, P., & Weinreich, M. (2018). DDK Has a Primary Role in Processing Stalled Replication Forks to Initiate Downstream Checkpoint Signaling. *Neoplasia*, *20*(10), 985–995.

Sato, N., Sato, M., Nakayama, M., Saitoh, R., Arai, K., & Masai, H. (2003). Cell cycle regulation of chromatin binding and nuclear localization of human Cdc7-ASK kinase complex. *Genes to Cells*, *8*(5), 451–463.

Schalbetter, S. A., Mansoubi, S., Chambers, A. L., Downs, J. A., & Baxter, J. (2015). Fork rotation and DNA precatenation are restricted during DNA replication to prevent chromosomal instability. *Proceedings of the National Academy of Sciences*, *112*(33), E4565–E4570.

Schauer, G. D., & O'Donnell, M. E. (2017). Quality control mechanisms exclude incorrect polymerases from the eukaryotic replication fork. *Proceedings of the National Academy of Sciences*, *114*(4), 675–680.

Schmidtke, P., & Barril, X. (2010). Understanding and Predicting Druggability. A High-Throughput Method for Detection of Drug Binding Sites. *Journal of Medicinal Chemistry*, *53*(15), 5858–5867.

Schuck, P. (2000). Size-distribution analysis of macromolecules by sedimentation velocity ultracentrifugation and lamm equation modeling. *Biophysical Journal*, *78*(3), 1606–1619.

Schwarz, J. K., Lovly, C. M., & Piwnica-Worms, H. (2003). Regulation of the Chk2 protein kinase by oligomerization-mediated cis- and trans-phosphorylation. *Molecular Cancer Research: MCR*, *1*(8), 598–609.

Schwob, E., & Nasmyth, K. (1993). CLB5 and CLB6, a new pair of B cyclins involved in DNA replication in Saccharomyces cerevisiae. *Genes & Development*, *7*(7a), 1160–

Scorah, J., & McGowan, C. H. (2009). Claspin and Chk1 regulate replication fork stability by different mechanisms. *Cell Cycle (Georgetown, Tex.)*, *8*(7), 1036–1043.

Scott, J. D., & Pawson, T. (2009). Cell Signaling in Space and Time: Where Proteins Come Together and When They're Apart. *Science*, *326*(5957), 1220–1224.

Segurado, M., & Tercero, J. A. (2009). The S-phase checkpoint: Targeting the replication fork. *Biology of the Cell*, *101*(11), 617–627.

Semple, J. W., Da-Silva, L. F., Jervis, E. J., Ah-Kee, J., Al-Attar, H., Kummer, L., … Duncker, B. P. (2006). An essential role for Orc6 in DNA replication through maintenance of pre-replicative complexes. *The EMBO Journal*, *25*(21), 5150–5158.

Shcherbakova, P. V., & Fijalkowska, I. J. (2006). Translesion synthesis DNA polymerases and control of genome stability. *Frontiers in Bioscience: A Journal and Virtual Library*, *11*, 2496–2517.

Sheu, Y.-J., & Stillman, B. (2006). Cdc7-Dbf4 phosphorylates MCM proteins via a docking site-mediated mechanism to promote S phase progression. *Molecular Cell*, *24*(1), 101–113.

Sheu, Y.-J., & Stillman, B. (2010). The Dbf4–Cdc7 kinase promotes S phase by alleviating an inhibitory activity in Mcm4. *Nature*, *463*(7277), 113–117.

Shi, T., Bunker, R. D., Mattarocci, S., Ribeyre, C., Faty, M., Gut, H., … Thomä, N. H. (2013). Rif1 and Rif2 Shape Telomere Function and Architecture through Multivalent Rap1 Interactions. *Cell*, *153*(6), 1340–1353. https://doi.org/10.1016/j.cell.2013.05.007

Shim, E. Y., Chung, W.-H., Nicolette, M. L., Zhang, Y., Davis, M., Zhu, Z., … Lee, S. E. (2010). Saccharomyces cerevisiae Mre11/Rad50/Xrs2 and Ku proteins regulate association of Exo1 and Dna2 with DNA breaks. *The EMBO Journal*, *29*(19), 3370–3380.

Shimmoto, M., Matsumoto, S., Odagiri, Y., Noguchi, E., Russell, P., & Masai, H. (2009). Interactions between Swi1-Swi3, Mrc1 and S phase kinase, Hsk1 may regulate cellular responses to stalled replication forks in fission yeast. *Genes to Cells*, *14*(6), 669–682.

Shyian, M., Mattarocci, S., Albert, B., Hafner, L., Lezaja, A., Costanzo, M., … Shore, D. (2016). Budding Yeast Rif1 Controls Genome Integrity by Inhibiting rDNA Replication. *PLOS Genetics*, *12*(11), e1006414.

Sikorski, R. S., & Hieter, P. (1989). A system of shuttle vectors and yeast host strains designed for efficient manipulation of DNA in Saccharomyces cerevisiae. *Genetics*, *122*(1), 19–27.

Silverman, J., Takai, H., Buonomo, S. B. C., Eisenhaber, F., & Lange, T. de. (2004). Human Rif1, ortholog of a yeast telomeric protein, is regulated by ATM and 53BP1 and functions in the S-phase checkpoint. *Genes & Development*, *18*(17), 2108–2119.

Smolka, M. B., Chen, S., Maddox, P. S., Enserink, J. M., Albuquerque, C. P., Wei, X. X., … Zhou, H. (2006). An FHA domain–mediated protein interaction network of Rad53 reveals its role in polarized cell growth. *The Journal of Cell Biology*, *175*(5), 743–753.

Sochocka, M., Ochnik, M., Sobczyński, M., Siemieniec, I., Orzechowska, B., Naporowski, P., & Leszek, J. (2019). New therapeutic targeting of Alzheimer's disease with the potential use of proline-rich polypeptide complex to modulate an innate immune response—Preliminary study. *Journal of Neuroinflammation*, *16*(1), 137.

Solomon, N. A., Wright, M. B., Chang, S., Buckley, A. M., Dumas, L. B., & Gaber, R. F. (1992). Genetic and molecular analysis of DNA43 and DNA52: Two new cell-cycle genes in Saccharomyces cerevisiae. *Yeast (Chichester, England)*, *8*(4), 273–289.

Sorenson, K. S., Mahaney, B. L., Lees-Miller, S. P., & Cobb, J. A. (2017). The non-homologous end-joining factor Nej1 inhibits resection mediated by Dna2-Sgs1 at DNA double strand breaks. *Journal of Biological Chemistry*, jbc.M117.796011.

Soutoglou, E., Dorn, J. F., Sengupta, K., Jasin, M., Nussenzweig, A., Ried, T., … Misteli, T. (2007). Positional stability of single double-strand breaks in mammalian cells. *Nature Cell Biology*, *9*(6), 675–682.

Souza, C. P. C. D., & Osmani, S. A. (2007). Mitosis, Not Just Open or Closed. *Eukaryotic Cell*, *6*(9), 1521–1527.

Speck, C., Chen, Z., Li, H., & Stillman, B. (2005). ATPase-dependent, cooperative binding of ORC and Cdc6p to origin DNA. *Nature Structural & Molecular Biology*, *12*(11), 965–971.

Speck, C., & Stillman, B. (2007). Cdc6 ATPase Activity Regulates ORC·Cdc6 Stability and the Selection of Specific DNA Sequences as Origins of DNA Replication. *Journal of Biological Chemistry*, *282*(16), 11705–11714.

Sperandio, O., Miteva, M. A., Segers, K., Nicolaes, G. A. F., & Villoutreix, B. O. (2008). Screening Outside the Catalytic Site: Inhibition of Macromolecular Interactions Through Structure-Based Virtual Ligand Screening Experiments. *The Open Biochemistry Journal*, *2*(1).

Sreesankar, E., Senthilkumar, R., Bharathi, V., Mishra, R. K., & Mishra, K. (2012). Functional diversification of yeast telomere associated protein, Rif1, in higher eukaryotes. *BMC Genomics*, *13*(1), 255.

Steensels, J., Snoek, T., Meersman, E., Nicolino, M. P., Voordeckers, K., & Verstrepen, K. J. (2014). Improving industrial yeast strains: Exploiting natural and artificial diversity. *Fems Microbiology Reviews*, *38*(5), 947–995.

Stein, A., & Aloy, P. (2010). Novel Peptide-Mediated Interactions Derived from High-Resolution 3-Dimensional Structures. *PLOS Computational Biology*, *6*(5), e1000789.

Stelter, P., & Ulrich, H. D. (2003). Control of spontaneous and damage-induced mutagenesis by SUMO and ubiquitin conjugation. *Nature*, *425*(6954), 188–191.

Storici, F., Lewis, L. K., & Resnick, M. A. (2001). In vivo site-directed mutagenesis using oligonucleotides. *Nature Biotechnology*, *19*(8), 773.

Sukackaite, R., Cornacchia, D., Jensen, M. R., Mas, P. J., Blackledge, M., Enervald, E., … Buonomo, S. B. C. (2017). Mouse Rif1 is a regulatory subunit of protein phosphatase 1 (PP1). *Scientific Reports*, *7*(1), 1–10.

Sun, Z., Hsiao, J., Fay, D. S., & Stern, D. F. (1998). Rad53 FHA domain associated with phosphorylated Rad9 in the DNA damage checkpoint. *Science (New York, N.Y.)*, *281*(5374), 272–274.

Sweeney, F. D., Yang, F., Chi, A., Shabanowitz, J., Hunt, D. F., & Durocher, D. (2005). Saccharomyces cerevisiae Rad9 acts as a Mec1 adaptor to allow Rad53 activation. *Current Biology: CB*, *15*(15), 1364–1375.

Symington, L. S. (2016). Mechanism and Regulation of DNA End Resection in Eukaryotes. *Critical Reviews in Biochemistry and Molecular Biology*, *51*(3), 195–212.

Szybalski, W. (2001). My Road to Øjvind Winge, the Father of Yeast Genetics. *Genetics*, *158*(1), 1–6.

Szyjka, S. J., Viggiani, C. J., & Aparicio, O. M. (2005). Mrc1 Is Required for Normal Progression of Replication Forks throughout Chromatin in S. cerevisiae. *Molecular Cell*, *19*(5), 691–697.

Tanaka, K., & Russell, P. (2001). Mrc1 channels the DNA replication arrest signal to checkpoint kinase Cds1. *Nature Cell Biology*, *3*(11), 966–972.

Tanaka, S., Nakato, R., Katou, Y., Shirahige, K., & Araki, H. (2011). Origin Association of Sld3, Sld7, and Cdc45 Proteins Is a Key Step for Determination of Origin-Firing Timing. *Current Biology*, *21*(24), 2055–2063.

Tanaka, S., Umemori, T., Hirai, K., Muramatsu, S., Kamimura, Y., & Araki, H. (2007). CDK-dependent phosphorylation of Sld2 and Sld3 initiates DNA replication in budding yeast. *Nature*, *445*(7125), 328–332.

Tazumi, A., Fukuura, M., Nakato, R., Kishimoto, A., Takenaka, T., Ogawa, S., … Masukata, H. (2012). Telomere-binding protein Taz1 controls global replication timing through its localization near late replication origins in fission yeast. *Genes & Development*, *26*(18), 2050–2062.

Tercero, J. A., Longhese, M. P., & Diffley, J. F. X. (2003). A Central Role for DNA Replication Forks in Checkpoint Activation and Response. *Molecular Cell*, *11*(5), 1323–1336.

Theis, J. F., & Newlon, C. S. (1997). The ARS309 chromosomal replicator of Saccharomyces cerevisiae depends on an exceptional ARS consensus sequence. *Proceedings of the National Academy of Sciences*, *94*(20), 10786–10791.

Tisato, V., Voltan, R., Gonelli, A., Secchiero, P., & Zauli, G. (2017). MDM2/X inhibitors under clinical evaluation: Perspectives for the management of hematological malignancies and pediatric cancer. *Journal of Hematology & Oncology*, *10*(1), 133.

Tishkoff, D. X., Filosi, N., Gaida, G. M., & Kolodner, R. D. (1997). A novel mutation avoidance mechanism dependent on S. cerevisiae RAD27 is distinct from DNA mismatch repair. *Cell*, *88*(2), 253–263.

Tissier, A., McDonald, J. P., Frank, E. G., & Woodgate, R. (2000). Polι, a remarkably error-prone human DNA polymerase. *Genes & Development*, *14*(13), 1642–1650.

Tomimatsu, N., Mukherjee, B., Catherine Hardebeck, M., Ilcheva, M., Vanessa Camacho, C., Louise Harris, J., … Burma, S. (2014). Phosphorylation of EXO1 by CDKs 1 and 2 regulates DNA end resection and repair pathway choice. *Nature Communications*, *5*, 3561.

Unnikrishnan, A., Gafken, P. R., & Tsukiyama, T. (2010). Dynamic changes in histone acetylation regulate origins of DNA replication. *Nature Structural & Molecular Biology*, *17*(4), 430–437.

Uzunova, S. D., Zarkov, A. S., Ivanova, A. M., Stoynov, S. S., & Nedelcheva-Veleva, M. N. (2014). The subunits of the S-phase checkpoint complex Mrc1/Tof1/Csm3: Dynamics and interdependence. *Cell Division*, *9*, 4.

Varrin, A. E., Prasad, A. A., Scholz, R.-P., Ramer, M. D., & Duncker, B. P. (2005). A Mutation in Dbf4 Motif M Impairs Interactions with DNA Replication Factors and Confers Increased Resistance to Genotoxic Agents. *Molecular and Cellular Biology*, *25*(17), 7494–7504.

Vialard, J. E., Gilbert, C. S., Green, C. M., & Lowndes, N. F. (1998). The budding yeast Rad9 checkpoint protein is subjected to Mec1/Tel1-dependent hyperphosphorylation and interacts with Rad53 after DNA damage. *The EMBO Journal*, *17*(19), 5679–5688.

Viggiani, C. J., Knott, S. R. V., & Aparicio, O. M. (2010). Genome-Wide Analysis of DNA Synthesis by BrdU Immunoprecipitation on Tiling Microarrays (BrdU-IP-chip) in Saccharomyces cerevisiae. *Cold Spring Harbor Protocols*, *2010*(2), pdb.prot5385.

Víglaský, V., Bauer, L., & Tlucková, K. (2010). Structural features of intra- and intermolecular G-quadruplexes derived from telomeric repeats. *Biochemistry*, *49*(10), 2110–2120.

Vinogradova, O., & Qin, J. (2012). NMR as a Unique Tool in Assessment and Complex Determination of Weak Protein–Protein Interactions. *Topics in Current Chemistry*, *326*, 35–45.

Virgilio, M. D., Callen, E., Yamane, A., Zhang, W., Jankovic, M., Gitlin, A. D., … Nussenzweig, M. C. (2013). Rif1 Prevents Resection of DNA Breaks and Promotes Immunoglobulin Class Switching. *Science*, *339*(6120), 711–715.

Virshup, D. M., & Shenolikar, S. (2009). From Promiscuity to Precision: Protein Phosphatases Get a Makeover. *Molecular Cell*, *33*(5), 537–545.

Waga, S., & Stillman, B. (1994). Anatomy of a DNA replication fork revealed by reconstitution of SV40 DNA replication in vitro. *Nature*, *369*(6477), 207–212.

Walker, J. R., Corpina, R. A., & Goldberg, J. (2001). Structure of the Ku heterodimer bound to DNA and its implications for double-strand break repair. *Nature*, *412*(6847), 607–614.

Wang, A. H.-J., Quigley, G. J., Kolpak, F. J., Crawford, J. L., Boom, J. H. van, Marel, G. van der, & Rich, A. (1979). Molecular structure of a left-handed double helical DNA fragment at atomic resolution. *Nature*, *282*(5740), 680–686.

Wang, H., Shi, L. Z., Wong, C. C. L., Han, X., Hwang, P. Y.-H., Truong, L. N., … Wu, X. (2013). The Interaction of CtIP and Nbs1 Connects CDK and ATM to Regulate HR–Mediated Double-Strand Break Repair. *PLOS Genetics*, *9*(2), e1003277.

Wang, J. C. (1998). Moving one DNA double helix through another by a type II DNA topoisomerase: The story of a simple molecular machine. *Quarterly Reviews of Biophysics*, *31*(2), 107–144.

Wang, W., Prosise, W. W., Chen, J., Taremi, S. S., Le, H. V., Madison, V., … Lesburg, C. A. (2008). Construction and characterization of a fully active PXR/SRC-1 tethered protein with increased stability. *Protein Engineering, Design and Selection*, *21*(7), 425–433.

Waterhouse, A. M., Procter, J. B., Martin, D. M. A., Clamp, M., & Barton, G. J. (2009). Jalview Version 2—A multiple sequence alignment editor and analysis workbench. *Bioinformatics*, *25*(9), 1189–1191.

Watson, J. D., & Crick, F. H. C. (1953). Molecular Structure of Nucleic Acids: A Structure for Deoxyribose Nucleic Acid. *Nature*, *171*(4356), 737–738.

Wehrman, T. S., Raab, W. J., Casipit, C. L., Doyonnas, R., Pomerantz, J. H., & Blau, H. M. (2006). A system for quantifying dynamic protein interactions defines a role for Herceptin in modulating ErbB2 interactions. *Proceedings of the National Academy of Sciences of the United States of America*, *103*(50), 19063–19068.

Wei, L., & Zhao, X. (2016). A new MCM modification cycle regulates DNA replication initiation. *Nature Structural & Molecular Biology*, *23*(3), 209–216.

Weinstock, D. M., Brunet, E., & Jasin, M. (2007). Formation of NHEJ-derived reciprocal chromosomal translocations does not require Ku70. *Nature Cell Biology*, *9*(8), 978–981.

Weng, J.-H., Hsieh, Y.-C., Huang, C.-C. F., Wei, T.-Y. W., Lim, L.-H., Chen, Y.-H., … Tsai, M.-D. (2015). Uncovering the Mechanism of Forkhead-Associated Domain-Mediated TIFA Oligomerization That Plays a Central Role in Immune Responses. *Biochemistry*, *54*(40), 6219–6229.

White, E. J., Emanuelsson, O., Scalzo, D., Royce, T., Kosak, S., Oakeley, E. J., … Schübeler, D. (2004). DNA replication-timing analysis of human chromosome 22 at high resolution and different developmental states. *Proceedings of the National Academy of Sciences*, *101*(51), 17771–17776.

Williams, S. J., Sohn, K. H., Wan, L., Bernoux, M., Sarris, P. F., Segonzac, C., … Jones, J. D. G. (2014). Structural Basis for Assembly and Function of a Heterodimeric Plant Immune Receptor. *Science*, *344*(6181), 299–303.

Wong, P. G., Winter, S. L., Zaika, E., Cao, T. V., Oguz, U., Koomen, J. M., … Alexandrow, M. G. (2011). Cdc45 limits replicon usage from a low density of preRCs in mammalian cells. *PloS One*, *6*(3), e17533.

Wybenga-Groot, L. E., Ho, C. S., Sweeney, F. D., Ceccarelli, D. F., McGlade, C. J., Durocher, D., & Sicheri, F. (2014). Structural basis of Rad53 kinase activation by dimerization and activation segment exchange. *Cellular Signalling*, *26*(9), 1825–1836.

Xu, H., Boone, C., & Klein, H. L. (2004). Mrc1 Is Required for Sister Chromatid Cohesion To Aid in Recombination Repair of Spontaneous Damage. *Molecular and Cellular Biology*, *24*(16), 7082–7090.

Xu, L., & Blackburn, E. H. (2004). Human Rif1 protein binds aberrant telomeres and aligns along anaphase midzone microtubules. *J Cell Biol*, *167*(5), 819–830.

Yabuuchi, H., Yamada, Y., Uchida, T., Sunathvanichkul, T., Nakagawa, T., & Masukata, H. (2006). Ordered assembly of Sld3, GINS and Cdc45 is distinctly regulated by DDK and CDK for activation of replication origins. *The EMBO Journal*, *25*(19), 4663–4674.

Yamazaki, S., Hayano, M., & Masai, H. (2013). Replication timing regulation of eukaryotic replicons: Rif1 as a global regulator of replication timing. *Trends in Genetics*, *29*(8), 449–460.

Yamazaki, S., Ishii, A., Kanoh, Y., Oda, M., Nishito, Y., & Masai, H. (2012). Rif1 regulates the replication timing domains on the human genome. *The EMBO Journal*, *31*(18), 3667–3677.

Yang, C.-C., Suzuki, M., Yamakawa, S., Uno, S., Ishii, A., Yamazaki, S., … Masai, H. (2016). Claspin recruits Cdc7 kinase for initiation of DNA replication in human cells. *Nature Communications*, *7*(1), 1–14.

Yao, R., Zhang, Z., An, X., Bucci, B., Perlstein, D. L., Stubbe, J., & Huang, M. (2003). Subcellular localization of yeast ribonucleotide reductase regulated by the DNA replication and damage checkpoint pathways. *Proceedings of the National Academy of Sciences of the United States of America*, *100*(11), 6628–6633.

Yeeles, J. T. P., Deegan, T. D., Janska, A., Early, A., & Diffley, J. F. X. (2015). Regulated eukaryotic DNA replication origin firing with purified proteins. *Nature*, *519*(7544), 431–435.

Yeeles, J. T. P., Janska, A., Early, A., & Diffley, J. F. X. (2017). How the Eukaryotic Replisome Achieves Rapid and Efficient DNA Replication. *Molecular Cell*, *65*(1), 105–116.

Yoshida, K., Poveda, A., & Pasero, P. (2013). Time to Be Versatile: Regulation of the Replication Timing Program in Budding Yeast. *Journal of Molecular Biology*, *425*(23), 4696–4705.

Yu, X., Chini, C. C. S., He, M., Mer, G., & Chen, J. (2003). The BRCT domain is a phospho-protein binding domain. *Science (New York, N.Y.)*, *302*(5645), 639–642.

Zarrinpar, A., Bhattacharyya, R. P., & Lim, W. A. (2003). The structure and function of proline recognition domains. *Science's STKE: Signal Transduction Knowledge Environment*, *2003*(179), RE8.

Zegerman, P., & Diffley, J. F. X. (2007). Phosphorylation of Sld2 and Sld3 by cyclin-dependent kinases promotes DNA replication in budding yeast. *Nature*, *445*(7125), 281–285.

Zegerman, P., & Diffley, J. F. X. (2009). DNA replication as a target of the DNA damage checkpoint. *DNA Repair*, *8*(9), 1077–1088.

Zegerman, P., & Diffley, J. F. X. (2010). Checkpoint-dependent inhibition of DNA replication initiation by Sld3 and Dbf4 phosphorylation. *Nature*, *467*(7314), 474–478.

Zhang, W., & Durocher, D. (2008). Dun1 Counts on Rad53 to Be Turned On. *Molecular Cell*, *31*(1), 1–2.

Zhang, Y. (2008). I-TASSER server for protein 3D structure prediction. *BMC Bioinformatics*, *9*(1), 40.

Zhang, Y., Hefferin, M. L., Chen, L., Shim, E. Y., Tseng, H.-M., Kwon, Y., … Tomkinson, A. E. (2007). Role of Dnl4–Lif1 in nonhomologous end-joining repair complex assembly and suppression of homologous recombination. *Nature Structural & Molecular Biology*, *14*(7), 639–646.

Zhang, Z.-X., Zhang, J., Cao, Q., Campbell, J. L., & Lou, H. (2018). The DNA Pol ϵ stimulatory activity of Mrc1 is modulated by phosphorylation. *Cell Cycle*, *17*(1), 64–72.

Zhao, H., Brown, P. H., & Schuck, P. (2011). On the distribution of protein refractive index increments. *Biophysical Journal*, *100*(9), 2309–2317.

Zhao, X., Muller, E. G. D., & Rothstein, R. (1998). A Suppressor of Two Essential Checkpoint Genes Identifies a Novel Protein that Negatively Affects dNTP Pools. *Molecular Cell*, *2*(3), 329–340.

Zhao, X., & Rothstein, R. (2002). The Dun1 checkpoint kinase phosphorylates and regulates the ribonucleotide reductase inhibitor Sml1. *Proceedings of the National Academy of Sciences*, *99*(6), 3746–3751.

Zhong, Y., Nellimoottil, T., Peace, J. M., Knott, S. R. V., Villwock, S. K., Yee, J. M., … Aparicio, O. M. (2013). The level of origin firing inversely affects the rate of replication fork progression. *The Journal of Cell Biology*, *201*(3), 373–383.

Zhou, Z., & Elledge, S. J. (1993). DUN1 encodes a protein kinase that controls the DNA damage response in yeast. *Cell*, *75*(6), 1119–1127.

Zhu, W., Ukomadu, C., Jha, S., Senga, T., Dhar, S. K., Wohlschlegel, J. A., … Dutta, A. (2007). Mcm10 and And-1/CTF4 recruit DNA polymerase α to chromatin for initiation of DNA replication. *Genes & Development*, *21*(18), 2288–2299.

Zhuang, L., Yang, Z., & Meng, Z. (2018). Upregulation of BUB1B, CCNB1, CDC7, CDC20, and MCM3 in Tumor Tissues Predicted Worse Overall Survival and Disease-Free Survival in Hepatocellular Carcinoma Patients. *BioMed Research International*, *2018*, 7897346.

Zimmermann, M., Lottersberger, F., Buonomo, S. B., Sfeir, A., & Lange, T. de. (2013). 53BP1 Regulates DSB Repair Using Rif1 to Control 5′ End Resection. *Science*, *339*(6120), 700–704.

Ziraldo, R., Hanke, A., & Levene, S. D. (2019). Kinetic pathways of topology simplification by Type-II topoisomerases in knotted supercoiled DNA. *Nucleic Acids Research*, *47*(1), 69–84.

Zou, L., & Elledge, S. J. (2003). Sensing DNA Damage Through ATRIP Recognition of RPA-ssDNA Complexes. *Science*, *300*(5625), 1542–1548.

Zou, L., Mitchell, J., & Stillman, B. (1997). CDC45, a novel yeast gene that functions with the origin recognition complex and Mcm proteins in initiation of DNA replication. *Molecular and Cellular Biology*, *17*(2), 553–563.

Appendix A

Chapter 3 Supporting Information

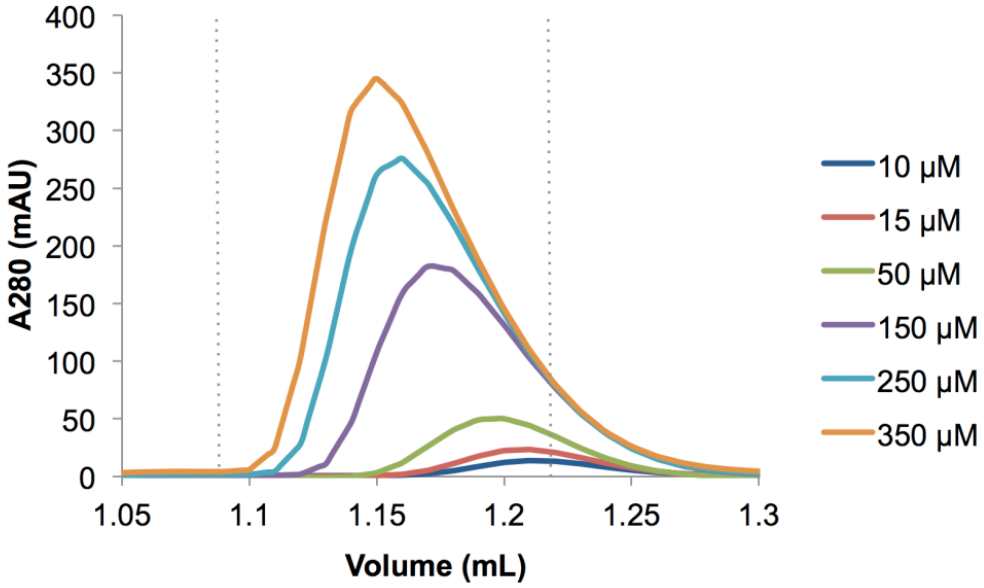

Appendix A Figure 1. **The Dbf4(0)Rad53 chimera exist in a monomer:dimer equilibrium.** Size exclusion chromatography profiles of Dbf4(L0)Rad53 at increasing concentrations.

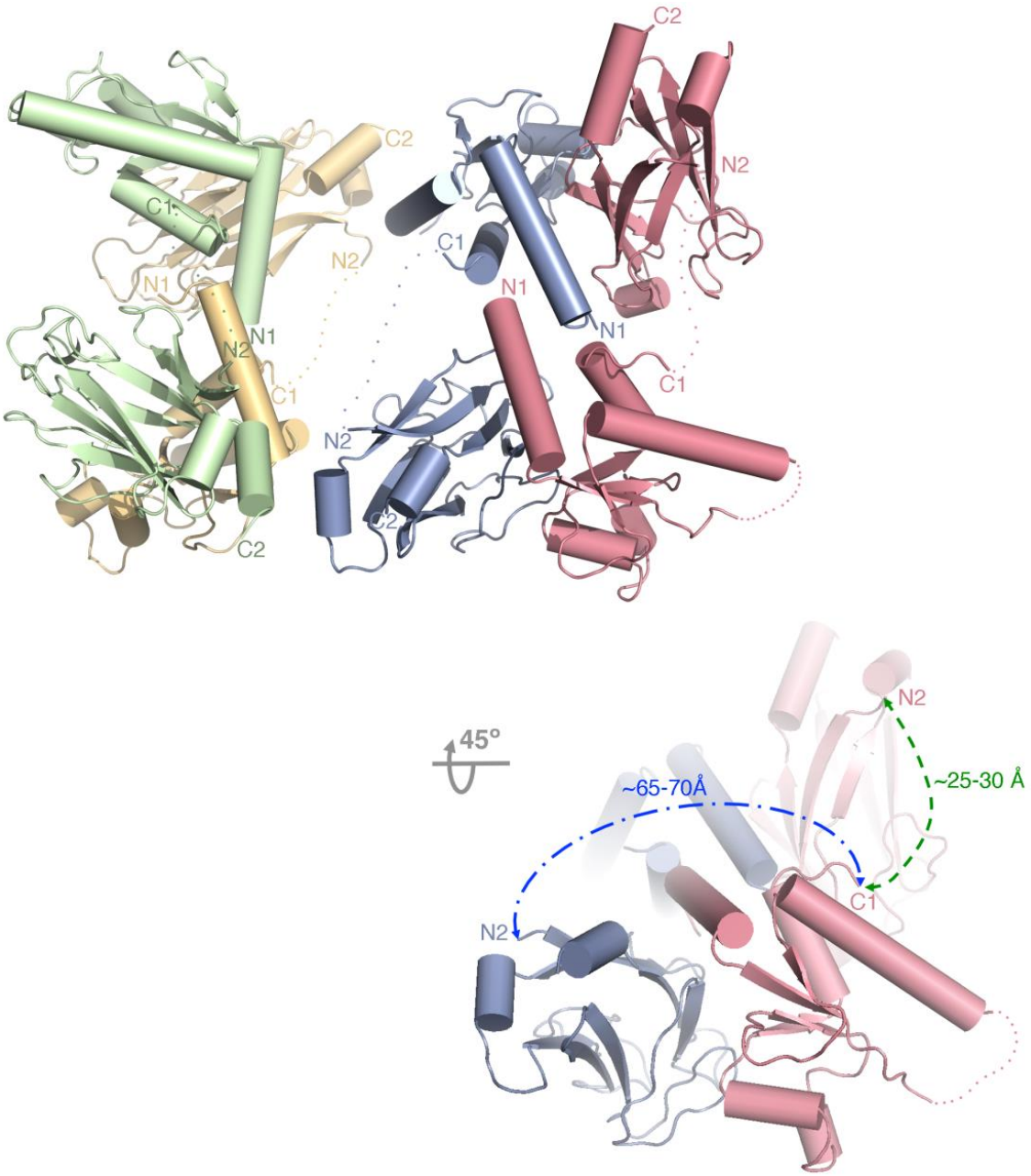

Appendix A Figure 2. Crystal packing of the binary complex. The four molecules in the asymmetric unit are shown color-coded with the N- and C-termini of the HBRCT and FHA1 domains labeled. The bottom panel shows the approximate distances between the C-terminus of the HBRCT and the N-terminus of its closest FHA1 neighbors.

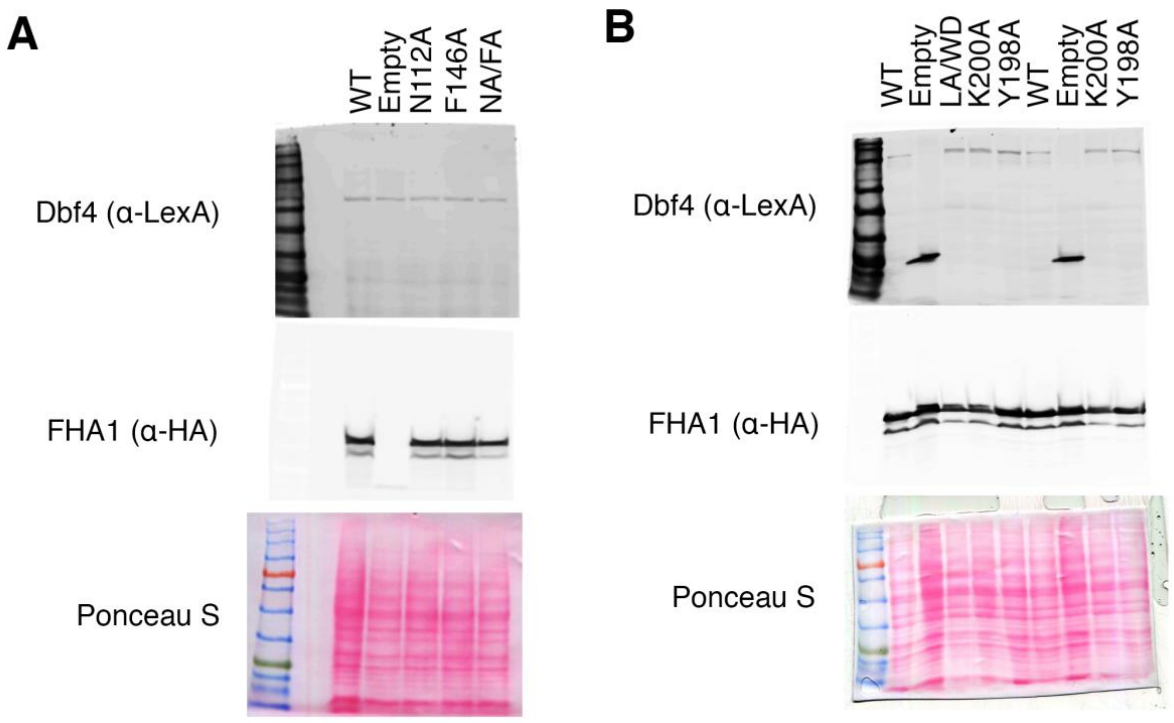

Appendix A Figure 3. Original gels and blots for Figure 3.3. To control for the two-hybrid bait and prey expression levels in Figure 3, whole cell extracts were prepared from transformants following prey induction and analyzed by Western blotting (of three independent experiments performed) using rabbit anti-LexA antibody (bait) and mouse anti-HA monoclonal antibody (prey), along with Alexa Fluor 647-conjugated goat anti-rabbit and Alexa Fluor 488-conjugated goat anti-mouse secondary antibodies, respectively. Prior to detection, the membrane was stained with Ponceau S to assess relative protein loading. Yeast two-hybrid analysis using variants of Rad53 FHA1 as the preys (A) or variants of Dbf4 (B) as the baits.

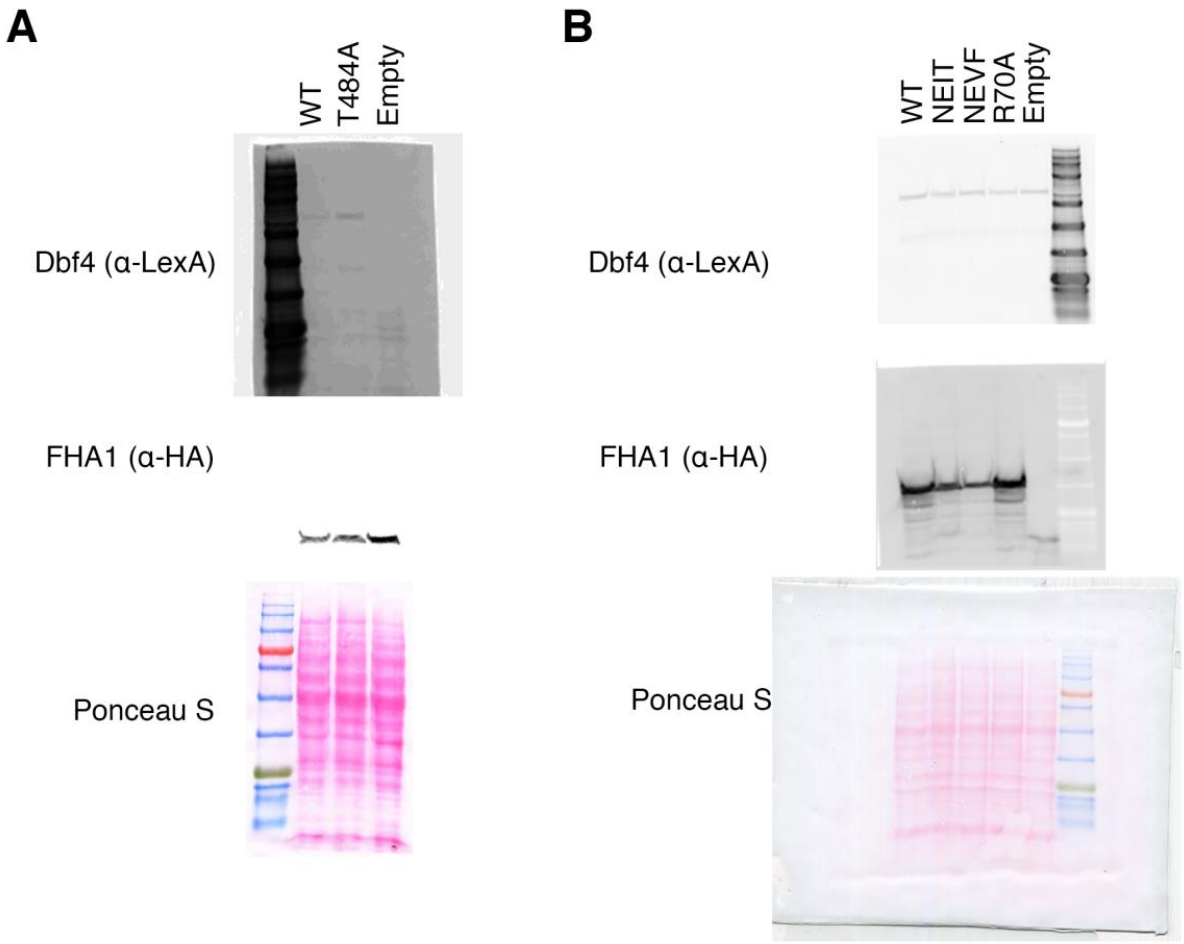

Appendix A Figure 4. Original gels and blots for Figure 3.4. To control for the two-hybrid bait and prey expression levels in Figure 4, whole cell extracts were prepared from transformants following prey induction and analyzed by Western blotting (of three independent experiments performed) using rabbit anti-LexA antibody (bait) and mouse anti-HA monoclonal antibody (prey), along with Alexa Fluor 647-conjugated goat anti-rabbit and Alexa Fluor 488-conjugated goat anti-mouse secondary antibodies, respectively. Prior to detection, the membrane was stained with Ponceau S to assess relative protein loading.

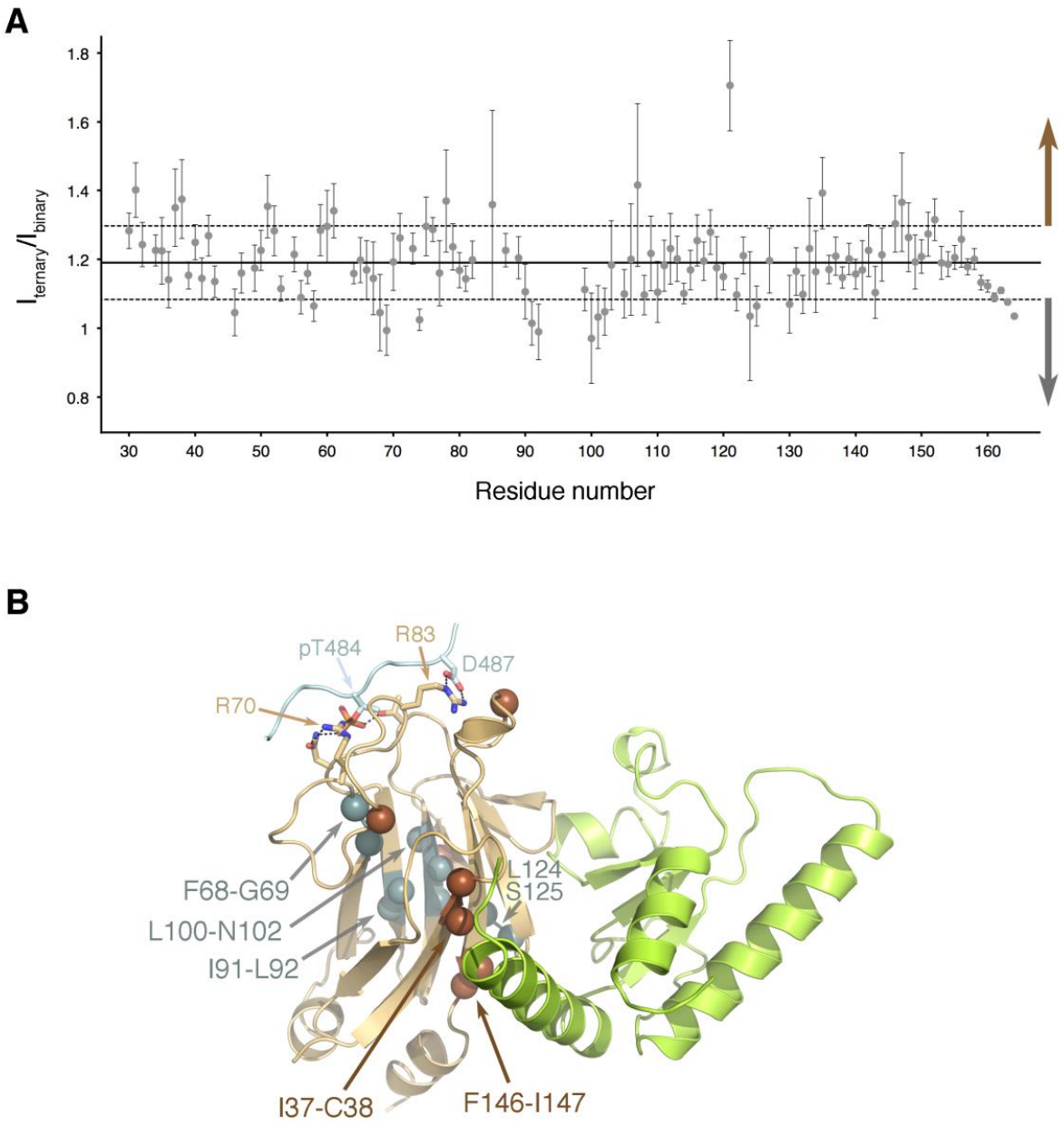

Appendix A Figure 5. ^{15}N-HSQC intensity changes confirm weakening of the Rad53:Dbf4 complex caused by binding of the phosphopeptide to Rad53. (A) Plot of residue specific ratios between cross-peak intensities in the ^{15}N-HSQC spectra of the binary (Rad53:Dbf4) and ternary (Rad53:Dbf4:Cdc7) complexes. The solid and dashed horizontal lines represent the average intensity ratio +/- one standard deviation. (B) Residues with values either greater or lower than the average +/- one standard deviation were plotted onto the X-ray structure of the ternary complex as brown or blue spheres, respectively.

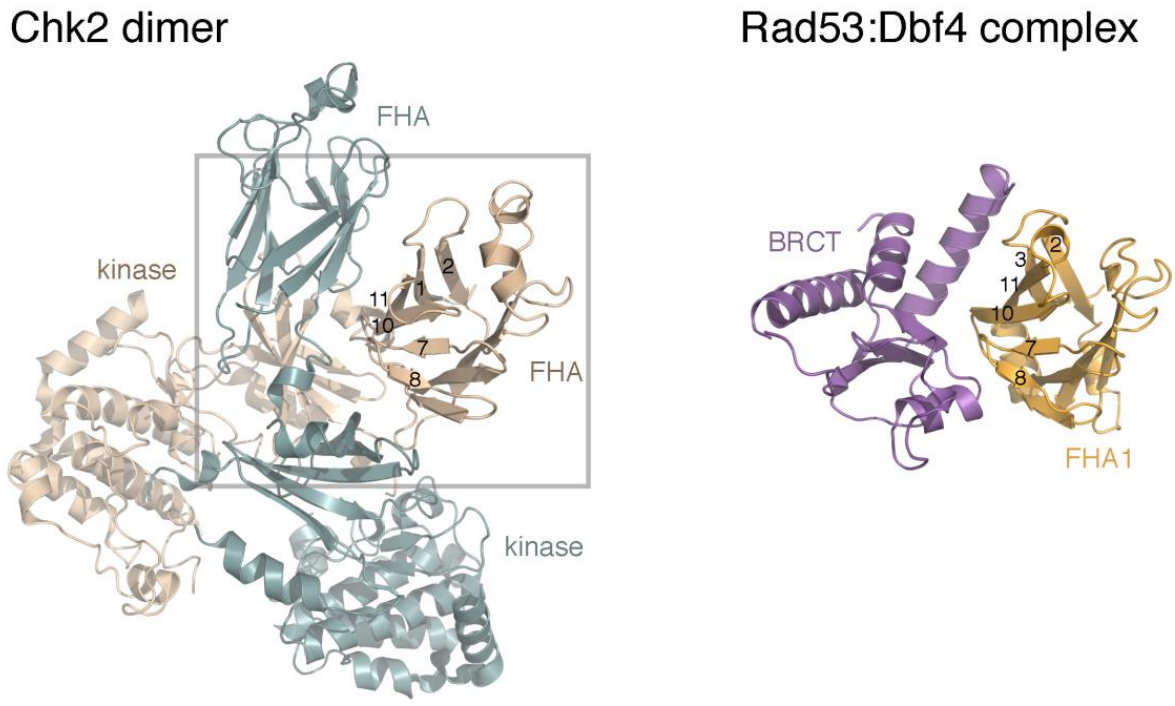

Appendix A Figure 6. Interaction surfaces mediating dimerization of Chk2 and the Rad53:Dbf4 complex. Ribbon diagram of the Chk2 crystal structure (left) showing with the two protomers of the dimer shown in steel blue and tan. The lateral surface of the FHA domain interacts with the FHA domain and the N-terminal lobe of the kinase domain on the second protomer. Comparison with the crystal structure of the Rad53:Dbf4 complex shows that the FHA1 domain of Rad53 (light orange) uses the equivalent lateral surface to interact with the BRCT domain of Dbf4 (purple).

Appendix B

Chapter 4 Supporting Information

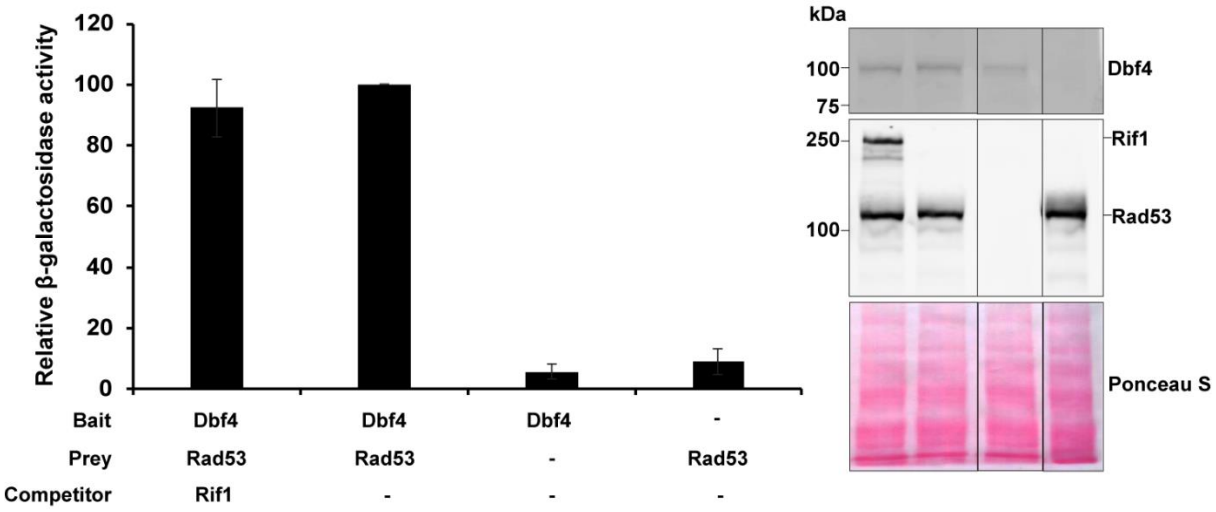

Appendix B Figure 1. Rif1 does not disrupt Rad53 binding to Dbf4. The interaction of Dbf4 and Rad53, with or without overexpression of Rif1, was assessed through yeast two-hybrid assays. The two-hybrid interaction values are presented as a percentage of the interaction of Dbf4 and Rad53 in the absence of Rif1 overexpression. Four independent replicates were performed, and error bars represent standard deviation. Representative Western blots (of four independent experiments performed) indicate protein expression levels and Ponceau S staining shows equal protein loading. Bait, prey and competitor proteins were detected with anti-LexA (Dbf4), anti-HA (Rad53) and anti-Myc (Rif1), antibodies, respectively.

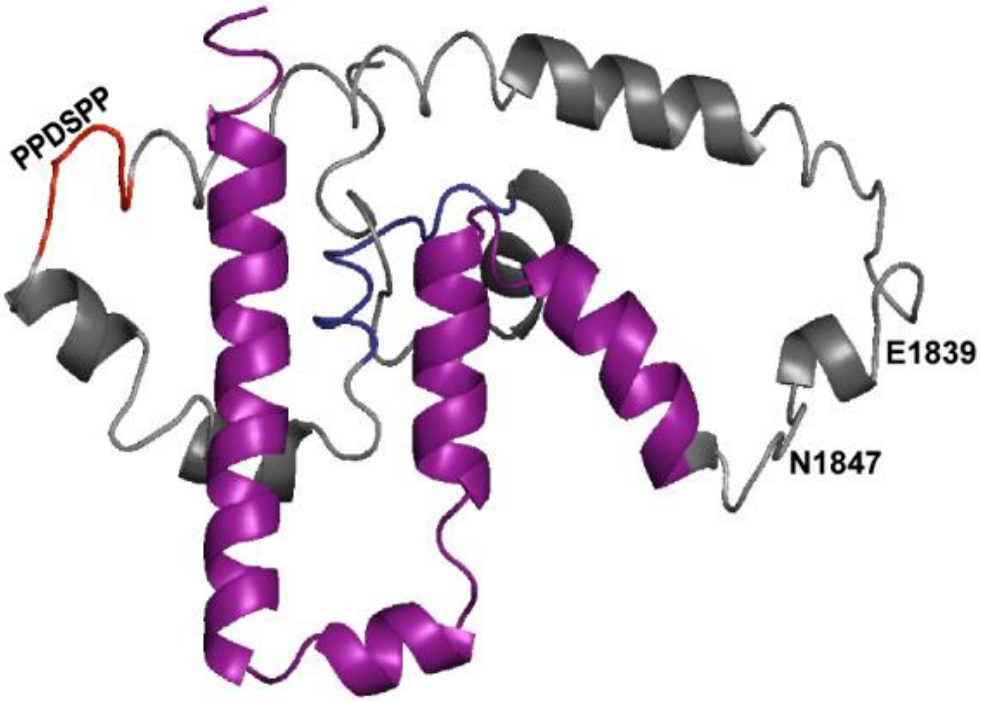

Appendix B Figure 2. I-TASSER structure prediction of Rif1 1739-1916. The tetramerization module is depicted in purple, PPDSPP region in red, and Rap1-binding module in blue.

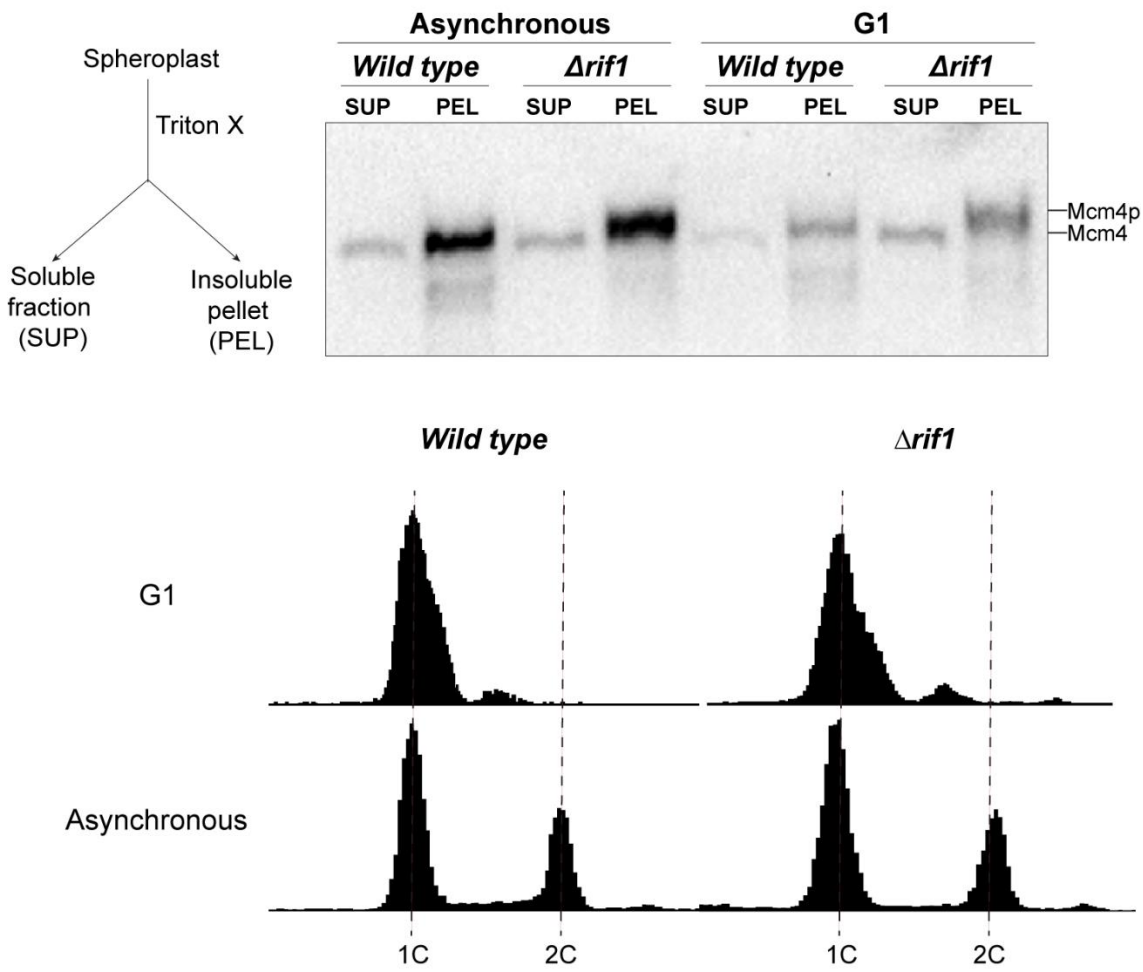

Appendix B Figure 3. Deletion of *RIF1* results in Mcm4 hyperphosphorylation in G1 phase. Both *wild type* and Δ*rif1* cells were arrested in G1 phase via incubation in YPD supplemented with 50 μg/ml α-factor for 3 hours. The cells were then harvested and spheroplasted. The protein extracts from both supernatant (SUP) and pellet (PEL) fractions were subjected to SDS-PAGE and transferred to a PVDF membrane for Mcm4 detection Expression and phosphorylation of Mcm4 were detected using an anti-Mcm4 antibody. FACS analysis was performed to confirm the efficiency of the G1 phase arrest.

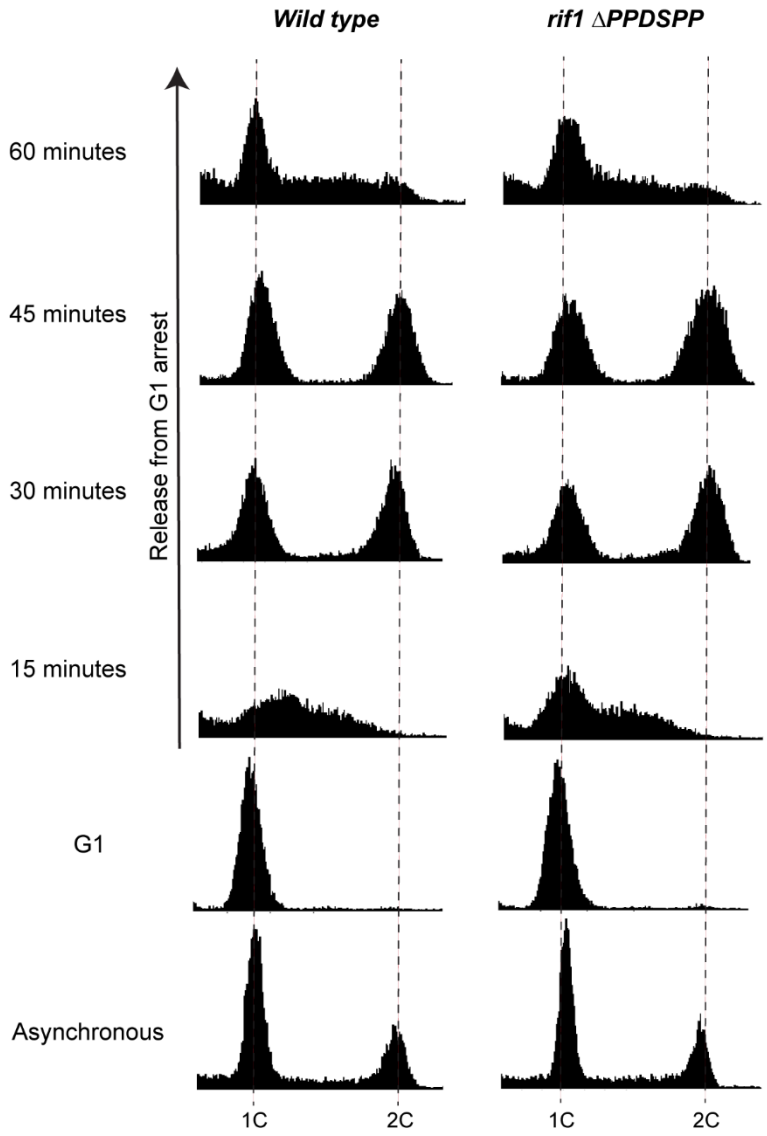

Appendix B Figure 4. ***rif1 ΔPPDSPP* shows a minor defect in cell cycle progression.** All strains were arrested in G1 via incubation in YPD supplemented with 30 µg/ml α-factor for 2.5 hours, harvested, washed, and then released to S phase with addition of 50 µg/ml Pronase E. *rif1 ΔPPDSPP* shows a delay in S phase entry at time point 15 minute after release.

Appendix C

Chapter 5 Supporting Information

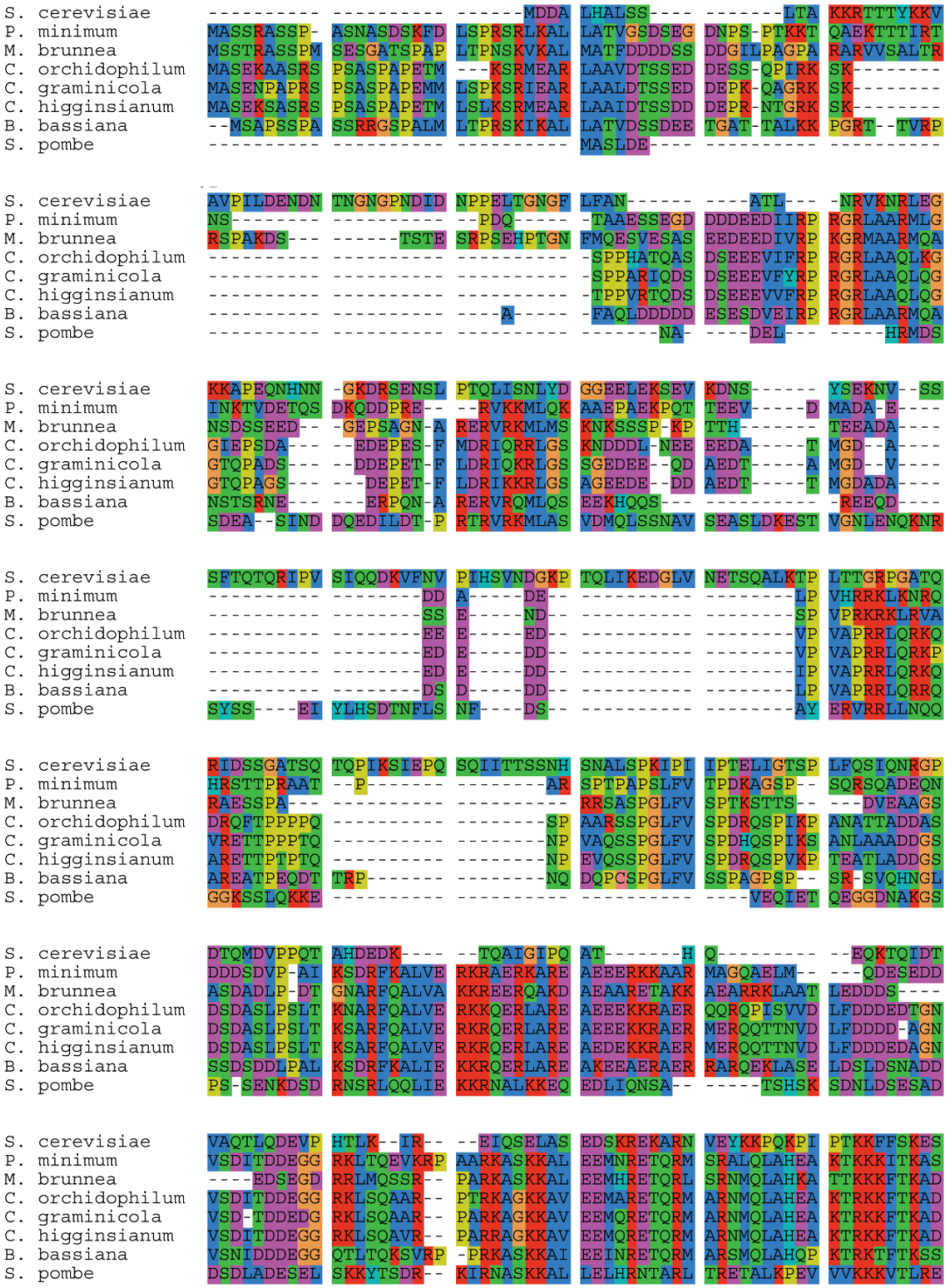

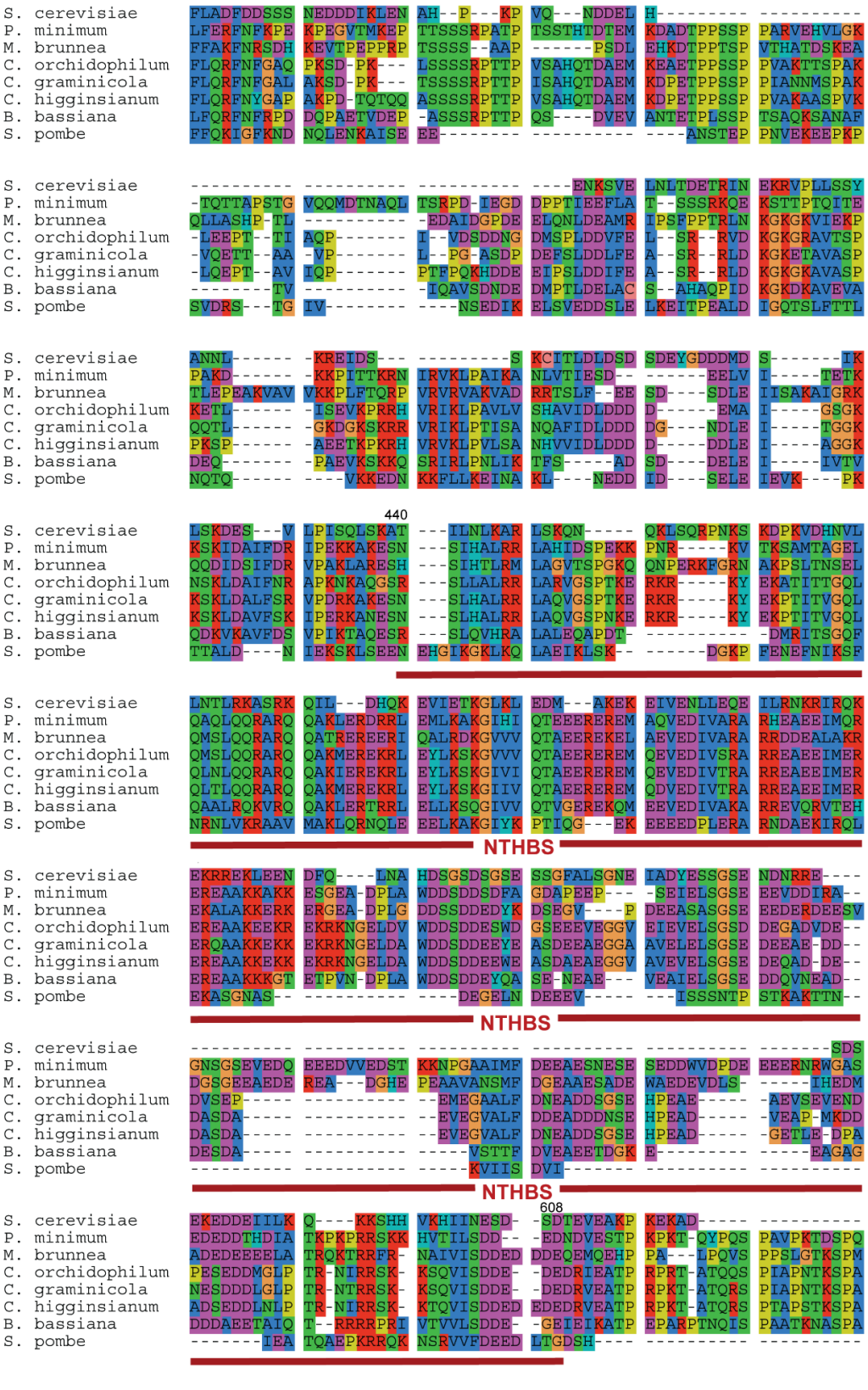
S. cerevisiae
P. minimum
M. brunnea
C. orchidophilum
C. graminicola
C. higginsianum
B. bassiana
S. pombe
440
NTHBS
NTHBS
NTHBS
608

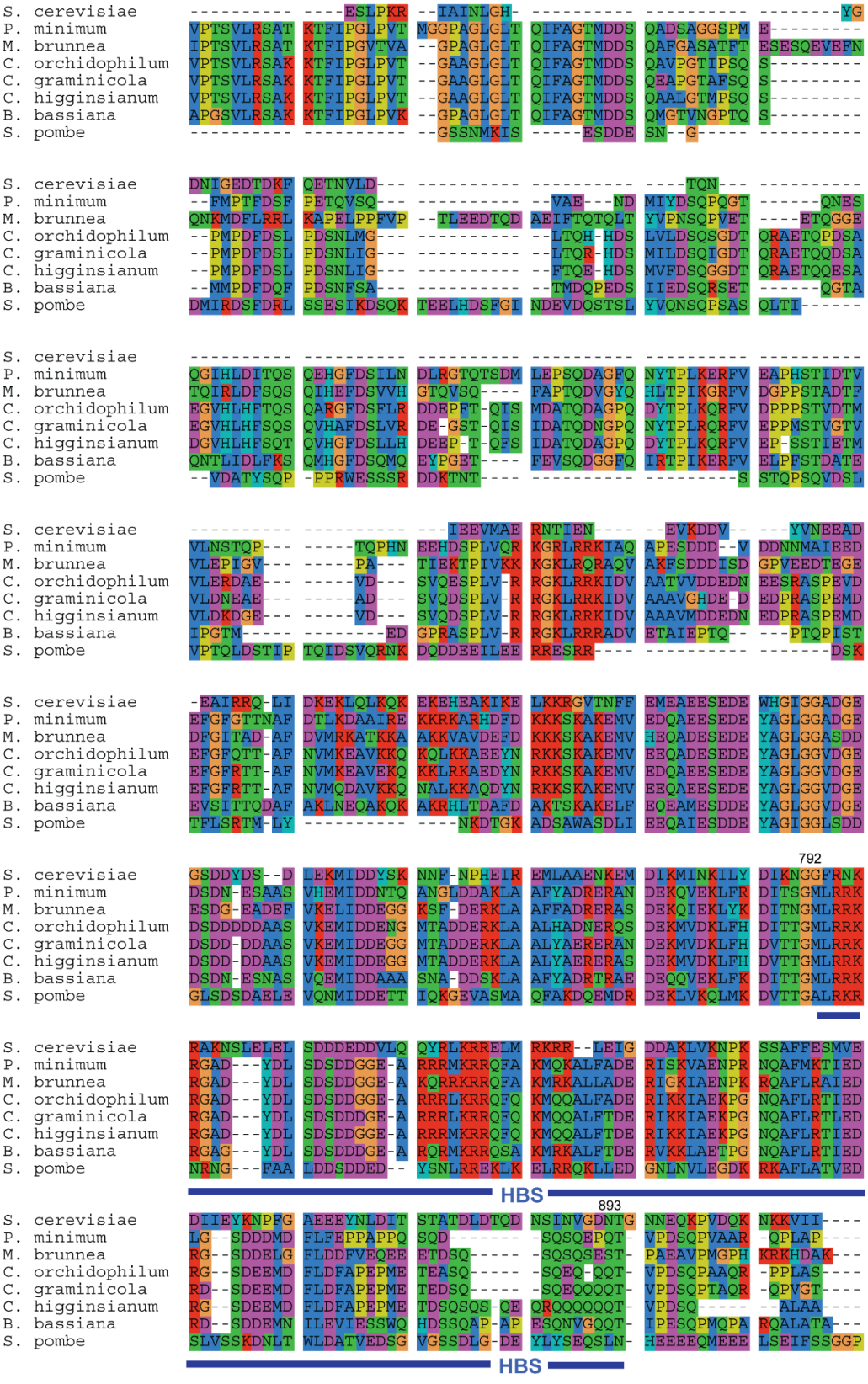
S. cerevisiae
P. minimum
M. brunnea
C. orchidophilum
C. graminicola
C. higginsianum
B. bassiana
S. pombe
792
HBS
893
HBS

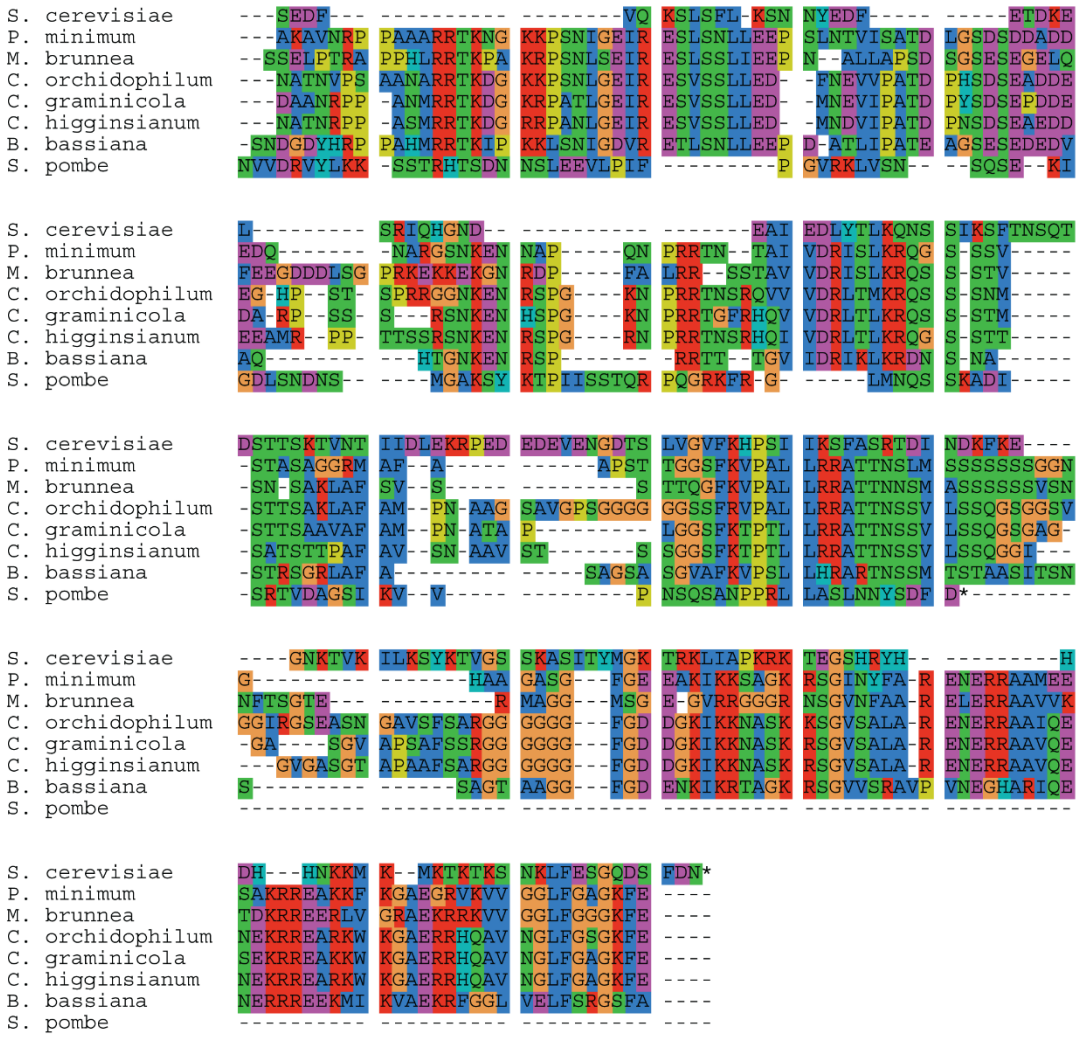

Appendix C Figure 1. Mrc1 multiple sequence alignment for different fungal species. Full-length Mrc1 sequences are from *Saccharomyces cerevisiae* (accession NP_009871), *Phaeoacremonium minimum* (accession XP_007917014), *Marssonina brunnea* (accession EKD12953), *Colletotrichum orchidophilum* (accession XP_022476293), *Colletotrichum graminicola* (accession EFQ28182), *Colletotrichum higginsianum* (accession XP_018156174), *Beauveria bassiana* (accession PMB72403), and *Schizosaccharomyces pombe* (accession NP_594486). The fission yeast Mrc1 NTHBS and HBS regions are indicated by red and blue lines, respectively.